WYDZIAŁ BIOLOGII
i OCHRONY ŚRODOWISKA
Uniwersytet Łódzki

Kierunek:
Interdyscyplinarne Studia Doktoranckie ,,InterDOC-STARt" realizowane na Wydziale Biologii i Ochrony Środowiska Uniwersytetu Łódzkiego

Anastazja Maria Poczta

NUMER ALBUMU: 5985

Aktywność przeciwnowotworowa nowych pochodnych melfalanu w komórkach białaczek szpikowych oraz szpiczaka mnogiego

Anticancer activity of new melphalan derivatives in myeloid leukemia and multiple myeloma cells

Praca doktorska

wykonana w Katedrze Biofizyki Medycznej
Instytutu Biofizyki na Wydziale Biologii
i Ochrony Środowiska UŁ

Promotor:
prof. dr hab. Agnieszka Marczak
Katedra Biofizyki Medycznej,
Instytut Biofizyki, Wydział Biologii
i Ochrony Środowiska,
Uniwersytet Łódzki

Promotor pomocniczy:
dr. inż. Piotr Krzeczyński
Sieć Badawcza Łukasiewicz–Instytut
Chemii Przemysłowej imienia Profesora
Ignacego Mościckiego, Warszawa

Łódź, 2023

Podziękowania

Składam serdeczne podziękowania dla Pani prof. dr hab. Agnieszki Marczak,
za ,,otwarcie" mi ciekawej, pełnej wyzwań oraz poszerzającej horyzonty drogi zawodowej.
Dziękuję za nieocenioną pomoc, poświęcony czas oraz opiekę merytoryczną
podczas realizacji niniejszej pracy doktorskiej.

Dziękuję Panu dr inż. Piotrowi Krzeczyńskiemu,
za opiekę merytoryczną oraz pomoc i zaangażowanie w przygotowanie pracy doktorskiej.

Dziękuję Kolegom, Koleżankom oraz Pracownikom Katedry Biofizyki Medycznej,
szczególnie Pani dr hab. Anecie Rogalskiej, prof. UŁ oraz Panu dr Arkadiuszowi Gajkowi,
za stworzenie miłej i przyjaznej atmosfery, cenne rady oraz wsparcie.

Szczególne podziękowania kieruję w stronę moich Najbliższych — Macieja, Rodziców,
Dziadków, za nieustające wsparcie i wiarę w moje możliwości, motywację, cierpliwość,
za każde słowo otuchy w chwilach kryzysu oraz radość z moich sukcesów.
Dzięki Wam dziś jestem w tym miejscu.

Spis treści

1. Finansowanie

Niniejsza praca doktorska została wykonana w ramach projektu "InterDOC-STARt – Interdyscyplinarne Studia Doktoranckie" realizowanego na Wydziale Biologii i Ochrony Środowiska Uniwersytetu Łódzkiego – Program Operacyjny Wiedza Edukacja Rozwój 2014–2020, Oś priorytetowa III. Szkolnictwo wyższe dla gospodarki i rozwoju, Działanie 3.2 Studia doktoranckie. Nr projektu: POWR.03.02.00–IP.08–00–DOK/16. Realizowany w latach 2018–2023. Kierownik — prof. dr hab. Agnieszka Marczak.

2. Współpraca naukowa

Sieć Badawcza Łukasiewicz–Instytut Biotechnologii i Antybiotyków w Warszawie przy współudziale dr inż. Małgorzaty Łukawskiej.

Sieć Badawcza Łukasiewicz–Instytut Chemii Przemysłowej imienia Profesora Ignacego Mościckiego w Warszawie przy współudziale dr inż. Piotra Krzeczyńskiego, pełniącego rolę promotora pomocniczego.

Translational Radiobiology, Department of Radiation Oncology, University Hospital Erlangen, Friedrich – Alexander – Universität Erlangen – Nürnberg, Niemcy, przy współudziale dr hab. n. med. Doroty Lubgan oraz Prof. Dr. Udo S. Gaipl podczas stażu naukowego w terminie 01.03. – 31.05.2022.

3. Spis publikacji wchodzących w skład rozprawy doktorskiej

Praca przeglądowa

I **Poczta A.**, Rogalska A., Marczak A.; *Treatment of Multiple Myeloma and the Role of Melphalan in the Era of Modern Therapies–Current Research and Clinical Approaches;* J Clin Med; 2021; 10(9):1841. IF: 4.964; punkty MEiN: 140 pkt.

Prace doświadczalne

II Gajek A*****., **Poczta A.***, Łukawska M., Cecuda–Adamczewska V., Tobiasz J.; Marczak A.; *Chemical modification of melphalan as a key to improving treatment of haematological malignancies;* Sci Rep; 2020; 11;10(1):4479. IF: 4.379; punkty MEiN: 140 pkt.
*****równoważny wkład autorów

III **Poczta A.**, Krzeczyński P., Tobiasz J., Rogalska A., Gajek A., Marczak A.; *Synthesis and In Vitro Activity of Novel Melphalan Analogs in Hematological Malignancy Cells;* Int J Mol Sci. 2022; 23(3):1760. IF: 6.208; punkty MEiN: 140 pkt.

IV **Poczta A.**, Krzeczyński P., Ionov M., Rogalska A., Gaipl U.S., Marczak A. Lubgan D.; *Newly Synthesized Melphalan Analogs Induce DNA Damage and Mitotic Catastrophe in Hematological Malignant Cancer Cells;* Int J Mol Sci. 2022; 23(22): 14258. IF: 6.208; punkty MEiN: 140 pkt.

Sumaryczna wartość IF: 21.759; punkty MEiN: 560.

4. Wprowadzenie

4.1. Uzasadnienie podjętej tematyki badawczej

Nowotwory układu krwiotwórczego są niejednorodną grupą chorób o złożonej patogenezie, co stwarza poważne wyzwanie dla współczesnej medycyny. Szacuje się, że największy odsetek wśród białaczek u dorosłych stanowi ostra białaczka szpikowa[1]. Szpiczak mnogi z kolei jest drugim co do częstości występowania, po chłoniaku nieziarniczym, nowotworem układu krwiotwórczego[2–4]. Jest to choroba wywodząca się z limfoidalnych komórek B i charakteryzująca klonalną proliferacją komórek plazmatycznych. Na obraz morfologiczny oraz kliniczny w pełni rozwiniętej choroby składają się: naciek z komórek plazmatycznych w szpiku kostnym lub innych tkankach, występowanie białka monoklonalnego w surowicy lub moczu, hiperkalcemia, niewydolność nerek, niedokrwistość, zmiany kostne oraz inne zaburzenia, do których zaliczyć można: zespół nadlepkości, amyloidozę i nawracające zakażenia bakteryjne[5–7]. Chociaż częstość występowania szpiczaka mnogiego wzrasta z wiekiem i częściej występuje u pacjentów 60 – 70 letnich, to jednak diagnozowany jest również u osób młodszych [8].

W arsenale terapeutycznym chorych na szpiczaka mnogiego znajdują się leki o różnych mechanizmach działania. Wymienić tu należy: leki alkilujące (melfalan, bendamustyna), immunomodulujące (talidomid, lenalidomid, pomalidomid), inhibitory deacetylazy histonowej (vorinostat, panobinostat), inhibitory proteasomu (bortezomib, carfilzomib, iksazomib) oraz przeciwciała monoklonalne (daratumumab, izatuksymab). Strategie leczenia różnią się w zależności od wieku pacjenta, chorób współistniejących, stadium choroby, wyników badań cytogenetycznych oraz innych czynników.

Terapia dużymi dawkami melfalanu (MEL) wspomagana przeszczepem komórek macierzystych od lat uważana jest za standard leczenia pierwszego rzutu chorych na szpiczaka mnogiego, którzy kwalifikują się do przeszczepu[5,9]. Lek ten jest pochodną iperytu azotowego i wykazuje silne działanie alkilujące. Każda z dwóch grup 2-chloroetylowych melfalanu tworzy karboniowe związki pośrednie, które wiążą się kowalencyjnie z atomem azotu guaniny lub adeniny DNA. Prowadzi to do między lub wewnątrz strukturalnego sieciowania DNA, powstawania monoadduktów oraz kompleksów DNA – białko[10–12]. Mechanizm ten ostatecznie prowadzi do zakłócenia

replikacji i transkrypcji DNA oraz zahamowania cyklu komórkowego co skutkuje śmiercią komórki. Leki alkilujące, w tym melfalan, są szczególnie aktywne w komórkach szybko proliferujących, w tym komórkach białaczkowych[6].

Komórki białaczkowe, ze względu na szybkość proliferacji, wymagają dużych ilości składników odżywczych i aminokwasów. Melfalan jest transportowany do komórek głównie przez duży neutralny transporter aminokwasów 1 (ang. *large neutral amino acid transporter 1*, LAT1)[13], którego poziom ekspresji w tkankach nowotworowych, a szczególnie w szybko dzielących się komórkach białaczkowych, jest znacząco wyższy w porównaniu z poziomem obserwowanym w prawidłowych, aktywowanych limfocytach T[13,14].

Pomimo, iż terapia dużymi dawkami melfalanu, a następnie przeszczep komórek krwiotwórczych, pozostaje kluczowym elementem terapii pacjentów chorujących na szpiczaka mnogiego, to jej stosowanie ograniczone jest przez występowanie licznych działań niepożądanych, w tym: kardiotoksyczność, hepatotoksyczność, mielosupresję, niewydolność nerek a także zmiany w tkance płuc. Wysokie dawki leków przeciwnowotworowych osłabiają układ odpornościowy pacjentów wpływając na system obronny organizmu[15]. Konsekwencją tej terapii może być również występowanie wtórnych nowotworów, w tym ostrych białaczek[16]. Innym problemem jest pojawienie się oporności wielolekowej podczas stosowania chemioterapii. Wszystko to skłania naukowców na całym świecie do poszukiwania nowych metod terapeutycznych, charakteryzujących się wyższą skutecznością przeciwnowotworową oraz lepszym profilem bezpieczeństwa.

Jedną z metod poprawy skuteczności terapeutycznej leków jest regulacja ich aktywności farmakologicznej poprzez modyfikację struktury chemicznej. Wiadomym jest, że budowa chemiczna leku determinuje jego właściwości fizykochemiczne oraz wpływa na aktywność farmakologiczną[17]. Modyfikacja struktury leków przeciwnowotworowych oraz określenie zależności między ich budową chemiczną, a aktywnością biologiczną jest podstawą do opracowania związków o optymalnej strukturze i właściwościach. Celowane projektowanie leków przeciwnowotworowych, a następnie przeprowadzenie wysokoprzepustowych badań *in vitro* minimalizuje ryzyko stworzenia cząsteczek nieaktywnych oraz pozwala na wybranie nowej struktury do dalszych badań przedklinicznych i klinicznych.

W niniejszej rozprawie doktorskiej oceniono skuteczność modyfikacji dwóch grup funkcyjnych – karboksylowej oraz aminowej obecnych w cząsteczce melfalanu. W I etapie badań dokonano analizy zależności struktura chemiczna cząsteczki – jej aktywność biologiczna. W tym celu w cząsteczce melfalanu zmodyfikowano kolejno: grupę karboksylową, grupę aminową oraz obie te grupy funkcyjne. Etap II badań miał na celu syntezę kolejnych pochodnych, zaprojektowanych na podstawie wyników aktywności biologicznej uzyskanych w I etapie. Po każdym etapie przeprowadzono selekcję związków. W jej wyniku wybrano najefektywniejsze modyfikacje struktury melfalanu, aby w etapie III przeprowadzić badania ich wpływu na DNA i poznać szlaki śmierci komórek nowotworowych: szpiczaka mnogiego (RPMI8226) ostrej białaczki monocytowej (THP1) oraz ostrej białaczki promielocytowej (HL60). Wykonano również analizę cytotoksyczności względem komórek prawidłowych – jednojądrzastych komórek krwi obwodowej człowieka (PBMC). Badania te pozwoliły na poznanie cytotoksycznego i genotoksycznego profilu nowych, nieopisanych jeszcze w literaturze, pochodnych melfalanu, analizę ich ścieżek sygnałowych w komórce oraz wykazanie zależności pomiędzy ich strukturą chemiczną a aktywnością biologiczną. Wykonana praca oraz otrzymane wyniki stanowią istotny wkład w wiedzę o samym leku (melfalanie), jak również o jego nowych analogach.

4.2. Hipoteza badawcza

Zastosowane modyfikacje struktury cząsteczki melfalanu zwiększają aktywność przeciwnowotworową macierzystego związku w komórkach białaczkowych (THP1, HL60) oraz komórkach szpiczaka mnogiego (RPMI8226).

4.3. Cel główny pracy

Celem nadrzędnym niniejszej rozprawy doktorskiej była analiza właściwości biologicznych nowych, otrzymanych drogą syntezy chemicznej, pochodnych melfalanu oraz wytypowanie tej struktury, która wykazuje wyższą aktywność przeciwnowotworową niż związek macierzysty względem komórek szpiczaka mnogiego oraz komórek ostrej białaczki monocytowej i promielocytowej.

4.4. Cele szczegółowe pracy

a. Opracowanie warunków syntezy oraz otrzymanie nowych pochodnych.
b. Przeprowadzenie metodą *in silico* analizy ADMET (ang. *Absorption, Distribution, Metabolism, Excretion and Toxicity*) badanych pochodnych pozwalająca na określenie ich właściwości lekopodobnych (ang. *drug – like*).
c. Analiza właściwości cytotoksycznych otrzymanych analogów melfalanu wobec komórek nowotworowych oraz komórek prawidłowych.
d. Analiza właściwości genotoksycznych nowych związków wobec komórek nowotworowych.
e. Ocena zdolności badanych związków do indukowania programowanej śmierci komórki.
f. Określenie głównych szlaków molekularnych odpowiedzialnych za aktywność biologiczną pochodnych melfalanu.
g. Analiza wpływu badanych związków na strukturę DNA.

4.5. Materiały i metody badawcze

Nowotworowe linie komórkowe oraz komórki prawidłowe

Materiał badawczy wykorzystany w eksperymentach stanowiły trzy linie komórkowe:

- **RPMI8226** (komórki szpiczaka mnogiego, ang. *multiple myeloma cell line*, ATCC® CCL–155™),
- **HL60** (komórki ludzkiej ostrej białaczki promielocytowej, ang. *acute promyelocytic leukemia cell line*, ATCC® CCL–240™),
- **THP1** (komórki ludzkiej ostrej białaczki monocytowej, ang. *acute monocytic leukemia cell line*, ATCC® TIB–202™).

Analizę cytotoksyczności badanych związków wykonano także względem komórek prawidłowych – **PBMC** (jednojądrzaste komórki krwi obwodowej, ang. *peripheral blood mononuclear cells*).

Melfalan oraz badane pochodne

W ramach niniejszej pracy doktorskiej zsyntetyzowano oraz oceniono biologiczną aktywność następujących związków (Rysunek 1):

MEL:

kwas 2–amino–3–[4–[bis(2–chloroetylo)amino]fenylo]propanowy;

EE–MEL:

ester etylowy kwasu 2–amino–3–[4–[bis(2–chloroetylo)amino]fenylo]propanowego;

EM–MEL:

ester metylowy kwasu 2–amino–3–[4–[bis(2–chloroetylo)amino]fenylo]propanowego;

MOR–MEL:

kwas 2–(morfolinometylidenoamino)–3–[4–[bis(2–chloroetylo)amino]fenylo]propanowy;

DIPR–MEL:

kwas 2–(*N*,*N*–di–(*n*–propylo)amino–3–[4–[bis(2–chloroetylo)amino]fenylo]propanowy;

EE–MOR–MEL:

ester etylowy kwasu 2–(morfolinometylidenoamino)–3–[4–[bis(2–chloroetylo)amino] fenylo]propanowego;

EM–MOR–MEL:

ester metylowy kwasu 2–(morfolinometylidenoamino)–3–[4–[bis(2–chloroetylo)amino] fenylo]propanowego;

EE–DIPR–MEL:

ester etylowy kwasu 2–(*N*,*N*–di–(*n*–propylo)amino–3–[4–[bis(2–chloroetylo)amino] fenylo] propanowego;

EM–DIPR–MEL:

ester metylowy kwasu 2–(*N*,*N*–di–(*n*–propylo)amino–3–[4–[bis(2–chloroetylo)amino] fenylo] propanowego;

EM–I–MEL:

ester metylowy kwasu 2–(indolinometylidenoamino)–3–[4–[bis(2–chloroetylo)amino] fenylo]propanowego;

EM–T–MEL:

ester metylowy kwasu 2–(tiomorfolinometylidenoamino)–3–[4–[bis(2–chloroetylo)amino] fenylo]propanowego;

EM–MORPIP–MEL:

ester metylowy kwasu 2–[(4–(4–morfolino)piperydynometylidenoamino]–3–[4–[bis(2–chloroetylo)amino]fenylo]propanowego.

Szczegółowy opis syntezy pochodnych otrzymanych w I etapie badań zawarty został w patencie PL220880 B1, natomiast syntezę pochodnych uzyskanych w II etapie badań opisano szczegółowo w publikacji III.

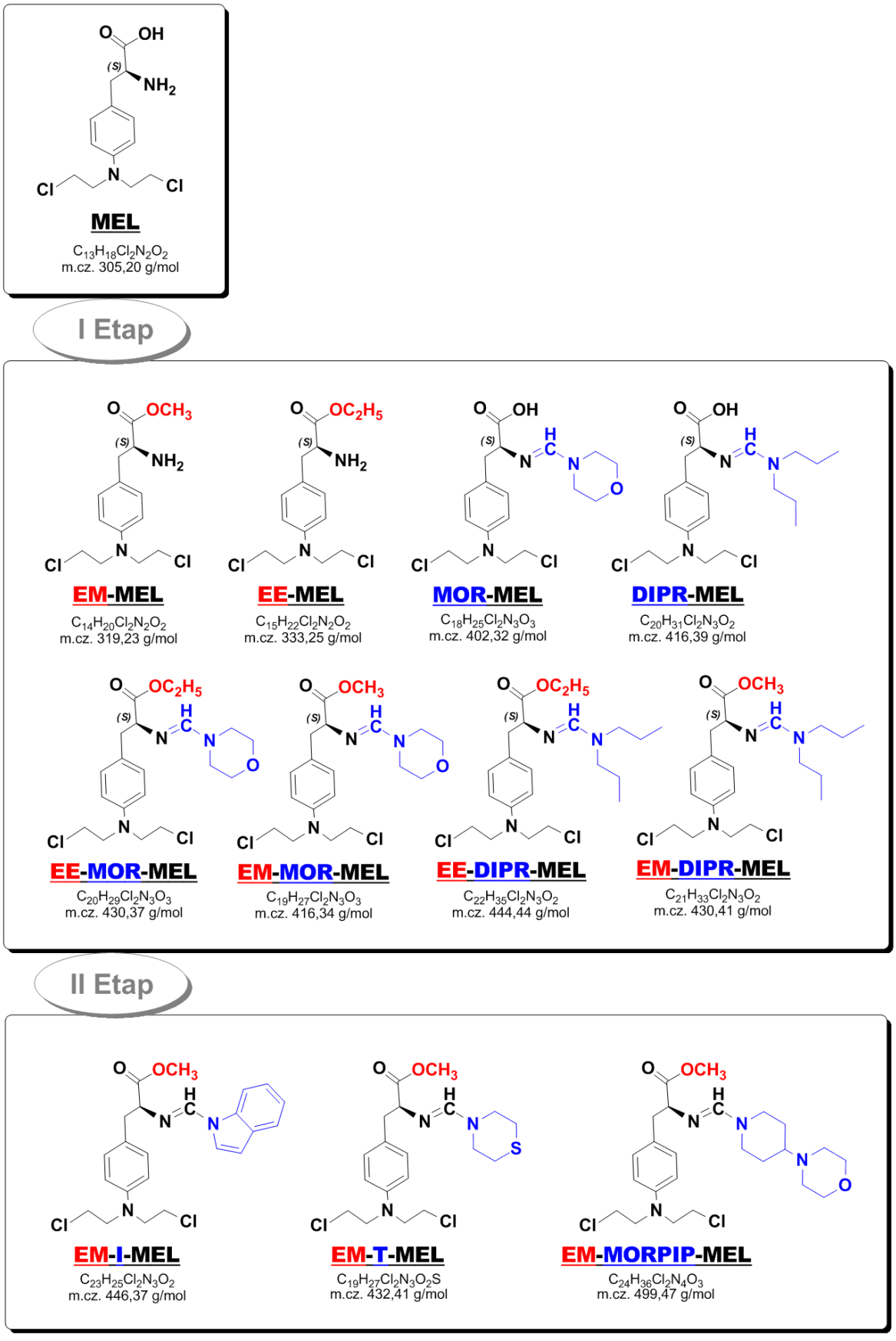

Rysunek 1. Struktura chemiczna badanych pochodnych melfalanu.

Metody badawcze

W celu realizacji badań wykorzystane zostały poniższe techniki badawcze:

1. Metody analityczne w syntezie chemicznej:
    - Chromatografia cienkowarstwowa,
    - Wysokosprawna chromatografia cieczowa.
2. Metody potwierdzające strukturę chemiczną związków:
    - Spektroskopia w podczerwieni,
    - Spektroskopia magnetycznego rezonansu jądrowego,
    - Spektroskopia masowa wysokiej rozdzielczości.

Ponadto, dla każdego z nowo otrzymanych związków zmierzono jego temperaturę topnienia oraz wyznaczono skręcalność właściwą.

3. Test cytotoksyczności z użyciem soli sodowej resazuryny.
4. Metody analizy fragmentacji DNA:
    - alkaliczna wersji testu kometowego,
    - test TUNEL (ang. *TdT – mediated dUTP Nick – End Labeling assay*).
5. Oznaczenie frakcji komórek apoptotycznych i nekrotycznych metodą podwójnego barwienia z wykorzystaniem mieszaniny fluorochromów: jodku propidyny oraz Hoechst 33342.
6. Zbadanie zaburzeń strukturalnych błony komórkowej metodą podwójnego barwienia z wykorzystaniem mieszaniny fluorochromów: jodku propidyny oraz aneksyny V sprzężonej z izotiocyjanianem fluoresceiny (FITC, ang. *fluorescein isothiocyanate*).
7. Analiza kondensacji chromatyny z wykorzystaniem mieszaniny fluorochromów: Vybrant® DyeCycle™ Violet oraz SYTOX® AADvanced™.
8. Badanie zmian potencjału błony mitochondrialnej za pomocą sondy fluorescencyjnej JC–1 (jodek 5,5’,6,6’–tetrachloro–1,1’,3,3’–tetraetylo-benzimidazolilokarbocyjaniny).
9. Badanie wewnątrzkomórkowego poziomu jonów wapnia za pomocą sondy fluorescencyjnej Fluo – 4NW.

10. Analiza aktywności kaspaz: 2, 3/7, 8, 9 metodą spektrofluorymetryczną z zastosowaniem sond fluorescencyjnych.
11. Badanie fosforylacji histonu H2AX poprzez barwienie immunofluorescencyjne.
12. Badanie struktury DNA metodą spektroskopii dichroizmu kołowego.
13. Pomiar potencjału zeta oraz dynamicznego rozpraszania światła.
14. Analiza rozkładu cyklu komórkowego metodą cytometrii przepływowej.
15. Analiza QSAR (ang. *Quantitative Structure Activity Relationship*) metodą *in silico.*
16. Analiza statystyczna otrzymanych danych eksperymentalnych.

5. Omówienie prac wchodzących w skład rozprawy doktorskiej

Istota problemu leczenia szpiczaka mnogiego oraz rola melfalanu zostały przeze mnie poruszone w pracy przeglądowej **[publikacja nr I]**. W publikacji tej opisana została zarówno farmakokinetyka oraz farmakodynamika melfalanu, skutki uboczne terapii, mechanizmy prowadzące do powstawania lekooporności, jak i kliniczne zastosowanie melfalanu w terapii skojarzonej z nowymi terapeutykami. Pochyliłam się nad analizą najnowszych badań klinicznych, aby odpowiedzieć na pytanie, czy terapia mieloablacyjna za pomocą wysokich dawek melfalanu połączona z autologicznym przeszczepem komórek macierzystych poprawia ogólną odpowiedź na leczenie oraz przeżycie wolne od progresji pomimo znacznej toksyczności ogólnoustrojowej. Badania wykazują, że nowe terapie stanowią kamień milowy w walce z nowotworami krwi i przyczyniają się do znacznego wzrostu przeżywalności pacjentów. Pomimo tego, terapia wysokimi dawkami melfalanu, a następnie przeszczep komórek macierzystych układu krwiotwórczego wciąż pozostają kluczowe w leczeniu chorych z nowo rozpoznanym szpiczakiem mnogim, którzy kwalifikują się do przeszczepu.

Ważną część tego artykułu stanowi przegląd prac naukowych, których celem było opracowanie związków na bazie melfalanu przezwyciężających problem wysokiej toksyczności ogólnoustrojowej, lekooporności oraz poprawiających aktywność przeciwnowotworową tego leku. Tworzenie koniugatów, proleku melfalanu, jak również celowana modyfikacja struktury jego cząsteczki są obiecującym kierunkiem w celu opracowania nowego leku o lepszych właściwościach terapeutycznych.

Cząsteczka melfalanu zawiera w swojej strukturze dwie grupy funkcyjne — grupę karboksylową oraz grupę aminową. Podstawą dla zaprojektowania nowych analogów melfalanu badanych przeze mnie w I etapie badań **[publikacja nr II]** były wnioski z wcześniejszych badań przeprowadzonych w zespole Pani Profesor Agnieszki Marczak, dotyczące oceny modyfikacji cząsteczek innych leków, takich jak doksorubicyna[18–20] czy kladrybina[21]. Ponadto, badania innych naukowców wykazały, że amidynowe analogi melfalanu w zastosowanym modelu *in vitro* zmniejszają liczbę komórek raka sutka[22,23]. Konkluzją wynikającą z tych badań jest to, że zamiana grupy di–*N*–propyloaminowej na amidynową stanowi skuteczny rodzaj modyfikacji struktury cząsteczki melfalanu

skutkujący wzrostem aktywności przeciwnowotworowej nowego związku w porównaniu do wyjściowego leku. Dlatego też jednym z celów modyfikacji chemicznej melfalanu przeprowadzonej w I etapie prac było zastąpienie grupy di–*N*–propyloaminowej resztą amidynową podstawioną pierścieniem morfolinowym lub dwoma łańcuchami *n*–propylowymi. Morfolina jest heterocyklicznym związkiem chemicznym zawierającym w swojej strukturze dwa heteroatomy – tlenu i azotu. Atom tlenu w tym pierścieniu zwiększa powinowactwo wiązania, uczestnicząc w interakcjach typu donor – akceptor. Ponadto, atom tlenu, poprzez swoją elektroujemność, zmniejsza zasadowość atomu azotu pierścienia morfolinowego[24,25]. Dwa heteroatomy w grupie amidynowej w pozycji 1,4 zapewniają elastyczną konformację pierścienia. Dzięki takiej konstrukcji grupa ta może uczestniczyć w interakcjach lipofilowo – hydrofilowych. Morfolina moduluje właściwości całej struktury, ponieważ obecność słabo zasadowego azotu w pozycji 4 w stosunku do atomu tlenu zwiększa rozpuszczalność takiego związku[26,27].

Dane literaturowe dostarczają natomiast dowodów na to, że dodanie estrowej grupy funkcyjnej zwiększa lipofilowość związku[28,29] oraz jego biodostępność[30–33]. Dlatego kolejnym celem modyfikacji chemicznej melfalanu była estryfikacja grupy karboksylowej. W rezultacie, w I etapie badań otrzymano osiem pochodnych melfalanu:

- zmodyfikowanych wyłącznie w grupie aminowej poprzez zastąpienie grupy di–*N*–propyloaminowej grupą amidynową zawierającą pierścień morfolinowy (MOR–MEL) lub dwa łańcuchy *n*–propylowe (DIPR–MEL),
- zmodyfikowanych wyłącznie w grupie karboksylowej poprzez otrzymanie estru metylowego (EM–MEL) oraz etylowego (EE–MEL) melfalanu,
- z modyfikacją w obu grupach funkcyjnych. W ten sposób uzyskano ester metylowy oraz etylowy melfalanu zawierający pierścień morfolinowy (EM–MOR–MEL, EE–MOR–MEL) oraz ester metylowy i etylowy zawierający dwa łańcuchy *n*–propylowe (EM–DIPR–MEL, EE–DIPR–MEL).

Według wytycznych National Cancer Institute (NCI) nowe związki chemiczne o potencjale przeciwnowotworowym powinny, w pierwszym etapie, zostać szczegółowo scharakteryzowane pod kątem ich aktywności cytotoksycznej w badaniach *in vitro*. Analizy nowo otrzymanych analogów melfalanu rozpoczęto więc od oceny ich właściwości cytotoksycznych oraz wyznaczenia stężeń do kolejnych badań. Cytotoksyczne działanie MEL

i jego pochodnych było zależne od dawki. Określono parametr IC_{50} (ang. *inhibitory concentration*), czyli stężenie niezbędne do zahamowania proliferacji o 50% w stosunku do komórek stanowiących grupę kontrolną. Wszystkie badane związki oprócz pochodnych, które uległy modyfikacji tylko w grupie aminowej (MOR–MEL i DIPR–MEL) wykazały wyższą cytotoksyczność względem komórek szpiczaka mnogiego oraz komórek białaczkowych niż związek macierzysty **[publikacja nr II, Figure 1]**. W przypadku komórek RPMI8226 najwyższą cytotoksyczność zaobserwowano po inkubacji z estrami melfalanu (EE–MEL oraz EM–MEL) natomiast komórki linii THP1 oraz HL60 były najbardziej wrażliwe na działanie cytotoksyczne po inkubacji z estrami melfalanu dodatkowo modyfikowanymi pierścieniem morfolinowym (EE–MOR–MEL oraz EM–MOR–MEL). Jednocześnie zaobserwowano słabsze działanie cytotoksyczne analogów EE–MEL, EM–MEL oraz EM–MOR–MEL względem jednojądrzastych komórek krwi obwodowej. Szczególnie pochodna EM–MOR–MEL charakteryzowała się niską cytotoksycznością względem komórek prawidłowych przy jednocześnie wysokim potencjale cytotoksycznym wobec komórek nowotworowych. Pochodne, które nie wykazywały wyższej cytotoksyczności niż lek macierzysty, czyli MOR–MEL oraz DIPR–MEL zostały wyeliminowane z dalszych badań. Do określenia kolejnych parametrów wybrano, na podstawie krzywych przeżywalności, po jednym stężeniu na linie komórkową: RPMI8226: 3 µM, HL60: 0,7 µM, THP1: 0,3 µM. Poszczególne stężenia stanowiły wartość średnią pomiędzy najsilniej, a najsłabiej działającą pochodną. Wybór jednego stężenia dla danej linii komórkowej miał na celu umożliwienie porównania działania związków na różnych etapach badań.

Kolejną częścią badań była analiza mechanizmów wewnątrzkomórkowych związanych z cytotoksycznym działaniem badanych związków. Ponieważ głównym mechanizmem działania melfalanu jest alkilowanie, oceniono wpływ nowych związków na strukturę DNA wykonując alkaliczną wersję testu kometowego oraz test TUNEL. Komórki wszystkich badanych linii wykazały zwiększony poziom uszkodzeń DNA po inkubacji z badanymi związkami **[publikacja nr II, Figure 4]**. Komórki szpiczaka mnogiego były szczególne podatne na indukcję uszkodzeń. Test kometowy jednoznacznie wykazał, że wszystkie badane pochodne, w szczególności po 24 i 48 godzinach inkubacji, wywołują uszkodzenia DNA, a zmiany te są istotne statystycznie w porównaniu nie tylko wobec kontroli ale zwłaszcza w stosunku do macierzystego leku.

Zdolność leków do indukcji apoptozy uznawana jest za ważne kryterium oceny ich skuteczności terapeutycznej. Dlatego kolejnym etapem badań była ocena właściwości proapoptotycznych pochodnych EE–MEL, EM–MEL, EE–MOR–MEL, EM–MOR–MEL, EE–DIPR–MEL oraz EM–DIPR–MEL. Wykonano szereg badań w celu oceny występowania zmian morfologicznych i biochemicznych, które sygnalizowałyby programowaną śmierć komórki. Podczas analizy kondensacji chromatyny oraz eksternalizacji fosfatydyloseryny zaobserwowano zmiany w komórkach charakterystyczne dla procesu apoptozy. Najwyższe zmiany zaobserwowano po 24 i 48 godzinach inkubacji, głównie z estrami melfalanu oraz estrami melfalanu zawierającymi resztę morfoliny, co korelowało z wynikami otrzymanymi w badaniach cytotoksyczności **[publikacja nr II, Figure 2, Figure 3]**.

Apoptoza jest złożonym molekularnie procesem śmierci komórki, w inicjację którego zaangażowanych jest wiele białek. Wyróżnić można kilka szlaków aktywacji apoptozy, w tym wewnątrzpochodny i zewnątrzpochodny. W ich przebiegu biorą udział enzymy z rodziny endopeptydaz zwane kaspazami, które można podzielić na inicjatorowe (kaspaza 2, 8, 9, 10 oraz 12) oraz efektorowe (kaspaza 3, 6 oraz 7). Opierając się na tej wiedzy, określono szczegółowy proces aktywowania apoptozy w komórkach nowotworowych po inkubacji z badanymi analogami. Zbadano aktywność: kaspazy 8 zaangażowanej głównie w zewnętrzny szlak apoptozy, 9 biorącej udział w wewnętrznym szlaku oraz kaspaz 3/7 zaangażowanych w oba te szlaki. W przypadku komórek linii HL60 oraz THP1 najwyższy wzrost aktywacji egzekutorowej kaspazy 3 zaobserwowano po 24–godzinnej inkubacji z pochodnymi EE–MEL, EM–MEL, EE–MOR–MEL, EM–MOR–MEL **[publikacja nr II, Figure 5]**. Zmiany w aktywności tej proteazy cysteinowej były od 1,5 do 2–krotnie wyższe względem macierzystego leku. W komórkach szpiczaka mnogiego obserwowano najniższy poziom aktywacji kaspazy 3. Aby ocenić mechanizmy molekularne leżące u podstaw aktywacji kaspazy 3 zbadano aktywność kaspazy 8 oraz kaspazy 9. Znaczące zmiany w aktywności tych enzymów zaobserwowano tylko w komórkach ostrej białaczki promielocytowej i monocytowej. Po 24–godzinnej inkubacji z badanymi analogami MEL, w komórkach białaczkowych zaobserwowano wzrost aktywności kaspazy 9, co świadczyć może o aktywacji wewnątrzpochodnej drogi apoptozy. Zaobserwowano również wzrost aktywności kaspazy 8. Poziom tej proteazy cysteinowej był niższy niż dla kaspazy 9. Sugeruje to dominację wewnętrznego szlaku apoptozy.

Innym ważnym markerem procesu apoptozy jest zmiana homeostazy wapnia. W komórkach, które uległy apoptozie obserwowane jest uwolnienie jonów wapnia z retikulum endoplazmatycznego oraz wzrost ich zawartości w cytozolu oraz mitochondriach. Najwyższy wzrost wewnątrzkomórkowego poziomu jonów wapnia zaobserwowano w komórkach linii THP1, a zmiany widoczne były już po 4 godzinach inkubacji z badanymi pochodnymi **[publikacja nr II, Figure 6]**. W przypadku komórek linii RPMI8226 zmiany homeostazy wapnia były nieznaczne. Dane te korelowały z wcześniejszymi wynikami oznaczania aktywności kaspaz egzekutorowych oraz inicjatorowych.

Podsumowując I etap badań można stwierdzić, że **kluczem dla zwiększenia cytotoksycznych, genotoksycznych oraz proapoptotycznych właściwości melfalanu jest modyfikacja grupy karboksylowej poprzez jej estryfikację oraz zamiana grupy di–*N*–propyloaminowej na amidynową zawierającą pierścień morfolinowy, który w swojej strukturze zawiera dwa heteroatomy.** Taka zmiana struktury melfalanu powoduje wzrost fragmentacji DNA co koreluje ze wzmocnieniem efektu cytotoksycznego. Właściwości proapoptotyczne badanych analogów również są istotnie wyższe w porównaniu do melfalanu. Natomiast ich mechanizm działania jest różny w zależności od rodzaju komórek nowotworowych. W przypadku komórek białaczkowych aktywacji ulega głównie mitochondrialny szlak apoptozy. W przypadku komórek szpiczaka mnogiego możliwa jest aktywacja innych proteaz zaangażowanych w fazę inicjatorową programowanej śmierci komórki lub inicjacja innego niż apoptoza mechanizmu śmierci komórki.

Etap II badań miał na celu potwierdzenie przyjętej strategii modyfikacji struktury melfalanu **[publikacja nr III]**. W związku z tym, w Sieci Badawczej Łukasiewicz–Instytucie Chemii Przemysłowej w Warszawie pod kierownictwem pana dr inż. Piotra Krzeczyńskiego zaprojektowano oraz zsyntetyzowano kolejne pochodne wykorzystując wiedzę zdobytą w I etapie badań. Otrzymano analogi estrów metylowych melfalanu podstawione w grupie amidynowej tiomorfoliną (EM–T–MEL), indoliną (EM–I–MEL) oraz 4–(4–morfolinylo)piperydyną (EM–MORPIP–MEL). Planowano otrzymać również pochodną podstawioną tiazoliną, jednakże próby jej syntezy nie powiodły się. Zsyntetyzowana w II etapie pochodna tiomorfolinowa wpisuje się w przyjętą wcześniej strategię, ponieważ posiada w swojej strukturze dwa heteroatomy — atom azotu w pozycji 1 oraz atom siarki

w pozycji 4. Ciekawym wydała się też próba syntezy i badań nad układem dotychczas nie testowanym, czyli zastosowaniem w grupie amidynowej struktury bicyklicznej składającej się z dwóch pierścieni (analog z resztą indoliny) oraz struktury bicyklicznej zawierającej dodatkowo dwa atomy azotu i atom tlenu (analog z resztą 4–(4–morfolinylo)piperydyny). Oprócz opisanych modyfikacji otrzymane pochodne przekształcono w estry metylowe zgodnie z wcześniejszymi wnioskami, że analogi z grupą estrową wykazują wyższą cytotoksyczność niż analogi zawierające wolną grupę karboksylową **[publikacja nr III, Figure 1]**.

Nowoczesne podejście do procesu opracowywania nowych leków wymaga zdefiniowania tzw. właściwości lekopodobnych cząsteczki o potencjale leczniczym, czyli ocenienia jej właściwości fizykochemicznych (rozpuszczalność, stabilność itp), jak również określenia, czy cząsteczka ta posiada na tyle zadowalające parametry absorbcji, dystrybucji, metabolizmu, wydalania oraz toksyczności (ang. *Absorption, Distribution, Metabolism, Excretion and Toxicity*; ADMET), że z dużym prawdopodobieństwem przejdzie pomyślnie pierwszy etap badań klinicznych[17]. Aby określić, czy zsyntetyzowane pochodne posiadają

właściwości lekopodobne, wykonano obliczenia *in silico* kilku parametrów dla badanych związków, a następnie sprawdzono czy spełniają one założenia reguły Piątek Lipińskiego i definicji Vebera. Zgodnie z regułami Lipińskiego kandydat na lek powinien spełniać następujące kryteria: masa cząsteczkowa (MW) ≤ 500 Da; lipofilowość opisana jako logP ≤ 5; liczba akceptorów wiązań wodorowych (HBA) ≤ 10; oraz liczba donorów wiązań wodorowych (HBD) ≤ 5[34]. Wszystkie badane związki wykazały zgodność z zasadami Lipińskiego oraz tylko jedno naruszenie zasad Vebera **[publikacja nr III, Table 1]**. Liczba wiązań rotacyjnych była nieco większa niż liczba określona w regule Vebera. Żaden z nowo zsyntetyzowanych związków nie był substratem dla glikoproteiny P — błonowego transportera, zdolnego do usuwania cząsteczek leku z komórki nowotworowej[35]. Wykonano również wykresy RADAR, które uwzględniają istotne właściwości fizykochemiczne cząsteczki, takie jak: lipofilowość, wielkość, polarność, rozpuszczalność, nasycenie oraz elastyczność. Dla wszystkich badanych związków pięć z sześciu analizowanych właściwości było zgodnych z właściwościami typowymi dla związków należących do grupy związków lekopodobnych **[publikacja nr III, Figure 2]**.

Można przewidywać, iż badane związki nie będą biodostępne w zadawalającym stopniu po podaniu doustnym. Zaleca się podanie dożylne.

Analogicznie jak w etapie I, kolejnym celem badań była analiza właściwości cytotoksycznych, genotoksycznych oraz proapoptotycznych pochodnych EM–I–MEL, EM–T–MEL oraz EM–MORPIP–MEL. Oceniono aktywność cytotoksyczną związków wobec komórek nowotworowych i prawidłowych oraz określono wartości IC_{50}. Pochodna EM–T–MEL wykazała najwyższą cytotoksyczność wobec komórek nowotworowych, a jej wartości IC_{50} były około 10–krotnie (THP1), 5–krotnie (HL60) i 2–krotnie (RPMI8226) niższe niż dla niezmodyfikowanego melfalanu. Jednocześnie EM–T–MEL okazał się znacznie mniej (2,5–krotnie) cytotoksyczny dla jednojądrzastych komórek krwi obwodowej niż melfalan. Analog EM–I–MEL również był bardziej cytotoksyczny niż MEL, wykazując znacząco niższe wartości IC_{50} głównie w linii komórkowej THP1 **[publikacja nr III, Figure 3]**. Zarówno w I jak i II etapie badań zaobserwowano znaczące różnice we wrażliwości komórek prawidłowych oraz białaczkowych na badane związki. Nowe pochodne, ze względu na mniejszą polarność cząsteczki w porównaniu z melfalanem, prawdopodobnie mogą być transportowane do komórek nowotworowych przez inne receptory błonowe, które ulegają nadekspresji w komórkach białaczkowych: MCT–1, –2, –4; OAT–1; OCTN–1; FLIPT–1 oraz OCT–6[36].

Aktywność cytotoksyczna pochodnej EM–MORPIP–MEL była porównywalna (THP1) lub mniejsza (HL60, PRMP8226) niż leku macierzystego, dlatego została ona wyeliminowana z dalszych analiz.

Z cytotoksycznością pochodnej EM–T–MEL względem komórek nowotworowych skorelowane były również jej właściwości genotoksyczne oraz proapoptotyczne. Tak zmodyfikowana cząsteczka MEL wywołała wysoki poziom uszkodzeń DNA we wszystkich badanych liniach komórkowych **[publikacja nr III, Figure 4]**. Badanie zmian morfologicznych po barwieniu mieszaniną fluorochromów: Hoechst 33342/ jodek propidyny oraz aneksyna V–FITC/ jodek propidyny wykazało, że pochodna EM–T–MEL aktywowała markery specyficzne dla apoptozy wyraźniej niż niezmodyfikowana cząsteczka MEL we wszystkich badanych liniach komórkowych. Analog EM–T–MEL spowodował znaczące zmiany w morfologii pojedynczych komórek, takie jak kurczenie się i fragmentacja czy tworzenie ciałek apoptotycznych. Komórki

po inkubacji z badanymi związkami, głównie EM–T–MEL, wykazywały wysoki poziom zielonej fluorescencji pochodzącej od aneksyny V–FITC i czerwonej fluorescencji pochodzącej z jodku propidyny, co wskazuje na translokację fosfatydyloseryny i uszkodzenie integralności błony komórkowej **[publikacja nr III, Figure 5, Figure 6]**.

Inny aspekt tych badań skupiał się na zmianach biochemicznych zachodzących podczas apoptozy indukowanej przez badane analogi melfalanu. Zakłócenie integralności mitochondriów jest kluczowym elementem programowanej śmierci komórki. Inkubacja komórek z pochodną EM–I–MEL, a zwłaszcza EM–T–MEL wiązała się ze spadkiem potencjału błony mitochondrialnej **[publikacja nr III, Figure 8]**. Pochodna EM–T–MEL najsilniej indukowała również aktywację kaspazy 3/7 we wszystkich testowanych liniach komórkowych. Wyniki oceny aktywności tej kaspazy były spójne z wynikami uzyskanymi w I etapie. Aktywacja tej egzekutorowej proteazy cysteinowej była poprzedzona inicjacją kaspazy 9 (głównie w linii komórkowej THP1) lub kaspazy 8 (głównie w linii komórkowej HL60), natomiast w komórkach linii RPMI8226 nie zaobserowano wzrostu aktywności żadnej z tych inicjatorowych kaspaz **[publikacja nr III, Figure 7]**.

Wyniki II etapu badań potwierdziły zależności obserwowane w I etapie. **Modyfikacja chemiczna melfalanu obejmująca estryfikację oraz zamianę grupy di–*N*–propyloaminowej na grupę amidynową zawierającą resztę tiomorfolinową, która w pozycji 1 posiada atom azotu a w pozycji 4 atom siarki, powoduje wzrost aktywności cytotoksycznej, genotoksycznej oraz proapototycznej melfalanu wobec komórek nowotworowych oraz obniżony efekt cytotoksyczny względem jednojądrzastych komórek krwi obwodowej.**

Wnioski otrzymane w I oraz II etapie badań pozwoliły mi na wybór pięciu analogów, których aktywność biologiczna była znacząco wyższa niż niemodyfikowanego leku. Wśród wyselekcjonowanych pochodnych znalazły się: ester etylowy melfalanu (EE–MEL), ester metylowy melfalanu (EM–MEL) oraz estry metylowe melfalanu zawierające pierścień morfolinowy (EM–MOR–MEL), tiomorfolinowy (EM–T–MEL) lub indolinowy (EM–I–MEL).

Wyjaśnienie mechanizmów, za pomocą których leki cytotoksyczne hamują proliferację komórek nowotworowych i indukują śmierć komórek jest kluczowe do oceny ich aktywności terapeutycznej oraz stanowi bazę do racjonalnego projektowania nowych

leków. Celem III-go etapu badań było poszerzenie wiedzy na temat wpływu wybranych analogów na DNA oraz poznanie szlaków śmierci komórek nowotworowych **[publikacja nr IV].**

Analiza rodzaju interakcji pomiędzy związkami terapeutycznymi, a makromolekułami takimi jak DNA i białka, pozwala na głębsze poznanie mechanizmów działania badanych leków[37]. Spektroskopia dichroizmu kołowego (ang. *circular dichroism*, CD) jest jedną z najczęściej stosowanych technik w badaniu struktur DNA. Aby przeanalizować mechanizm interakcji DNA z melfalanem i jego pochodnymi, przeprowadzono eksperymenty z wykorzystaniem techniki dichroizmu kołowego **[publikacja nr IV, Figure 1 A, B]**. Cząsteczki liganda mogą oddziaływać z DNA na kilka sposobów: interkalacja, wiązanie w małym lub dużym rowku, niespecyficzne wiązanie na zewnątrz nici DNA, wiązanie kowalencyjne czy mieszany sposób wiązania[38]. Klasyczny interkalator ustawia się sztywno w orientacji prostopadłej do osi heliksu, co prowadzi do zwiększenia długości nici DNA, gdyż odległości pomiędzy dwiema sąsiadującymi parami zasad kompleksu interkalacyjnego ulegają zwiększeniu. Taki mechanizm działania powoduje zmianę eliptyczności molowej i zwiększenie intensywności dodatnich i ujemnych pików DNA z jednoczesnym przesunięciem ich w stronę wyższych długości fal[38–41]. Analogi EM–MOR–MEL oraz EM–T–MEL spowodowały duże zmiany w intensywności i położeniu pików DNA. Analiza widm CD dla DNA inkubowanego z badanymi analogami sugeruje, że nastąpiła częściowa interkalacja. Dodatkowo, przesunięcie pików w stronę wyższych długości fal związane jest ze zmianą konformacji DNA z formy B do formy A[42]. Wykonano przykładową wizualizację pokazującą miejsce wiązania melfalanu i EM–T–MEL z DNA **[publikacja nr IV, Figure 1 C]**. Analizę badanych analogów rozszerzono następnie o pomiar potencjału zeta i średnicy hydrodynamicznej. Pomiar potencjału zeta badanej cząsteczki lub jej kompleksu z DNA dostarcza informacji o ładunku powierzchniowym. Wykazano, że zarówno melfalan jak i badane analogi są naładowane ujemnie i nie powodują wzrostu średnicy hydrodynamicznej DNA **[publikacja nr IV, Figure 2]**.

Kolejnym celem tego etapu badań była analiza mechanizmów wewnątrzkomórkowych związanych z działaniem badanych pochodnych na DNA. Odpowiedź komórkowa na uszkodzenie DNA obejmuje złożoną sieć szlaków sygnałowych, które ostatecznie prowadzą do zatrzymania cyklu komórkowego lub śmierci komórki.

Jednym z kluczowych zdarzeń molekularnych w komórce, w związku z powstaniem dwuniciowych pęknięć DNA, jest fosforylacja histonu H2AX w pozycji seryny 139[43]. Efektem tego jest tworzenie się w jądrze ognisk histonu γH2AX, które są widoczne pod mikroskopem dzięki specyficznemu barwieniu immunofluorescencyjnemu. Test ten jest skutecznym farmakodynamicznym markerem tworzenia międzysieciowych wiązań poprzecznych DNA zarówno dla leków na bazie iperytu azotowego, jak i platyny[44,45]. Przeprowadzone badania *in vitro* wykazały, że odpowiedź na uszkodzenie DNA w postaci powstania ognisk γH2AX po inkubacji z badanymi związkami była zależna od czasu dla wszystkich trzech badanych linii komórkowych (RPMI8226, HL60 i THP1) **[publikacja nr IV, Figure 3, Table 1]**. Najwyższą zdolność do fosforylacji histonu H2AX wykazała pochodna EM–T–MEL. Zmiany obserwowane po inkubacji z tym analogiem były kilkukrotnie wyższe niż w przypadku melfalanu. Istotne zmiany dla tego molekularnego markera są spójne z wcześniejszymi badaniami właściwości genotoksycznych dla tej pochodnej.

Następstwem stresu genotoksycznego jest aktywacja kaskady zjawisk molekularnych zakończona zahamowaniem podziałów komórkowych. Jednym z pożądanych i często występujących efektów działania leków cytostatycznych jest blokowanie cyklu komórkowego na drodze różnych procesów farmakodynamicznych. Potencjał danej substancji aktywnej do hamowania podziałów komórkowych można analizować za pomocą techniki cytometrii przepływowej, gdyż w metodzie tej wykorzystuje się zjawisko zmiany poziomu ilości DNA w komórce w trakcie cyklu. Kolejny etap badań miał na celu ocenę zdolności melfalanu oraz badanych analogów do hamowania cyklu podziałowego komórek nowotworowych w wyniku ich genotoksycznego działania **[publikacja nr IV, Figure 4]**. Wszystkie badane związki powodowały akumulację komórek w fazach S i G2/M cyklu komórkowego kosztem fazy G1. Jednakże analog zawierający resztę tiomorfoliny najsilniej wpływał na rozkład faz cyklu komórkowego prowadząc do zatrzymania cyklu komórek linii RPMI8226 i HL60 w fazie G2/M natomiast komórki linii THP1 były dodatkowo blokowane w fazie S. Procent komórek zatrzymanych w fazie G2/M po 24 i 48 godzinach inkubacji z tą pochodną wzrósł około 2–krotnie w porównaniu z próbą kontrolną. Jednocześnie zmniejszyła się populacja komórek w fazie G1 powodując w ten sposób odwrócenie profilu cyklu komórkowego. Mniejsze, ale istotne zmiany w rozkładzie cyklu komórkowego zaobserwowano również po inkubacji

komórek z pochodnymi EE–MEL, EM–MEL, MOR–MEL (24 h, 48 h) oraz EM–I–MEL (po 48 godz.). Melfalan również indukował zatrzymanie cyklu komórkowego, głównie w fazie G2/M, jednakże zmiany te były istotnie mniejsze w porównaniu z EM–T–MEL.

Kolejny etap badań miał na celu określenie szlaków śmierci badanych komórek nowotworowych po inkubacji z melfalanem oraz analizowanymi pochodnymi. W etapie I oraz II ocenie poddano analizę właściwości proapoptotycznych nowych pochodnych melfalanu, która opierała się na licznych zmianach morfologicznych i biochemicznych w komórkach. Wykazano, że mechanizm działania melfalanu oraz jego pochodnych jest różny w zależności od rodzaju komórek nowotworowych. W przypadku komórek białaczkowych (THP1 oraz HL60) badane parametry oceny właściwości proapoptotycznych jednoznacznie wskazywały na aktywację tego typu śmierci po inkubacji z badanymi związkami. W przypadku komórek szpiczaka mnogiego molekularny szlak prowadzący do śmierci pozostawał niejasny. W komórkach tych, w odpowiedzi na badane związki, dochodziło do zmian morfologicznych charakterystycznych dla późnych etapów apoptozy. Nieznacznej aktywacji ulegała kaspaza 3/7, a inicjacja tej proteazy egzekutorowej nie była poprzedzona wzrostem aktywności kaspazy 8 czy 9. To skłoniło mnie do oceny aktywności kaspazy 2, która, jako jeden z najważniejszych regulatorów katastrofy mitotycznej, jest zaangażowana w utrzymanie stabilności genomu. Jako część kompleksu PIDDosome (ang. *p53–induced death domain protein*), kaspaza 2 uczestniczy w eliminacji dodatkowych centrosomów oraz reguluje ploidalność i proliferację komórek[46,47]. Z drugiej strony, proteaza ta uczestniczy w regulacji cyklu komórkowego poprzez stabilizację p53 i rozszczepianie jego inhibitora Mdm2 (ang. *Mouse double minute 2 homolog*), które są niezbędne dla odpowiedzi komórkowej podczas nieprawidłowej segregacji chromosomów i rozwoju katastrofy mitotycznej[46].

Analiza aktywności kaspazy 2 w komórkach szpiczaka mnogiego i komórkach białaczkowych po inkubacji z melfalanem oraz badanymi pochodnymi wykazała znaczny wzrost aktywności tej proteazy cysteinowej, głównie po 24 godzinach inkubacji **[publikacja nr IV, Figure 5]**. Najwyższe zmiany po inkubacji z badanymi związkami zaobserwowano w komórkach szpiczaka mnogiego, co wskazywać może na wysoką niestabilność genomową. Pochodna EM–T–MEL najsilniej indukowała aktywację tej kaspazy a istotnie statystycznie zmiany względem niemodyfikowanego melfalanu zaobserwowano już

po 4 godzinach inkubacji z tym związkiem. Wynik ten okazał się spójny z badaniami innej grupy badawczej[48], które również wykazały, że melfalan aktywuje kaspazę 2 w komórkach szpiczaka mnogiego i prowadzi do aktywacji katastrofy mitotycznej w tych komórkach.

Warto podkreślić, że katastrofa mitotyczna prowadzi do licznych zmian morfologicznych i biochemicznych w komórkach[49]. Komórki niezdolne do zakończenia procesu mitozy charakteryzują się nieprawidłowym wzrostem poziomu cykliny B1 i blokadą cyklu w fazie G2/M co prowadzi do zmian w jądrze komórkowym[50,51]. Po inkubacji komórek szpiczaka mnogiego z badanymi związkami następowało zatrzymanie cyklu komórkowego głównie w fazie G2/M. Ponadto, wiadomym jest, że komórki ulegające katastrofie mitotycznej nie wykazują fragmentacji DNA typowej dla apoptozy, czy pęknięć DNA wykrywanych metodą TUNEL[52]. W I etapie badań analiza procesu apoptozy z wykorzystaniem tej metody wykazała słaby sygnał fragmentacji DNA na odcinki równe wielokrotności długości nukleosomów, co jest szczególną cechą komórek apoptotycznych. Co ważne, rekonfiguracja sieci mitochondrialnej również uważana jest za morfologiczną cechę katastrofy mitotycznej[46]. W II etapie badań wykazano, że inkubacja komórek z badanymi związkami powoduje spadek potencjału błony mitochondrialnej. Oprócz zmian morfologicznych w jądrze komórkowym i mitochondriach, proces katastrofy mitotycznej charakteryzuje się również wzrostem poziomu ufosforylowanego histonu H2AX[46,53]. Na podstawie wniosków z przeprowadzonych badań można zatem sądzić, że jednym ze szlaków śmierci komórek szpiczaka mnogiego jest katastrofa mitotyczna.

Podsumowując ten etap badań, można stwierdzić, że **głównym celem molekularnym dla melfalanu oraz badanych analogów jest DNA. Pochodne EM–MOR–MEL oraz EM–T–MEL, wpływają na konformację struktury B–DNA, poprzez częściową interkalację, co skutkuje wzrostem poziomu ufosforylowanego histonu H2AX. W wyniku genotoksycznego działania badanych analogów cykl komórkowy zostaje zatrzymany w fazach S i G2/M. Wykazano również, że śmierć komórek szpiczaka mnogiego następuje poprzez aktywację katastrofy mitotycznej.** Nie zaobserwowano różnic w skuteczności działania estru metylowego i etylowego melfalanu. Obydwie modyfikacje skutkowały wzrostem aktywności macierzystego leku. Analogi EM–MOR–MEL i EM–T–MEL, w warunkach badań *in vitro*, charakteryzują się najlepszą aktywnością przeciwnowotworową w komórkach białaczkowych oraz szpiczaka mnogiego.

6. Wnioski

Przeprowadzone badania pozwoliły mi pozytywnie zweryfikować postawioną hipotezę badawczą zakładającą, że zastosowane modyfikacje struktury cząsteczki melfalanu zwiększają aktywność przeciwnowotworową w komórkach ostrej białaczki promielocytowej i monocytowej oraz szpiczaka mnogiego (Rysunek 2).

Na podstawie przeprowadzonych badań można wnioskować, że:

1. Kluczem dla zwiększenia skuteczności przeciwnowotworowej melfalanu, jest modyfikacja grupy karboksylowej poprzez jej estryfikację oraz zamiana grupy di–*N*–propyloaminowej na amidynową, zawierającą pierścień heterocykliczny (pierścień morfolinowy lub tiomorfolinowy). Przeprowadzone badania wskazują, że takie analogi, w warunkach badań *in vitro*, charakteryzują się lepszą aktywnością cytotoksyczną, genotoksyczną i proapoptotyczną w komórkach białaczkowych oraz szpiczaka mnogiego niż obecnie stosowany melfalan. Jednocześnie związki te były znacznie mniej cytotoksyczne wobec komórek prawidłowych.
2. Głównym celem molekularnym melfalanu oraz badanych analogów, u podstawy którego leżą ich właściwości przeciwnowotworowe, jest ich interakcja z DNA.
3. Mechanizm aktywacji molekularnych szlaków śmierci przez melfalan oraz badane pochodne jest różny w zależności od rodzaju komórek nowotworowych. Komórki białaczkowe indukują śmierć komórki głównie poprzez aktywację mitochondrialnego (ostra białaczka monocytowa) lub receptorowego (ostra białaczka promielocytowa) szlaku apoptozy, natomiast śmierć komórek szpiczaka mnogiego następuje głównie przez inicjację katastrofy mitotycznej.

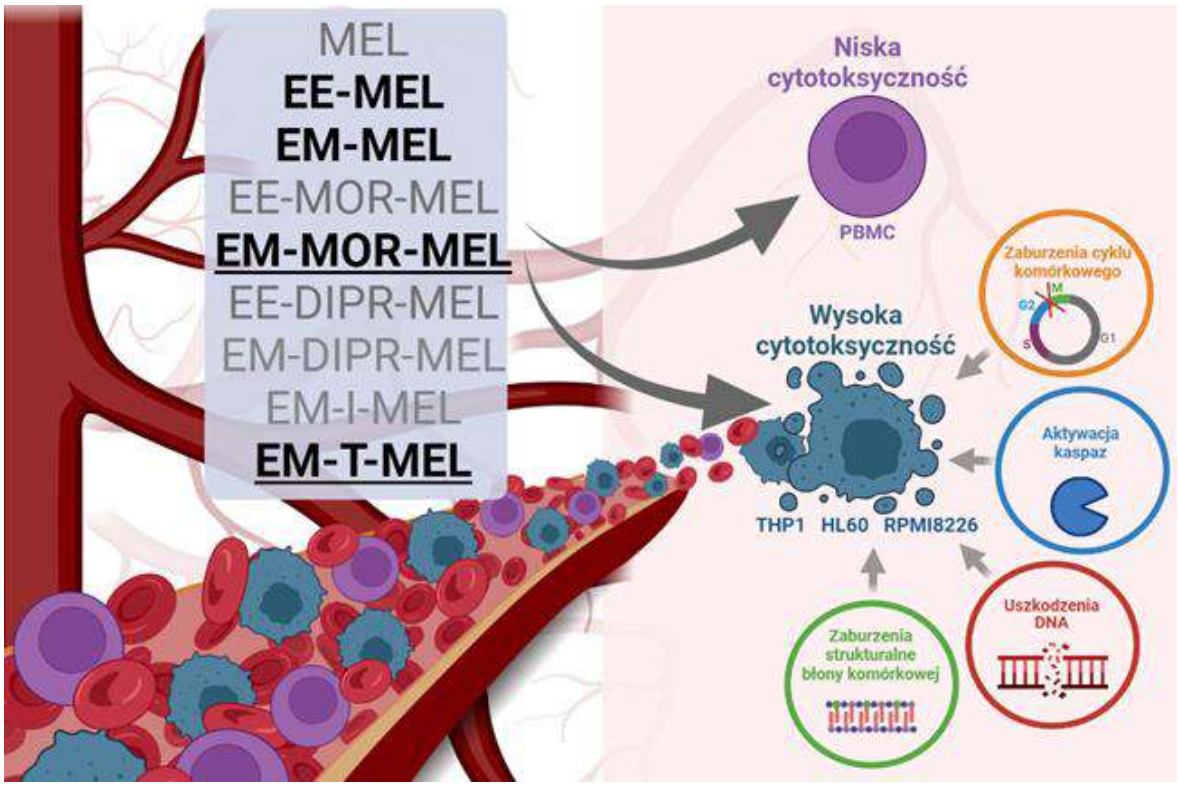

Rysunek 2. Mechanizm działania badanych związków w oparciu o przeprowadzone badania *in vitro*.

Literatura

1. Padmakumar, D. *et al.* A concise review on the molecular genetics of acute myeloid leukemia. *Leuk Res* 111, 106727 (2021).
2. Joshua, D. E., Bryant, C., Dix, C., Gibson, J. & Ho, J. Biology and therapy of multiple myeloma. *Medical Journal of Australia* vol. 210 375–380 Preprint at https://doi.org/10.5694/mja2.50129 (2019).
3. Castaneda, O. & Baz, R. Multiple Myeloma Genomics - A Concise Review. *Acta medica academica* vol. 48 57–67 Preprint at https://doi.org/10.5644/ama2006-124.242 (2019).
4. Rajkumar, S. V. Multiple myeloma: Every year a new standard? *Hematol Oncol* 37, 62–65 (2019).
5. Aksenova, A. Y. *et al.* Genome instability in multiple myeloma: Facts and factors. *Cancers* vol. 13 Preprint at https://doi.org/10.3390/cancers13235949 (2021).
6. Pinto, V. *et al.* Multiple myeloma: Available therapies and causes of drug resistance. *Cancers (Basel)* 12, 1–32 (2020).
7. Jurczyszyn, Artur., Skotnicki, A. B. & Belowski, Jacek. *Szpiczak mnogi : wybrane zagadnienia. T. 2*. (Fundacja Centrum Leczenia Szpiczaka, 2011).
8. Motais, B. *et al.* A bird's-eye view of cell sources for cell-based therapies in blood cancers. *Cancers* vol. 12 Preprint at https://doi.org/10.3390/cancers12051333 (2020).
9. Perrot, A. How I treat frontline transplantation-eligible multiple myeloma. *Blood* 139, 2882–2888 (2022).
10. van Kan, M., Burns, K. E. & Helsby, N. A. A systematic review of inter-individual differences in the DNA repair processes involved in melphalan monoadduct repair in relation to treatment outcomes. *Cancer Chemotherapy and Pharmacology* vol. 88 755–769 Preprint at https://doi.org/10.1007/s00280-021-04340-z (2021).
11. Loeber, R. L. *et al.* Proteomic Aanalysis of DNA-protein cross-linking by antitumor nitrogen mustards. *Chem Res Toxicol* 22, 1151–1162 (2009).
12. Mohamed, D. & Linscheid, M. Separation and identification of trinucleotide-melphalan adducts from enzymatically digested DNA using HPLC-ESI-MS. in *Analytical and Bioanalytical Chemistry* vol. 392 805–817 (2008).
13. Zhao, Y., Wang, L. & Pan, J. The role of L-type amino acid transporter 1 in human tumors. *Intractable Rare Dis Res* 4, 165–169 (2015).
14. Hayashi, K., Jutabha, P., Endou, H., Sagara, H. & Anzai, N. LAT1 Is a Critical Transporter of Essential Amino Acids for Immune Reactions in Activated Human T Cells. *The Journal of Immunology* 191, 4080–4085 (2013).
15. Singh, R. K., Kumar, S., Prasad, D. N. & Bhardwaj, T. R. Therapeutic journery of nitrogen mustard as alkylating anticancer agents: Historic to future perspectives. *Eur J Med Chem* 151, 401–433 (2018).
16. Cohen, Y. C. *et al.* Identification of resistance pathways and therapeutic targets in relapsed multiple myeloma patients through single-cell sequencing. *Nat Med* 27, 491–503 (2021).

17. Mao, F. *et al.* Chemical structure-related drug-like criteria of global approved drugs. *Molecules* 21, (2016).

18. Denel-Bobrowska, M. *et al.* Identification of the key pathway of oxazolinoanthracyclines mechanism of action in cells derived from human solid tumors. *Toxicol Appl Pharmacol* 313, 159–169 (2016).

19. Denel-Bobrowska, M. *et al.* Molecular mechanism of action of oxazolinoanthracyclines in cells derived from human solid tumors. Part 2. *Toxicology in Vitro* 46, 323–334 (2018).

20. Denel-Bobrowska, M. & Marczak, A. Structural modifications in the sugar moiety as a key to improving the anticancer effectiveness of doxorubicin. *Life Sci* 178, 1–8 (2017).

21. Poczta, A., Rogalska, A., Łukawska, M. & Marczak, A. Antileukemic activity of novel adenosine derivatives. *Sci Rep* 9, 14135 (2019).

22. Bielawska, A., Bielawski, K. & Anchim, T. Amidine analogues of melphalan: Synthesis, cytotoxic activity, and DNA binding properties. *Arch Pharm (Weinheim)* 340, 251–257 (2007).

23. Bielawski, K. *et al.* Novel amidine analogue of melphalan as a specific multifunctional inhibitor of growth and metabolism of human breast cancer cells. *Biochem Pharmacol* 72, 320–331 (2006).

24. Al-Ghorbani, M., Vigneshwaran, V., Ranganatha, V. L., Prabhakar, B. T. & Khanum, S. A. Synthesis of oxadiazole-morpholine derivatives and manifestation of the repressed CD31 Microvessel Density (MVD) as tumoral angiogenic parameters in Dalton's Lymphoma. *Bioorg Chem* 60, 136–146 (2015).

25. Al-Ghorbani, M., Bushra Begum, A., Zabiulla, Z., Mamatha, S. v. & Khanum, S. A. Piperazine and morpholine: Synthetic preview and pharmaceutical applications. *Research Journal of Pharmacy and Technology* vol. 8 611–628 Preprint at https://doi.org/10.5958/0974-360X.2015.00100.6 (2015).

26. Lenci, E., Calugi, L. & Trabocchi, A. Occurrence of Morpholine in Central Nervous System Drug Discovery. *ACS Chem Neurosci* 12, 378–390 (2021).

27. Arshad, F. *et al.* Revealing quinquennial anticancer journey of morpholine: A SAR based review. *European Journal of Medicinal Chemistry* vol. 167 324–356 Preprint at https://doi.org/10.1016/j.ejmech.2019.02.015 (2019).

28. Daré, R. G. *et al.* Abilities of protocatechuic acid and its alkyl esters, ethyl and heptyl protocatechuates, to counteract UVB-induced oxidative injuries and photoaging in fibroblasts L929 cell line. *J Photochem Photobiol B* 203, 111771 (2020).

29. Chalas, J. *et al.* Effect of ethyl esterification of phenolic acids on low-density lipoprotein oxidation. *Biomedicine & Pharmacotherapy* 55, 54–60 (2001).

30. Bulumulla, C. *et al.* Investigating the effect of esterification on retinal pigment epithelial uptake using rhodamine B derivatives. *Transl Vis Sci Technol* 9, 1–19 (2020).

31. Wang, C. lin, Guo, C., Zhou, Y. & Wang, R. In vitro and in vivo characterization of opioid activities of C-terminal esterified endomorphin-2 analogs. *Peptides (N.Y.)* 30, 1697–1704 (2009).

32. Oliveira, D. P. de *et al.* Esterification of trans-aconitic acid improves its anti-inflammatory activity in LPS-induced acute arthritis. *Biomedicine and Pharmacotherapy* 99, 87–95 (2018).

33. Chvapil, M., Kielar, F., Liska, F., Silhankova, A. & Brendel, K. Synthesis and evaluation of long-acting D-penicillamine derivatives. *Connect Tissue Res* 46, 242–250 (2005).

34. Małkiewicz, M. A. *et al.* Blood-brain barrier permeability and physical exercise. *J Neuroinflammation* 16, 1–16 (2019).

35. Robinson, K. & Tiriveedhi, V. Perplexing Role of P-Glycoprotein in Tumor Microenvironment. *Frontiers in Oncology* vol. 10 Preprint at https://doi.org/10.3389/fonc.2020.00265 (2020).

36. Mynott, R. L. & Wallington-Beddoe, C. T. Drug and Solute Transporters in Mediating Resistance to Novel Therapeutics in Multiple Myeloma. *ACS Pharmacology and Translational Science* vol. 4 1050–1065 Preprint at https://doi.org/10.1021/acsptsci.1c00074 (2021).

37. Subastri, A. *et al.* Exploration of disulfiram dealings with calf thymus DNA using spectroscopic, electrochemical and molecular docking techniques. *J Lumin* 170, 255–261 (2016).

38. Kellett, A., Molphy, Z., Slator, C., McKee, V. & Farrell, N. P. Molecular methods for assessment of non-covalent metallodrug-DNA interactions. *Chem Soc Rev* 48, 971–988 (2019).

39. Molphy, Z. *et al.* A phosphate-targeted dinuclear Cu(II) complex combining major groove binding and oxidative DNA cleavage. *Nucleic Acids Res* 46, 9918–9931 (2018).

40. Pawar, S. K. & Jaldappagari, S. Intercalation of a flavonoid, silibinin into DNA base pairs: Experimental and theoretical approach. *Journal of Molecular Recognition* 33, (2020).

41. Inamdar, P. R. & Sheela, A. Spectroscopic investigations on partial intercalative binding behaviour of terpyridine based copper(II) complexes with DNA. *J Photochem Photobiol B* 159, 133–141 (2016).

42. Meenongwa, A. *et al.* DNA-interacting and biological properties of copper(II) complexes from amidino-O-methylurea. *New Journal of Chemistry* 39, 664–675 (2015).

43. Rahmanian, N., Shokrzadeh, M. & Eskandani, M. Recent advances in γH2AX biomarker-based genotoxicity assays: A marker of DNA damage and repair. *DNA Repair* vol. 108 Preprint at https://doi.org/10.1016/j.dnarep.2021.103243 (2021).

44. Clingen, P. H. *et al.* Histone H2AX phosphorylation as a molecular pharmacological marker for DNA interstrand crosslink cancer chemotherapy. *Biochem Pharmacol* 76, 19–27 (2008).

45. Spanswick, V. J. *et al.* Evidence for different mechanisms of 'unhooking' for melphalan and cisplatin-induced DNA interstrand cross-links in vitro and in clinical acquired resistant tumour samples. *BMC Cancer* 12, (2012).

46. Sazonova, E. v., Petrichuk, S. v., Kopeina, G. S. & Zhivotovsky, B. A link between mitotic defects and mitotic catastrophe: detection and cell fate. *Biology Direct* vol. 16 Preprint at https://doi.org/10.1186/s13062-021-00313-7 (2021).

47. Vitale, I., Manic, G., Castedo, M. & Kroemer, G. Caspase 2 in mitotic catastrophe: The terminator of aneuploid and tetraploid cells. *Molecular and Cellular Oncology* vol. 4 Preprint at https://doi.org/10.1080/23723556.2017.1299274 (2017).

48. Cives, M. *et al.* Bendamustine overcomes resistance to melphalan in myeloma cell lines by inducing cell death through mitotic catastrophe. *Cell Signal* 25, 1108–1117 (2013).

49. Castedo, M. *et al.* Cell death by mitotic catastrophe: A molecular definition. *Oncogene* vol. 23 2825–2837 Preprint at https://doi.org/10.1038/sj.onc.1207528 (2004).

50. Mc Gee, M. M. Targeting the Mitotic Catastrophe Signaling Pathway in Cancer. *Mediators of Inflammation* vol. 2015 Preprint at https://doi.org/10.1155/2015/146282 (2015).

51. Verhees, F. *et al. The Antiviral Agent Cidofovir Induces DNA Damage and Mitotic Catastrophe in HPV-Positive and-Negative Head and Neck Squamous Cell Carcinomas In Vitro*. (2019).

52. Roninson, I. B., Broude, E. v. & Chang, B. D. If not apoptosis, then what? Treatment-induced senescence and mitotic catastrophe in tumor cells. *Drug Resistance Updates* vol. 4 303–313 Preprint at https://doi.org/10.1054/drup.2001.0213 (2001).

53. Imreh, G., Norberg, H. V., Imreh, S. & Zhivotovsky, B. Correction to Chromosomal breaks during mitotic catastrophe trigger γH2AX-ATM-p53-mediated apoptosis [J. Cell Sci., 124 (2016) 2951-2963]. *Journal of Cell Science* vol. 129 1950 Preprint at https://doi.org/10.1242/jcs.190132 (2016).

7. Streszczenie w języku polskim

Nowotwory układu krwiotwórczego są heterogenną grupą chorób o złożonej patogenezie, co stanowi poważne wyzwanie dla współczesnej medycyny. Największy odsetek wśród białaczek u dorosłych stanowi ostra białaczka szpikowa. Natomiast szpiczak mnogi jest drugim co do częstości występowania nowotworem układu krwiotwórczego. Terapia mieloablacyjna za pomocą dużych dawek melfalanu wspomagana przeszczepem komórek macierzystych od lat uważana jest za standard leczenia pierwszego rzutu chorych na szpiczaka mnogiego, którzy kwalifikują się do przeszczepu. Problemy związane ze stosowaniem tej terapii to brak selektywności, wysoka toksyczność oraz rozwój oporności na lek. Wszystko to sprawia, że poszukiwane są nowe terapeutyki, charakteryzujące się wyższą skutecznością przeciwnowotworową i lepszym profilem bezpieczeństwa.

Jedną z metod poprawy skuteczności terapeutycznej leków jest regulacja ich aktywności farmakologicznej poprzez modyfikację struktury chemicznej. Celem pracy doktorskiej była analiza właściwości biologicznych nowych, otrzymanych drogą syntezy chemicznej pochodnych melfalanu oraz wytypowanie tej struktury, która wykazuje wyższą aktywność przeciwnowotworową niż związek macierzysty względem komórek szpiczaka mnogiego (RPMI8226) oraz komórek ostrej białaczki monocytowej (THP1) i promielocytowej (HL60).

Badania *in vitro*, będące podstawą tej pracy pozwoliły na wytypowanie najskuteczniejszej modyfikacji struktury melfalanu. Wykazano, że kluczem dla zwiększenia aktywności cytotoksycznej, genotoksycznej i proapoptotycznej w komórkach białaczkowych oraz szpiczaka mnogiego jest modyfikacja grupy karboksylowej poprzez jej estryfikację oraz zamiana grupy di–*N*–propyloaminowej na amidynową, zawierającą pierścień heterocykliczny (pierścień morfolinowy lub tiomorfolinowy). Jednocześnie taka zmiana struktury melfalanu powoduje obniżenie aktywności cytotoksycznej wobec komórek prawidłowych — jednojądrzastych komórek krwi obwodowej. Zbadano mechanizm aktywacji molekularnych szlaków śmierci przez melfalan oraz badane pochodne. Badania pozwoliły na poznanie zależności pomiędzy strukturą chemiczną melfalanu oraz nowych pochodnych a ich aktywnością biologiczną. Otrzymane wyniki stanowią istotny wkład w wiedzę o obecnie stosowanym leku — melfalanie, jak również o jego nowych analogach.

8. Streszczenie w języku angielskim I Summary

Hematopoietic neoplasms are a heterogeneous disease group and a major challenge for contemporary medicine. Acute myeloid leukemia accounts for the largest proportion among adult leukemias. Multiple myeloma is the second most common hematopoietic malignancy. Myeloablative therapy with high – dose melphalan followed by autologous stem cell transplantation is considered the standard of treatment for multiple myeloma patients who are eligible for transplantation. Problems associated with the use of this therapy include lack of selectivity, high toxicity and the development of drug resistance. All this leads to the search for new therapeutics with higher anti–tumor efficacy and a better safety profile.

One way to improve the therapeutic efficacy of drugs is to regulate their pharmacological activity by modifying their chemical structure. The aim of this dissertation was to analyze the biological properties of new melphalan derivatives obtained by chemical synthesis and to select this modification of its structure which exhibits higher anticancer activity than the parent compound against multiple myeloma cells (RPMI8226), acute monocytic (THP1) and promyelocytic (HL60) leukemia cells.

In vitro studies have identified the most effective structural modification of melphalan. It was shown that the key to enhancing cytotoxic, genotoxic and proapoptotic activity in leukemia and multiple myeloma cells is the modification of the carboxyl group by its esterification and the replacement of the di–*N*–propylamine group with an amidine group containing a heterocyclic ring (morpholine or thiomorpholine one). Simultaneously, such a change in the structure of melphalan causes a reduction in cytotoxic activity against normal cells — peripheral blood mononuclear cells. The mechanism of activation of molecular death pathways by melphalan and the derivatives studied was investigated. The study allowed us to understand the relationship between the chemical structure of melphalan and the new derivatives and their biological activity. The obtained results are an important contribution to the knowledge of the currently used drug — melphalan, as well as its new analogues.

Kopie publikacji wchodzących w zakres rozprawy doktorskiej

PUBLIKACJA NR I

Poczta A., Rogalska A., Marczak A.; *Treatment of Multiple Myeloma and the Role of Melphalan in the Era of Modern Therapies–Current Research and Clinical Approaches;* J Clin Med; 2021; 10(9):1841.

- **Praca przeglądowa**
- **IF: 4.964**
- **punkty MEiN: 140 pkt.**

Journal of
Clinical Medicine

MDPI

Review

Treatment of Multiple Myeloma and the Role of Melphalan in the Era of Modern Therapies—Current Research and Clinical Approaches

Anastazja Poczta *, Aneta Rogalska and Agnieszka Marczak

Department of Medical Biophysics, Faculty of Biology and Environmental Protection, Institute of Biophysics, University of Lodz, Pomorska 141/143, 90-236 Lodz, Poland; aneta.rogalska@biol.uni.lodz.pl (A.R.); agnieszka.marczak@biol.uni.lodz.pl (A.M.)

* Correspondence: anastazja.poczta@edu.uni.lodz.pl; Tel.: +48-(42)-635-4481; Fax: +48-(42)-635-4479

Abstract: Multiple myeloma (MM) accounts for 10% of all hematological malignancies, and it is the second most common hematological neoplasm for which chemotherapy is an important pharmacological treatment. High dose melphalan followed by autologous stem cell transplantation remains the standard of treatment for transplant-eligible patients with MM. In this review, we describe aspects of the pharmacokinetics and pharmacodynamics of melphalan therapy and related compounds. In addition, we describe the use of melphalan in innovative therapies for the treatment of MM, including the development of drug carriers to reduce systemic toxicity, combination therapy to improve the effectiveness of cancer therapy, and the chemical modification of the melphalan molecule to improve antitumor activity.

Keywords: autologous stem cell transplantation; clinical study; combination chemotherapy; high dose melphalan therapy; in vitro and in vivo studies; multiple myeloma

Citation: Poczta, A.; Rogalska, A.; Marczak, A. Treatment of Multiple Myeloma and the Role of Melphalan in the Era of Modern Therapies—Current Research and Clinical Approaches. *J. Clin. Med.* **2021**, *10*, 1841. https://doi.org/10.3390/jcm10091841

Academic Editor: Shaji Kumar

Received: 6 March 2021
Accepted: 16 April 2021
Published: 23 April 2021

1. Introduction

Despite constant advances in medicine, cancer remains a major health problem. It affects patients of all ages, often leading to death. Many effective anti-cancer drugs have the potential to alkylate DNA, RNA, and several proteins. DNA alkylation is the major change leading to anticancer activity. One important milestone in the fight against cancer was the discovery of nitrogen mustard as an alkylating agent in 1942. Nitrogen mustard-based DNA alkylating agents were the first effective antitumor compounds developed, and they remain important drugs for the treatment of many types of cancer. Many years of research on nitrogen mustard have resulted in the identification of a wide range of therapeutically useful compounds. Active molecules can be designed by reducing the electrophilicity of mustard agents, thereby obtaining safer analogues. This approach was used to develop clinically useful anti-cancer agents such as chlorambucil, mechlorethamine, melphalan, cyclophosphamide, and estramustine. The biological activity of this noteworthy group of compounds is based on DNA binding, cross-linking two strands, preventing DNA replication, and inducing cell cycle arrest, which leads to cell death. These alkylating agents bind to the N7 nitrogen on guanine DNA bases. DNA alkylation occurs in two stages. First, the bis(2-chloroethyl) amine undergoes first order SN2 cyclization at neutral or alkaline pH in a one-step reaction, resulting in the formation of a highly reactive and unstable aziridinium cation. In the second step, the resulting aziridine cation is subjected to nucleophilic addition by a DNA nucleophile to form a monoalkylation adduct through the SN2 mechanism. These reactions can then be repeated with another involving CH2CH2Cl to obtain a cross-link between two complementary DNA strands [1]. Many drugs and chemicals that form reactive electrophiles, including alkylating compounds, bind to cellular macromolecules such as proteins, and increase heat shock proteins synthesis by binding

covalently to nucleophilic functional groups. Alkylating agents also cause secondary cytotoxic signals, such as depletion of glutathione, increased cellular calcium, oxidative stress, and lipid peroxidation, which induce a heat shock response [2].

Melphalan (MEL, trade name Alkeran™) is an alkylating drug that belongs to the nitrogen mustard group of alkylating agents. This drug was first synthesized in the second half of the 20th century. Melphalan is the phenylalanine derivative of nitrogen mustard [3]. The intracellular cytotoxic activity of melphalan is based on inter- or intra-structural DNA cross-linking and DNA-protein cross-linking via two chlororethyl groups on the molecule. These cross-links lead to deletion of nitrogen bases, strand cleavage, and open ring formation in the DNA molecule, which disrupts DNA replication and transcription. The ability of melphalan to induce both inter- and intra-strand links classifies this drug as a bifunctional alkylating agent [4].

In this review, we describe aspects of the pharmacokinetics, and pharmacodynamics of melphalan therapy and related compounds and define how melphalan is used in the treatment of multiple myeloma (MM).

2. Multiple Myeloma Is the Second Most Common Hematological Malignancy: Current Treatment Strategies

Plasma cell disorders are a wide group of diseases [5]. MM accounts for 1% of all malignancies, and 10% of all hematological cancers, and it is the second most common hematologic tumor after non-Hodgkin's lymphoma [6,7]. MM is a B-cell malignancy characterized by clonal proliferation of plasma cells, overproduction of paraproteins, renal failure, hypercalcemia, anemia, osteolytic bone damage, and numerous infections [8]. Although the incidence of MM increases with age, and it is more common at 60–70 years of age, younger patients have also been diagnosed. In recent years, the median overall survival (OS) has increased from 2–3 years to 8–10 years, which is mostly due to an improved understanding of the heterogeneity of the disease, as well as the introduction of new therapeutic drugs. The use of autologous stem cell transplantation [7] or allogeneic stem cell transplantation (Allo-SCT), which is a potentially curative treatment, has also increased the survival of MM patients [9].

The treatment of MM involves different combinations of drugs with different mechanisms of action, including alkylating agents, corticosteroids, anthracyclines, immunomodulatory drugs (IMID), histone deacetylase inhibitors (iHDAC), proteasome inhibitors (PIs), monoclonal antibodies (mAbs), and high-dose chemotherapy followed by autologous stem cell transplantation (ASCT). Alkylating agents such as melphalan attack rapidly proliferating cells [7], cross-linking the two strands and arresting DNA replication, which causes cell death. In addition to melphalan, bendamustine is another alkylating agent that has been successfully used in both the upfront and relapse/refractory settings of MM patients, including those with renal impairment. This drug attracted attention because of its specific mechanism of action. Although it is structurally similar to both alkylating agents and antimetabolities, it does not show cross-resistance with alkylating drugs [10]. Glucocorticoids (especially dexamethasone), which are steroid hormones, have been used for more than 50 years in the treatment of MM. Dexamethasone works by activating the mitochondrial apoptotic pathway, upregulating pro-apoptotic genes, downregulating anti-apoptotic genes, promoting the cleavage of poly (ADP-ribose) polymerase (PARP), and activating caspase 3 [11–13]. The mechanistic target of rapamycin (mTOR) pathway is also involved in the mechanism of action of dexamethasone, and inhibitors of mTOR sensitize MM cells to dexamethasone-induced apoptosis [14,15]. Proteasome inhibitors such as bortezomib, carfilzomib, and ixazomib, exhibit their biological activities through various mechanisms, such as direct effects on MM cells, suppression of several adhesion molecules, inhibition of cytokines, and angiogenesis. By blocking the degradation of the kappa B inhibitor (IκB), bortezomib inhibits the NFκB signaling pathway, which plays a key role in MM cell survival and proliferation. Bortezomib inhibits the expression and secretion of vascular endothelial growth factor, thereby inhibiting angiogenesis in the bone marrow microenvironment. In addition, bortezomib inhibits oseoclasts and directly stimulates osteoblast proliferation and differentiation [7,16]. Monoclonal antibodies such as daratumumab and isatuximab bind to specific antigens on the surface of MM

cells. This induces MM cell death through antibody-dependent cellular cytotoxicity (ADCC), complement dependent cytotoxicity (CDC), and/or antibody-dependent cellular phagocytosis (ADCP) [17]. Histone deacetylase inhibitors such as vorinostat and panobinostat act on malignant plasma cells by opening the chromatin structure, which leads to changes in the expression of many genes involved in signaling pathways, cell cycle inhibition, and angiogenesis. This leads to cell growth arrest, activation of external, and/or internal apoptotic pathways, induction of autophagy, activation of mitotic cell death, and senescence [18,19]. A promising agent for the treatment of patients with relapsed or refractory MM is venetoclax (ABT-199), a selective, orally bioavailable B cell lymphoma 2 (BCL-2) inhibitor. It is particularly effective in MM harboring t(11;14), which is characterized by high expression of BCL-2 relative to B-cell lymphoma-extra large (BCL-XL) and myeloid cell leukemia-1 (MCL-1) [20,21]. Immunomodulatory drugs such as thalidomide, lenalidomide, and pomalidomide modulate the inflammatory environment of the bone marrow, causing MM cell death by inhibiting angiogenesis and antiproliferative properties [22]. Cereblon (CRBN) is a target for immunomodulatory drugs [23], and lenalidomide-bound cereblon acquires the ability to target two specific B cell transcription factors, Ikaros family zinc finger proteins 1 and 3 (IKZF1 and IKZF3), for proteasomal degradation [24]. Another promising treatment for MM is anti-B cell maturation antigen (BCMA) chimeric antigen receptor (CAR) T cell therapy. It has shown improved efficacy with the bivalent BM38 CAR-T therapy for relapsed/refractory MM with a high overall response rate (ORR) [25].

3. Pharmacokinetics and Pharmacodynamics of Melphalan

The pharmacokinetic parameters of melphalan were tested in several research centers [26–32], and the results showed large interindividual differences in the parameters analyzed. The dominant half-life (t1/2β) values range between 25 and 96 min, and the melphalan plasma clearance is 127–797 mL/min/m^2 [26,27]. The average volume of distribution ranges from 6 to 108 L/m^2 [28–30]. Research of melphalan administered at a high dose (180 mg/m^2) shows that plasma levels of melphalan decline bi-exponentially, with a mean terminal half-life (t1/2β) of 61 min (range 40.3–132.8 min). The estimated peak concentrations are 5.45–16.57 mcg/mL. The average volume of distribution at steady state and clearance are 0.479 ± 0.164 L/kg and 6.73 ± 1.60 mL/min/kg, respectively. These kinetic parameters are similar to those observed for lower doses of melphalan [33]. Melphalan administered in oral form is rapidly absorbed after administration. Absorption lag-time is <1 h [34]. Alberts et al. showed that oral melphalan has a mean plasma terminal phase half-life (t1/2) of 90 ± 17 min. The mean area under the plasma concentration: time curve (CXT) is 53 ± 33 µg/ min/mL. Urinary excretion averages 10.9 ± 4.9% during the first 24 h. The average CXT ratio (oral: intravenous) is 0.56 (range, 0.25–0.89) [35]. A large variation in bioavailability between individuals has been observed after p.o. treatment. Although this parameter is not dependent on the dose administered, it decreases with the duration of the treatment. This suggests that it may be advantageous to administer oral melphalan for fewer days to achieve higher bioavailability. Absorption of melphalan is consistent with first order kinetics at the dose intervals tested [34]. Reece et al. [36] confirmed that to achieve the best bioavailability, melphalan should be administered on an empty stomach, as administration with food, especially fat food, reduces the melphalan exposure (AUC) by up to 39%.

Melphalan enters the cells mainly via the neutral leucine active amino acid pathway [37]. Studies using murine L12106 leukemia cells show that the transport of melphalan is mediated equally by two separate amino acid transport systems: one system is mediated by a monovalent-dependent cation that has the highest affinity for leucine, and the second is the L system, the classic leucine-preferable sodium independent transport system. The model synthetic substrate for the L system is 2-aminobicyclo[2.2.1]heptane-2-carboxylic acid (BCH) [1]. Identical carrier systems have been identified for L-PAM transport in LPC-1 plasmacytoma cells and L5178Y lymphoblasts [38,39]. Studies on the mechanism of melphalan uptake by L5178Y lymphoblasts have been extended by focusing on the chemical specificity of the transport mechanism.

Melphalan uptake is an active carrier mediated process. It proceeds "uphill" against a concentration gradient, is temperature-sensitive, partly sodium-dependent, and is in-

hibited by several metabolic antagonists. Studies indicate that melphalan uptake follows Michaelis-Menten two-phase kinetics, suggesting the involvement of at least two carrier systems, and it is inhibited by various amino acids [40,41]. A strong inhibitor of melphalan uptake is β-2-aminobicyclo[2.2.1]heptane-2-carboxylic acid, a specific inhibitor of the L-amino acid transport system (preferring leucine), but not by 2-aminoisobutyric acid or 2-(methylamino)-isobutyric acid-specific inhibitors of the amino acid system A (preferring alanine). Under conditions of full saturation of the L and A systems with β-2-aminobicyclo[2.2.1]heptane-2-carboxylic acid and 2-aminoisobutyric acid, drug uptake is inhibited by serine, an amino acid that is transported through the ASC system (alanine, serine and cysteine). In experiments using leucine as a substrate, melphalan inhibited the uptake of the amino acid by both the L system and the second ASC-like system. Carrier-dependent melphalan uptake can be explained by transport through these two systems. When the drug concentration range is 3.33–20 μM, the carrier-mediated uptake of melphalan is mediated equally by the L system and the ASC system, whereas in the 20–100 μM concentration range, the L system becomes increasingly dominant [40].

Large neutral amino acid transporter 1 (LAT1 or SLC7A5) is a sodium- and pH-independent transporter that provides vital amino acids (e.g., leucine and phenylalanine) to cells. Melphalan is transported to the brain via cerebrovascular LAT1, demonstrating the usefulness of LAT1 for drug delivery in the central nervous system. This drug has strong structural similarity to endogenous LAT1 substrates. Prodrugs directed at LAT1 show structural similarity: they are composed of a parent drug attached to the amino acid side chain via a biodegradable bond and an unsubstituted α-carboxyl and α-amino group to achieve effective LAT binding [42].

Melphalan is eliminated both by the kidneys and by spontaneous chemical degradation to mono- and dihydroxy metabolites. The latter pathway has a relatively small share (just over 5%) because plasma protein binding delays the rate of melphalan hydrolysis. However, melphalan is degraded rapidly in the urine, which leads to a very variable dose percentage that can be recovered from urine within 24 h. This led to some confusion about the role of kidney function in the elimination of melphalan. The fact that more than 60% of the dose was recovered in three of nine patients in one study suggests that renal excretion is the main route of melphalan elimination [43].

4. Autologous Stem Cell Transplantation (ASCT) in Combination with High Doses of Melphalan (HDM) as the Standard Treatment for Newly Diagnosed Patients with Multiple Myeloma

The current treatment regimen for newly diagnosed MM (NDMM) involves obtaining the deepest remission of the disease followed by maintenance of this response through continuous therapy [44,45].

Initial use of high-dose melphalan (HDM) results in a higher response; however, the high toxicity associated with bone marrow recovery time outweighs the benefits. The combination of autologous stem cell infusion with HDM reduces toxicity and leads to better outcomes. HDM-ASCT for the treatment of MM was first developed by Barlogie, McElwain, and others in the mid-1980s and was the first treatment milestone leading to better outcomes [3,46]. In the age of modern therapy, HDM-ASCT remains the standard approach for the treatment of patients with newly diagnosed MM who are eligible for transplantation [44,47,48]. High-dose therapy combined with ASCT is considered to be the standard of care for MM patients <65 years of age. MM is a disease of the elderly, as the median age at diagnosis is 70 years. Therefore, a large proportion of patients are considered ineligible for high-dose therapy because of increased treatment-related toxicity and mortality associated with a melphalan dose of 200 mg/m^2 [49]. However, high-dose therapy with melphalan 200 mg/m^2 is safe in selected elderly patients with NDMM, even in those older than 70 years without increased mortality [50].

Randomized trials comparing HDM-ASCT with conventional chemotherapy have demonstrated the clinical benefit of HDM-ASCT. HDM-ASCT was compared with various chemotherapy combinations including doxorubicin, vincristine, melphalan, cyclophos-

phamide, carmustine, and prednisone [47,48]. An overview of phase III clinical trials comparing the MM regimen with or without ASCT is provided in Table 1.

In 1996, Attal et al. [51] published the first such studies on NDMM. The study showed that high-dose melphalan therapy combined with ASCT improves response rate, event free survival, and OS in patients with myeloma [51]. Another randomized, multicenter phase III study conducted by Attal et al. [52] in patients with MM showed that treatment with lenalidomide, bortezomib, and dexamethasone (RVD) plus ASCT resulted in longer progression-free survival (PFS) than RVD alone; however, OS did not differ significantly between the two treatment arms [52].

The use of ASCT as an intensification therapy and consolidation therapy in patients with NDMM compared with new therapies (bortezomib-melphalan-prednisone, with or without bortezomib-lenalidomide-dexamethasone consolidation therapy and lenalidomide-dexamethasone maintenance) was supported by a multicenter, randomized, open-label phase III study conducted by the team of Prof. Cavo [53]. The results of the study support the use of ASCT as intensification therapy and the use of consolidation therapy in patients with NDMM, even in the era of novel treatments. PFS, but not OS, was significantly improved with ASCT compared with VMP (bortezomib–melphalan–prednisone) [53].

In a randomized, phase III study by Gay et al. [54] in patients with NDMM, consolidation of chemotherapy (cyclophosphamide and dexamethasone) with lenalidomide significantly increased the risk of progression or death and decreased OS compared with HDM-ASCT. The results of this study confirmed that consolidation with HDM-ASCT remains the preferred therapeutic option in transplant-eligible patients with NDMM. This regimen improves PFS and OS at the expense of increased, but manageable, adverse events. A phase III randomized trial by Palumbo et al. [55] compared melphalan 200 mg and ASCT with melphalan, prednisone and lenalidomide (MPR); the results favored melphalan and ASCT. Both PFS and OS were significantly longer with HDM-ASCT than with MPR [55].

More than 30 years after the introduction of ASCT to the therapy of patients with multiple myeloma, there are steel studying at different aspects of ASCT as: early or delayed, single or tandem [56,57]. The randomized, open-label phase III study BSBMT/UKMF Myeloma X Relapse showed that salvage ASCT increases OS during consolidation of reinduction treatment in patients with MM at first relapse following the first ASCT. Delaying salvage ASCT to third-line treatment or later may not be as beneficial as using salvage ASCT at first relapse [58].

For over 10 years, numerous studies have compared single and tandem ASCT with melphalan conditioning [59]. Tandem ASCT refers to the re-administration of ASCT within 6 months of the first application. Patients randomly assigned to a second autologous hematopoietic cell transplantation (AHCT/AHCT + lenalidomide) received high-dose melphalan (200 mg/m^2) followed by autologous peripheral-blood stem-cell infusion [59]. In another study of tandem transplantation, the second high-dose regimen was administered at 140 mg/m^2 [60]. Despite numerous clinical trials, tandem ASCT remains controversial and is recommended for patients who did not achieve a very good partial response (VGPR) after the first ASCT or NDMM patients with high-risk disease characteristics, including patients with high-risk cytogenetics [57,59].

The Phase III BMT CTN 0702 study was designed to improve PFS by comparing ASCT, tandem ASCT, and ASCT with four consecutive cycles of RVD. The results showed that a second consolidation of ASCT or RVD as post-ASCT interventions in the initial treatment of transplant-eligible MM patients did not improve PFS or OS. A single ASCT and lenalidomide should remain the standard approach [59]. The latest clinical trials involving new MM treatment regimens include the use of HDM-ASCT (Table 2).

More than 30 years after its introduction, HDM-ASCT remains in the arsenal of therapy for patients with newly diagnosed MM. Many clinical trials are currently underway to assess the efficacy of combination therapy with melphalan for the treatment of MM (Table 3). Novel therapies represent a milestone in the treatment of MM, and have contributed to a significant increase in the survival of MM patients over the past two decades [48,61,62].

Table 1. Clinical trials assessing the efficacy of combination therapy for the treatment of MM, including melphalan-new directions. Overview of phase III clinical studies comparing the MM treatment regimen with or without Autologous Stem Cell Transplantation.

Ref.	Type of Study	No. of Patients	Treatment Regimen	Results			
				Response	PFS	OS	MRD Negativity
[53,61]	Multicenter, randomized, open-label, phase III study	1503	I: MEL (200 mg/m^2) + ASCT (intensification therapy) + RVD/no cons.	VGPR: 84%	56.7 months (95% CI 49.3–64.5)	NA	36% (10-5)
			II: VMP (intensification therapy) + RVD/no cons.	VGPR: 75%	41·9 months (95% CI 37.5–46.9)	NA	64% (10-5)
				HR for PFS of ASCT compared with VMP: 0.73, 0.62–0.85; $p = 0.0001$.			
[55,61]	Open-label, randomized, phase III study	402	I: MEL (200 mg/m^2) + ASCT (consolidation therapy) ± Rm.	CR (post-consolidation): 23%	43.0 months	4-year 81.6%	NA
			II: MPR (consolidation therapy) ± Rm.	CR (post-consolidation): 18%	22.4 months	4-year 65.3%	NA
				HR for PFS: 0.44; 95% CI: 0.32–0.61; $p < 0.001$. HR for OS: 0.55; 95% CI, 0.32–0.93; $p = 0.02$.			
[54,61]	Multicenter, randomized, open-label, phase III study	389	I: MEL (200 mg/m^2) +ASCT (consolidation therapy) +Rm./RPm.	CR: 33% (MEL-ASCT +Rm.) CR: 37% (MEL-ASCT +RPm.)	43.3 months (95% CI 33.2–52.2);	4-year OS: 75% (MEL-ASCT + Rm.) 4-year OS: 77% (MEL-ASCT + RPm.)	NA
			II: CRD (consolidation therapy) +Rm./RPm.	CR: 27% (CRD + Rm.)CR: 23% (CRD + RPm.)	28.6 months (95% CI 20.6–36.7)	4-year OS: 77% (CRD + Rm.) 4-year OS:76% (CRD + RPm.)	NA
				HR for the first 24 months 2.51, 95% CI 1.60–3.94; $p < 0.0001$			
[59]	Prospective, randomized, phase III study	758	I: MEL+ ASCT (consolidation therapy) + Rm.	1-year ORR: 47.1% ($n = 208$)	53.9% (95% CI: 47.4–60%)	38-month OS: 83.7% (95% CI: 78.4–87.8%)	NA
			II: MEL+ ASCT/ASCT (consolidation therapy) + Rm.	1-year ORR: 50.5% ($n = 192$)	58.5% (95% CI: 51.7–64.6%)	38-month OS: 81.8% (95% CI: 76.2–86.2%)	NA
			III: MEL+ ASCT +RVD (consolidation therapy) +Rm.	1-year ORR: 58.4% ($n = 209$)	57.8% (95% CI: 51.4–63.7%)	38-month OS: 85.4% (95% CI: 80.4–89.3%)	NA
				Patients with high-risk disease experienced higher rates of treatment failure (progression or death; HR, 1.66; 95% CI: 1.30–2.11) and overall mortality (HR, 1.49; 95% CI: 1.01– 2.20) compared with patients with standard-risk disease.			
[52,61]	Open-label, randomized, phase III study	700	I: MEL (200 mg/m^2) + ASCT+ RVD (consolidation therapy) + Rm.	CR: 59%	50 months	4-year OS: 81%	79% (10-4)
			II: RVD (consolidation therapy) +Rm.	CR: 48%	36 months	4-year OS: 82%	65% (10-4)
				HR for disease progression or death, 0.65; $p < 0.001$			
[58,63]	Open-label, randomized, phase III study	297	I: MEL (200 mg/m^2) + sASCT (consolidation therapy)	CR: 92.1%	19 months (95% CI 16–26)	67 months (95% CI 55–not estimable)	NA
			II: cyclophosphamine (consolidation therapy)	CR: 94.1%	11 months (95% CI: 9–12)	52 months (95% CI 42–60)	NA
				HR for PFS: 0.45 (95% CI 0.31–0.64), $p < 0.0001$ HR for OS: 0.56 (0.35–0.90), $p = 0.0169$			

Abbreviations: ASCT, autologous stem cell transplantation; sASCT, salvage autologous stem cell transplantation; CR, complete remission; CRD, cyclophosphamide + lenalidomide + dexamethasone; HR, hazard ratio; MM, multiple myeloma; MPR, melphalan + prednisone + lenalidomide; MRD, minimal residual disease; NA, not available; ORR, overall response rate; OS, overall survival; PFS, progression-free survival; Rm, lenalidomide maintenance; RPm, lenalidomide + prednisone maintenance; RVD, lenalidomide + bortezomib + dexamethasone; VGPR, very good partial response; VMP, bortezomib + melphalan + prednisone.

Table 2. Clinical trials assessing the efficacy of combination therapy for the treatment of MM, including melphalan-new directions. Published clinical studies featuring new MM treatment regimens with Autologous Stem Cell Transplantation.

Ref.	Type of Study	No. of Patients	Treatment Regimen	Results
[64]	Randomized, a double-blind, placebo-controlled phase III trial	656	I: ixazomib maintenance therapy II: placebo both groups had undergone standard induction therapy with MEL (200 mg/m^2) conditioning and a single ASCT	There was a 28% reduction in the risk of PFS with ixazomib vs. placebo (26.5 months (95% CI 23.7–33.8) vs. 21.3 months (18.0–24.7); HR 0.72, 95% CI 0.58–0.89; $p = 0.0023$). At the time of this analysis no increase in secondary malignancies was observed with ixazomib therapy (3% patients) compared with placebo (3% patients).
[65–67]	Open-label, randomized, phase III study	458	RVD (induction therapy) + BU (12 mg/kg)- MEL (140 mg/m^2) + ASCT /MEL (200 mg/m^2) +ASCT + RVD (consolidation therapy)	Conditioning with BU-MEL in comparison to MEL was associated with longer PFS (41 vs. 31 months; $p = 0.009$), although OS was similar to that in the melphalan 200 mg/m^2 group. This should be counterbalanced against the higher frequency of veno-occlusive disease-related deaths. Access to novel agents as a salvage therapy after relapse/progression was decreased for patients receiving BU-MEL (43%) vs. MEL (58%; $p = 0.01$).
[68]	Prospective, investigator-initiated, nonrandomized, multicenter, open-label, phase II study	100	RVD (induction therapy) + MEL (200 mg/m^2) + ASCT + Rm ± PCD	PCD was an effective therapy after first relapse with RVD. Responses were obtained in 85% of patients evaluated: CR (1%), VGPR (33%).After 4 cycles, the rate of PR (or better) was 85%. 94% of planned ASCTs were performed.
[69]	Single-arm, prospective phase II study	125	I: MEL (200 mg/m^2) + ASCT + Lipegfilgrastim (LIP) II: MEL (200 mg/m^2) + ASCT + Filgrastim (FIL)	The median duration of grade 4 neutropenia was 5 days in both LIP and FIL groups. The incidence of FN was significantly lower in the LIP than in the FIL group (29% vs. 49%, respectively, $p = 0.024$). The HR of ANC $\geq 0.5 \times 10(9)$/L was 3.5 times higher in patients treated with LIP than in those treated with FIL (HR 3.50, 95% CI 2.28–5.38, $p < 0.001$), indicating that the response was faster in LIP treated patients than in those treated with FIL.

Abbreviations: ANC, absolute neutrophil count; ASCT, autologous stem cell transplantation; BU-MEL, busulfan + melphalan; CR, complete remission; FN, febrile neutropenia; HR, hazard ratio; MM, multiple myeloma; OS, overall survival; PCD, pomalidomide + cyclophosphamide + dexamethasone; PFS, progression-free survival; PR, partial remission; Rm, lenalidomide maintenance; RVD, lenalidomide + bortezomib + dexamethasone; VGPR, very good partial response.

Table 3. Clinical trials assessing the efficacy of combination therapy for the treatment of MM, including melphalan-new directions. New clinical studies of the treatment of MM with combination therapy including melphalan.

Clinical Trial Identifier	Trial Phase	Treatment Regimen	Objective of Trial
NCT03829371	1	VMP, MPT and lenalidomide with low-dose dexamethasone	Comparison of treatment regimens in an autologous stem cell transplantation ineligible population affected by MM.
NCT03346135	2	melphalan, daratumumab	Daratumumab after stem cell transplant for the treatment of MM.
NCT03481556	2	melphalan, dexamethasone, bortezomib, daratumumab	Assessing patients with relapsed or relapsed-refractory MM following 1–4 lines of prior therapy.
NCT04466475	1	astatine at 211 anti-cd38 monoclonal antibody okt10-b10, melphalan	Radioimmunotherapy and chemotherapy before stem cell transplantation. Therapy based on 211At-OKT10-B10 in combination with melphalan before a stem cell transplant may be more effective than melphalan monotherapy in MM.
NCT03556332	1	carfilzomib, lenalidomide, dexamethasone, daratumumab, Procedure: autologous hematopoietic cell transplantation (melphalan)	Assessing patients with relapsed or refractory myeloma with re-administration of ASCT to a patient with symptoms of disease progression. The effect of the drugs in combinations will be compared before and after ASCT in MM.
NCT02581007	2	fludarabine, melphalan, cyclophosphamide	Evaluation of the safety and efficacy of a reduced intensity allogeneic HSCT from partially HLA-mismatched first-degree relatives utilizing PBSC as the stem cell source.
NCT04008888	1	melphalan, fludarabine, PI and dexamethasone as maintenance therapy, PI + IMids + dexamethasone as consolidated chemotherapy	Assessing efficacy and safety of the holistic treatment of young high-risk MM patients who were designed to receive a combination of high-dose chemotherapy with allogeneic or autologous HSCT.
NCT01453088	3	melphalan, bortezomib	Assessing a standard regimen and the newly established melphalan and bortezomib regimen in patients with MM 65 years or older.
NCT02780609	$\frac{1}{2}$	selinexor, melphalan, dexamethasone, fosaprepitant	Determination of the maximum tolerated dose of selinexor in combination with high-dose melphalan as a conditioning regimen for hematopoietic cell transplant in MM.
NCT03570983	2	allopurinol, carmustine, etoposide, cytarabine, melphalan	Comparing melphalan to carmustine, etoposide, cytarabine, and melphalan (beam) as a conditioning regimen for patients with MM undergoing high dose therapy followed by autologous stem cell reinfusion.
NCT02043847	1	radiation: total marrow irradiation drug:melphalan, filgrastim (g-csf)	Assessing patients with relapsed or refractory MM will receive high dose melphalan with autologous stem cell rescue. The pre-transplant conditioning is based on total marrow irradiation.

Abbreviations: ASCT, autologous stem cell transplantation; HSCT, hematopoietic stem cell transplantation; IMID, immunomodulatory drugs; MM, multiple myeloma; MPT, melphalan-prednisone- thalidomide; PBSC, peripheral blood stem cell; PI, proteasome inhibitors; VMP, bortezomib + melphalan + prednisone.

5. Clinical Usage of Combination Treatment with Melphalan to Improve the Effectiveness of Cancer Therapy

Oral administration of melphalan and prednisone as an immunosuppressant against MM was first described by Alexanian et al. in 1969 [70]. This combination resulted in an increase in the response rate and median survival of 6 months compared with melphalan alone [37].

The introduction of novel therapies is an important milestone in the treatment of MM that has markedly increased the survival of MM patients over the last two decades. The immunomodulatory drug thalidomide and its lenalidomide derivative, and the proteasome inhibitor bortezomib have improved the natural history of MM. The usage and optimization of the combination of these drugs have improved the OS of patients with MM. These drugs are currently included as induction and maintenance therapy [37,48].

The aim of induction treatment of MM patients eligible for transplantation is to obtain the earliest possible response for rapid disease control and the maximum possible response without excessive toxicity to safely enter ASCT. Three-drug combinations including a PI with an IMiD and dexamethasone are currently considered as the gold standard regimens [48,71]. The combination of bortezomib, thalidomide, and dexamethasone (VTD) shows superiority over the combinations of the two drugs thalidomide-dexamethasone (TD) and bortezomib-dexamethasone (VD) in terms of response rates and long-term outcomes [56,72,73]. Lenalidomide in combination with bortezomib and dexamethasone (RVD) has advantages over lenalidomide-dexamethasone (RD) and is associated with deeper and sustained responses and increased survival [74]. RVD is also associated with improved OS compared with the combination of bortezomib, cyclophosphamide and dexamethasone (VCD) [75]. Induction therapy with RVD showed high rates of deep response in the Phase III clinical trial, as more than one-third of NDMM patients eligible for transplantation were minimal residual disease (MRD) negative. RVD therapy has become the predominant induction regimen in the United States, although VTD or even VCD are feasible options depending on drug availability [74,76].

Another approach for patients with newly diagnosed MM who are not eligible for ASCT is the inclusion of daratumumab in standard therapy. Daratumumab is a human IgGκ monoclonal antibody against a CD38 cell surface marker that is expressed on the surface of hematopoietic cells, and is overexpressed on MM cells. CD38 acts as a receptor and as an ectoenzyme, thereby performing many functions, and its multi-faceted mechanisms of action include direct antitumor and immunomodulatory activity [17,77,78]. Daratumumab may also sensitize myeloma cells to other drugs by decreasing CD38 expression levels and/or restoring depleted T cell responses [78,79]. Combination therapy consisting of intravenous administration of daratumumab, bortezomib, melphalan, and prednisone (Dara-VMP) in patients with newly diagnosed MM who are not eligible for ASCT has been approved based on the results of the phase III ALCYONE trial. This therapy significantly extended the median PFS compared with therapy without daratumumab [77,80,81]. The MAIA study (NCT02252172) confirmed the efficacy and safety of daratumumab in NDMM patients who were not eligible for ASCT, although it compared the use of daratumumab in combination with lenalidomide and dexamethasone (Dara-RD) vs. lenalidomide and dexamethasone alone. The results of this phase III trial showed that treatment with daratumumab plus lenalidomide and dexamethasone results in significantly longer PFS than lenalidomide and dexamethasone alone; the risk of disease progression or death was 44% lower in the daratumumab group than in the control group. The addition of daratumumab improved the efficacy of both VMP and RD [82]. Choosing between Dara-VMP and Dara-RD can be difficult because there is currently no direct comparison of the two combinations. In Italy, a study performing a head-to-head comparison of VMP vs. RD (NCT03829371) is underway [83]. New melphalan treatment regimens are constantly being developed and are currently in the early stages of clinical trials (Table 3). The proposed therapies are, among others, based on the next-generation proteasome in-

hibitor carfilzomib (Kyprolis®) (NCT03556332) and the exportin 1 inhibitor selinexor (NCT0278 0609). Exportin 1 is overexpressed 2- to 4-fold in MM. Despite considerable advances, there are still problems with systemic toxicity, which hampers optimal VMP administration and extends the duration of treatment. Carfilzomib is a proteasome inhibitor that selectively and irreversibly binds to the constitutive proteasome and immunoproteasome. In a preclinical model, carfilzomib showed a stronger anti-myeloma effect than bortezomib. In addition, this new generation proteasome inhibitor has a different safety profile than bortezomib, showing a very low incidence of neuropathy [84]. The side effects of drugs were described in the phase III ENDEAVOR clinical trial. This study compared the safety profiles of the two regimens, carfilzomib and dexamethasone and bortezomib and dexamethasone. The safety profiles were similar, although the carfilzomib group showed a higher number of grade 3 adverse events and serious adverse events; however, these were deemed to be manageable and may be accounted for by the longer average treatment period than that of the bortezomib group [85].

6. "Weak Side" of Melphalan

High-dose therapy is burdened by plenty of side effects, significant morbidity, and rarely, treatment-related mortality [86]. Melphalan-induced side effects depend strongly on the dose [87]. HDM-ASCT leads to high-grade toxicities such as prolonged bone marrow suppression, nausea, vomiting [88], diarrhea, alopecia, rash, pruritus, mouth ulceration, hypersensitivity reactions [89], mucositis [67,90], infections (bacteremia, pneumonia, *Clostridium difficile*, fungal infection, sepsis, septic shock), vascular disorders, and thromboembolic events (pulmonary embolism, ischemic cardiopathy, ischemic stroke) [52]. Uncommon but potentially serious side effects include veno-occlusive disease, autologous graft-versus-host disease, graft failure [86], irreversible myelosuppression, hemolytic anemia, pulmonary fibrosis, anaphylaxis [89], nutrition problems, and weight loss [91].

A common side effect of high-dose melphalan therapy is cardiotoxicity, which is manifested as supraventricular tachycardia and atrial fibrillation [92,93]. The use of a high concentration of melphalan in myeloablative therapy in preparation for hematopoietic cell transplantation is highly hepatotoxic, as it is associated with high enzyme growth rates and acute liver damage due to sinusoidal obstruction syndrome. In most patients, serum aminotransferase levels increase markedly (5–20 times the normal upper limit) [89].

A population-based study that aimed to determine in-hospital mortality and complications after ASCT showed that elderly patients (>65 years) are at increased risk of complications after transplantation, including severe sepsis, acute respiratory failure, septic shock, pulmonary disease, acute renal failure, cardiac arrhythmias, and prolonged mechanical ventilation compared with patients under 65 years of age. In-hospital mortality in MM patients following ASCT is rare (1.5%), and in in-hospital mortality does not differ significantly between elderly and younger patients [94,95] (Figure 1).

HEMATOLOGIC TOXICITY

	[94]	[95]	[96]	[97]	[53]		
					G1-2	G3	G4
Anemia	11.8%	28.5%	NR	71.2%	51%	15%	1%
Febrile neutropenia	21.1%	16.5%	NR	NR	5%	17%	1%
Neutropenia	37.6%	NR	62%	NR	2%	6%	73%
Thrombocytopenia	7.1%	6.2%	NR	NR	2%	11%	72%

GASTROINTESTINAL

	[94]	[95]	[53]
Diarrhea	32.2%	NR	17%
Nausea or vomiting	29.5%	NR	15%
Mucositis	42.9%	44.7%	21%

RESPIRATORY

	[94]	[95]
Acute respiratory failure	1.8%	2.1%
Mechanical ventilation	1.8%	1.7%

INFECTIOUS

	[94]	[95]	[97]
Bacteremia	15.5%	NR	NR
Clostridium difficile	5.4%	5.6%	NR
Fungal infection	4.3%	0.4%	NR
Pneumonia	5.2%	5.8%	5.6%
Septic shock	1.5%	NR	NR
Sepsis	3.8%	15.0%	14.2%
Severe sepsis	2.0%	NR	NR

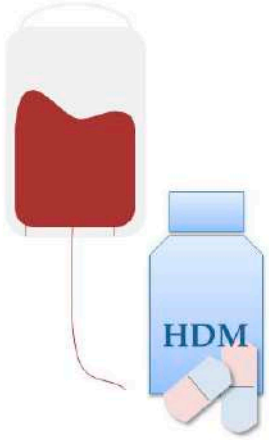

RENAL AND CARDIAC

	[94]	[95]	[97]
Acute renal failure	4.8%	5.8%	NR
Acute heart failure	1.9%	3%	NR
Cardiac arrhythmia	11.%	NR	14.8%

Figure 1. Side effects of HDM-ASCT therapy include: hematologic toxicity, infection, gastrointestinal complaints, pulmonary disease, acute renal failure, and cardiac arrhythmias. Figure based on [53,94–97]. G-grade (adverse events grades 1–2 occurring in at least 10% of patients and adverse events grades 3–4 in all patients [53]); NR, not reported.

7. Drug Resistance to Melphalan

Multiple drug resistance (MDR) contributes to the failure of cancer treatment leading to clinical relapse. MDR is the phenomenon by which cancer cells become resistant to a wide variety of unrelated drugs after exposure to a single chemotherapeutic agent. Despite advancements in MM treatment, drug resistance develops frequently during the antimyeloma therapy [98]. Melphalan is administered at low concentrations for initial therapy of patients that are not eligible for ASCT and is, at high concentration, the most common conditioning treatment for patients undergoing ASCT. VMP data from 59 patients newly diagnosed with MM were collected and analyzed. Of these patients, 78% received 9-cycle regimens. As many as 84% of patients underwent a reduction in the dose of drugs during the cycles. There were no statistically significant differences in PFS and OS between the high dose ($\geq$52.1 mg/m^2) and low dose (<52.1 mg/m^2) groups. The reason for reducing the dose of drugs in patients was non-hematological toxicity (92.7%) including peripheral neuropathy (36.6%). Chromosomal abnormalities were identified in 17 (28.8%) patients [99]. On the other hand, new clinical studies suggest that combination therapies may overcome drug resistance and may have additive or even synergistic effects with melphalan. In the phase III ALCYONE study, melphalan, as one of the drugs in the Dara-VMP regimen, was administered orally at a dose of 9 mg/m^2, once daily on days 1–4 of each cycle. Treatment with this combination led to grade 3 or 4 infection-related side effects and adverse infusion reactions despite increasing the OS of MM patients [100].

High doses of melphalan, as well as low doses administered over a long period of time, can lead to the development of drug resistance. A commonly accepted practice before ASCT is the administration of high doses of melphalan. A study analyzed 27 patients with advanced MM who received 220 mg/m^2 i.v. melphalan (HDM220) followed by ASCT. The study group consisted of nine patients with primary refractory disease and 18 patients who relapsed after

responding to the previous high-dose therapy. In the group of patients who had previously received intensive care and then relapsed, high-dose melphalan was effective only when the disease was chemosensitive. In patients with relapsed disease that showed resistance to treatment, increasing the melphalan dose was ineffective, with an event-free survival (EFS) rate of 0% after 1 year. The major adverse side effect was grade 4 mucositis in 63% of patients [101]. Another study analyzed 1964 patients to determine whether melphalan 200 mg/m^2 and melphalan 140 mg/m^2 are equally effective and tolerable at first single autologous transplantation episodes. Studies show that the disease state at the time of transplantation affects OS and PFS. These indicators were significantly greater in patients with poor clinical responses to induction therapies who received melphalan at a dose of 200 mg/m^2. Research has also shown that transplantation in patients with very good partial or complete response significantly preferred melphalan 140 mg/m^2 for OS (adjusted hazard ratio: 2.02) [102]. However, resistance to melphalan can occur and can lead to relapse after ASCT, and early relapse results in reduced survival [103]. Another study identified an association between polymorphisms of genes involved in DNA repair and melphalan resistance in MM. In a group of MM patients treated with high-dose melphalan and ASCT, single nucleotide polymorphisms of Poly (ADP-ribose) Polymerase *(PARP)*, RAD51 Recombinase *(RAD51)*, Proliferating Cell Nuclear Antigen *(PCNA)*, 8-Oxoguanine DNA Glycosylase *(OGG1),* Xeroderma Pigmentosum, Complementation Group C (*XPC*), Breast And Ovarian Cancer Susceptibility Protein 1 *(BRCA1)*, Excision Repair 1, Endonuclease Non-Catalytic Subunit (*ERCC1*), *BRCA1* Associated RING Domain 1 *(BARD1*), and Tumor Protein P53 Binding Protein 1 *(TP53BP1*) were associated with the outcome and OS of patients [104]. *ERCC2* and *XRCC3* gene polymorphisms are also associated with treatment outcome and drug resistance in patients treated with high-dose melphalan and ASCT [105]. Moreover, a combination of IMiD followed by HDM-ASCT leads to adverse outcomes associated with somatic mutations in the peripheral blood named clonal hematopoiesis of indeterminate potential (CHIP). In a study of 629 MM patients treated by ASCT, CHIP was detected in 136/629 patients (21.6%). Cell sequencing indicated a mutation mainly of DNA Methyltransferase 3 Alpha *(DNMT3A),* Tet Methylcytosine Dioxygenase 2 *(TET2),* Tumor Protein P53 *(TP53),* Additional Sex Combs Like 1, Transcriptional Regulator *(ASXL1)*, and Protein Phosphatase, Mg2+/Mn2+ Dependent 1D *(PPM1D)* genes, which were associated with a significantly reduced PFS and OS as compared to patients without CHIP. It is suggested that the presence of CHIP might be associated with worse outcomes, which indicates the benefit of performing research in this direction to newly diagnosed MM patients before ASCT [106]. A few mechanisms of resistance to melphalan have been described. A study reported that MM cells from patients previously treated with melphalan can repair DNA crosslinks in vitro [107]. DNA repair in the course of leukemia occurs mainly through the base excision repair and Fanconi anemia (FA)/BRCA repair pathways [108]. DNA damage in peripheral blood mononuclear cells is a predictor of clinical outcome in patients treated with high-dose melphalan and ASCT [109]. Moreover, genetic lesions affecting both alleles of the tumor suppressor gene *TP53* are major indicators of unfavorable prognosis in newly diagnosed MM [110]. Only 3.7% of patients are diagnosed with biallelic changes in the *TP53* gene in the form of a loss or mutation (called double-hit myeloma) [111]. By contrast, in a cohort of patients with relapsed MM, *TP53* abnormalities were identified in 45% of the patients, and the double hit event del(17p)/TP53mut or del(17p)/TP53del was present in 15% of the cases [112,113]. Second hits (del17p+ TP53 point mutation) abolish the remaining p53 activity and increase resistance to melphalan [110]. Deletions of chromosome 17p13 in *TP53* result in shorter median event-free survival (EFS) (14.6 months) and median OS (22.4 months) [114]. Increasingly accurate diagnostics of tumors in terms of damage to the *TP53* gene will facilitate therapeutic decisions that are beneficial for the patient [110].

Genetic and epigenetic changes in MM correlate with the stage of the disease. H3K9 acetylation at *c-myc* and cyclin D gene (*CCND1*) promoters increases in individual MM patients after melphalan treatment [115]. Moreover, platelet-derived growth factor BB (PDGF-BB) affects the expression of the *c-myc* gene through the *c-myc* promoter. PDGF-BB upregulates the expression of *myc* and at the same time reduces the sensitivity of

cancer cells to the effects of melphalan [116]. Nevertheless, in the presence of cytostatics, further growth of neoplastic cells is observed. This is mainly due to the development of multidrug resistance. Overexpression of ATP binding cassette (ABC) transporters in the plasma membrane of MM cells contributes to the increase of MDR. A study indicated that melphalan is a glycoprotein P (P-gp) substrate [117]. Multidrug resistance protein 1 (MDR1) and baculoviral inhibitor of apoptosis repeat-containing 5 (survivin) are overexpressed, and Bcl-2-like protein 11 (Bim) is suppressed in RPMI8226 melphalan resistant cells [107]. One study compared the expression of microRNAs (miRNAs) between MM resistant and sensitive cell lines. Decreased MM cell growth induced by inhibition of miR-221/222 plus melphalan is associated with upregulation of the pro-apoptotic BBC3/ Bcl-2-binding component 3 (PUMA) protein, a miR-221/222 target, as well as with modulation of the drug influx–efflux L-type amino acid transporter 1 (LAT1 or SLC7A5) and the ABC transporter ABCC1/ multidrug resistance-associated protein 1 (MRP1) [118]. Overexpression of the long non-coding RNA linc00515 is detected in LP1 melphalan-resistant cells, indicating that linc00515 not only promotes carcinogenesis but also enhances the drug resistance of MM cells. The authors confirmed that knockdown of linc00515 inhibits autophagy and chemoresistance by upregulating miR-140-5p and downregulating autophagy related 14 (ATG14) in MM cells [119].

Interactions between MM cells and the bone marrow microenvironment may also be a source of resistance to melphalan. Increased concentrations of interleukin-6 (IL-6) induced by high-dose melphalan facilitate the survival of melphalan-resistant cells. Patients treated with high-dose melphalan, stem cell transplantation, and anti-IL-6 antibody have a better chance of survival [120]. Several inhibitors of the IL-6/Janus kinase (JAK)/ Signal transducer and activator of transcription 3 (STAT3) pathway have been investigated to reduce the proliferation of MM cells [121]. Cell-adhesion mediated drug resistance (CAM-DR) to melphalan is induced in MM cell lines and in patient primary cells through adhesion to fibronectin or bone marrow stromal cells (BMSCs), which is mediated by very late antigen-4 (VLA4) integrin (α4β1) and VLA-5 (α5β1) [122]. Suppression of integrin β7 decreases adhesion to fibronectin and E-cadherin and inhibits CAM-DR to bortezomib or melphalan in MM cells [123]. Epithelial–mesenchymal transition (EMT)-like features mediated by integrin-α8 may also contribute to melphalan resistance. The mRNA expression of the growth factor receptors platelet-derived growth factor receptor alpha (PDGFRA) and platelet-derived growth factor receptor beta (PDGFRB) is upregulated following integrin-α8 overexpression [124]. Overexpression of ATP-dependent DNA helicase Q1 (RECQ1) helicase is also a factor that protects MM cells from melphalan cytotoxicity, as shown in a group of patients with poor outcomes. RECQ helicases are involved in the maintenance of chromosome stability during replication and recombination. RECQ1 overexpression protects MM cells against bortezomib or melphalan. The comet assay showed that despite overexpression of RECQ1, melphalan induced DNA damage, although the rate of DNA repair increased over time [125].

Research suggests that oxidative stress plays a role in inducing mutations and enhancing the growth of cancer cells. Deregulation of genes involved in the response to oxidative stress is associated with poor outcomes and melphalan resistance in MM. Melphalan induces reactive oxygen species and decreases glutathione (GSH) concentration. Pretreatment with a physiological concentration of GSH protects MM cells from melphalan-induced cell cycle arrest and cytotoxicity [126].

8. Attempts to Find a "Better Melphalan"

The currently available melphalan therapy is associated with decreased selectivity, high toxicity, and the potential for the development of drug resistance. Side effects and the development of resistance are, in fact, the main obstacles to most existing cancer therapies. Because of numerous undesirable actions related to melphalan therapies, the introduction of new treatment regimens is essential. According to the literature, the most promising research has led to the solutions listed in the next paragraphs.

8.1. Drug Carriers as a Way to Reduce Systemic Toxicity

Polymer-drug conjugates play an important role in improving the targeting of cancer cells and increasing the selectivity of anti-cancer drugs. Safe and efficient drug carriers capable of delivering anti-cancer drugs specifically to their destination without causing side effects are currently sought. Loss molecular weight anti-cancer drugs are conjugated to polymeric carriers to produce a polymer-drug conjugate, which generally improves the distribution of the anti-cancer drug molecule. The main roles of polymer-drug conjugates are as follows: (1) to increase the bioavailability of the chemotherapeutic agent by increasing the water solubility of poorly soluble or insoluble drugs; (2) to protect the drugs against deactivation, and to preserve their activity during circulation; (3) to reduce the body's immune response by decreasing the antigenic activity of the drug; and (4) to actively target the drug specifically to its site of action. In a study by Xu et al. [48], quantum dots (QDs) and melphalan were attached to a hyaluronic acid (HA) skeleton to synthesize a polymer-drug conjugate. The rate of drug release was significantly higher under acidic conditions (pH = 5.8), which simulate the microenvironment of cancer cells or tissues, than under basic conditions (pH = 7.4) [127]. HA binds specifically to various cancer cells that overexpress the CD44 receptor [128]. The advantage of HA is its property of natural degradation in the body. This process is mainly regulated by the enzyme hyaluronidase, which cleaves N-acetyl-d-glucosaminidic bonds in the HA backbone. Normal tissue is weakly alkaline (pH > 7.00), and tumor tissues and their surroundings are acidic (pH 4.5–6.0) with high expression of CD44 receptors that can direct HA-QDs-MEL towards tumor sites. Hence, the HA-QDs-MEL conjugate was stable in blood and normal tissues, and the drug was released in cancerous tissues. The HA-QDs-MEL conjugate shows excellent drug release properties, and may be a potential candidate for cancer chemotherapy with very high selectivity and low adverse effects on normal tissues [127].

To improve water solubility, systemic circulation time, and pharmacokinetic profiles, a research team led by Lu [129] synthesized and investigated a number of MEL-OCM-chitosan conjugates combined with various amino acid spacers (including glycine, l-phenylalanine, l-leucine, and 1-proline). OCM-chitosan shows no toxicity, high water solubility, biodegradability, and biocompatibility, and is thus one of the most useful candidate drug carriers. In addition, OCM-chitosan contains a large number of -COOH and-NH2 groups in the molecule that can be easily conjugated to drugs and proteins via a direct link or through a linker. MEL-OCM-chitosan conjugates show satisfactory water solubility compared with free melphalan. In vitro studies show that conjugates are stable in plasma, although they are rapidly degraded in an enzyme solution [129,130].

To solve the problems associated with the poor water solubility and rapid elimination of the drug, which reduce the specificity of melphalan, poly (amidoamine) (PAMAM) porphyrin conjugates with melphalan were synthesized and characterized. The dendrimeric conjugates show satisfactory water solubility compared with free melphalan. The size of the dendrimer plays a key role in controlling the drug content and the diameter of the melphalan conjugates. In vitro cellular cytotoxicity studies show that the dendrimeric conjugation strategy and the use of PAMAM dendritic arms as spacers improves the antitumor activity of the conjugates, which also show lower toxicity than free melphalan [131].

Melphalan-flufenamide (melflufen; L-melphalanyl-p-L-fluoro-phenylalanine ethyl) is an enzyme-activated melphalan prodrug that provides faster and greater intracellular melphalan accumulation in cancer cells. Melflufen is a newly constructed alkylating dipeptide that exhibits significantly higher anti-tumor activity than melphalan in vitro and in vivo. Chemically, melflufen is a dipeptide ethyl ester consisting of melphalan and para-fluoro-L-phenylalanine [132]. Melflufen, which is activated by hydrolytic cleavage of the peptide bond in a process that leads to high intracellular concentrations of melphalan, is capable of interacting with nucleic acids in cancer cells. Aminopeptidase N metalloprotease (APN; CD13) is directly involved in the activation of melflufen [133]. Melflufen targets tumor cells because it is a substrate for aminopeptidases that are overexpressed in cancer cells [134]. By using a simple peptide bond, melflufen activity is directed at cells expressing APN, thereby providing a peptidase-potentiated effect [132].

Melflufen transport to cells is rapid; it hydrolyzes in the cytoplasm almost immediately, forming a free and more hydrophilic form of melphalan [134]. Exposure of various tumor cells to melflufen in vitro results in at least a 10 to 20-fold higher intracellular concentration of melphalan than equimolar doses of melphalan [135]. Chauhan et al. [136] showed that melflufen is (1) 10 times more active against hematological cancer cells than melphalan; (2) blocks the migration of MM cells and inhibits tumor-associated angiogenesis; (3) induces DNA damage associated with γ-H2A histone family member X (γ-H2AX) and p53 induction; and (4) is associated with caspase activation and poly-ADP ribose polymerase (PARP) cleavage via melflufen-induced apoptosis. In vitro results were confirmed in a human MM xenograft model, which showed better inhibition of tumor growth and longer survival for melflufen than for melphalan. Melflufen causes rapid, strong, and irreversible DNA damage, which may explain its ability to overcome melphalan resistance in MM cells. Peripheral blood-derived mononuclear cells (PBMCs) are at least 10 times less sensitive to melphalan than cancer cells [132,136]. It shows high anti-tumor activity in cell lines and primary lymphoma cell cultures, as well as in a xenograft mouse model [135]. Numerous studies have also demonstrated the activity of melflufen in solid tumor cells [132,134,137,138]. Studies using solid tumor models show that melflufen induces at least a 10-fold higher melphalan load associated with high cytotoxicity against tumor cells [135]. When tested in primary cultures of human cells representing 20 different types of human malignancies, melflufen showed 50 to 100-fold greater potency than melphalan [134]. Melflufen can overcome melphalan resistance and induce synergistic anti-MM activity in combination with bortezomib, lenalidomide or dexamethasone. A recent multicenter, international, open-label, phase I–II study showed that melflufen is active in patients with relapsed and refractory MM (RRMM). These results demonstrate the feasibility of this scheme and support the initiation of additional clinical studies with melflufen in MM, both in combination with dexamethasone and in triplet with additional drug classes [139,140]. In a Phase I study, the established maximum tolerated dose was 40 mg melflufen plus dexamethasone. In Phase II, patients treated with combination therapy (meflufen + dexamethasone) achieved an ORR of 31%, achieved a clinical benefit ratio of 49%, duration of response was 8.4 months, PFS was 5.7 months, and OS was 20.7 months [141]. The phase II HORIZON clinical study (NCT02963493) is currently underway to assess the efficacy and safety of melflufen + dexamethasone in 157 patients with RRMM resistant to pomalidomide and/or daratumumab. The ongoing phase III OCEAN clinical trial (NCT03151811) is investigating the efficacy and safety of melflufen in combination with dexamethasone versus pomalidomide/dexamethasone in patients with RRMM. Eligible patients are refractory to both lenalidomide and last-line treatment and have not received prior pomalidomide. The primary endpoint is PFS and the secondary endpoints are OS, ORR, response time, and safety [141].The studies of melflufen and dexamethasone carried out recently by Richardson et al. showed clinically significant efficacy of these compounds and a manageable safety profile in patients with heavily pretreated RRMM, including those with triple-class-refractory and extramedullary disease [140]. Based on these results, in February 2021, the Food and Drug Administration approved PEPAXTO® (melphalan flufenamide, also known as melflufen), in combination with dexamethasone, to treat adult patients with relapsed or refractory multiple myeloma, who received at least four prior lines of treatment and whose disease is resistant to at least one proteasome inhibitor, one immunomodulatory drug, and one CD38-directed monoclonal antibody.

8.2. Chemical Modifications of the Melphalan Molecule as a Way to Improve Antitumor Activity

The structure of the melphalan molecule is noteworthy because of the presence of two modifiable functional groups: a carboxyl group and an amino group. These modifications provide extensive comparisons. Gajek et al. [142] synthesized and investigated new melphalan analogues modified in both functional groups. The resulting compounds are methyl and ethyl esters of melphalan (EE-MEL/EM-MEL), followed by melphalan esters also modified with a morpholine ring (EE-MOR-MEL/EM-MOR-MEL) or a dipropylene chain (EE-MOR-MEL/EM-DIPR-MEL). The derivatives were used to assess the potential antitumor properties of the structural changes compared with melphalan. The study was performed using three

models of hematological malignancy: RPMI8226 (myeloma cancer cells), THP1 (acute monocytic leukemia cells), and HL60 (promyelocytic leukemia cells). Modification of the carboxyl group by esterification of the compound showed the highest efficacy, and the results indicated that the ester group is necessary to increase the cytotoxic activity of melphalan [142,143]. In vitro studies conducted by this group of researchers showed that new MEL analogues have better antitumor activity than the parent drug. The compounds are characterized by high cytotoxicity and genotoxicity. Determining the potential ability of melphalan derivatives to activate cysteine proteases (caspase-3, -8, and -9), a characteristic mechanism in the course of programmed cell death, is an important element of the study, because the ability of drugs to induce apoptosis is considered an important criterion for assessing their therapeutic efficacy. This is the preferred type of cell death, as it is a physiological process that does not cause inflammation. The cellular response to the test compounds varies depending on the cell type. In MM cells, these compounds activate mechanisms of cell death other than apoptosis, such as mitotic disaster, autophagy, or necroptosis. Furthermore, the most promising derivatives (EE-MEL, EM-MEL, EM-MOR-MEL) were selected to assess the cytotoxic effects of these compounds on normal cells, namely, PBMCs. Chemical modifications, in particular esterification, can increase the antitumor activity of melphalan by increasing the lipophilicity of the drug. However, this study is limited to in vitro data only and must be verified by in vivo experiments [142] (Figure 2).

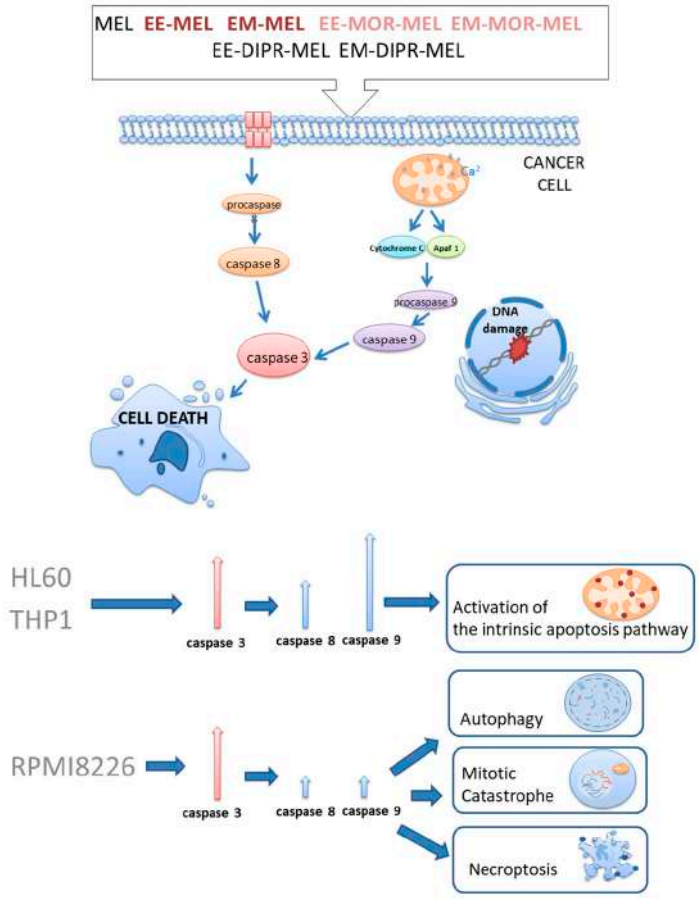

Figure 2. Mechanism of action of melphalan and new derivatives of melphalan. The cellular response to the test compounds varied depending on the cell type. Melphalan and its analogues activate the intrinsic pathway of apoptosis in acute monocytic leukemia cells and promyelocytic leukemia cells. In MM cells, these compounds activate mechanisms of cell death other than apoptosis, such as mitotic disaster, autophagy, or necroptosis. Figure is adapted from previous publication [142].

9. Conclusions

The use of high dose melphalan was first described by McElwain and Powles in 1983 [46]. After 37 years of its application in the treatment of MM therapy, the drug remains a part of treatment regimens. High-dose melphalan and ASCT are safe in patients with MM. Despite the current difficulty in accessing oncology centers, work on the development of further MM therapies has not stopped. Here, we described the use of therapy involving combinations of drugs with different mechanisms of action, including alkylating agents, immunomodulatory drugs, histone deacetylase inhibitors, proteasome inhibitors, and monoclonal antibodies. We showed that the use of various drugs is effective in the fight against MM. Changing the structure of melphalan by modifying the carboxyl and amino groups, as well as creating transporters for melphalan, are more effective strategies for the treatment of MM than the use of the unmodified melphalan molecule. The new analogues are characterized by higher cytotoxicity and genotoxicity, or the ability to induce apoptosis in hematological malignancies, and thus represent an important step in finding an effective anti-cancer therapy.

Author Contributions: A.P. and A.R. performed the literature research and wrote the manuscript. A.M. revised and supervised the manuscript. All authors have read and agreed to the published version of the manuscript.

Funding: Anastazja Poczta was supported by the Polish National Centre for Research and Development (POWR.03.02.00-00-I033/16-00).

Institutional Review Board Statement: Not applicable.

Informed Consent Statement: Not applicable.

Data Availability Statement: Not applicable.

Conflicts of Interest: The authors declare no conflict of interest.

References

1. Singh, R.K.; Kumar, S.; Prasad, D.N.; Bhardwaj, T.R. Therapeutic journery of nitrogen mustard as alkylating anticancer agents: Historic to future perspectives. *Eur. J. Med. Chem.* **2018**, *151*, 401–433. [CrossRef]
2. Liu, H.; Lightfoot, R.; Stevens, J.L. Activation of Heat Shock Factor by Alkylating Agents is Triggered by Glutathione Depletion and Oxidation of Protein Thiols. *J. Biol. Chem.* **1996**, *271*, 4805–4812. [CrossRef] [PubMed]
3. Bergel, F.; Stock, J.A. Cyto-active Amino-acid and Peptide Derivatives. *J. Chem. Soc.* **1954**, 2409–2417. [CrossRef]
4. Falco, P.; Bringhen, S.; Avonto, I.; Gay, F.; Morabito, F.; Boccadoro, M.; Palumbo, A. Melphalan and its role in the management of patients with multiple myeloma. *Expert Rev. Anticancer Ther.* **2007**, *7*, 945–957. [CrossRef]
5. Saikia, T.K. Developments in the Field of Myeloma in the Last Decade. *Indian J. Hematol. Blood Transfus.* **2017**, *33*, 3–7. [CrossRef]
6. Dehghanifard, A.; Kaviani, S.; Abroun, S.; Mehdizadeh, M.; Saiedi, S.; Maali, A.; Ghaffari, S.; Azad, M. Various Signaling Pathways in Multiple Myeloma Cells and Effects of Treatment on These Pathways. *Clin. Lymphoma Myeloma Leuk.* **2018**, *18*, 311–320. [CrossRef]
7. Pinto, V.; Bergantim, R.; Caires, H.R.; Seca, H.; Guimarães, J.E.; Vasconcelos, M.H. Multiple Myeloma: Available Therapies and Causes of Drug Resistance. *Cancers* **2020**, *12*, 407. [CrossRef]
8. Esma, F.; Salvini, M.; Troia, R.; Boccadoro, M.; LaRocca, A.; Pautasso, C. Melphalan hydrochloride for the treatment of multiple myeloma. *Expert Opin. Pharmacother.* **2017**, *18*, 1127–1136. [CrossRef] [PubMed]
9. Martino, M.; Paviglianiti, A.; Gentile, M.; Martinelli, G.; Cerchione, C. Allogenic stem cell transplantation in multiple myeloma: Dead or alive and kicking? *Panminerva Medica* **2021**, *62*, 234–243. [CrossRef]
10. Gentile, M.; Vigna, E.; Recchia, A.G.; Morabito, L.; Mendicino, F.; Giagnuolo, G.; Morabito, F. Bendamustine in multiple myeloma. *Eur. J. Haematol.* **2015**, *95*, 377–388. [CrossRef]
11. Chauhan, D.; Hideshima, T.; Rosen, S.; Reed, J.C.; Kharbanda, S.; Anderson, K.C. Apaf-1/Cytochrome c-independent and Smac-dependent Induction of Apoptosis in Multiple Myeloma (MM) Cells. *J. Biol. Chem.* **2001**, *276*, 24453–24456. [CrossRef]
12. Chauhan, D.; Pandey, P.; Ogata, A.; Teoh, G.; Treon, S.; Urashima, M.; Kharbanda, S.; Anderson, K.C. Dexamethasone induces apoptosis of multiple myeloma cells in a JNK/SAP kinase independent mechanism. *Oncogene* **1997**, *15*, 837–843. [CrossRef] [PubMed]
13. Chauhan, D.; Pandey, P.; Ogata, A.; Teoh, G.; Krett, N.; Halgren, R.; Rosen, S.; Kufe, D.; Kharbanda, S.; Anderson, K. Cytochrome c-dependent and -independent Induction of Apoptosis in Multiple Myeloma Cells. *J. Biol. Chem.* **1997**, *272*, 29995–29997. [CrossRef] [PubMed]

14. Yan, H.; Frost, P.; Shi, Y.; Hoang, B.; Sharma, S.; Fisher, M.; Gera, J.; Lichtenstein, A. Mechanism by Which Mammalian Target of Rapamycin Inhibitors Sensitize Multiple Myeloma Cells to Dexamethasone-Induced Apoptosis. *Cancer Res.* **2006**, *66*, 2305–2313. [CrossRef]
15. Burwick, N.; Sharma, S. Glucocorticoids in multiple myeloma: Past, present, and future. *Ann. Hematol.* **2019**, *98*, 19–28. [CrossRef] [PubMed]
16. Okazuka, K.; Ishida, T. Proteasome inhibitors for multiple myeloma. *Jpn. J. Clin. Oncol.* **2018**, *48*, 785–793. [CrossRef] [PubMed]
17. McKeage, K.; Lyseng-Williamson, K.A. Daratumumab in multiple myeloma: A guide to its use as monotherapy in the EU. *Drugs Ther. Perspect.* **2016**, *32*, 463–469. [CrossRef]
18. Lakshmaiah, K.C.; Jacob, L.A.; Aparna, S.; Lokanatha, D.; Saldanha, S.C. Epigenetic therapy of cancer with histone deacetylase inhibitors. *J. Cancer Res. Ther.* **2014**, *10*, 469–478.
19. Xu, W.S.; Parmigiani, R.B.; Marks, P.A. Histone deacetylase inhibitors: Molecular mechanisms of action. *Oncogene* **2007**, *26*, 5541–5552. [CrossRef]
20. Kumar, S.; Kaufman, J.L.; Gasparetto, C.; Mikhael, J.; Vij, R.; Pegourie, B.; Benboubker, L.; Facon, T.; Amiot, M.; Moreau, P.; et al. Efficacy of venetoclax as targeted therapy for relapsed/refractory t(11;14) multiple myeloma. *Blood* **2017**, *130*, 2401–2409. [CrossRef]
21. Vaxman, I.; Sidiqi, M.H.; Gertz, M. Venetoclax for the treatment of multiple myeloma. *Expert Rev. Hematol.* **2018**, *11*, 915–920. [CrossRef] [PubMed]
22. Quach, H.; Ritchie, D.; Stewart, A.K.; Neeson, P.; Harrison, S.; Smyth, M.J.; Prince, H.M. Mechanism of action of immunomodulatory drugs (IMiDS) in multiple myeloma. *Leukemia* **2009**, *24*, 22–32. [CrossRef]
23. Tachita, T.; Kinoshita, S.; Ri, M.; Aoki, S.; Asano, A.; Kanamori, T.; Yoshida, T.; Totani, H.; Ito, A.; Kusumoto, S.; et al. Expression, mutation, and methylation of cereblon-pathway genes at pre- and post-lenalidomide treatment in multiple myeloma. *Cancer Sci.* **2020**, *111*, 1333–1343. [CrossRef]
24. Lu, G.; Middleton, R.E.; Sun, H.; Naniong, M.; Ott, C.J.; Mitsiades, C.S.; Wong, K.-K.; Bradner, J.E.; Kaelin, W.G., Jr. The Myeloma Drug Lenalidomide Promotes the Cereblon-Dependent Destruction of Ikaros Proteins. *Science* **2014**, *343*, 305–309. [CrossRef]
25. Li, C.; Mei, H.; Hu, Y.; Guo, T.; Liu, L.; Jiang, H.; Tang, L.; Wu, Y.; Ai, L.; Deng, J.; et al. A Bispecific CAR-T Cell Therapy Targeting Bcma and CD38 for Relapsed/Refractory Multiple Myeloma: Updated Results from a Phase 1 Dose-Climbing Trial. *Blood* **2019**, *134*, 930. [CrossRef]
26. Kergueris, M.F.; Milpied, N.; Moreau, P.; Harousseau, J.L.; Larousse, C. Pharmacokinetics of high-dose melphalan in adults: Influence of renal function. *Anticancer Res.* **1994**, *14*, 2379–2382.
27. Bosanquet, A.G.; Gilby, E.D. Pharmacokinetics of oral and intravenous melphalan during routine treatment of multiple myeloma. *Eur. J. Cancer Clin. Oncol.* **1982**, *18*, 355–362. [CrossRef]
28. Pinguet, F.; Martel, P.; Fabbro, M.; Petit, I.; Canal, P.; Culine, S.; Astre, C.; Bressolle, F. Pharmacokinetics of high-dose intravenous melphalan in patients undergoing peripheral blood hematopoietic progenitor-cell transplantation. *Anticancer Res.* **1997**, *17*, 605–611.
29. Moreau, P.; Kergueris, M.-F.; Milpied, N.; Le Tortorec, S.; Mahé, B.; Bulabois, C.-E.; Rapp, M.-J.; Larousse, C.; Bataille, R.; Harousseau, J.-L. A pilot study of 220 mg/m^2 melphalan followed by autologous stem cell transplantation in patients with advanced haematological malignancies: Pharmacokinetics and toxicity. *Br. J. Haematol.* **1996**, *95*, 527–530. [CrossRef] [PubMed]
30. Reece, P.; Hill, H.; Green, R.; Morris, R.; Dale, B.; Kotasek, D.; Sage, R. Renal clearance and protein binding of melphalan in patients with cancer. *Cancer Chemother. Pharmacol.* **1988**, *22*, 348–352. [CrossRef] [PubMed]
31. Mougenot, P.; Fabbro, M.; Poujol, S.; Pinguet, F.; Culine, S.; Astre, C.; Bressolle, F. Population pharmacokinetics of melphalan, infused over a 24-hour period, in patients with advanced malignancies. *Cancer Chemother. Pharmacol.* **2004**, *53*, 503–512. [CrossRef]
32. Pinguet, F.; Culine, S.; Bressolle, F.; Astre, C.; Serre, M.P.; Chevillard, C.; Fabbro, M. A phase I and pharmacokinetic study of melphalan using a 24-hour continuous infusion in patients with advanced malignancies. *Clin. Cancer Res.* **2000**, *6*, 57–63. [PubMed]
33. Hersh, M.R.; Ludden, T.M.; Kuhn, J.G.; Knight, W.A. Pharmacokinetics of high dose melphalan. *Investig. New Drugs* **1983**, *1*, 331–334. [CrossRef] [PubMed]
34. Ehrsson, H.; Eksborg, S.; Osterborg, A.; Mellstedt, H.; Lindfors, A. Oral melphalan pharmacokinetics–relation to dose in patients with multiple myeloma. *Cancer Immunol. Immunother.* **1989**, *6*, 151–154.
35. Alberts, D.S.; Chang, S.Y.; Chen, H.-S.G.; Evans, T.L.; Moon, T.E. Oral melphalan kinetics. *Clin Pharmacol Ther.* **1979**, *26*, 737–745. [CrossRef]
36. Reece, P.A.; Kotasek, D.; Morris, R.G.; Dale, B.M.; Sage, R.E. The effect of food on oral melphalan absorption. *Cancer Chemother. Pharmacol.* **1986**, *16*, 194–197. [CrossRef]
37. Kuczma, M.; Ding, Z.-C.; Zhou, G. Immunostimulatory Effects of Melphalan and Usefulness in Adoptive Cell Therapy with Antitumor CD4+ T Cells. *Crit. Rev. Immunol.* **2016**, *36*, 179–191. [CrossRef]
38. Haines, D.R.; Fuller, R.W.; Ahmad, S.; Vistica, D.T.; Marquez, V.E. Selective cytotoxicity of a system L specific amino acid nitrogen mustard. *J. Med. Chem.* **1987**, *30*, 542–547. [CrossRef] [PubMed]
39. Vistica, D. Cytotoxicity as an indicator for transport mechanism: Evidence that murine bone marrow progenitor cells lack a high-affinity leucine carrier that transports melphalan in murine L1210 leukemia cells. *Blood* **1980**, *56*, 427–429. [CrossRef] [PubMed]

40. Begleiter, A.; Lam, H.Y.; Grover, J.; Froese, E.; Goldenberg, G.J. Evidence for active transport of melphalan by two amino acid carriers in L5178Y lymphoblasts in vitro. *Cancer Res.* **1979**, *39*, 353–359.
41. Goldenberg, G.; Lam, H.; Begleiter, A. Active carrier-mediated transport of melphalan by two separate amino acid transport systems in LPC-1 plasmacytoma cells in vitro. *J. Biol. Chem.* **1979**, *254*, 1057–1064. [CrossRef]
42. Singh, N.; Ecker, G.F. Insights into the Structure, Function, and Ligand Discovery of the Large Neutral Amino Acid Transporter 1, LAT1. *Int. J. Mol. Sci.* **2018**, *19*, 1278. [CrossRef] [PubMed]
43. Shaw, P.J.; Nath, C.E.; Lazarus, H.M. Not too little, not too much—Just right! (Better ways to give high dose melphalan). *Bone Marrow Transpl.* **2014**, *49*, 1457–1465. [CrossRef]
44. Maybury, B.; Cook, G.; Pratt, G.; Yong, K.; Ramasamy, K. Augmenting Autologous Stem Cell Transplantation to Improve Outcomes in Myeloma. *Biol. Blood Marrow Transpl.* **2016**, *22*, 1926–1937. [CrossRef]
45. Diamond, B.; MacLachlan, K.; Chung, D.J.; Lesokhin, A.M.; Landgren, C.O. Maintenance therapy and need for cessation studies in multiple myeloma: Focus on the future. *Best Pract. Res. Clin. Haematol.* **2020**, *33*, 101140. [CrossRef] [PubMed]
46. McElwain, T.J.; Powles, R.L. High-dose intravenous melphalan for plasma-cell leukaemia and myeloma. *Lancet* **1983**, *322*, 822–824. [CrossRef]
47. Mateos, M.-V.; Miguel, J.F.S. Management of multiple myeloma in the newly diagnosed patient. *Hematology* **2017**, *2017*, 498–507. [CrossRef] [PubMed]
48. Kazandjian, D.; Dew, A.; Hill, E. The changing role of high dose melphalan with stem cell rescue in the treatment of newly diagnosed multiple myeloma in the era of modern therapies-back to the future! *Best Pract. Res. Clin. Haematol.* **2020**, *33*, 101150. [CrossRef]
49. Cavo, M.; Rajkumar, S.V.; Palumbo, A.; Moreau, P.; Orlowski, R.; Bladé, J.; Sezer, O.; Ludwig, H.; Dimopoulos, M.A.; Attal, M.; et al. International Myeloma Working Group consensus approach to the treatment of multiple myeloma patients who are candidates for autologous stem cell transplantation. *Blood* **2011**, *117*, 6063–6073. [CrossRef]
50. Merz, M.; Neben, K.; Raab, M.S.; Sauer, S.; Egerer, G.; Hundemer, M.; Hose, D.; Kunz, C.; Heiß, C.; Ho, A.D.; et al. Autologous stem cell transplantation for elderly patients with newly diagnosed multiple myeloma in the era of novel agents. *Ann. Oncol.* **2014**, *25*, 189–195. [CrossRef]
51. Attal, M.; Harousseau, J.-L.; Stoppa, A.-M.; Sotto, J.-J.; Fuzibet, J.-G.; Rossi, J.-F.; Casassus, P.; Maisonneuve, H.; Facon, T.; Ifrah, N.; et al. A Prospective, Randomized Trial of Autologous Bone Marrow Transplantation and Chemotherapy in Multiple Myeloma. *N. Engl. J. Med.* **1996**, *335*, 91–97. [CrossRef]
52. Attal, M.; Lauwers-Cances, V.; Hulin, C.; Leleu, X.; Caillot, D.; Escoffre, M.; Arnulf, B.; Macro, M.; Belhadj, K.; Garderet, L.; et al. Lenalidomide, Bortezomib, and Dexamethasone with Transplantation for Myeloma. *N. Engl. J. Med.* **2017**, *376*, 1311–1320. [CrossRef]
53. Cavo, M.; Gay, F.; Beksac, M.; Pantani, L.; Petrucci, M.T.; Dimopoulos, M.A.; Dozza, L.; van der Holt, B.; Zweegman, S.; Oliva, S.; et al. Autologous haematopoietic stem-cell transplantation versus bortezomib–melphalan–prednisone, with or without bortezomib–lenalidomide–dexamethasone consolidation therapy, and lenalidomide maintenance for newly diagnosed multiple myeloma (EMN02/HO95): A multicentre, randomised, open-label, phase 3 study. *Lancet Haematol.* **2020**, *7*, e456–e468. [CrossRef] [PubMed]
54. Gay, F.; Oliva, S.; Petrucci, M.T.; Conticello, C.; Catalano, L.; Corradini, P.; Siniscalchi, A.; Magarotto, V.; Pour, L.; Carella, A.; et al. Chemotherapy plus lenalidomide versus autologous transplantation, followed by lenalidomide plus prednisone versus lenalidomide maintenance, in patients with multiple myeloma: A randomised, multicentre, phase 3 trial. *Lancet Oncol.* **2015**, *16*, 1617–1629. [CrossRef]
55. Palumbo, A.; Cavallo, F.; Gay, F.; Di Raimondo, F.; Ben Yehuda, D.; Petrucci, M.T.; Pezzatti, S.; Caravita, T.; Cerrato, C.; Ribakovsky, E.; et al. Autologous Transplantation and Maintenance Therapy in Multiple Myeloma. *N. Engl. J. Med.* **2014**, *371*, 895–905. [CrossRef] [PubMed]
56. Ntanasis-Stathopoulos, I.; Gavriatopoulou, M.; Kastritis, E.; Terpos, E.; Dimopoulos, M.A. Multiple myeloma: Role of autologous transplantation. *Cancer Treat. Rev.* **2020**, *82*, 101929. [CrossRef]
57. Al Hamed, R.; Bazarbachi, A.H.; Malard, F.; Harousseau, J.-L.; Mohty, M. Current status of autologous stem cell transplantation for multiple myeloma. *Blood Cancer J.* **2019**, *9*, 1–10. [CrossRef]
58. Cook, G.; Ashcroft, A.J.; Cairns, D.A.; Williams, C.D.; Brown, J.M.; Cavenagh, J.D.; Snowden, J.A.; Parrish, C.; Yong, K.; Cavet, J.; et al. The effect of salvage autologous stem-cell transplantation on overall survival in patients with relapsed multiple myeloma (final results from BSBMT/UKMF Myeloma X Relapse [Intensive]): A randomised, open-label, phase 3 trial. *Lancet Haematol.* **2016**, *3*, e340–e351. [CrossRef]
59. Stadtmauer, E.A.; Pasquini, M.C.; Blackwell, B.; Hari, P.; Bashey, A.; Devine, S.; Efebera, Y.; Ganguly, S.; Gasparetto, C.; Geller, N.; et al. Autologous Transplantation, Consolidation, and Maintenance Therapy in Multiple Myeloma: Results of the BMT CTN 0702 Trial. *J. Clin. Oncol.* **2019**, *37*, 589–597. [CrossRef] [PubMed]
60. Stojanoski, Z.; Georgievski, B.; Cevreska, L.; Stojanovic, A.; Pivkova, A.; Genadieva-Stavric, S.; Stankovic, S.; Karadzova-Stojanoska, A. Autologous stem-cell trans-plantation in patients with multiple myeloma. *Prilozi* **2008**, *29*, 265–279.
61. Garderet, L.; Morris, C.; Beksac, M.; Gahrton, G.; Schönland, S.; Yakoub-Agha, I.; Hayden, P.J. Are Autologous Stem Cell Transplants Still Required to Treat Myeloma in the Era of Novel Therapies? A Review from the Chronic Malignancies Working Party of the EBMT. *Biol. Blood Marrow Transpl.* **2020**, *26*, 1559–1566. [CrossRef] [PubMed]

62. Soekojo, C.Y.; Kumar, S.K. Stem-cell transplantation in multiple myeloma: How far have we come? *Ther. Adv. Hematol.* **2019**, *10*. [CrossRef]
63. Cook, G.; Royle, K.; O'Connor, S.; Cairns, D.A.; Ashcroft, A.J.; Williams, C.D.; Hockaday, A.; Cavenagh, J.D.; Snowden, J.A.; Ademokun, D.; et al. The impact of cytogenetics on duration of response and overall survival in patients with relapsed multiple myeloma (long-term follow-up results from BSBMT / UKMF Myeloma X Relapse [Intensive]): A randomised, open-label, phase 3 trial. *Br. J. Haematol.* **2019**, *185*, 450–467. [CrossRef] [PubMed]
64. Dimopoulos, M.A.; Gay, F.; Schjesvold, F.; Beksac, M.; Hajek, R.; Weisel, K.C.; Goldschmidt, H.; Maisnar, V.; Moreau, P.; Min, C.K.; et al. Oral ixazomib maintenance following autologous stem cell transplantation (TOURMALINE-MM3): A double-blind, randomised, placebo-controlled phase 3 trial. *Lancet* **2019**, *393*, 253–264. [CrossRef]
65. Rosiñol, L.; Oriol, A.; Rios, R.; Sureda, A.; Blanchard, M.J.; Hernández, M.T.; Martínez-Martínez, R.; Moraleda, J.M.; Jarque, I.; Bargay, J.; et al. Bortezomib, lenalidomide, and dexamethasone as induction therapy prior to autologous transplant in multiple myeloma. *Blood* **2019**, *134*, 1337–1345. [CrossRef] [PubMed]
66. Lahuerta, J.J.; Mateos, M.V.; Martínez-López, J.; Grande, C.; de La Rubia, J.; Rosinol, L.; Sureda, A.; García-Laraña, J.; Díaz-Mediavilla, J.; Hernández-García, M.T.; et al. Busulfan 12 mg/kg plus melphalan 140 mg/m^2 versus melphalan 200 mg/m^2 as conditioning regimens for autologous transplantation in newly diagnosed multiple myeloma patients included in the PETHEMA/GEM2000 study. *Haematologica* **2010**, *95*, 1913–1920. [CrossRef]
67. Bashir, Q.; Thall, P.F.; Milton, D.R.; Fox, P.S.; Kawedia, J.D.; Kebriaei, P.; Shah, N.; Patel, K.; Andersson, B.S.; Nieto, Y.L.; et al. Conditioning with busulfan plus melphalan versus melphalan alone before autologous haemopoietic cell transplantation for multiple myeloma: An open-label, randomised, phase 3 trial. *Lancet Haematol.* **2019**, *6*, e266–e275. [CrossRef]
68. Garderet, L.; Kuhnowski, F.; Berge, B.; Roussel, M.; Escoffre-Barbe, M.; Lafon, I.; Facon, T.; Leleu, X.; Karlin, L.; Perrot, A.; et al. Pomalidomide, cyclophosphamide, and dexamethasone for relapsed multiple myeloma. *Blood* **2018**, *132*, 2555–2563. [CrossRef]
69. Martino, M.; Gori, M.; Tripepi, G.; Recchia, A.G.; Cimminiello, M.; Provenzano, P.F.; Naso, V.; Ferreri, A.; Moscato, T.; Console, G.; et al. A comparative effectiveness study of lipegfilgrastim in multiple myeloma patients after high dose melphalan and autologous stem cell transplant. *Ann. Hematol.* **2020**, *99*, 331–341. [CrossRef]
70. Alexanian, R. Treatment for multiple myeloma. Combination chemotherapy with different melphalan dose regimens. *JAMA* **1969**, *208*, 1680–1685. [CrossRef]
71. Kazandjian, D.; Landgren, O. Delaying the use of high-dose melphalan with stem cell rescue in multiple myeloma is ready for prime time. *Clin. Adv. Hematol. Oncol.* **2019**, *17*, 559–568.
72. Terpos, E.; Ntanasis-Stathopoulos, I. Multiple Myeloma: Clinical Updates from the American Society of Hematology Annual Meeting 2018. *Clin. Lymphoma Myeloma Leuk.* **2019**, *19*, e324–e336. [CrossRef]
73. Sekine, L.; Ziegelmann, P.K.; Manica, D.; Pithan, C.D.F.; Sosnoski, M.; Morais, V.D.; Falcetta, F.S.; Ribeiro, M.R.; Salazar, A.P.; Ribeiro, R.A. Frontline treatment for transplant-eligible multiple myeloma: A 6474 patients network meta-analysis. *Hematol. Oncol.* **2019**, *37*, 62–74. [CrossRef] [PubMed]
74. Durie, B.G.M.; Hoering, A.; Abidi, M.H.; Rajkumar, S.V.; Epstein, J.; Kahanic, S.P.; Thakuri, M.; Reu, F.; Reynolds, C.M.; Sexton, R.; et al. Bortezomib with lenalidomide and dexamethasone versus lenalidomide and dexamethasone alone in patients with newly diagnosed myeloma without intent for immediate autologous stem-cell transplant (SWOG S0777): A randomised, open-label, phase 3 trial. *Lancet* **2017**, *389*, 519–527. [CrossRef]
75. Uttervall, K.; Bruchfeld, J.B.; Gran, C.; Wålinder, G.; Månsson, R.; Lund, J.; Gahrton, G.; Alici, E.; Nahi, H. Upfront bortezomib, lenalidomide, and dexamethasone compared to bortezomib, cyclophosphamide, and dexamethasone in multiple myeloma. *Eur. J. Haematol.* **2019**, *103*, 247–254. [CrossRef]
76. Goldschmidt, H.; Ashcroft, J.; Szabo, Z.; Garderet, L. Navigating the treatment landscape in multiple myeloma: Which combinations to use and when? *Ann. Hematol.* **2019**, *98*, 1–18. [CrossRef]
77. Syed, Y.Y. Daratumumab: A Review in Combination Therapy for Transplant-Ineligible Newly Diagnosed Multiple Myeloma. *Drugs* **2019**, *79*, 447–454. [CrossRef]
78. Morandi, F.; Horenstein, A.L.; Costa, F.; Giuliani, N.; Pistoia, V.; Malavasi, F. CD38: A Target for Immunotherapeutic Approaches in Multiple Myeloma. *Front. Immunol.* **2018**, *9*, 2722. [CrossRef] [PubMed]
79. Nooka, A.K.; Kaufman, J.L.; Hofmeister, C.C.; Joseph, N.S.; Heffner, T.L.; Gupta, V.A.; Sullivan, H.C.; Neish, A.S.; Dhodapkar, M.V.; Lonial, S. Daratumumab in multiple myeloma. *Cancer* **2019**, *125*, 2364–2382. [CrossRef]
80. Mateos, M.-V.; Dimopoulos, M.A.; Cavo, M.; Suzuki, K.; Jakubowiak, A.; Knop, S.; Doyen, C.; Lúcio, P.; Nagy, Z.; Kaplan, P.; et al. Daratumumab plus Bortezomib, Melphalan, and Prednisone for Untreated Myeloma. *N. Engl. J. Med.* **2018**, *378*, 518–528. [CrossRef]
81. Palumbo, A.; Chanan-Khan, A.; Weisel, K.; Nooka, A.K.; Masszi, T.; Beksac, M.; Spicka, I.; Hungria, V.; Munder, M.; Mateos, M.V.; et al. Daratumumab, Bortezomib, and Dexamethasone for Multiple Myeloma. *N. Engl. J. Med.* **2016**, *375*, 754–766. [CrossRef]
82. Facon, T.; Kumar, S.; Plesner, T.; Orlowski, R.Z.; Moreau, P.; Bahlis, N.; Basu, S.; Nahi, H.; Hulin, C.; Quach, H.; et al. Daratumumab plus Lenalidomide and Dexamethasone for Untreated Myeloma. *N. Engl. J. Med.* **2019**, *380*, 2104–2115. [CrossRef]
83. Bonello, F.; Grasso, M.; D'Agostino, M.; Celeghini, I.; Castellino, A.; Boccadoro, M.; Bringhen, S. The Role of Monoclonal Antibodies in the First-Line Treatment of Transplant-Ineligible Patients with Newly Diagnosed Multiple Myeloma. *Pharmaceuticals* **2020**, *14*, 20. [CrossRef]

84. Leleu, X.; Fouquet, G.; Richez, V.; Guidez, S.; Duhamel, A.; Machuron, F.; Karlin, L.; Kolb, B.; Tiab, M.; Araujo, C.; et al. Carfilzomib Weekly plus Melphalan and Prednisone in Newly Diagnosed Transplant-Ineligible Multiple Myeloma (IFM 2012-03): A Phase I Trial. *Clin. Cancer Res.* **2019**, *25*, 4224–4230. [CrossRef] [PubMed]
85. Dimopoulos, M.A.; Goldschmidt, H.; Niesvizky, R.; Joshua, D.; Chng, W.-J.; Oriol, A.; Orlowski, R.Z.; Ludwig, H.; Facon, T.; Hajek, R.; et al. Carfilzomib or bortezomib in relapsed or refractory multiple myeloma (ENDEAVOR): An interim overall survival analysis of an open-label, randomised, phase 3 trial. *Lancet Oncol.* **2017**, *18*, 1327–1337. [CrossRef]
86. Kazandjian, D.; Mo, C.C.; Landgren, O.; Richardson, P.G. The role of high-dose melphalan with autologous stem-cell transplant in multiple myeloma: Is it time for a paradigm shift? *Br. J. Haematol.* **2020**, *191*, 692–703. [CrossRef]
87. Kühne, A.; Sezer, O.; Heider, U.; Meineke, I.; Muhlke, S.; Niere, W.; Overbeck, T.; Hohloch, K.; Trümper, L.; Brockmöller, J.; et al. Population Pharmacokinetics of Melphalan and Glutathione S-transferase Polymorphisms in Relation to Side Effects. *Clin. Pharmacol. Ther.* **2008**, *83*, 749–757. [CrossRef]
88. Isoda, A.; Saito, R.; Komatsu, F.; Negishi, Y.; Oosawa, N.; Ishikawa, T.; Miyazawa, Y.; Matsumoto, M.; Sawamura, M.; Manaka, A. Palonosetron, aprepitant, and dexamethasone for prevention of nausea and vomiting after high-dose melphalan in autologous transplantation for multiple myeloma: A phase II study. *Int. J. Hematol.* **2016**, *105*, 478–484. [CrossRef]
89. LiverTox: Clinical and Research Information on Drug-Induced Liver Injury. Bethesda (MD): National Institute of Diabetes and Digestive and Kidney Diseases; 2012–2020. Melphalan. [Updated 2020 Jan 15]. Available online: https://www.ncbi.nlm.nih.gov/books/NBK548280/ (accessed on 18 April 2021).
90. Spencer, A.; Horvath, N.; Gibson, J.; Prince, H.M.; Herrmann, R.; Bashford, J.; Joske, D.; Grigg, A.; McKendrick, J.; Deveridge, S.; et al. Prospective randomised trial of amifostine cytoprotection in myeloma patients undergoing high-dose melphalan conditioned autologous stem cell transplantation. *Bone Marrow Transpl.* **2005**, *35*, 971–977. [CrossRef] [PubMed]
91. Chou, T.; Tobinai, K.; Uike, N.; Asakawa, T.; Saito, I.; Fukuda, H.; Mizoroki, F.; Ando, K.; Iida, S.; Ueda, R.; et al. Melphalan-Prednisolone and Vincristine-Doxorubicin-Dexamethasone Chemotherapy followed by Prednisolone/Interferon Maintenance Therapy for Multiple Myeloma: Japan Clinical Oncology Group Study, JCOG0112. *Jpn. J. Clin. Oncol.* **2011**, *41*, 586–589. [CrossRef]
92. Ma, L.-L.; Liu, Y.; Jia, S.-X.; Lv, H.-C.; Fang, M.-Y.; Xia, Y.-L. A case report: High dose melphalan as a conditioning regimen for multiple myeloma induces sinus arrest. *Cardio-Oncology* **2020**, *6*, 4. [CrossRef]
93. Tuzovic, M.; Mead, M.; Young, P.A.; Schiller, G.; Yang, E.H. Cardiac Complications in the Adult Bone Marrow Transplant Patient. *Curr. Oncol. Rep.* **2019**, *21*, 28. [CrossRef] [PubMed]
94. Sanchez, L.; Sylvester, M.; Parrondo, R.; Mariotti, V.; Eloy, J.A.; Chang, V.T. In-Hospital Mortality and Post-Transplantation Complications in Elderly Multiple Myeloma Patients Undergoing Autologous Hematopoietic Stem Cell Transplantation: A Population-Based Study. *Biol. Blood Marrow Transpl.* **2017**, *23*, 1203–1207. [CrossRef] [PubMed]
95. Savani, B.N.; Mukherjee, A.; Savani, G.T.; Ankit, C. Utilization Trend and in-Hospital Complications of Autologous Hematopoietic Stem Cell Transplantation in Multiple Myeloma in the United States: 13 Years Perspective. *Blood* **2014**, *124*, 3978. [CrossRef]
96. Bachier-Rodriguez, L.; Shah, G.L.; Knezevic, A.; Devlin, S.M.; Maloy, M.; Koehne, G.; Chung, D.J.; Landau, H.; Giralt, S.A. Engraftment Kinetics after High-Dose Melphalan Autologous Stem Cell Transplant in Patients with Multiple Myeloma. *Biol. Blood Marrow Transpl.* **2018**, *24*, S144. [CrossRef]
97. Bakalov, V.; Tang, A.; Shaikh, H.G.; Shah, S.; Chahine, Z.; Kaplan, R.B.; Lister, J.; Sadashiv, S. In-Hospital Complications and Outcomes of Autologous Stem Cell Transplantation in Multiple Myeloma Patients Older Than 65-Years Old in the United States: National Inpatient Sample Analysis, 2011–2015. *Blood* **2019**, *134*, 4764. [CrossRef]
98. Abdi, J.; Chen, G.; Chang, H. Drug resistance in multiple myeloma: Latest findings and new concepts on molecular mechanisms. *Oncotarget* **2013**, *4*, 2186–2207. [CrossRef] [PubMed]
99. Cho, S.-H.; Shin, H.-J.; Jung, K.S.; Kim, D.Y. Dose Adjustment Helps Obtain Better Outcomes in Multiple Myeloma Patients with Bortezomib, Melphalan, and Prednisolone (VMP) Treatment. *Turk. J. Hematol.* **2019**, *36*, 106–111. [CrossRef]
100. Hungria, V.; Martínez-Baños, D.M.; Mateos, M.-V.; Dimopoulos, M.A.; Cavo, M.; Heeg, B.; Garcia, A.; Lam, A.; Machnicki, G.; He, J.; et al. Daratumumab Plus Bortezomib, Melphalan, and Prednisone Versus Standard of Care in Latin America for Transplant-Ineligible Newly Diagnosed Multiple Myeloma: Propensity Score Matching Analysis. *Adv. Ther.* **2020**, *37*, 4996–5009. [CrossRef]
101. Moreau, P.; Milpied, N.; Mahé, B.; Juge-Morineau, N.; Rapp, M.-J.; Bataille, R.; Harousseau, J.-L. Melphalan 220 mg/m2 followed by peripheral blood stem cell transplantation in 27 patients with advanced multiple myeloma. *Bone Marrow Transpl.* **1999**, *23*, 1003–1006. [CrossRef]
102. Auner, H.W.; Iacobelli, S.; Sbianchi, G.; Knol-Bout, C.; Blaise, D.; Russell, N.H.; Apperley, J.F.; Pohlreich, D.; Browne, P.V.; Kobbe, G.; et al. Melphalan 140 mg/m 2 or 200 mg/m 2 for autologous transplantation in myeloma: Results from the Collaboration to Collect Autologous Transplant Outcomes in Lymphoma and Myeloma (CALM) study. A report by the EBMT Chronic Malignancies Working Party. *Haematologica* **2018**, *103*, 514–521. [CrossRef]
103. Kumar, S.K.; Dispenzieri, A.; Fraser, R.; Mingwei, F.; Akpek, G.; Cornell, R.; Kharfan-Dabaja, M.; Freytes, C.; Hashmi, S.; Hildebrandt, G.; et al. Early relapse after autologous hematopoietic cell transplantation remains a poor prognostic factor in multiple myeloma but outcomes have improved over time. *Leukemia* **2018**, *32*, 986–995. [CrossRef] [PubMed]
104. Dumontet, C.; Landi, S.; Reiman, T.; Perry, T.E.; Plesa, A.; Bellini, I.; Barale, R.; Pilarski, L.M.; Troncy, J.; Tavtigian, S.V.; et al. Genetic polymorphisms associated with outcome in multiple myeloma patients receiving high-dose melphalan. *Bone Marrow Transpl.* **2009**, *45*, 1316–1324. [CrossRef] [PubMed]

105. Vangsted, A.J.; Gimsing, P.; Klausen, T.W.; Nexø, B.A.; Wallin, H.; Andersen, P.; Hokland, P.; Lillevang, S.T.; Vogel, U. Polymorphisms in the genes ERCC2, XRCC3 and CD3EAP influence treatment outcome in multiple myeloma patients undergoing autologous bone marrow transplantation. *Int. J. Cancer* **2006**, *120*, 1036–1045. [CrossRef] [PubMed]
106. Mouhieddine, T.H.; Sperling, A.S.; Redd, R.; Park, J.; Leventhal, M.; Gibson, C.J.; Manier, S.; Nassar, A.H.; Capelletti, M.; Huynh, D.; et al. Clonal hematopoiesis is associated with adverse outcomes in multiple myeloma patients undergoing transplant. *Nat. Commun.* **2020**, *11*, 1–9. [CrossRef]
107. Tsubaki, M.; Satou, T.; Itoh, T.; Imano, M.; Komai, M.; Nishinobo, M.; Yamashita, M.; Yanae, M.; Yamazoe, Y.; Nishida, S. Overexpression of MDR1 and survivin, and decreased Bim expression mediate multidrug-resistance in multiple myeloma cells. *Leuk. Res.* **2012**, *36*, 1315–1322. [CrossRef]
108. Sousa, M.M.L.; Zub, K.A.; Aas, P.A.; Hanssen-Bauer, A.; Demirovic, A.; Sarno, A.; Tian, E.; Liabakk, N.B.; Slupphaug, G. An Inverse Switch in DNA Base Excision and Strand Break Repair Contributes to Melphalan Resistance in Multiple Myeloma Cells. *PLoS ONE* **2013**, *8*, e55493. [CrossRef]
109. Lin, J.; Raoof, D.A.; Thomas, D.G.; Greenson, J.K.; Giordano, T.J.; Robinson, G.S.; Bourner, M.J.; Bauer, C.T.; Orringer, M.B.; Beer, D.G. L-Type Amino Acid Transporter-1 Overexpression and Melphalan Sensitivity in Barrett's Adenocarcinoma. *Neoplasia* **2004**, *6*, 74–84. [CrossRef]
110. Munawar, U.; Roth, M.; Barrio, S.; Wajant, H.; Siegmund, D.; Bargou, R.C.; Kortüm, K.M.; Stühmer, T. Assessment of TP53 lesions for p53 system functionality and drug resistance in multiple myeloma using an isogenic cell line model. *Sci. Rep.* **2019**, *9*, 1–9. [CrossRef]
111. Walker, B.A.; Mavrommatis, K.; Wardell, C.P.; Ashby, T.C.; Bauer, M.; Davies, F.; Rosenthal, A.; Wang, H.; Qu, P.; Hoering, A.; et al. A high-risk, Double-Hit, group of newly diagnosed myeloma identified by genomic analysis. *Leukemia* **2019**, *33*, 159–170. [CrossRef]
112. Weinhold, N.; Ashby, C.; Rasche, L.; Chavan, S.S.; Stein, C.; Stephens, O.W.; Tytarenko, R.; Bauer, M.A.; Meissner, T.; Deshpande, S.; et al. Clonal selection and double-hit events involving tumor suppressor genes underlie relapse in myeloma. *Blood* **2016**, *128*, 1735–1744. [CrossRef]
113. Jovanović, K.K.; Escure, G.; Demonchy, J.; Willaume, A.; van de Wyngaert, Z.; Farhat, M.; Chauvet, P.; Facon, T.; Quesnel, B.; Manier, S. Deregulation and Targeting of TP53 Pathway in Multiple Myeloma. *Front. Oncol.* **2019**, *8*. [CrossRef]
114. Avet-Loiseau, H.; Attal, M.; Moreau, P.; Charbonnel, C.; Garban, F.; Hulin, C.; Leyvraz, S.; Michallet, M.; Yakoub-Agha, I.; Garderet, L.; et al. Genetic abnormalities and survival in multiple myeloma: The experience of the Intergroupe Francophone du Myélome. *Blood* **2007**, *109*, 3489–3495. [CrossRef]
115. Krejčí, J.; Harničarová, A.; Štreitová, D.; Hajek, R.; Pour, L.; Kozubek, S.; Bártová, E. Epigenetics of multiple myeloma after treatment with cytostatics and gamma radiation. *Leuk. Res.* **2009**, *33*, 1490–1498. [CrossRef] [PubMed]
116. Greco, C.; D'Agnano, I.; Vitelli, G.; Vona, R.; Marino, M.; Mottolese, M.; Zuppi, C.; Capoluongo, E.; Ameglio, F. C-Myc Deregulation is Involved in Melphalan Resistance of Multiple Myeloma: Role of PDGF-BB. *Int. J. Immunopathol. Pharmacol.* **2006**, *19*, 67–79. [CrossRef]
117. Abraham, J.; Salama, N.N.; Azab, A.K. The role of P-glycoprotein in drug resistance in multiple myeloma. *Leuk. Lymphoma* **2014**, *56*, 26–33. [CrossRef] [PubMed]
118. Gullà, A.; Di Martino, M.T.; Cantafio, M.E.G.; Morelli, E.; Amodio, N.; Botta, C.; Pitari, M.R.; Lio, S.G.; Britti, D.; Stamato, M.A.; et al. A 13 mer LNA-i-miR-221 Inhibitor Restores Drug Sensitivity in Melphalan-Refractory Multiple Myeloma Cells. *Clin. Cancer Res.* **2016**, *22*, 1222–1233. [CrossRef]
119. Lu, D.; Yang, C.; Zhang, Z.; Cong, Y.; Xiao, M. Knockdown of Linc00515 Inhibits Multiple Myeloma Autophagy and Chemoresistance by Upregulating miR-140-5p and Downregulating ATG14. *Cell Physiol Biochem.* **2018**, *48*, 2517–2527. [CrossRef] [PubMed]
120. Rossi, J.-F.; Fegueux, N.; Lu, Z.Y.; Legouffe, E.; Exbrayat, C.; Bozonnat, M.-C.; Navarro, R.; Lopez, E.; Quittet, P.; Daures, J.-P.; et al. Optimizing the use of anti-interleukin-6 monoclonal antibody with dexamethasone and 140 mg/m2 of melphalan in multiple myeloma: Results of a pilot study including biological aspects. *Bone Marrow Transpl.* **2005**, *36*, 771–779. [CrossRef] [PubMed]
121. Hunsucker, S.A.; Magarotto, V.; Kuhn, D.J.; Kornblau, S.M.; Wang, M.; Weber, D.M.; Thomas, S.K.; Shah, J.J.; Voorhees, P.M.; Xie, H.; et al. Blockade of interleukin-6 signalling with siltuximab enhances melphalan cytotoxicity in preclinical models of multiple myeloma. *Br. J. Haematol.* **2011**, *152*, 579–592. [CrossRef] [PubMed]
122. Damiano, J.S.; Cress, A.E.; Hazlehurst, L.A.; Shtil, A.A.; Dalton, W.S. Cell adhesion mediated drug resistance (CAM-DR): Role of in-tegrins and resistance to apoptosis in human myeloma cell lines. *Blood* **1999**, *93*, 1658–1667. [CrossRef] [PubMed]
123. Neri, P.; Ren, L.; Azab, A.K.; Brentnall, M.; Gratton, K.; Klimowicz, A.C.; Lin, C.; Duggan, P.; Tassone, P.; Mansoor, A.; et al. Integrin β7-mediated regulation of multiple myeloma cell adhesion, migration, and invasion. *Blood* **2011**, *117*, 6202–6213. [CrossRef] [PubMed]
124. Ryu, J.; Koh, Y.; Park, H.; Kim, D.Y.; Kim, D.C.; Byun, J.M.; Lee, H.J.; Yoon, A.S.-S. Highly Expressed Integrin-α8 Induces Epithelial to Mesenchymal Transition-Like Features in Multiple Myeloma with Early Relapse. *Mol. Cells* **2016**, *39*, 898–908. [CrossRef] [PubMed]
125. Viziteu, E.; Klein, B.; Basbous, J.; Lin, Y.-L.; Hirtz, C.; Gourzones, C.; Tiers, L.; Bruyer, A.; Vincent, L.; Grandmougin, C.; et al. RECQ1 helicase is involved in replication stress survival and drug resistance in multiple myeloma. *Leukemia* **2017**, *31*, 2104–2113. [CrossRef]

126. Gourzones, C.; Bellanger, C.; Lamure, S.; Gadacha, O.C.; de Paco, E.G.; Vincent, L.; Cartron, G.; Klein, B.; Moreaux, J. Antioxidant Defenses Confer Resistance to High Dose Melphalan in Multiple Myeloma Cells. *Cancers* **2019**, *11*, 439. [CrossRef]
127. Xu, H.; He, J.; Zhang, Y.; Fan, L.; Zhao, Y.; Xu, T.; Nie, Z.; Li, X.; Huang, Z.; Lu, B.; et al. Synthesis and in vitro evaluation of a hyaluronic acid–quantum dots–melphalan conjugate. *Carbohydr. Polym.* **2015**, *121*, 132–139. [CrossRef]
128. Mattheolabakis, G.; Milane, L.; Singh, A.P.; Amiji, M.M. Hyaluronic acid targeting of CD44 for cancer therapy: From receptor biology to nanomedicine. *J. Drug Target.* **2015**, *23*, 605–618. [CrossRef]
129. Lu, B.; Huang, D.; Zheng, H.; Huang, Z.; Xu, P.; Xu, H.; Yin, Y.; Liu, X.; Li, D.; Zhang, X. Preparation, characterization, and in vitro efficacy of O-carboxymethyl chitosan conjugate of melphalan. *Carbohydr. Polym.* **2013**, *98*, 36–42. [CrossRef]
130. Li, D.; Lu, B.; Huang, Z.; Xu, P.; Zheng, H.; Yin, Y.; Xu, H.; Liu, X.; Chen, L.; Lou, Y.; et al. A novel melphalan polymeric prodrug: Preparation and property study. *Carbohydr. Polym.* **2014**, *111*, 928–935. [CrossRef]
131. Ramírez-Arroniz, J.C.; Klimova, E.M.; Pedro-Hernández, L.D.; Organista-Mateos, U.; Cortez-Maya, S.; Ramírez-Ápan, T.; Nieto-Camacho, A.; Calderón-Pardo, J.; Martínez-García, M. Water-soluble porphyrin-PAMAM-conjugates of melphalan and their anticancer activity. *Drug Dev. Ind. Pharm.* **2018**, *44*, 1342–1349. [CrossRef]
132. Wickström, M.; Nygren, P.; Larsson, R.; Harmenberg, J.; Lindberg, J.; Sjöberg, P.; Jerling, M.; Lehmann, F.; Richardson, P.; Anderson, K.; et al. Melflufen—A peptidase-potentiated alkylating agent in clinical trials. *Oncotarget* **2017**, *8*, 66641–66655. [CrossRef] [PubMed]
133. Strese, S.; Wickström, M.; Fuchs, P.F.; Fryknäs, M.; Gerwins, P.; Dale, T.; Larsson, R.; Gullbo, J. The novel alkylating prodrug melflufen (J1) inhibits angiogenesis in vitro and in vivo. *Biochem. Pharmacol.* **2013**, *86*, 888–895. [CrossRef] [PubMed]
134. Berglund, Å.; Ullén, A.; Lisyanskaya, A.; Orlov, S.; Hagberg, H.; Tholander, B.; Lewensohn, R.; Nygren, P.; Spira, J.; Harmenberg, J.; et al. First-in-human, phase I/IIa clinical study of the peptidase potentiated alkylator melflufen administered every three weeks to patients with advanced solid tumor malignancies. *Investig. New Drugs* **2015**, *33*, 1232–1241. [CrossRef]
135. Delforoush, M.; Strese, S.; Wickström, M.; Larsson, R.; Enblad, G.; Gullbo, J. In vitro and in vivo activity of melflufen (J1) in lymphoma. *BMC Cancer* **2016**, *16*, 263. [CrossRef]
136. Chauhan, D.; Ray, A.; Viktorsson, K.; Spira, J.; Paba-Prada, C.; Munshi, N.; Richardson, P.; Lewensohn, R.; Anderson, K.C. In Vitro and In Vivo Antitumor Activity of a Novel Alkylating Agent, Melphalan-Flufenamide, against Multiple Myeloma Cells. *Clin. Cancer Res.* **2013**, *19*, 3019–3031. [CrossRef]
137. Viktorsson, K.; Shah, C.-H.; Juntti, T.; Hååg, P.; Zielinska-Chomej, K.; Sierakowiak, A.; Holmsten, K.; Tu, J.; Spira, J.; Kanter, L.; et al. Melphalan-flufenamide is cytotoxic and potentiates treatment with chemotherapy and the Src inhibitor dasatinib in urothelial carcinoma. *Mol. Oncol.* **2016**, *10*, 719–734. [CrossRef]
138. Carlier, C.; Strese, S.; Viktorsson, K.; Velander, E.; Nygren, P.; Uustalu, M.; Juntti, T.; Lewensohn, R.; Larsson, R.; Spira, J.; et al. Preclinical activity of melflufen (J1) in ovarian cancer. *Oncotarget* **2016**, *7*, 59322–59335. [CrossRef]
139. Richardson, P.G.; Bringhen, S.; Voorhees, P.; Plesner, T.; Mellqvist, U.-H.; Reeves, B.; Paba-Prada, C.; Zubair, H.; Byrne, C.; Chauhan, D.; et al. Melflufen plus dexamethasone in relapsed and refractory multiple myeloma (O-12-M1): A multicentre, international, open-label, phase 1–2 study. *Lancet Haematol.* **2020**, *7*, e395–e407. [CrossRef]
140. Richardson, P.G.; Oriol, A.; Larocca, A.; Bladé, J.; Cavo, M.; Rodriguez-Otero, P.; Leleu, X.; Nadeem, O.; Hiemenz, J.W.; Hassoun, H.; et al. Melflufen and Dexamethasone in Heavily Pretreated Relapsed and Refractory Multiple Myeloma. *J. Clin. Oncol.* **2021**, *39*, 757–767. [CrossRef] [PubMed]
141. Schjesvold, F.; Robak, P.; Pour, L.; Aschan, J.; Sonneveld, P. OCEAN: A randomized Phase III study of melflufen + dexamethasone to treat relapsed refractory multiple myeloma. *Futur. Oncol.* **2020**, *16*, 631–641. [CrossRef] [PubMed]
142. Gajek, A.; Poczta, A.; Łukawska, M.; Adamczewska, V.-C.; Tobiasz, J.; Marczak, A. Chemical modification of melphalan as a key to improving treatment of haematological malignancies. *Sci. Rep.* **2020**, *10*, 4479. [CrossRef]
143. Antoni, F.; Bernhardt, G. Derivatives of nitrogen mustard anticancer agents with improved cytotoxicity. *Arch. Pharm.* **2020**, e2000366. [CrossRef]

PUBLIKACJA NR II

Gajek A*****., **Poczta A.***, Łukawska M., Cecuda-Adamczewska V., Tobiasz J.; Marczak A.; *Chemical modification of melphalan as a key to improving treatment of haematological malignancies;* Sci Rep; 2020; 11;10(1):4479.

*****równoważny wkład autorów

- **Praca doświadczalna**
- **IF: 4.379**
- **punkty MEiN: 140 pkt.**

SCIENTIFIC REPORTS
nature research

OPEN

Chemical modification of melphalan as a key to improving treatment of haematological malignancies

Arkadiusz Gajek[1,3*], Anastazja Poczta[1,3], Małgorzata Łukawska[2], Violetta Cecuda-Adamczewska[2], Joanna Tobiasz[2] & Agnieszka Marczak[1]

Chemical modification of known, effective drugs is one method to improve chemotherapy. Thus, the object of this study was to generate melphalan derivatives with improved cytotoxic activity in human cancer cells (RPMI8226, HL60 and THP1). Several melphalan derivatives were synthesised, modified in their two important functional groups. Nine analogues were tested, including melphalan compounds modified: only at the amino group, by replacing the amine with an amidine group containing a morpholine ring (MOR-MEL) or with an amidino group and dipropyl chain (DIPR-MEL); only at the carboxyl group to form methyl and ethyl esters of melphalan (EM-MEL, EE-MEL); and in a similar manner at both functional groups (EM-MOR-MEL, EE-MOR-MEL, EM-DIPR-MEL, EE-DIPR-MEL). Melphalan derivatives were evaluated for cytotoxicity (resazurin viability assay), genotoxicity (comet assay) and the ability to induce apoptosis (terminal deoxynucleotidyl transferase dUTP nick end labelling, TUNEL, phosphatidylserine externalisation, chromatin condensation, activity of caspases 3/7, 8 and 9 and intracellular concentration of calcium ions) in comparison with the parent drug. Almost all derivatives, with the exception of MOR-MEL and DIPR-MEL, were found to be more toxic than melphalan in all cell lines evaluated. Treatment of cultures with the derivatives generated a significant higher level of DNA breaks compared to those treated with melphalan, especially after longer incubation times. In addition, all the melphalan derivatives demonstrated a high apoptosis-inducing ability in acute monocytic and promyelocytic leukemia cells. This study showed that the mechanism of action of the tested compounds differed depending on the cell line, and allowed the selection of the most active compounds for further, more detailed investigations.

Cancer is considered to be one of the most serious health problems. Multiple myeloma (MM) is malignant plasma cell disorder that is characterized by the presence of clonal plasma cell proliferation in bone marrow and over production of monoclonal paraprotein in the blood and/or urine[1,2].

The nitrogen mustards, as alkylating agents, belong to the earliest effective antitumor drugs used in cancer chemotherapy[3]. This cytotoxic drug exerts its pharmacological activity by inducing interstrand links in the main DNA groove, crosslinking of two strands, and preventing DNA replication, resulting in cell death. At the molecular level, individual pairs of nitrogen generate a strained intermediate "aziridinium ion" that is very reactive to cell DNA, and binds to the N7 nitrogen on the DNA base guanine. This linkage represents the most toxic of all alkylation events[4,5]. The alkylating agent- melphalan (MEL) has been used in the treatment of several types of haematological malignancies and solid tumor[6]. Nowadays, clinical usage of melphalan is limited to multiple myeloma treatment[7]. An observation that has fundamentally changed the standard of MM treatment, was that melphalan used in large doses (100 mg/m^2 and more) breaks myeloma resistance to low doses very effectively. Melphalan at these doses also destroys healthy hematopoietic cells, so such treatment requires prior collection of these cells from the patient (usually from peripheral blood), storage and transplantation after melphalan administration

[1]Department of Medical Biophysics, Institute of Biophysics, Faculty of Biology and Environmental Protection, University of Lodz, Pomorska 141/143, 90-236, Lodz, Poland. [2]ŁUKASIEWICZ Research Network-Institute of Biotechnology and Antibiotics, 5 Staroscinska St., 02-516, Warsaw, Poland. [3]These authors contributed equally: Arkadiusz Gajek and Anastazja Poczta. *email: arkadiusz.gajek@biol.uni.lodz.pl

(autologous stem cell transplantation, ASCT). This therapy involves significant toxicity and can therefore be used only in younger patients, not affected by significant accompanying diseases. Thus, the possibility of using this treatment has become the basis for the division of patients into two main categories: patients eligible for high doses of melphalan and transplantation of their own hematopoietic cells and patients not eligible for such treatment. High-dose melphalan (range: 140–200 mg/m^2) plus ASCT currently serves as the standard treatment approach for patients with newly diagnosed, transplant-eligible multiple myeloma[1,2,6].

The occurrence of drug resistant, lack of selectivity and high toxicity are the primary limiting factor for the long-term success of this treatment[2,3,8]. Side effects are mainly restricted to the bone marrow, though at very high doses it also involves the gastrointestinal tract and bone marrow supression[9]. For these reasons, there is an urgent need to develop new antitumour drugs for a wide variety of tumours, especially those showing primary resistance to conventional therapy, or that have developed resistance after treatment with conventional cancer chemotherapies.

Although much effort has been made to find new melphalan derivatives that will overcome all the above-mentioned problems and increase uptake of the drug into cells, none of them has found a clinical application[4,10,11]. Our previous studies have indicated that oxazoline and formamidine modification of anthracyclines are promising way of enhancing a drug, compared to its native form. The conclusion from that study was this type of improvement is detrimental to cancer cells, making it a potential approach in devising cell therapy strategies[12–18]. Although belonging to a completely different group of anticancer compounds, we decided to verify the effectiveness of these modifications for the anti-cancer activity of melphalan, and to select the most active compounds for further, more detailed studies. Due to the presence of two important functional groups on the melphalan molecule, modifications were made at both sites, -COOH and -NH2, to assess their effect on the cytotoxic properties of the compound. The derivatives were also assayed to determine which modification was the best. Our research aims not only to increase the antitumor activity of melphalan but also to extend its spectrum of activity (promyelocytic leukemia and acute monocytic leukemia).

Chemical modifications included a carboxyl group, with synthesised compounds being methyl and ethyl esters (EM-MEL, EE-MEL). In addition, these derivatives were modified at their amino groups by replacing the amine group with an amidine group containing a morpholine ring (EM-MOR-MEL, EE-MOR-MEL), or with an amidine group and dipropyl chain (EM-DIPR-MEL, EE-DIPR-MEL). For a systematic analysis of structure-activity relationships, melphalan derivatives modified only at the amino group were also added to the study. These modifications were made in the same manner as described above; however, the compounds were not modified at the carboxyl group (MOR-MEL, DIPR-MEL). This group of analogues were used to assess the potential anticancer properties of the structural changes in comparison to the parent compound, melphalan.

Results

Cytotoxicity of melphalan and its derivatives in selected human cell line models. Sensitivities of myeloma cells (RPMI8226), acute promyelocytic leukemia cells (HL60) and acute monocytic leukemia cells (THP1) to melphalan and its derivatives were estimated from the drugs half maximal inhibitory (IC_{50}) concentrations. Figure 1 shows the influence of the tested compounds on the viability of human cancer cells, as estimated by the resazurin viability assay.

The modifications of the melphalan molecule were designed to evaluate, the importance and desirability of modifications of melphalan at two functional groups of its molecule, with as few compounds as possible.

(a) *The cytotoxicity of the parent drug, melphalan (**MEL**)*
The individual cell lines exhibited notably different sensitivities to the reference drug. The IC_{50} values for melphalan in RPMI8226, THP1 and HL60 cells were 8.9 µM, 6.26 µM and 3.78 µM, respectively.

(b) *The cytotoxicity of melphalan compounds modified only at the amino group by replacing the amine group with an amidine group containing a morpholine ring or an amidino group with a dipropyl chain (**MOR-MEL, DIPR-MEL**)*
Chemical modifications only at the amine group abolish the cytotoxic activity of melphalan against all the investigated cancer cell lines. MOR-MEL and DIPR-MEL derivatives did not differentially influence cell viability to any measurable extent during the incubation period.

(c) *The cytotoxicity of melphalan compounds modified only at carboxyl group: methyl and ethyl esters of melphalan (**EE-MEL** and **EM-MEL**)*
By contrast, modifications only at the carboxyl group had the opposite effect, with EM-MEL and EE-MEL derivatives showing the highest activity of any of the compounds against myeloma cancer cells. In general, melphalan esters were considerably more cytotoxic, having approximately an 8-fold lower IC_{50} concentration (1.05 µM for EM-MEL and 1.17 µM for EE-MEL) than the unmodified drug (8.9 µM) in RPMI8226 cell line, 5.5-fold lower IC_{50} concentration (0.77 µM for EM-MEL and 0.7 µM for EE-MEL) in HL60 cell line and 20-fold lower IC_{50} concentration (0.32 µM for EM-MEL and 0.35 µM for EE-MEL) in THP1 cell in comparison to MEL (3.78 µM-HL60 and 6.26 µM-THP1).

(d) *The cytotoxicity of melphalan compounds modified at both the amino and carboxyl functional groups (**EE-MOR-MEL, EM-MOR-MEL** and **EE-DIPR-MEL, EM-DIPR-MEL**)*

Cytotoxicity of EE-MOR-MEL, EM-MOR-MEL, EE-DIPR-MEL and EM-DIPR-MEL to RPMI8226 cancer cells were considerably lower than for melphalan compounds modified only at the carboxyl group. However, IC_{50} concentrations obtained for this group were still lower than that observed for MEL. EE-MOR-MEL showed the highest activity ($IC_{50} = 3.13$ µM), more than 2.8-fold that of melphalan. EM-MOR-MEL showed the second highest activity ($IC_{50} = 3.6$ µM) in this group. EE-DIPR-MEL and EM-DIPR-MEL had IC_{50} values of 5.94 µM and 4.85 µM, respectively, in both cases showing greater activity than MEL ($IC_{50} = 8.9$ µM).

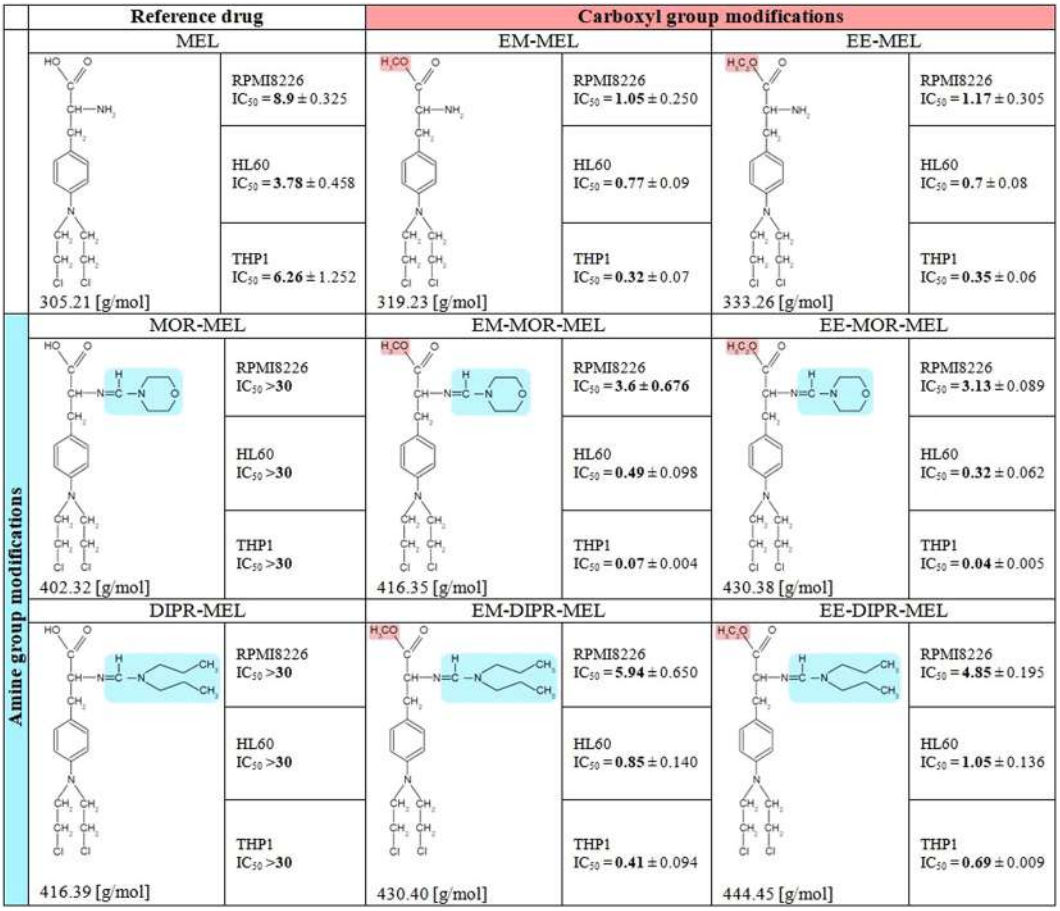

Figure 1. $IC_{50} \pm SD$ values [μM] of compounds in RPMI8226, HL60 and THP1 human cancer cell lines.

By contrast, in leukemia cells, both investigated cell lines were significantly more sensitive to EE-MOR-MEL and EM-MOR-MEL than myeloma cancer cells. IC_{50} concentrations obtained for the most active compound (EE-MOR-MEL) were around 12- (HL60, $IC_{50} = 0.32\,\mu M$) and 160- (THP1, $IC_{50} = 0.04\,\mu M$) fold lower than that for the unmodified drug (MEL). EE-DIPR-MEL ($IC_{50} = 1.05\,\mu M$ in HL60, $IC_{50} = 0.69\,\mu M$ in THP1), EM-DIPR-MEL ($IC_{50} = 0.85\,\mu M$ in HL60, $IC_{50} = 0.41\,\mu M$ in THP1), though having lower cytotoxity, showed similar changes in IC_{50} values to the methyl and ethyl esters (EE-MOR-MEL, EM-MOR-MEL).

Taken together, these results indicate that the ester group was essential for the compounds high cytotoxicity. Additional substituents at the amino group, whether with an amidine group containing a morpholine ring or an amidino group with a dipropyl chain, decreased (RPMI8226 cells) or enhanced (THP1 and HL60 cells) the activity. Due to the observed toxic effects, measurements of phosphatidylserine externalisation, chromatin condensation, labelling of Br-dUTP to 3′OH ends of single- and double-stranded DNA fragments and comet assay experiments were performed for all compounds at concentrations of 0.3 μM for THP1 cells, 0.7 μM for HL60 cells and 3 μM for RPMI8226 cells.

We performed study to evaluate the cytotoxic effect of selected melphalan derivatives (EE-MEL, EM-MEL and EM-MOR-MEL) on normal peripheral blood-derived mononuclear cells (PBMC). Reduced cytotoxicity of the tested derivatives in PBMC and increased cytotoxic effect in tumor cell lines were observed. The IC_{50} values for esters of melphalan in PMBC (EE-MEL - $IC_{50} = 2.20 \pm 0.25\,\mu M$; EM – MEL - $IC_{50} = 2.39 \pm 1.08\,\mu M$) was around 4.5-fold higher than leukemia and 2-fold higher for multiple myeloma cells. The most beneficial effect (the biggest difference between normal and cancer cells) was noted for EM-MOR-MEL. The IC_{50} value was around 90-fold higher in PBMC ($IC_{50} = 6.41 \pm 0.85\,\mu M$) in comparison to THP1, 15-fold in HL60 and 2-fold in RPMI8226 cells.

Evaluation of impact on parameters directly related to apoptotic processes - measurement of phosphatidylserine externalisation and chromatin condensation. To evaluate the possible role of apoptotic features on the cytotoxicity of melphalan and its derivatives, the mode of cell death triggered by these compounds was investigated. Using annexin V/propidium iodide and Vybrant® DyeCycle™ Violet/SYTOX® AADvanced™ double staining methods, quantitative (Fig. 2) and qualitative (Fig. 3) assessments were made of molecular events connected with apoptosis. The average effect of unmodified and modified melphalan compounds on cell populations, as well as morphological changes at the single cell level was investigated.

As opposed to RPMI8226 and THP1 cells, HL60 cells were a little bit more susceptible to annexin V externalisation after exposure to the drugs. In all investigated cancer cells, following exposure to all derivatives, a

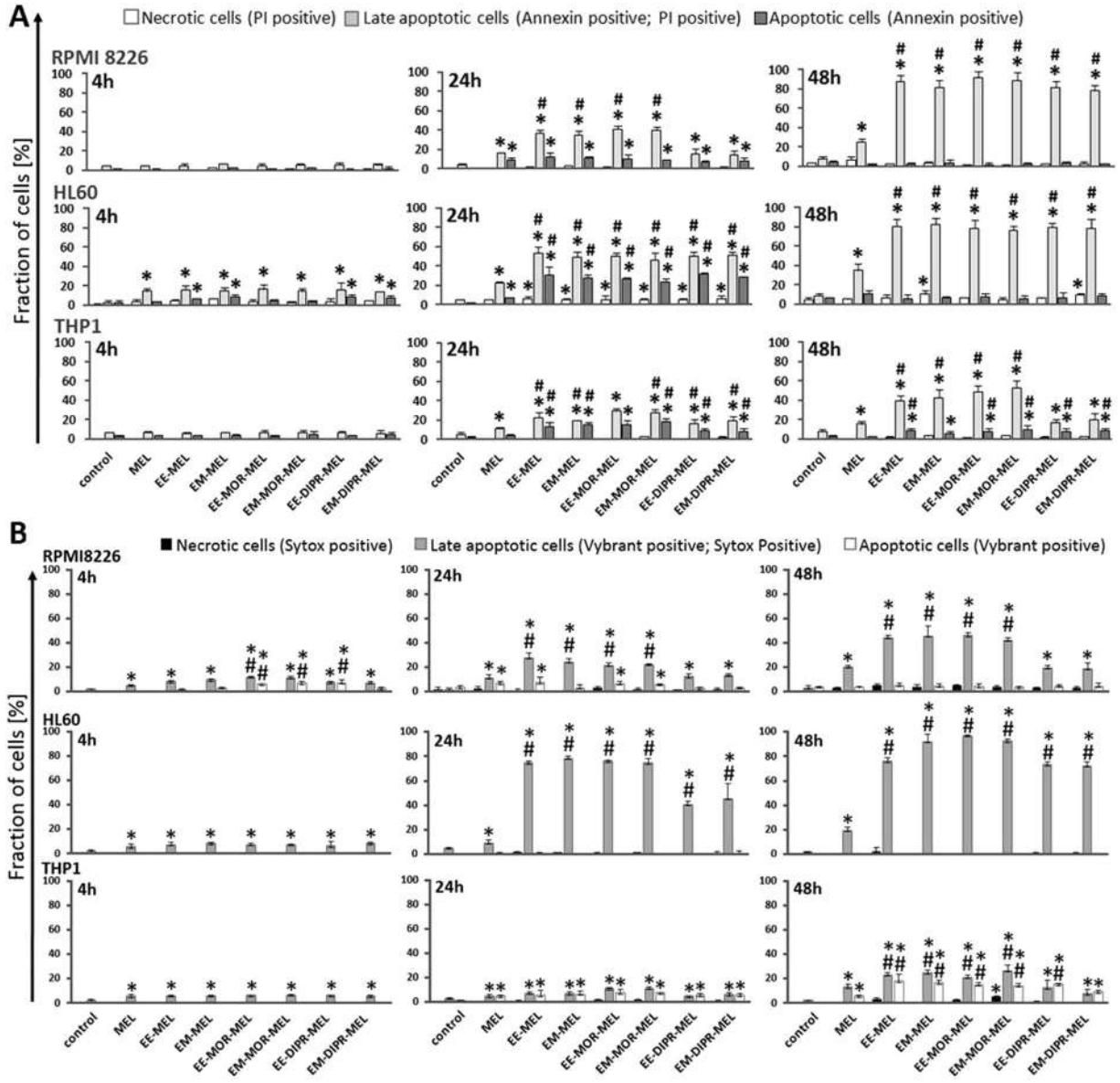

Figure 2. Influence of melphalan and its derivatives on the induction of apoptosis in RPMI8226, HL60 and THP1 cancer cell lines, as estimated by annexin V/propidium iodide (**A**) and Vybrant® DyeCycle™ Violet/SYTOX® AADvanced™ (**B**) assays. Quantitative results of the compounds effect on the level of necrotic, and early and late apoptotic cells are represent by the mean ± standard deviation (SD) for three independent experiments.

pronounced increase in the number of late apoptotic cells was found after 48 h (approximately 80–90% for RPMI8226 and HL60 cells, and 20–50% for THP1), while a smaller increase (approximately 25% for RPMI8226, 35% for HL60 and 17% for THP1) was observed in cells treated with unmodified melphalan, for the same concentrations and time. It should also be taken into account that by 48 h of treatment, the percentage of the late apoptotic fraction for all investigated compounds increased greatly in comparison to the 24 h incubation time, whereas the early apoptotic fraction continued to strongly decrease. For the THP1 cell line at 48 h, EE-DIPR-MEL, EM-DIPR-MEL were the least potent derivatives at inducing apoptosis, with an effect comparable to that of the unmodified drug. Under the same conditions, a constant number of necrotic cells were observed for all cell lines. In the case of chromatin condensation measurements, similar results were observed, correlating with data from studies using annexin V/propidium iodide staining. In summary, biochemical changes connected with apoptotic cell death was dominant, whereas necrotic changes were not associated.

Measurements of DNA damage by comet assay and the terminal deoxynucleotidyl transferase dUTP nick end labelling (TUNEL) method. In the current study the alkaline version of the DNA comet assay (pH > 13) was performed to assess the degree of DNA damage in RPMI8226, HL60 and THP1 cells. Quantitative data obtained from agarose gel electrophoresis are presented in Fig. 4A. Results indicated that

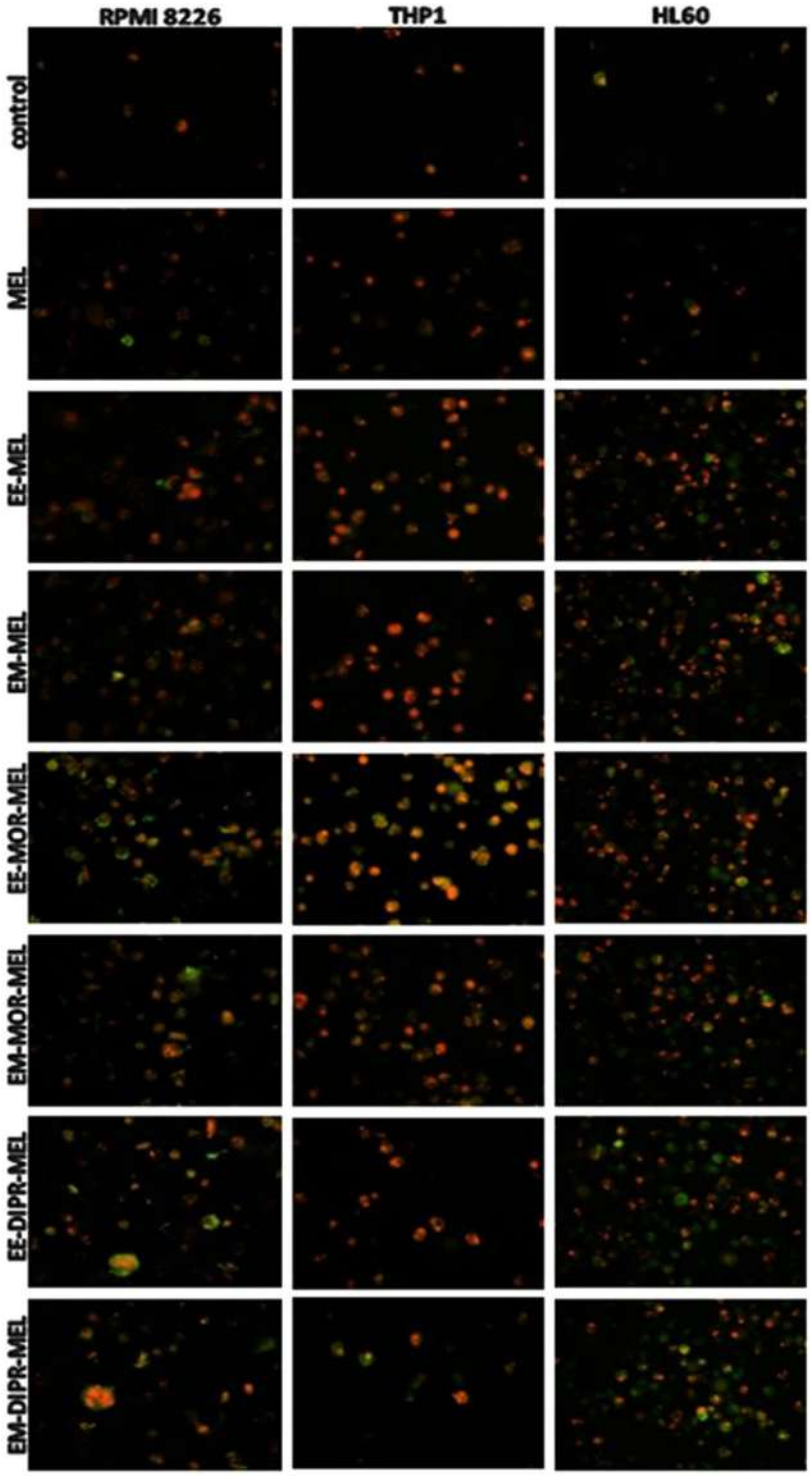

Figure 3. Fluorescence images of RPMI8226, HL60 and THP1 cells at 48 h after treatment with melphalan and its derivatives. The cells were stained with an annexin V/propidium iodide mixture and visualised by fluorescence microscopy, magnification ×200. After drug treatment, high green (derived from annexin V-fluorescein isothiocyanate, FITC) and red fluorescence (derived from propidium iodide) in cells with exposed phosphatidylserine (PS) indicated damage to the integrity of cellular membranes, characteristic symptoms of the late stages of programmed cell death. (For interpretation of the references to colours in this figure legend, the reader is referred to the web version of this article).

THP1and HL60 cell lines were less susceptible to DNA damage by both melphalan and the melphalan derivatives, compared to RPMI8226 cells. Treatment with the modified drugs generated a higher level of DNA breaks in comparison to untreated (control) cells, as well as melphalan-treated cultures, especially after longer incubation times.

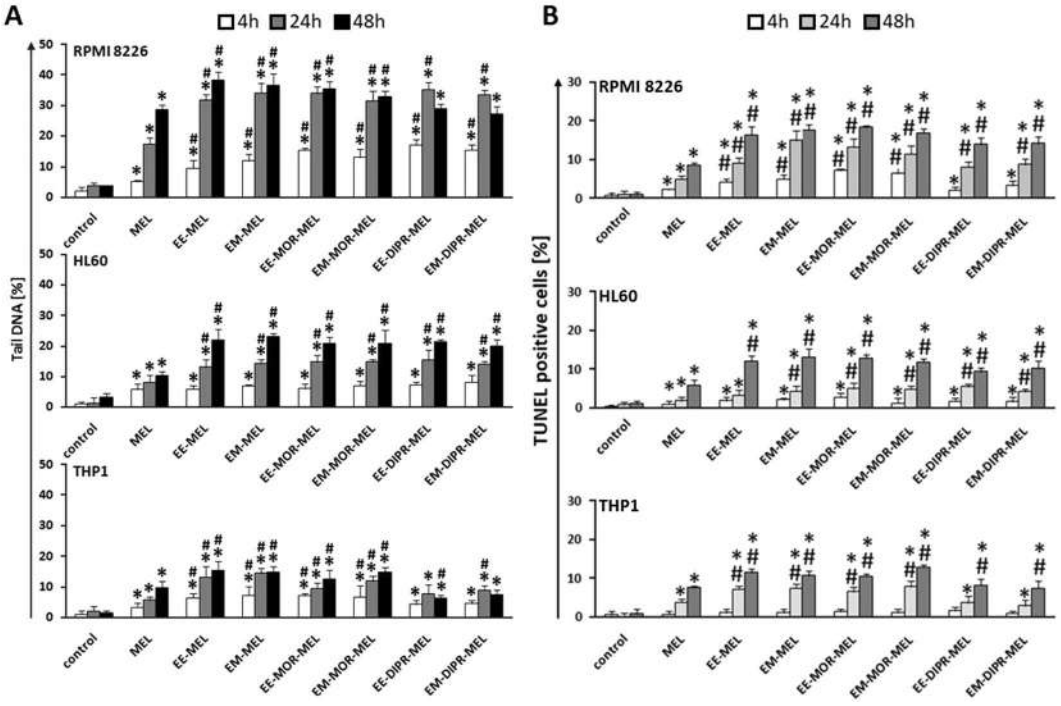

Figure 4. (**A**) Tail DNA (%) of cells treated with investigated compounds for 4, 24 and 48 h in RPMI8226, HL60 and THP1 cell lines. The number of analysed cells in each treatment was 100, and the analysis was repeated three times. (**B**) Influence of melphalan and its derivatives on the induction of DNA damage correlated with apoptosis in RPMI8226, HL60 and THP1 cancer cell lines, as estimated by TUNEL assay. Error bars denote SD.

In myeloma cancer, after 48 h of treatment, the maximum level of cells with damaged DNA was observed for EE-MEL and EM-MEL (~38%). A slightly lower percentage of damaged cells was noted after treatment with EE-MOR-MEL and EM-MOR-MEL. EE-DIPR-MEL and EM-DIPR-MEL were the least potent compounds in inducing DNA damage, with an effect comparable to that of melphalan. A similar effect was observed in the THP1 cell line, where EE-DIPR-MEL and EM-DIPR-MEL caused DNA damage at the level of ~7% in comparison to EE-MEL and EM-MEL (~15%), and EE-MOR-MEL and EM-MOR-MEL (~13%). In HL60 cells, a 48 h incubation with modified drugs led to a similar increase in DNA in the comet tail (~21%). In order to confirm these results, an alternative method, TUNEL assay, was used to measure DNA damage (Fig. 4B).

All investigated cell lines showed an increase in the number of cells with damaged DNA after exposure to melphalan derivatives. Moreover, the sensitivity to DNA damage differed between these cell lines, and increased in the following order, THP1 < HL60 < RPMI8226, which correlated with susceptibility of cells to DNA damage as determined by comet assay. Once again, EE-DIPR-MEL and EM-DIPR-MEL derivatives were the least effective in comparison to EE-MEL, EM-MEL, EE-MOR-MEL and EM-MOR-MEL for the cell lines under evaluation.

Detection of caspase-8, -9, -3/-7 activity. Changes in caspase-3, -8 and -9 activity in HL60, THP1 and RPMI8226 cells exposed to melphalan derivatives and to MEL are shown in Fig. 5. The final results were expressed as percentage activity of a particular cysteine protease, where the fluorescence value (caspase-3/-7) or luminescence (caspase-8 and -9) of the control not treated with the compound was taken as 100%. The highest increase in caspase-3/-7 activity was observed after incubation for 24 h with all tested derivatives, EE-MEL, EM-MEL, EE-MOR-MEL, EM-MOR-MEL, EE-DIPR-MEL and EM-DIPR-MEL. The HL60 cell line was the most sensitive to activation of caspase-3/-7, followed by THP1 and then RPMI8226. In THP1 and HL60 cells, the highest increase in caspase-3/-7 activity was observed after incubation with the EE-MEL and EE-MOR-MEL derivatives. These values were 1.5 to 2-fold higher than for the reference drug (HL60, 736.92 ± 105.48%; THP1, 429.08 ± 48.10%), and were 1225.64 ± 155.22% (EE-MEL) and 1127.68 ± 39.24% (EE-MOR-MEL) for HL60, and 981.93 ± 51.79% (EE-MOR-MEL) and 788.85 ± 83.40% (EE-MEL) for THP-1. For RPMI8226 cells, increase in caspase -3/-7 activity were observed after 24 h incubation with EE-MEL (656.19 ± 221.7%) and EM-MEL (625.09 ± 75.7%) while the value for the reference drug was 463.75 ± 64.5% (Fig. 5).

In order to better understand the molecular mechanisms underlying the activation of caspase-3 in THP1, HL60 and RPMI8226 cells in response to the new derivatives, the measurement of caspase-8 and caspase-9 activity was examined. Significant changes were observed only in HL60 and THP1 cells. A strong increase in the activity of caspase-9 was noted after 24 hours of incubation with all the derivatives. The activity of this enzyme for MEL was 185.53 ± 23.12% (HL60) and 316.5 ± 17.31% (THP1). Results for all analogues were similar, and ranged from 213.60 ± 26.83% to 275.02 ± 41.32% for HL60, and from 395.68 ± 21.46% to 468.30 ± 23.43% for THP1. For THP1 cells, all tested compounds also caused an increase in caspase-8 activation after 4 and 24 hours

HL-60		Caspase 3	Caspase 9	Caspase 8
MEL	4	97,52 ± 9,1	116,81 ± 18,2	120,65 ± 20,7
	24	736,92 ± 105,5	185,5 ± 23,5	144,36 ± 17,7
	48	272,18 ± 52,2	108,89 ± 4,5	123,00 ± 9,6
EE-MEL	4	109,89 ± 19,1	110,2 ± 11,6	122,64 ± 9,8
	24	1225,64 ± 155,2	265,52 ± 36,9	177,98 ± 11,7
	48	423,56 ± 43,2	102,37 ± 4,3	123,27 ± 8,8
EM-MEL	4	107,4 ± 3,5	105,7 ± 5,2	141,23 ± 25,0
	24	1060,53 ± 81,5	275,02 ± 41,3	178,55 ± 18,5
	48	424,92 ± 38,7	104,01 ± 5,9	114,23 ± 3,4
EE-MOR	4	95,47 ± 18,4	111,7 ± 22,1	131,83 ± 22,7
	24	1127,68 ± 39,2	215,2 ± 43,1	151,89 ± 12,5
	48	419,82 ± 28,1	110,45 ± 25,3	141,29 ± 24,1
EM-MOR	4	96,31 ± 1,9	107,7 ± 11,6	134,01 ± 16,4
	24	913,92 ± 141,7	214,78 ± 32,3	149,43 ± 15,0
	48	381,96 ± 82,8	103,57 ± 3,5	127,87 ± 8,9
EE-DIPR	4	90,99 ± 1,9	105,6 ± 8,1	123,51 ± 8,1
	24	750,47 ± 115,4	213,60 ± 26,8	158,64 ± 13,9
	48	279,14 ± 16,6	106,73 ± 10,4	116,86 ± 7,5
EM-DIPR	4	88,77 ± 4,8	108,33 ± 12,9	125,47 ± 8,8
	24	714,21 ± 31,3	224,39 ± 31,9	157,94 ± 17,5
	48	264,30 ± 67,3	106,51 ± 8,7	125,21 ± 1,5

THP1		Caspase 3	Caspase 9	Caspase 8
MEL	4	115,34 ± 10,4	116,81 ± 18,2	159,93 ± 33,2 *
	24	429,08 ± 48,1 *	316,52 ± 17,3 *	155,51 ± 15,4 *
	48	129,50 ± 28,1	118,42 ± 16,4	125,16 ± 26,2
EE-MEL	4	127,82 ± 15,5	138,74 ± 3,5	161,35 ± 11,2 *
	24	788,85 ± 83,4 *	395,68 ± 21,5 *	193,51 ± 7,7 *
	48	157,07 ± 36,1	139,37 ± 25,6	133,97 ± 22,5
EM-MEL	4	118,40 ± 25,3	133,05 ± 0,3	156,80 ± 15,8 *
	24	635,56 ± 72,4 *	425,71 ± 31,1 *	198,27 ± 31,7 *
	48	158,10 ± 19,7	129,19 ± 8,3	133,41 ± 10,8
EE-MOR-MEL	4	105,37 ± 11,0	139,40 ± 5,5	177,39 ± 4,8 *
	24	981,93 ± 51,7 *	464,45 ± 22,3 *	186,28 ± 3,5 *
	48	131,29 ± 8,4	109,45 ± 6,4	111,54 ± 17,1
EM-MOR-MEL	4	111,21 ± 25,7	134,92 ± 4,6	169,59 ± 10,9 *
	24	858,72 ± 15,3 *	463,55 ± 14,6 *	208,45 ± 24,8 *
	48	136,82 ± 20,2	110,81 ± 10,5	109,88 ± 9,6
EE-DIP-MEL	4	113,24 ± 30,4	135,57 ± 6,1	167,23 ± 18,0 *
	24	365,62 ± 70,0 *	438,48 ± 33,6 *	211,99 ± 7,6 *
	48	119,13 ± 17,0	107,96 ± 23,0	177,31 ± 15,4 *
EM-DIPR-MEL	4	113,42 ± 13,0	133,38 ± 9,2	165,78 ± 3,3 *
	24	459,18 ± 81,7 *	468,30 ± 23,4 *	204,91 ± 16,9 *
	48	159,46 ± 17,1	98,66 ± 26,7	141,72 ± 23,1 *

RPMI8226		Caspase 3	Caspase 9	Caspase 8
MEL	4	113,67 ± 12,5	102,29 ± 2,8	101,83 ± 3,5
	24	463,75 ± 64,5 *	131,55 ± 6,3	117,87 ± 11,4
	48	168,23 ± 37,8	116,39 ± 1,7	112,84 ± 14,4
EE-MEL	4	110,95 ± 10,8	106,04 ± 7,9	100,06 ± 5,5
	24	656,19 ± 221,7 *	125,67 ± 9,2	122,01 ± 6,3
	48	203,09 ± 125,2	103,06 ± 4,5	106,97 ± 8,4
EM-MEL	4	115,39 ± 19,6	100,50 ± 10,7	102,74 ± 6,6
	24	625,09 ± 75,7 *	128,56 ± 7,8	119,08 ± 11,9
	48	183,11 ± 1,8	109,92 ± 2,6	102,83 ± 4,9
EE-MOR-MEL	4	119,39 ± 16,3	106,80 ± 3,4	104,85 ±2 ,6
	24	509,76 ± 61,6 *	121,02 ± 10,5	114,20 ± 2,7
	48	145,19 ± 63,9	94,97 ± 0,8	95,58 ± 3,6
EM-MOR-MEL	4	105,52 ± 16,4	105,22 ± 10,9	101,67 ± 2,5
	24	492,25 ± 90,3 *	135,19 ± 12,2	134,24± 8,5
	48	166,57 ± 19,9	114,86 ± 10,9	104,22 ± 11,1
EE-DIP-MEL	4	107,47 ± 17,2	104,40 ± 6,1	102,63 ± 2,7
	24	454,68 ± 152,0 *	126,29 ± 0,8	112,77 ± 10,7
	48	168,81 ± 20,5	98,99 ± 5,8	104,17 ± 2,9
EM-DIPR-MEL	4	113,42 ± 13,1	99,90 ± 4,1	98,54 ± 1,3
	24	459,18 ± 162,1 *	116,01 ± 6,1	105,76 ± 12,5
	48	159,46 ± 17,8	98,59 ± 10,3	100,12 ± 6,6

Figure 5. Changes in activity of caspase-9, caspase-8 and caspase-3 after exposure of RPMI8226, HL60, THP1 cell lines to melphalan and analogues for 4, 24, 48 h. The measurements were carried out in the presence or absence of inhibitors. The cells were treated with an IC_{50} dose of MEL and its derivatives. The final result obtained was a percentage activity of a particular caspase, where the fluorescence value (caspase-3) or luminescence (caspase-8 and -9) of the control, not treated with the compound, was taken as 100%. Each point represents the average ± SD of three independent experiments. Values shaded in grey indicate differences between samples incubated with new derivatives and those incubated with MEL.

of incubation, whereas in HL60 cells, changes were observed after 24 and 48 hours of incubation. In the case of RPMI8226 cells, no significant changes in the activation of this cysteine protease were observed after incubation with all compounds (MEL and MEL derivatives).

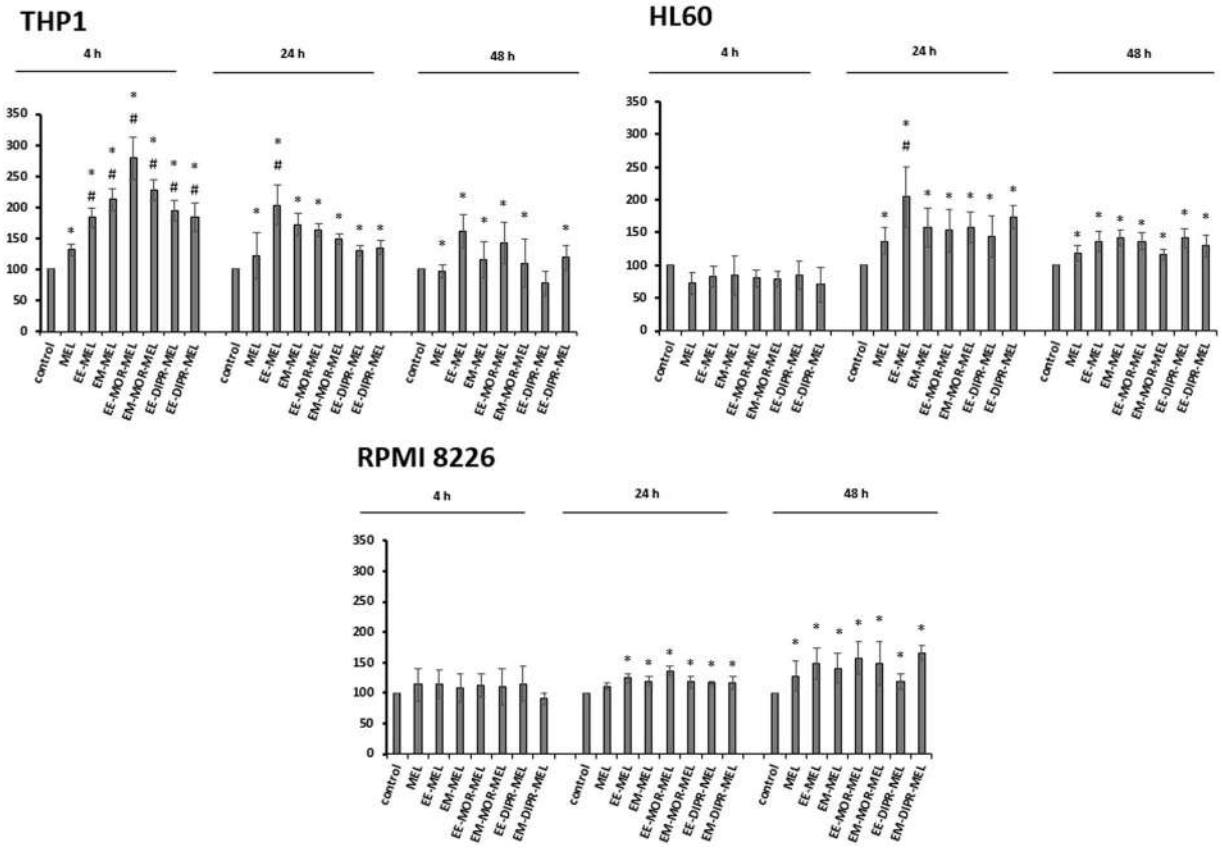

Figure 6. The effect of melphalan and its derivatives on Ca^{2+} concentration in THP1, HL60 and RPMI8226 cell lines. The cells were treated with an IC_{50} dose of the test compounds and then incubated for 2, 4, 24 or 48 h. The intensity of Fluo-4-NW probe fluorescence measured in control cells after 2, 24 or 48 h of incubation was taken as 100%. Each point represents the average ± SD of three independent experiments.

The experiments were also carried out simultaneously with caspase-3/-7, -8 and -9 activity inhibitors to ensure that the enzymes activated by the test compounds were the cysteine proteases being tested. Inhibitors caused a decrease in the percentage of the activity, indicating that the reactions were specific and resulted from the action of the tested compounds.

Intracellular calcium measurement. To examine whether the changes of intracellular calcium (Ca^{2+}) were involved in apoptosis induced by melphalan analogues, the release of calcium was studied using the fluorescence probe Fluo-4-NW. Figure 6 shows that melphalan and its derivatives induced different effects on the distribution of calcium ions in HL60, THP1 and RPMI8226 cells. In treated cells, changes in calcium level were detected, which was strongly dependent on the cell line, the type of chemical modification of the basal compound and the duration of the treatment. Generally, all analogues caused greater changes in intracellular calcium level, compared to melphalan.

With regard to THP1 cells, the biggest changes were observed after short-term incubation with all tested compound (4 h). While the level of intracellular calcium for MEL was 131.27 ± 10.08%, results for all analogues were similar and ranged from 183.14 ± 22.86% to 279.15 ± 34.15%. Under these particular conditions, the greatest changes in the level of intracellular calcium ions were observed after treatment with EE-MOR-MEL (approx. 2.8-fold increase). Extending the incubation time of the experiment resulted in a gradual reduction in the percentage of calcium released with all the compounds.

By contrast, short-term incubation (4 h) of HL60 cells with the analogues did not cause any significant change in the distribution of calcium. However, the most striking changes (approx. 2-fold increase) were found after longer treatment (24 h) with the ethyl ester of melphalan (EE-MEL). Further, but lower increases (around 1.2–1.4 fold) were observed after longer incubation with all investigated compounds (48 h).

Surprisingly, an opposite effect was observed in RPMI 8226 cells. The maximal increase in the percentage of calcium level was noted at 48 h after treatment with melphalan analogues.

Discussion

To strengthen the position of chemotherapy in fighting cancer more efficient methods of identifying new drugs need to be implemented. Identification of restrictions in chemical structure of certain groups of compounds in terms of their biological activity might constitute a valuable source of knowledge, useful in planning subsequent compound synthesis.

The object of this study was to identify melphalan derivatives with the enhanced cytotoxic activity in human cancer cells. The structure of melphalan molecule is notable for the presence of two modifiable functional groups, amino and carboxyl group. Systemic modification of both of these groups gives the possibility of extensive comparisons.

In vitro validation of cytotoxic, antiproliferative and proapoptotic properties of these compounds against various cancer cells, as well as results of investigation of their structure activity relationship (SAR) may provide a basis for the development of derivatives having optimal structure to serve as future anticancer drugs. For our research, RPMI8226- myeloma cancer, HL60- promyelocytic leukemia, and THP1- acute monocytic leukemia cell lines were chosen as haematological malignancy models.

This study used well known methods as screening tools. Initially, melphalan and its derivatives were evaluated for cytotoxicity in the selected model cells. Almost all derivatives, with the exception of MOR-MEL and DIPR-MEL, were recognized to be more toxic than the parent compound, MEL, in all three cell lines. Furthermore, significant differences in analogues' toxicity against the cell lines were detected. The toxicity of derivatives was the highest against the HL60 and THP1 cell line, while RPMI8226 cells showed the lowest sensitivity. EM-MOR MEL and EE-MOR MEL showed the highest efficacy against cancer cell lines HL60 and THP1, while RPMI8226 cells were more sensitive to EE-MEL and EM-MEL. Pilot studies also showed that EE-MEL, EM-MEL, EM-MOR-MEL are less cytotoxic to normal peripheral blood mononuclear cells.

Considering the interaction of all the aforementioned compounds with the three cell lines, the most effective melphalan structure had a free amino group and a modified carboxyl group, which was either a methyl or ethyl ester. Esters are known to be useful in modification of the drug lipophilicity. Additionally, aliphatic esters generally enhance lipid solubility[19]. However it should be noted that the influence on modification activity in one part of a molecule is not easy to be determined unequivocally, even for one specific cell line, because it can depend, to a large extent, on modifications observed in other parts of the molecule. It should be taken into account that the anticancer effectiveness of drug is often combined with its dose and its accumulation in individual cells. Therefore various cell types could demonstrate different levels of sensitivity to identical doses of a drug. Comparison of the chemical modifications of the derivatives with their cytotoxicity results confirmed the importance of certain chemical groups. Hence, we shall be able to successfully plan the synthesis of melphalan derivatives with anticipated high cytotoxicity capacity.

Distinguishing between mechanisms that induce cancer cell death is extremely important in terms of drug efficacy. Therefore one of the main assumptions of our investigations was to obtain information about the mechanism of cell death induced by melphalan derivatives.

Inhibition and inability to undergo apoptosis is a critical point in the development of cancer and a major barrier to its effective treatment. Due to numerous genes' mutation cancer cells gain immortality and are not annihilated by programmed cell death (PCD) and may proliferate excessively, which leads to tumor development and growth. Therefore the potential of chemotherapeutic agents and any cancer therapy to induce apoptosis of cancer cells is one of the most desirable properties. Given the above, principal aim of the study was to analyze the cytotoxicity of the tested melphalan derivatives and their contribution to cancer cell apoptosis.

Proposed detailed research assignments was aimed to estimate whether the melphalan derivatives can show proapoptotic activities in investigated cancer cells and if so, by which molecular mechanisms. For this reasons the effect of the investigated compounds on nucleic acid degradation (by comet and TUNEL assays) and parameters directly related to apoptosis (by PS externalisation and chromatin condensation) were measured. A number of characteristic biochemical changes occur at an early stages of apoptotic cell death. Unlike conventional cytotoxicity measurements which only assess parameters proportional to the degree of cell death, these parameters are measured for shorter incubation times. For this purpose, analysis of the contribution of apoptosis process in cytotoxicity of investigated compounds were examined after increasing times of incubation (4–48 h).

In this study DNA comet assay was performed under alkaline conditions. This method allowed detection of various types of DNA damages, such as single and double stranded DNA breaks (SSB and DSB respectively), DNA fragmentation induced by free radicals, cross-type DNA-DNA bonds and DNA-protein interactions[20]. This assay permits the quantification of DNA damage in a single cell preparation and is applicable to any eukaryotic cell. The assay can be used in both *in vitro* and *in vivo* testing and has been shown to be a powerful and sensitive predictor of genetic toxicity[21]. Our research clearly revealed that melphalan analogues generated a significant higher level of DNA breaks in comparison to unmodified drug, especially as a result of extended incubation times. Unexpectedly, in comparison to the comet assay, the TUNEL assay taken as an alternative method of DNA damage measurement connected with apoptosis, gave a poor signal response upon treatment with all test compounds. DNA is digested into regular oligonucleosomal fragments or multiples thereof. This phenomenon is the characteristic feature of apoptosis versus DNA degraded into irregular pieces in necrosis. However, in particular incidents DNA scission may stop and not progress into intranucleosomal fragments. As such, these apoptotic cells will be characterized by low levels of BrdU-FITC fluorescence. Hence, it is advised that other markers should be used in the identification of apoptotic cells than the ones dependent on the presence of DSB[22]. In addition, the DNA comet assay, used in this research, does not give an unambiguous answer to the question of whether DNA breaks are the result of mobilization of the apoptotic cell death machinery, because DNA may also be degraded in necrotic cells[20]. Criteria for apoptotic and necrotic death, including biochemical and molecular changes, indicate that both types of death are interdependent.

For these reasons, we studied cellular alterations connected with the leading processes responsible for cancer cell death activated by investigated derivatives, PS externalisation and chromatin condensation.

Morphological and biochemical changes such as the asymmetry of the cell membrane, nucleus shrink and compaction of chromatin are characteristic for the process of apoptosis. As a result of all complex molecular mechanisms involved in apoptotic process, progressive degradation of DNA occurs, which is dependent on active endonucleases. Thus, rating of apoptogenic properties of melphalan compounds were made on the basis of changes in plasma membrane (PS externalization) involved in apoptotic process.

Our studies have shown that all new analogues of melphalan induced apoptosis hallmarks; however, mainly at the late stages (irrespective of incubation time). More to the point, the results of the current study furnished proof that melphalan derivatives were considerably more effective against the three cell lines than the parent drug, MEL, and increased the anticancer activity.

Apoptosis, depending on the type of inducing agent, can take place with the participation of various evolutionarily conserved molecular mechanisms responsible for signal transmission initiating this process. Most proteolytic processes during apoptosis occur in the presence of a family of cysteine-dependent proteases catalysing the hydrolysis of proteins – caspases. Having confirmed that MEL and its derivatives induced apoptosis, the next stage of this study was aimed at determination of the apoptosis pathway (internal or external). For this purpose, we examined the activity of caspase-8, involved in the external pathway, caspase-9, which is a part of the internal apoptosis pathway, and caspase-3, which is involved in both pathways. In addition, the effect of the tested compounds on the increase of intracellular calcium levels was observed. HL60 was the most sensitive line for activation of caspase-3, followed by THP1 and RPMI8226, respectively. In case of THP1 and HL60, the highest increase in this cysteine protease was observed upon 24 hours of incubation with EE-MEL and EE-MOR-MEL. Contrary, for RPMI8226, the highest increase was found after incubation with methyl and ethyl melphalan esters.

The intrinsic apoptotic pathway is mediated by caspase-9 activation, which causes the release of mitochondrial cytochrome c and the formation of the apoptosome[23]. In THP1 and HL60 cells the strongest increase in caspase-9 activity was found after 24 h of incubation with the derivatives; changes that were statistically significant in comparison with cells incubated with MEL. In case of THP1 cells, this increase might be related to the high sensitivity of this line to oxidative stress and reactive oxygen species[24]. In HL60 and THP1, an increase in caspase-8 activity was also detected; however, the level of this cysteine protease was lower than for caspase-9. This suggested a dominance of the intrinsic apoptotic pathway.

No increase in caspase-9 or caspase-8 activity was observed for RPMI8226 cells. This might suggest the induction of cell death mechanisms other than apoptosis, such as mitotic catastrophe, autophagy, necroptosis or alternations of the apoptotic pathways. Pan *et al*. (2011) showed that melphalan, especially at low doses, induces autophagy in myeloma cells, and the use of inhibitors of this process significantly augments proapoptotic activity of DNA-damaging chemotherapy, both *in vitro* using MM cell lines or purified patient MM cells and *in vivo* in a human plasmacytoma xenograft mouse model[25]. It also should be mentioned that in addition to the best-known proteases - caspases involved in the effector phase of programmed cell death- there are other proteases like both cysteine (calpain, cathepsin B and L isoforms), aspartate (cathepsin D) and serine (granzyme B, AP24 protease). There have been suspicion that perhaps the proteolytic activity of calpain and caspase-3 is hierarchical. It has been observed that calpain activates (through proteolytic cleavage) caspase-3, -7 and -9. Activation of calpain by caspase-3 has also been reported. It is also possible that caspase-3 (but also -1 and -7) may be responsible for the proteolysis of calpastatin, thus causing the activation of calpain[26–29].

The current studies indicated that the cellular response to the test compounds varied depending on the type of cells (leukemia and myeloma cells). Therefore, further research will be carried out to describe the type of cell death caused by derivatives in a detailed way, including the possibility of the simultaneous participation of different pathways leading to cell death.

It was demonstrated that changes in calcium homeostasis play a key role in necrotic and apoptotic processes. Moreover, additional types of cell death, particularly anoikis as well as autophagy, are modulated by transient Ca^{2+} levels[27]. Ca^{2+} ions are also indispensable for the activation of some enzymes that reorganize the chromatin complex and its availability on the nucleolytic attack and also affect, directly or indirectly, the induction of expression (initiation of transcriptional activity) of genes associated with the execution of the PCD[26–31].

All the analogues investigated in the current study caused greater changes in intracellular calcium levels. In THP-1 cells, the biggest changes were observed after short-term incubation (4 h), mainly with EM-MOR-MEL. In case of HL60 cells, significant changes were observed after incubation for 24 hours only, mainly with the ethyl ester of melphalan (EE-MEL). However, in RPMI8226 cells, maximal increase in the percentage of calcium level was noted upon treatment for 48 h with all melphalan analogues. These results were consistent with the previously reported studies on the induction of apoptosis in HL60, THP1 and RPMI8226 cells.

Conclusions

A new series of nine melphalan analogues were designed, synthesised and tested. A comprehensive approach to the structure-antiproliferative activity relationship was proposed by attempting to compare the modification of both the carboxyl and amino groups of the parent molecule. As a result of that comparison, novel analogues EM-MOR-MEL and EE-MOR-MEL showed better activities (cytotoxicity, genotoxicity and ability to induce apoptosis) than melphalan, a drug still on the market.

All investigated derivatives (with a particular mention for EE-MEL, EM-MEL, EE-MOR-MEL and EM-MOR-MEL) caused significant changes in cells, compared to those treated with melphalan, indicating once again that these proposed modifications might serve as a potent drug therapeutic system. However, the presented study is limited to only *in vitro* cell line data. The results generate hypothesis and require validation with *in vivo* experiments. These studies allowed us to select the most active compounds for further, more detailed investigations, significantly advancing our understanding of toxic mechanisms of specific chemicals (Fig. 7).

Materials and methods

Chemicals. All tested compounds (Fig. 8) with purity over 98.5% (HPLC) were synthesized in the ŁUKASIEWICZ Research Network-Institute of Biotechnology and Antibiotics, Warsaw, Poland, method described in the Polish Patent PL220880 B1 (Espacenet database). HPLC analysis were performed using a Waters liquid chromatographic system consisting of DAD detector. A Chromolith Performance RP-18e (100-4.6 mm)

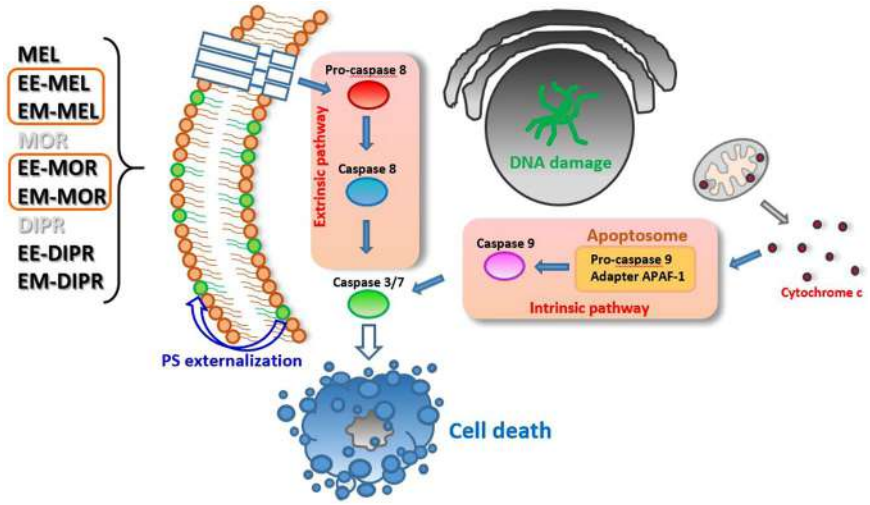

Figure 7. Proposed model of the molecular and cellular responses to the new MEL derivatives.

column was used. at constant flow rate of 1.0 ml/min. The mobile phase consisted of laurylosulfate buffer and acetonitrile; solvent were filtered under vacuum, mixed and degassed by a helium before use.

Cell culture. RPMI8226 (ATCC® CCL-155™) myeloma cancer cells, HL60 (ATCC® CCL-240™) promyelocytic leukemia cells and THP1 (ATCC® TIB-202™) acute monocytic leukemia cells were purchased from American Type Culture Collection (ATCC, Rockville, USA). Peripheral Blood Mononuclear Cells (PBMC) were isolated from buffy coat obtained from the Central Blood Bank (Lodz, Poland). PBMCs were isolated with Histopaque 1077 (Sigma Aldrich) at density gradient by centrifugation at 300 × g for 15 min.

All investigated cells were grown as a monolayer with RPMI 1640 medium, 1% phytohemaglutinin (only in PBMCs growth medium) supplemented with 10% fetal bovine serum, penicillin (10 U/ml) and streptomycin (50 μg/ml), in standard conditions: 37 °C, 100% humidity, the atmosphere being 5% CO_2 and 95% air. The cell viability was systematically controlled using trypan blue (0.4%, Sigma). In all experiments, cells in logarithmic phase of growth were used when their viability was above 95%.

Cytotoxicity assay. The effect of melphalan and its derivatives on RPMI8226, THP1, HL60 and PBMCs growth was determined by using resazurin viability assay. Cells subcultured into 96-well black plates at a density of 1.5×10^4 cells/well were incubated with various concentrations of selected compounds at 37 °C for 48 h. After incubation resazurin solution was added to each well (10 μg/ml, final concentration) and the plates were incubated for 90 minutes. Fluorescence measurement was performed at ~530 nm excitation and ~590 nm emission using an Fluoroskan Ascent FL plate reader (Labsystems, Sweden).

Measurements of phosphatidylserine externalization. Double staining of cells with Annexin V and propidium iodide (PI) was used according to the protocol described in our previous article[32]. This method is a useful tool for distinguishing viable cells (unstained with either fluorochrome) from early apoptotic cells (stained only with Annexin V), late apoptotic (stained with Annexin V and propidium iodide) and necrotic (dead) cells (stained only with PI).

Briefly, 5×10^5 control and drug treated cells were washed with cold PBS and resuspended in 500 μl binding buffer (delivered from producer) that contained 5 μl of Annexin V fluorescein isothiocyanate (FITC), 5 μl of PI and stained for 15 minutes in room temperature. Finally, at least 10^4 cells were analyzed for FITC and PI fluorescence (Ex ~488 nm; Em ~530 nm) using a flow cytometer (LSR II, Becton Dickinson). The cells stained with the annexin V/propidium iodide mixture were then visualized using fluorescence microscopy (Olympus IX70, Japan), magnification × 200.

Measurements of chromatin condensation. Violet Chromatin Condensation/Dead Cell Apoptosis Kit with Vybrant® DyeCycle™ Violet and SYTOX® AADvanced™ was used in order to examine chromatin condensation during apoptosis (Molecular probes®, Invitrogen™). Briefly, 5×10^5 control and drug treated cells were washed and suspended in 1 ml of Hank's Balanced Salt Solution buffer (HBSS) containing Vybrant® DyeCycle™ Violet and SYTOX® AADvanced™ dyes, according to manufacturer's protocol. Immediately after the incubation period (30 min, protected from light), stained cells were analyzed without washing by flow cytometry (LSR II, Becton Dickinson), using ~405/488 nm dual excitation while measuring the fluorescence emission at ~440/660 nm.

Measurements of DNA damage – comet assay. Comet assay was performed under alkaline conditions according to the protocol described in our previous article[33]. Cells were suspended in 0.75% low melting point agarose in PBS, pH 7.4. Next, 50 μl of this suspension was spread on frosted microscope slides precoated with 1% normal melting agarose. After gelling, the slides were treated with lysing buffer consisting of 2.5 M NaCl, 100 mM

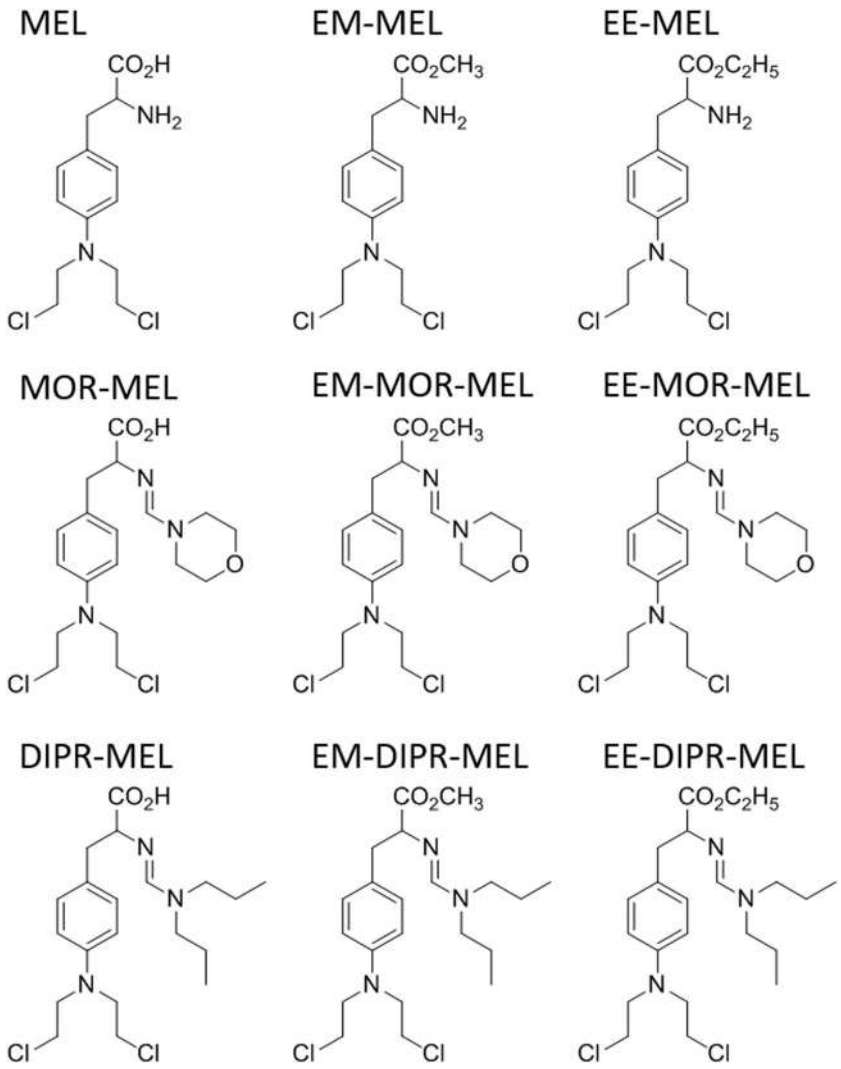

Figure 8. Chemical structures of melphalan derivatives.

EDTA, 1% Triton X-100, 10% DMSO and 10 mM Tris, pH 10 at 4 °C for 1 h. Then slides were placed in the electrophoresis solution (300 mM NaOH, 1 mM EDTA, pH > 13) for 40 min to allow DNA unwinding. Electrophoresis was carried out at 0.73 V/cm and 30 mA for 30 min. Then the slides were stained with 2 μg/ml DAPI. All these steps were performed in the dark to prevent additional DNA damage. 100 randomly selected cells from each slide were analyzed using fluorescence microscope (Olympus IX70, Tokyo, Japan) equipped with a CC12 video camera, a UV filter and image analysis system - CaspLab v. 1.2.3b2. The percentage of DNA in the comet tail was chosen as an indicator of DNA damage.

Measurements of DNA damage during apoptosis – TUNEL assay. ApoBrdU DNA Fragmentation Assay Kit (BioVision) was used in order to examine DNA damage during apoptosis according to the protocol described in our previous article[34]. This method enables the detection of the early stage of apoptosis by labeling 3′OH ends of single- and double-stranded DNA fragments with Br-dUTP (bromolated deoxyuridine triphosphate nucleotides). The Br-dUTP fragments are detected by the fluorescein labeled anti-BrdU monoclonal antibody, which enables a brighter signal. Control and drug treated cells were fixed in a 4% paraformaldehyde freshly prepared in PBS and incubated for 1 h at 37 °C in DNA Labeling Solution containing a TdT Reaction Buffer, a terminal deoxynucleotidyl transferase (TdT) and the Br-dUTP. Next, the cells were resuspended in an antibody solution containing an anti-BrdU-FITC antibody (in total darkness for 30 min at room temperature) and incubated with the propidium iodide/RNase A solution. The cells fluorescence was measured with the flow-cytometry (LSR II, Becton Dickinson). The green fluorescence of FITC at 520 nm and the red fluorescence of propidium iodide at 623 nm were detected. The number of TUNEL-positive cells was expressed as a percentage of the total number of cells in the sample.

Measurement of caspase 3/7, 8 and 9 activation. The activity of caspases-3 and -7 were estimated with Apo-ONE® Homogeneous Caspase 3/7 Assay and Caspase-Glo® 9/8 Assay Systems according to the manufacturer's protocols (Promega Corporation, Madison, WI, USA). Measurement of caspases activation in control and

treated cells seeded in 96-well plates (black or white), was recorded by monitoring changes in the fluorescence (caspase-3/7) or luminescence (caspase-8 and -9) after 4 h, 24 h and 48 h incubation of cells with investigated compounds. The intensity of fluorescence or luminescence were measured using a Fluoroskan Ascent FL plate reader (Labsystem, Sweden). Cysteine proteases activity were expressed as a ratio of fluorescence or luminescence of the treated samples relative to the corresponding untreated controls taken as 100%. The proper inhibitors were used in the control experiments to confirm that the observed fluorescence in both the control and the drug-treated cells is due to caspase-3, -9, -8 presences in the samples[32].

Intracellular calcium measurement. Intracellular calcium level was determined using the fluorescent probe Fluo-4NW according to the protocol described in our previous article[32]. After entering the cell, Fluo-4NW is converted by cytosolic hydrolases to the active form, having the possibility of binding of calcium ions. As a result of joining of calcium ions, the probe emits fluorescence ($\lambda_{em} = 538$ nm) after excitation with light of wavelength 485 nm.

Cells were cultured and treated with investigated compounds on Petri dishes. Next, the cells were plated in 96-well black fluorimetric plates (2×10^4 cells/well). The growth medium was removed and the cells were washed with PBS in order to eliminate sources of baseline fluorescence. Finally a dye loading solution (Fluo-4-NW dye, 4-[(Dipropylamino)sulfonyl] benzoic acid (Probenecid) - used to inhibit extrusion of the indicator out of the cell by organic anion transporters, Hanks' balanced salt solution (HBSS), 20 mM N-(2- hydroxyethyl) piperazine-N'-(2-ethanesulfonic acid) buffer solution (HEPES)) was added in a volume of 100 µl per well and incubated for 30 min in the total darkness at 37 °C, and then for next 30 min. at room temperature. The measurement was done on Fluoroskan Ascent FL microplate reader (Labsystems, Sweden) using 494 nm excitation and 516 nm emission wavelengths.

Statistical analysis. The data was presented as a mean ± S.D. An analysis of ANOVA variance with a Tukey post hoc test was used for multiple comparisons. All statistics were calculated using the STATISTICA program (StatSoft, Tulsa, OK, USA). A p-value of < 0.05 was considered significant. All figures contain identical descriptions for statistically significant changes: $^{*}p < 0.05$ statistically significant differences in comparison to control cells, $^{\#}p < 0.05$ statistically significant differences between samples incubated with melphalan and melphalan derivatives.

Received: 14 June 2019; Accepted: 24 February 2020;
Published online: 11 March 2020

References

1. Mateos, M. V. & San Miguel, J. F. Management of multiple myeloma in the newly diagnosed patient. *Hematology Am Soc Hematol Educ Program.* **8**, 498–507 (2017).
2. Falco, P. *et al.* Melphalan and its role in the management of patients with multiple myeloma. *Expert Rev Anticancer Ther.* **7**, 945–957 (2007).
3. Saha, P., Debnath, C. & Bérubé, G. Steroid-linked nitrogen mustards as potential anticancer therapeutics: a review. *J Steroid Biochem Mol Biol.* **137**, 271–300 (2013).
4. Bielawski, K. *et al.* Novel amidine analogue of melphalan as a specific multifunctional inhibitor of growth and metabolism of human breast cancer cells. *Biochem Pharmacol.* **72**, 320–331 (2006).
5. Singh, R. K., Kumar, S., Prasad, D. N. & Bhardwaj, T. R. Therapeutic journery of nitrogen mustard as alkylating anticancer agents: Historic to future perspectives. *Eur J Med Chem.* **151**, 401–433 (2018).
6. Kuczma, M., Ding, Z. C. & Zhou, G. Immunostimulatory Effects of Melphalan and Usefulness in Adoptive Cell Therapy with Antitumor CD4+ T Cells. *Crit Rev Immunol.* **2**, 179–191 (2016).
7. Gourzones, C. *et al.* Antioxidant Defenses Confer Resistance to High Dose Melphalan in Multiple Myeloma Cells. *Cancers (Basel).* **11**, 439 (2019).
8. Hu, X. *et al.* Design and synthesis of novel nitrogen mustard-evodiamine hybrids with selective antiproliferative activity. *Bioorg Med Chem Lett.* **27**, 4989–4993 (2017).
9. Carpenter, J. T. Jr. & Maddox, W. A. Melphalan adjuvant therapy in breast cancer. *Lancet.* **2**, 450–451 (1983).
10. Bogomilova, A. *et al.* A polyphosphoester conjugate of melphalan as antitumoral agent. *Eur J Pharm Sci.* **50**, 410–419 (2013).
11. Strese, S. *et al.* The novel alkylating prodrug melflufen (J1) inhibits angiogenesis *in vitro* and *in vivo*. *Biochem Pharmacol.* **86**, 888–895 (2013).
12. Marczak, A., Denel-Bobrowska, M., Łukawska, M. & Oszczapowicz, I. Formamidinodoxorubicins are more potent than doxorubicin as apoptosis inducers in human breast cancer cells. *Anticancer Research.* **35**, 1935–1940 (2015).
13. Marczak, A., Denel-Bobrowska, M., Rogalska, A., Łukawska, M. & Oszczapowicz, I. Cytotoxicity and induction of apoptosis by formamidinodoxorubicins in comparison to doxorubicin in human ovarian adenocarcinoma cells. *Environ Toxicol Pharmacol.* **39**, 369–383 (2015).
14. Denel-Bobrowska, M. *et al.* Identification of the key pathway of oxazolinoanthracyclines mechanism of action in cells derived from human solid tumors. *Toxicol Appl Pharmacol.* **313**, 159–169 (2016).
15. Denel-Bobrowska, M., Lukawska, M., Oszczapowicz, I. & Marczak, A. Histological subtype of ovarian cancer as a determinant of sensitivity to formamidine derivatives of doxorubicin - *in vitro* comparative studies with SKOV-3 and ES-2 cancer cell lines. *Asian Pac J Cancer Prev.* **17**, 4223–4231 (2016).
16. Lukawska, M., Wietrzyk, J., Opolski, A., Oszczapowicz, J. & Oszczapowicz, I. Synthesis and biological properties of oxazolinodaunorubicin- a new derivative of daunorubicin with a modified daunosamine moiety. *Invest New Drugs.* **28**, 600–608 (2010).
17. Lukawska, M. *et al.* Oxazolinodoxorubicin - a promising new anthracycline. *Anticancer Research.* **32**, 2959–2965 (2012).
18. Kik, K., Wasowska-Lukawska, M., Oszczapowicz, I. & Szmigiero, L. Cytotoxicity and cellular uptake of doxorubicin and its formamidine derivatives in HL60 sensitive and HL60/MX2 resistant cells. *Anticancer Res.* **29**, 1429–1433 (2009).
19. Chalas, J. *et al.* Effect of ethyl esterification of phenolic acids on low-density lipoprotein oxidation. *Biomed Pharmacother.* **55**, 54–60 (2001).
20. Tice, R. R. *et al.* Single cell gel/comet assay: guidelines for *in vitro* and *in vivo* genetic toxicology testing. *Environ Mol Mutagen.* **35**, 206–221 (2000).

21. Nandhakumar, S. *et al*. Evaluation of DNA damage using single-cell gel electrophoresis (Comet Assay). *J Pharmacol Pharmacother.* **2**, 107–111 (2011).
22. Darzynkiewicz, Z., Galkowski, D. & Zhao, H. Analysis of apoptosis by cytometry using TUNEL assay. *Methods.* **44**, 250–254 (2008).
23. Xue, X. *et al*. Curcumin induces apoptosis in SGC-7901 gastric adenocarcinoma cells via regulation of mitochondrial signaling pathways. *Asian Paci J Cancer Prev.* **15**, 3987–3992 (2014).
24. Zhou, F. *et al*. Jab1/Csn5-Thioredoxin Signaling in Relapsed Acute Monocytic Leukemia under Oxidative Stress. *Clin Cancer Res.* **23**, 4450–4461 (2017).
25. Pan, Y. *et al*. Targeting autophagy augments *in vitro* and *in vivo* antimyeloma activity of DNA-damaging chemotherapy. *Clin Cancer Res.* **17**, 3248–3258 (2011).
26. Harwood, S. M., Yaqoob, M. M. & Allen, D. A. Caspase and calpain function in cell death: bridging the gap between apoptosis and necrosis. *Ann Clin Biochem.* **42**, 415–431 (2005).
27. Fadeel, B., Orrenius, S. & Zhivotovsky, B. The most unkindest cut of all: on the multiple roles of mammalian caspases. *Leukemia.* **14**, 1514–1525 (2000).
28. Yamashima, T. Implication of cysteine proteases calpain, cathepsin and caspase in ischemic neuronal death of primates. *Prog. Neurobiol.* **62**, 273–295 (2000).
29. Wright, S. C., Wang, H., Wei, Q. S., Kinder, D. H. & Larrick, J. W. Bcl-2-mediated resistance to apoptosis is associated with glutathione-induced inhibition of AP24 activation of nuclear DNA fragmentation. *Cancer Res.* **58**, 5570–5576 (1998).
30. Zhivotovsky, B. & Orrenius, S. Calcium and cell death mechanisms: a perspective from the cell death community. *Cell Calcium.* **50**, 211–221 (2011).
31. Nicotera, P. & Rossi, A. D. Nuclear Ca2+: physiological regulation and role in apoptosis. *Mol. Cell. Biochem.* **135**, 89–98 (1994).
32. Gajek, A. *et al*. Early Activation of Apoptosis and Caspase-independent Cell Death Plays an Important Role in Mediating the Cytotoxic and Genotoxic Effects of WP 631 in Ovarian Cancer Cells. *Asian Pac J Cancer Prev.* **16**, 8503–8512 (2015).
33. Gajek, A., Rogalska, A. & Koceva-Chyła, A. Aclarubicin in subtoxic doses reduces doxorubicin cytotoxicity in human non-small cell lung adenocarcinoma (A549) and human hepatocellular carcinoma (HepG2) cells by decreasing DNA damage. *Toxicol In Vitro.* **55**, 140–150 (2019).
34. Rogalska, A., Gajek, A. & Marczak, A. Epothilone B induces extrinsic pathway of apoptosis in human SKOV-3 ovarian cancer cells. *Toxicol In Vitro.* **28**, 675–683 (2014).

Acknowledgements

The investigation was supported by a statutory research grant provided for the Department of Medical Biophysics (B1811000000190.01). Publication's printing cost was co-financed by the European Union from the European Social Fund under the "InterDOC-STARt" project (POWR.03.02.00-00-I033/16-00).

Author contributions

A.G. and A.P. contributed equally to this work. A.M., A.G., A.P. and M.Ł. formed the hypothesis and designed the study. A.G., A.P. participated in the experimental design and conducted most of the experiments and collected data. V.C.A. performed some experiments. A.G. and A.P. analyzed the results. M.Ł. and J.T. synthesized compounds. All authors contributed to manuscript preparation. All authors read and approved the manuscript.

Competing interests

The authors declare no competing interests.

Additional information

Correspondence and requests for materials should be addressed to A.G.

Reprints and permissions information is available at www.nature.com/reprints.

Publisher's note Springer Nature remains neutral with regard to jurisdictional claims in published maps and institutional affiliations.

PUBLIKACJA NR III

Poczta A., Krzeczyński P., Tobiasz J., Rogalska A., Gajek A., Marczak A.; *Synthesis and In Vitro Activity of Novel Melphalan Analogs in Hematological Malignancy Cells;* Int J Mol Sci. 2022; 23(3):1760.

- **Praca doświadczalna**
- **IF: 6.208**
- **punkty MEiN: 140 pkt.**

International Journal of
Molecular Sciences

MDPI

Article

Synthesis and In Vitro Activity of Novel Melphalan Analogs in Hematological Malignancy Cells

Anastazja Poczta [1,*], Piotr Krzeczyński [2], Joanna Tobiasz [2], Aneta Rogalska [1], Arkadiusz Gajek [1] and Agnieszka Marczak [1]

[1] Department of Medical Biophysics, Institute of Biophysics, Faculty of Biology and Environmental Protection, University of Lodz, 141/143 Pomorska Street, 90-236 Lodz, Poland; aneta.rogalska@biol.uni.lodz.pl (A.R.); arkadiusz.gajek@biol.uni.lodz.pl (A.G.); agnieszka.marczak@biol.uni.lodz.pl (A.M.)
[2] Department of Pharmacy, Cosmetic Chemistry and Biotechnology, Team of Chemistry, Łukasiewicz Research Network—Industrial Chemistry Institute, 8 Rydygiera Street, 01-793 Warsaw, Poland; piotr.krzeczynski@ichp.pl (P.K.); joanna.tobiasz@ichp.pl (J.T.)
* Correspondence: anastazja.poczta@edu.uni.lodz.pl

Abstract: Despite the continuous developments in pharmacology and the high therapeutic effect of new treatment options for patients with hematological malignancies, these diseases remain a major health issue. Our study aimed to synthesize, analyze in silico, and determine the biological properties of new melphalan derivatives. We obtained three methyl esters of melphalan having in their structures amidine moieties substituted with thiomorpholine (EM–T–MEL), indoline (EM–I–MEL), or 4-(4-morpholinyl) piperidine (EM–MORPIP–MEL). These have not yet been described in the literature. The in vitro anticancer properties of the analogs were determined against THP1, HL60, and RPMI8226 cells. Melphalan derivatives were evaluated for cytotoxicity (resazurin viability assay), genotoxicity (alkaline comet assay), and their ability to induce apoptosis (Hoechst33342/propidium iodide double staining method; phosphatidylserine translocation; and caspase 3/7, 8, and 9 activity measurements). Changes in mitochondrial membrane potential were examined using the specific fluorescence probe JC–1 (5,5′,6,6′-tetrachloro-1,1′,3,3′–tetraethylbenzimidazol carbocyanine). The EM–T–MEL derivative had the highest biological activity, showing higher cytotoxic and genotoxic properties than the parent drug. Moreover, it showed a high ability to induce apoptosis in the tested cancer cells. This compound also had a beneficial effect in peripheral blood mononuclear cells (PBMC). In conclusion, we verified and confirmed the hypothesis that chemical modifications of the melphalan structure improved its anticancer properties. The conducted study allowed the selection of the compound with the highest biological activity and provided a basis for chemical structure-biological activity analyses.

Keywords: apoptosis assay; chemical modification; DNA damage; in silico study; leukemia cell lines; melphalan

Citation: Poczta, A.; Krzeczyński, P.; Tobiasz, J.; Rogalska, A.; Gajek, A.; Marczak, A. Synthesis and In Vitro Activity of Novel Melphalan Analogs in Hematological Malignancy Cells. *Int. J. Mol. Sci.* **2022**, *23*, 1760. https://doi.org/10.3390/ijms23031760

Academic Editor: Alessia Ligresti

Received: 20 December 2021
Accepted: 1 February 2022
Published: 3 February 2022

1. Introduction

Blood cancers are currently among the most serious medical problems. Recent data have shown that one in eight cancer cases worldwide come from blood cells, bone marrow, or the lymphatic system. Malignant hematopoiesis, such as leukemia and lymphomas, is divided into more than 100 subtypes with varying survival rates [1]. Multiple myeloma (MM) is characterized by the infiltration of monoclonal plasma cells into the bone marrow, which secretes monoclonal immunoglobulin that is found in the urine and/or blood. The accumulation of these immunoglobulins leads to organ dysfunction, which causes hypercalcemia, renal failure, anemia, or lytic bone changes [2–4].

Treatment of MM involves a combination of drugs with distinct mechanisms of action, including immunomodulating drugs, proteasome inhibitors, monoclonal antibodies, alkylating agents, and histone deacetylase inhibitors. Despite these numerous modern therapies, high doses of melphalan followed by autologous stem cell transplantation remain key in

treating MM patients eligible for transplantation. Melphalan is a bifunctional alkylating agent. Each of the two bis-2-chloroethyl melphalan groups forms carbonium intermediates that cause alkylation by covalent bonding with nitrogen atoms in the DNA of the guanine molecule at the 7-position. This leads to cross-links between the two DNA strands, preventing transcription and DNA replication and inhibiting the cell cycle. By targeting highly proliferating cells, including malignant plasma cells, this drug causes cell death [4].

A major limitation of chemotherapy, including melphalan treatment, is the lack of drug selectivity, which has adverse effects on healthy tissues. High doses of anticancer drugs also weaken patients' immunity by affecting the body's biomolecular defense system [5]. The therapeutic activity of melphalan, despite the high remission of the disease, is limited by melphalan numerous side effects, such as cardiotoxicity, irreversible myelosuppression, anemia, numerous infections, and kidney failure. Therapy-related secondary primary malignancies (SPMs) in myeloma patients have been recognized as a consequence of treatment with alkylating agents [6]. Another issue is the emergence of multidrug resistance during antimyeloma therapy [7]. Because of these problems, finding new forms of therapy is crucial for improving the effectiveness of therapy. Modifications of melphalan's structure to improve its anticancer properties have been studied for years. As early as the 1950s and 1960s, scientists worked with melphalan derivatives and studied their activity on cell lines and in animal models [8–10]. Today, this topic is still relevant, and various melphalan analogs are being evaluated that will be more effective than the parent drug [2,11,12]. Chemical modifications of the drug structure could serve as the basis for an improved chemotherapy system for MM patients. Chemical modification of the structure and determination of the relationship between the chemical structure and its biological activity may be the basis for developing derivatives with optimal structure that can be used as future anticancer drugs. Targeted design of anticancer drugs based on well-designed and -conducted basic research may in the future replace long and expensive in vivo tests, preceding the qualification of a new structure for further preclinical research through its candidate for a future drug.

Our previous studies [13] have shown that chemical modifications of melphalan are a promising way of enhancing the activity of this molecule compared to that of the parent drug. It was shown that esterification of the carboxyl group and replacement of the amino group with an amidine group containing a morpholine ring caused significant changes in cells. The modified structures exceeded the cytotoxic, genotoxic, and proapoptotic activity of the unmodified melphalan. Based on this knowledge, in the current research, we performed further chemical modifications of both the carbonyl and amino groups of melphalan to find derivatives with higher anticancer activity. As a result, we obtained methyl esters of melphalan containing amidine residues, including thiomorpholine (EM–T–MEL), indoline (EM–I–MEL), and 4-(4-morpholinyl) piperidine (EM–MORPIP–MEL). Our current research aimed to determine the cytotoxicity and genotoxicity of the new melphalan derivatives, as well as the ability of these derivatives to induce apoptosis and generate changes in the mitochondrial membrane potential. Such derivatives could potentially be therapeutically important.

2. Results

2.1. Chemistry

Samples of melphalan derivatives used in biological research were obtained by three-stage chemical synthesis from commercially available substrates (Figure 1).

The first step in the synthesis involved the reaction of commercial melphalan (MEL) with a 50% molar excess of N-formylmorpholine dimethylacetal (DMA–MOR) in methanol at room temperature. The morpholine derivative of melphalan (MOR–MEL) obtained was the starting material for the further synthesis of all new derivatives.

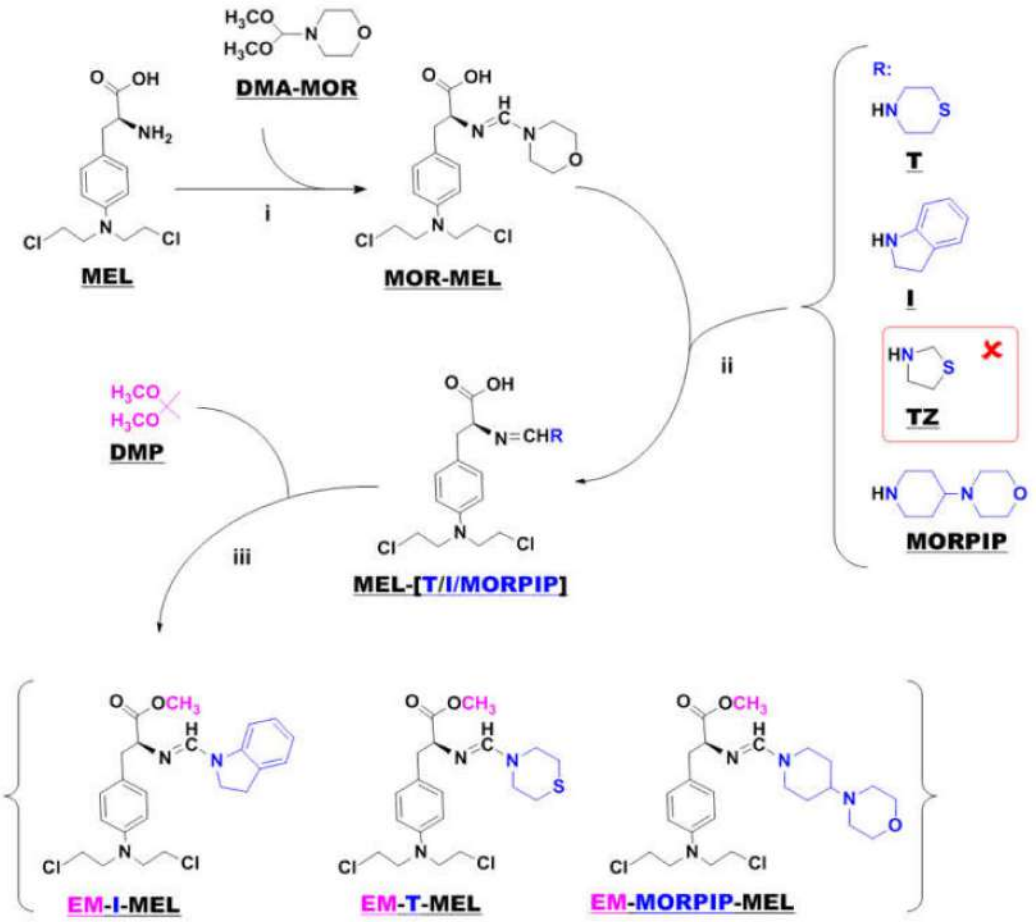

Figure 1. Synthesis of new melphalan derivatives. Conditions: (**i**): methanol, room temperature, 1 h; (**ii**): methanol, room temperature; (**iii**): 2,2–dimethoxypropane, concentrated hydrochloric acid, room temperature, 1 h.

MOR–MEL was then reacted with a 100% molar excess of the appropriate amine (thiomorpholine (T), indoline (I), or 4-(4-morpholinyl) piperidine (MORPIP)) in methanol at room temperature to obtain the appropriate amine derivative of melphalan (MEL–T, MEL–I, and MEL–MORPIP). Initially, we intended to obtain a thiazolidine derivative of melphalan in place of MEL–MORPIP, but during the experiments, it turned out that MOR–MEL did not react with thiazolidine (TZ). Attempts to change the reaction conditions and the synthesis method were unsuccessful. Therefore, it was decided to discontinue further work and replace the thiazolidine derivative with 4-(4-morpholinyl) piperidine.

In the last stage, the amine derivatives of melphalan (MEL–(T/I/MORPIP)) were esterified. Ester synthesis was carried out with 2,2-dimethoxypropane (DMP) in an acidic environment (approximately 10% addition of concentrated hydrochloric acid) to give the corresponding amine derivatives of melphalan methyl esters in the form of thick oils free of amines. All three amines were then converted to a hydrochloride form with a 5 M solution of hydrogen chloride gas in ethyl acetate.

Because of these structural changes, their molecules were much less polar than melphalan itself. This was confirmed by HPLC analysis (Figure S1), which showed the composition of the peaks of individual compounds. The analysis was performed on the reversed phases. The retention times of the tested derivatives ranged from 13,424 min to 20,531 min, while the retention time of melphalan under the same conditions was 12,151 min, which indicated the greater polarity of the melphalan molecule than of the described derivatives.

2.2. In Silico Analysis

To determine whether the test compounds belonged to the druglike group, the rules of Lipinski and the definition of Veber were used. According to the five Lipinski rules, a drug candidate should meet the following criteria: molecular weight (MW) $\leq$ 500 Da; lipophilicity described as logP $\leq$ 5; number of hydrogen bond acceptors (HBAs) $\leq$ 10; and number of hydrogen bond donors (HBDs) $\leq$ 5 [14]. The data obtained for the new test compounds are summarized in Table 1.

Table 1. Druglikeness parameters estimated according to Lipinski's and Veber's rules. HBDs [a]: number of hydrogen bond donors; HBAs [b]: number of hydrogen bond acceptors; NBR [c]: number of rotatable bonds; TPSA [d]: total polar surface area.

Compound	Lipinski's Rules				Veber's Rule	
	MW ≤500 Da	LogP ≤5	HBDs [a] ≤5	HBAs [b] ≤10	NBR [c] ≤10	TPSA [d] ≤140
EM–I–MEL	448.39	4.46	0	3	11	45.14
EM–T–MEL	432.41	3.61	0	3	11	70.44
EM–MORPIP–MEL	499.47	3.36	0	5	12	57.61

All the test compounds complied with Lipinski's rules and had only one violation of Veber's rules. The number of rotational bonds was slightly greater than the number specified in Veber's rule. We also considered that none of the new compounds was a substrate for P-glycoprotein.

To illustrate the distribution of the most important physicochemical properties in the body, we also prepared radar charts (Figure 2) from the SwissADME website, which consider six important physicochemical properties. The pink area represents the optimal range for each property: lipophilicity (LIPO), XLOGP3 between −0.7 and +5.0; size (SIZE), MW between 150 and 500 g/mol; polarity (POLAR), TPSA between 20 and 130 Å^2; solubility (INSOLU), log S not higher than 6; saturation (INSATU), fraction of carbons in the sp^3 hybridization not less than 0.25; and flexibility (FLEX), no more than nine rotatable bonds.

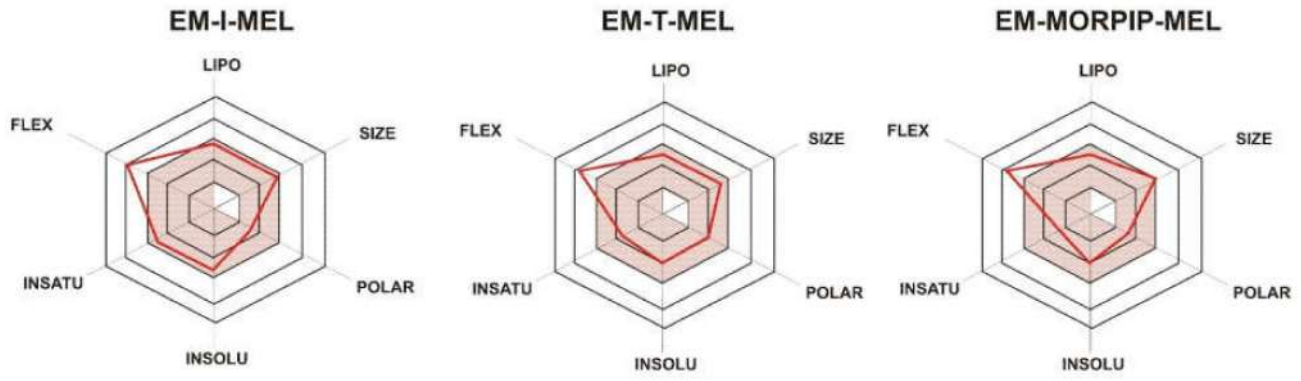

Figure 2. RADAR charts for the physicochemical properties of lipophilicity (LIPO), size, polarity (POLAR), solubility (INSOLU), saturation (INSATU), and flexibility (FLEX) determined for EM–I–MEL, EM–T–MEL, and EM–MORPIP–MEL.

For all the compounds tested, five of the six properties analyzed were located in the pink area, which proved their optimality and compliance with the properties typical for compounds belonging to the group of druglike compounds. Based on these properties, it was also concluded that the test compounds were predicted not to be orally bioavailable because they were too flexible. Intravenous administration would be recommended.

2.3. Chemical Modifications of Melphalan Alter Its Cytotoxicity in Human Cells in In Vitro Study

The cytotoxic activity of the compounds was assessed using a resazurin reduction assay after 48 h of incubation. The sensitivity of cells to the test compounds was determined using the IC_{50} parameter (Figure 3).

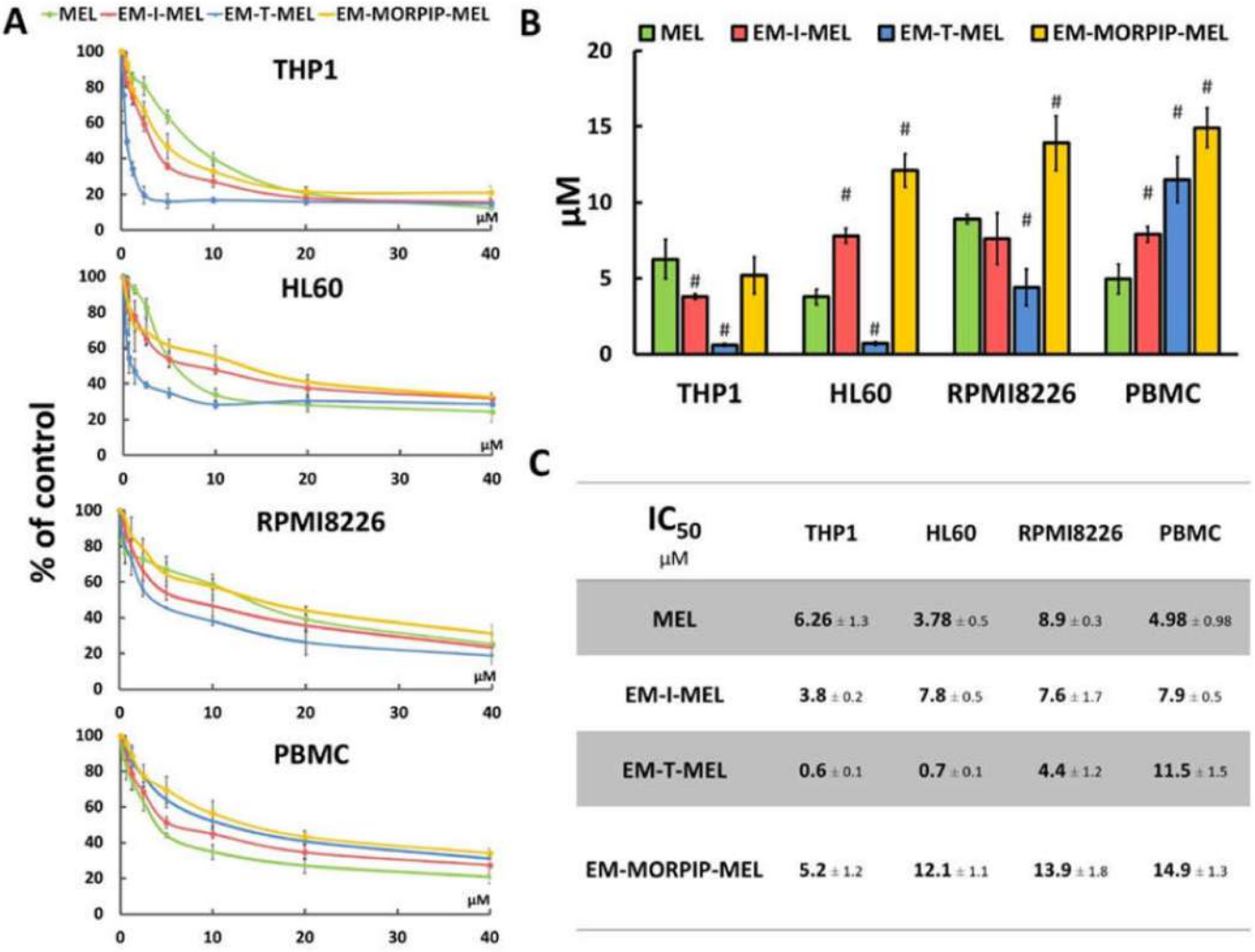

IC_{50} μM	THP1	HL60	RPMI8226	PBMC
MEL	6.26 ± 1.3	3.78 ± 0.5	8.9 ± 0.3	4.98 ± 0.98
EM-I-MEL	3.8 ± 0.2	7.8 ± 0.5	7.6 ± 1.7	7.9 ± 0.5
EM-T-MEL	0.6 ± 0.1	0.7 ± 0.1	4.4 ± 1.2	11.5 ± 1.5
EM-MORPIP-MEL	5.2 ± 1.2	12.1 ± 1.1	13.9 ± 1.8	14.9 ± 1.3

Figure 3. Chemical modifications of the melphalan molecule significantly increased cytotoxicity against leukemic cells and reduced cytotoxic activity against normal cells. (**A**) Concentration-dependent cytotoxic effects of MEL and its derivatives on HL60, THP1, RPMI8226, and PBMC growth measured by the resazurin assay. Cells without any treatment were used as controls and taken as 100%. (**B**) Graphical interpretation of IC_{50} values. (#) $p < 0.05$ statistically significant differences between samples incubated with melphalan and melphalan derivatives. (**C**) IC_{50} values for melphalan and melphalan derivatives against the cancer cell lines tested.

The cell lines tested showed different sensitivities to the parent compound and the obtained derivatives. The THP1 cells showed the highest sensitivity to the test analogs, while the RPMI8226 line had the lowest sensitivity. EM–I–MEL had higher (about 1.5 times) cytotoxicity than the parent drug in only the THP1 cells. In all cancer cell lines tested, the highest cytotoxicity was observed after incubation with EM–T–MEL. The highest activity of this compound (and the largest difference between the IC_{50} of melphalan and the IC_{50} of the derivative) was observed in human acute monocytic leukemia cells. The IC_{50} concentration of this derivative in this cell line was nearly 10 times lower than that of melphalan. In HL60 cells, the IC_{50} value of the EM–T–MEL derivative was approximately five times lower than that of the unmodified compound. Cells of the multiple myeloma

line also showed high (two times higher than melphalan) cytotoxic activity after incubation with EM–T–MEL. At the same time, a decreased cytotoxic effect of EM–T–MEL was observed against peripheral blood mononuclear cells (PBMC). This analog was approximately 2.5 times less cytotoxic to PBMCs than melphalan. The cytotoxicity of EM–MORPIP–MEL was similar against THP1 and higher against HL60, RMPI8226, and PBMCs compared to the parent drug. Because of this, EM–MORPIP–MEL was eliminated from further analyses. One concentration per cell line was selected for testing of the next parameters: RPMI8226, 3 μM; HL60, 0.7 μM; THP1, 0.3 μM, which were the same as in previous studies evaluating the biological properties of melphalan analogs [13].

2.4. Tested Melphalan Analogs Caused DNA Fragmentation in Leukemic Cells

The level of DNA damage in THP1, HL60, and RPMI8226 cells was analyzed by performing an alkaline version of the comet assay. Cells were incubated with melphalan and its derivatives (EM–I–MEL, EM–T–MEL) for 4, 24, and 48 h. Cells not treated with any compound were taken as control. Figure 4 shows DNA damage measured as a percentage of DNA in the comet tails of the cells tested. It was shown that melphalan and its derivatives induced DNA damage in the cells, and this increase was dependent on the incubation time. The most cytotoxic derivative, EM–T–MEL, also generated the highest level of DNA damage in all tested cells, mainly after 24 and 48 h of incubation. After as little as 4 h of incubation of the cells with the compounds, increased levels of DNA damage were observed. In THP1 cells at this time, unmodified melphalan caused 5.5% DNA strand breaks, while the EM–I–MEL derivative caused 9.2% DNA strand breaks. The EM–T–MEL derivative caused 11.7% DNA strand breaks. Statistically significant changes compared to melphalan were observed after 24 h incubation with EM–I–MEL and 24 and 48 h incubation with EM–T–MEL. Similar relationships were also observed in the HL60 cells. Treating HL60 cells for 48 h with the EM–T–MEL derivative (30.1%) was associated with twofold higher levels of DNA damage than was treating them with MEL (15.6%). The maximum level of myeloma cells with damaged DNA was observed after 48 h of treatment with derivatives EM–I–MEL (34.1%) and EM–T–MEL (38.5%).

2.5. Chemical Modifications Increase the Proapoptotic Properties of Melphalan: Using Double Staining to Determine the Mechanism of Leukemia Cell Death

2.5.1. Hoechst 33342 and Propidium Iodide Double Staining

The simultaneous use of two fluorescent dyes—propidium iodide (PI) and Hoechst 33342—enabled the identification of four populations of cells in the microscope image field: live, early-apoptotic, late-apoptotic, and necrotic cells. The experiment was carried out after 4, 24, and 48 h of incubation with the test compounds. Figure 5B,C shows the morphological changes, while the quantitative analysis of the live cell fraction and the early apoptotic, late apoptotic, and necrotic cells are shown in Figure 5A.

In the case of THP1 cells, after 24 h of incubation with the test compounds, a significant increase in the number of cells in the early stage of apoptosis was observed with EM–I–MEL (23% of the total population) and EM–T–MEL (31% of the total population) compared to MEL (13% of the total population). After a 4-h incubation, significant changes were observed only in relation to the control. The greatest changes were observed after 48 h incubation with the EM–T–MEL derivative. There was a significant increase in the pool of late apoptotic cells (49% of the total population) compared to control cells (2.5%) and cells treated with melphalan (4%). There was also a significant increase in the number of cells in the early stage of apoptosis (25%). It is also worth noting that treatment of THP1 cells resulted in the appearance of a fraction of necrotic cells. The necrotic cell content in the entire population was 13%. These changes were statistically significant relative to the control and parent drug. The EM–I–MEL derivative led mainly to an increase in the number of early apoptotic cells (29% of the total population) and late apoptotic cells (13%) in the longest incubation period with the compound. The 48 h incubation of THP1 cells

with the parent drug was associated mainly with an increase in the pool of early apoptotic cells (20%).

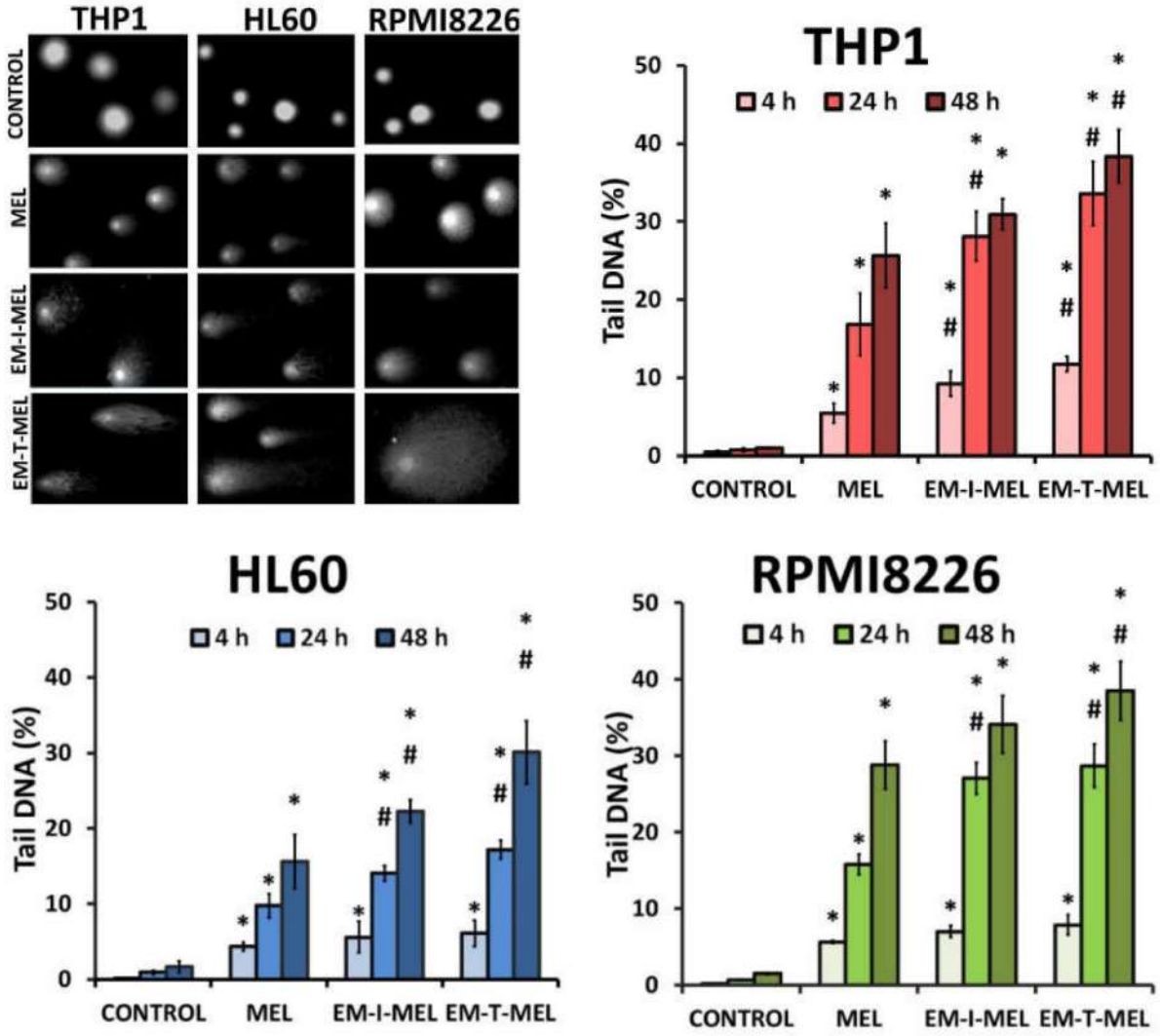

Figure 4. Melphalan analogs increased DNA damage (percentage of DNA in the comet tail) in THP1, HL60, and RPMI8226 cells after 4, 24, and 48 h of incubation. The characteristic tails of comets with damaged DNA are shown under a fluorescence microscope after electrophoresis and 4′,6-diamidino-2-phenylindole (DAPI) gel staining. All data are from three biological assays and are graphed as the mean ± SD. (*) Statistically significant differences compared to control cells, $p < 0.05$. (#) Statistically significant differences compared to MEL, $p < 0.05$.

The 24 and 48 h incubations of HL60 cells with MEL and MEL derivatives resulted in significant increases in the population of apoptotic and necrotic cells. After 24 h of incubation, the EM–I–MEL derivative initiated the appearance of about 31% of the apoptotic cell fraction (early apoptotic cells: 17% of the entire population; late apoptotic cells: 14%; necrotic cells: 8.5%). In the case of the EM–T–MEL derivative, an even greater percentage of apoptotic cells was recorded, approximately 40% (early-apoptotic cells: 25% of the total population; late-apoptotic cells: 15%), and 19% of the entire population was necrotic cells. The 48 h incubation of HL60 cells resulted in a significant increase in the fraction of late apoptotic cells for both the EM–I–MEL derivative and the EM–T–MEL derivative compared to the parent compound.

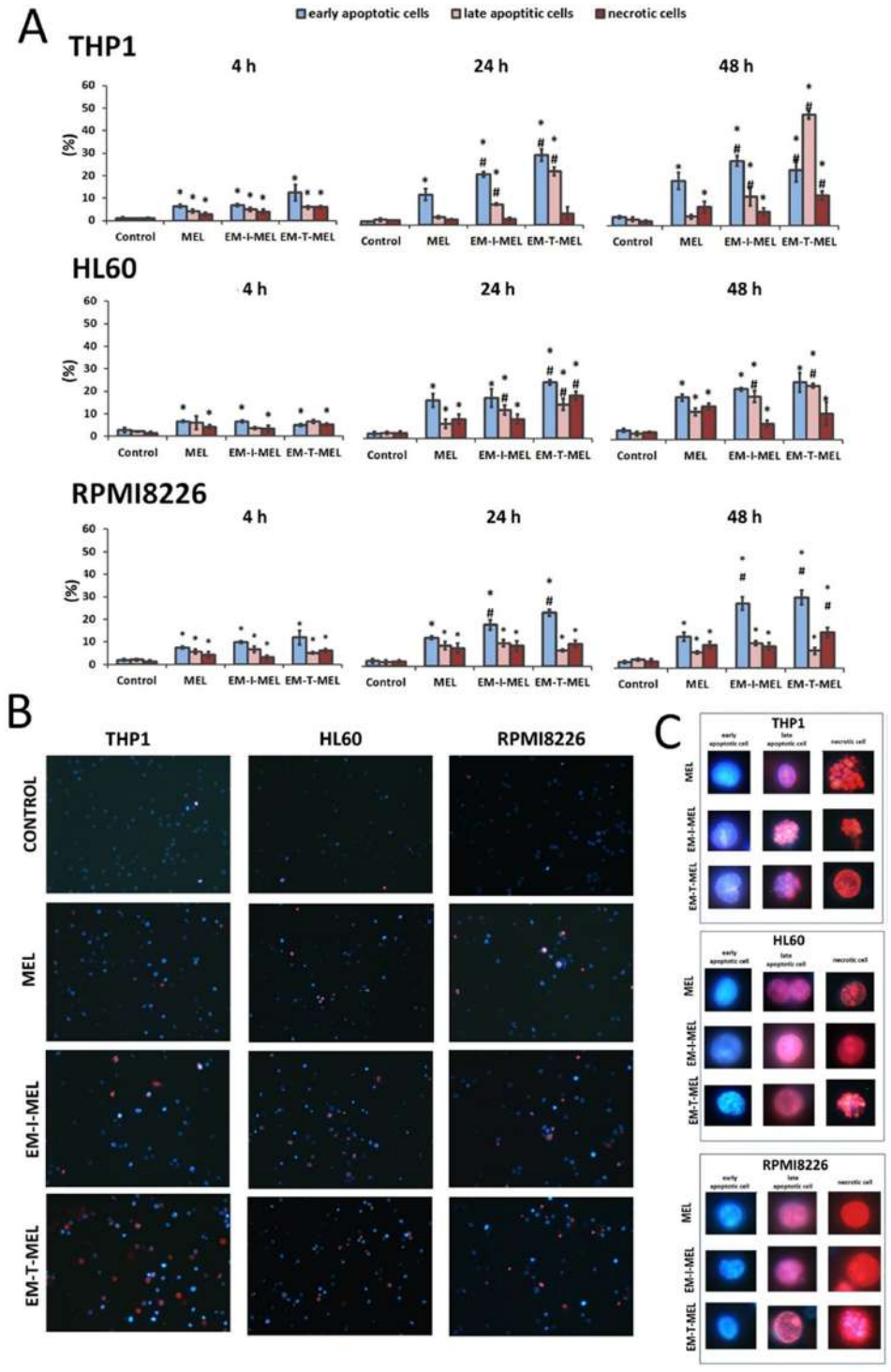

Figure 5. Novel melphalan analogs showed higher proapoptotic activity than the unmodified compound. (**A**) Fractions of apoptotic and necrotic cells after 4–48 h of incubation with MEL and test melphalan derivatives. Results are presented as the mean ± SD. (*) Statistically significant differences compared to control cells, $p < 0.05$. (#) Statistically significant differences compared to MEL, $p < 0.05$. (**B**) Determination of the fraction of apoptotic and necrotic cells after 48 h incubation with melphalan and melphalan derivatives. Cells were stained with the fluorescent dyes Hoechst 33342 and propidium iodide (PI) to determine the fraction of live cells (pale blue fluorescence), early-apoptotic (bright blue fluorescence), late-apoptotic (pink–violet fluorescence), and necrotic (red fluorescence) cells. (**C**) Morphological changes observed in the THP1, HL60, and RPMI8226 lines after 48 h of incubation with melphalan and the derivatives EM–I–MEL and EM–T–MEL. The cells were visualized under a fluorescence microscope (Olympus IX70).

In the case of multiple myeloma cells, after 24 and 48 h of incubation with melphalan and the test analogs, a significant increase in the number of early-apoptotic cells was found. Furthermore, 48-h incubation with EM–I–MEL or EM–T–MEL derivatives resulted in the appearance of about 40% of the total population as apoptotic cells (early and late apoptosis). This increase was about two times higher than that in the cells treated with the parent drug. There was also a significant increase in the number of necrotic cells after incubation with the EM–T–MEL derivative (16% of the total population) compared to after incubation with MEL (10%).

2.5.2. Annexin V-Fluorescein Isothiocyanate, and Propidium Iodide Double Staining

One marker of cell death by apoptosis is a disruption in the cell membrane asymmetry and externalization of phosphatidylserine. Therefore, we performed a qualitative assessment of the molecular events associated with apoptosis using the annexin V–fluorescein isothiocyanate (FITC) and PI double staining method (Figure 6). We also included bright-field observation images in order to visualize morphological changes after treatment with the investigated compounds. EM–T–MEL caused the most significant changes in single-cell morphology, such as shrinkage, apoptotic body formation, and cell fragmentation. At the same time, cells after incubation with the test compounds, mainly EM–T–MEL, showed high green (derived from annexin V–FITC) and red fluorescence (derived from propidium iodide), indicating phosphatidylserine translocation and damage to cell membrane integrity.

2.6. Melphalan Derivatives Activated Caspase-Dependent Apoptosis: Determining the Apoptotic Pathway in Cancer Cells

The anticancer properties of compounds are primarily due to their ability to induce apoptosis. We assayed the activity of the executive caspase 3/7 and initiator caspases 8 and 9, which are directly involved in the activation of this process. The final results are expressed as the percentage of activity of a specific cysteine protease, with the fluorescence value of the untreated control taken as 100%.

In the case of THP1 cells, increased activity of mainly caspase 3/7 was observed (Figure 7). After a 24 h incubation with the EM–T–MEL (1506%) derivative, the increase in activity of this cysteine protease was about six times higher than that after incubation with the unmodified MEL (243%). Incubations for 4 h and 24 h of THP1 cells with all test compounds resulted in activation of caspase 9. However, the changes were statistically significant only relative to the control. HL60 cells were also highly sensitive to caspase 3/7 activation. Significant changes in the activity of this caspase were observed mainly after 24 h of incubation with the EM–T–MEL derivative (1307%) compared to the parent drug (233%). After 48 h incubation, statistically significant changes were also observed for the derivative EM–I–MEL (1044%). The increased activity of this caspase was preceded mainly by the activation of the initiating caspase 8 after incubation with all test compounds. The changes were statistically significant only compared to the control. RPMI8226 cells induced caspase 3/7 mainly after 24 and 48 h of incubation. In contrast, the most cytotoxic EM–T–MEL derivative caused an increase in the activity of this caspase after only 4 h of incubation. In contrast, this line was the least sensitive to the activation of this cysteine protease. There was also no increase in the activity of the analyzed initiating caspases (8 and 9) during the tested incubation times with the compounds.

2.7. The New Derivatives of Melphalan Caused Loss of Mitochondrial Membrane Potential

The disruption of mitochondrial integrity is a key event in apoptosis. Depolarization of the mitochondrial membrane is often associated with apoptosis by the release of proapoptotic proteins, such as cytochrome c, from the mitochondria and the formation of a proapoptotic complex. The impact of MEL, EM–I–MEL, and EM–T–MEL on the mitochondrial membrane potential ($\Delta\Psi m$) in HL60, RPMI8226, and THP1 cells was assessed using fluorometric analysis after staining with the fluorescent dye 5,5′,6,6′-tetrachloro-1,1′,3,3′-tetraethylbenzimidazolcarbocyanine (JC–1) (Figure 8). Red fluorescence of JC–1

dimers (high mitochondrial potential) was observed in control cells. Treatment with new compounds dramatically increased the green fluorescence of JC–1 monomers, indicating decreases in the mitochondrial membrane potential. All compounds induced time-dependent changes. In all the cell lines studied, the greatest changes in the mitochondrial potential took place after EM–T–MEL treatment.

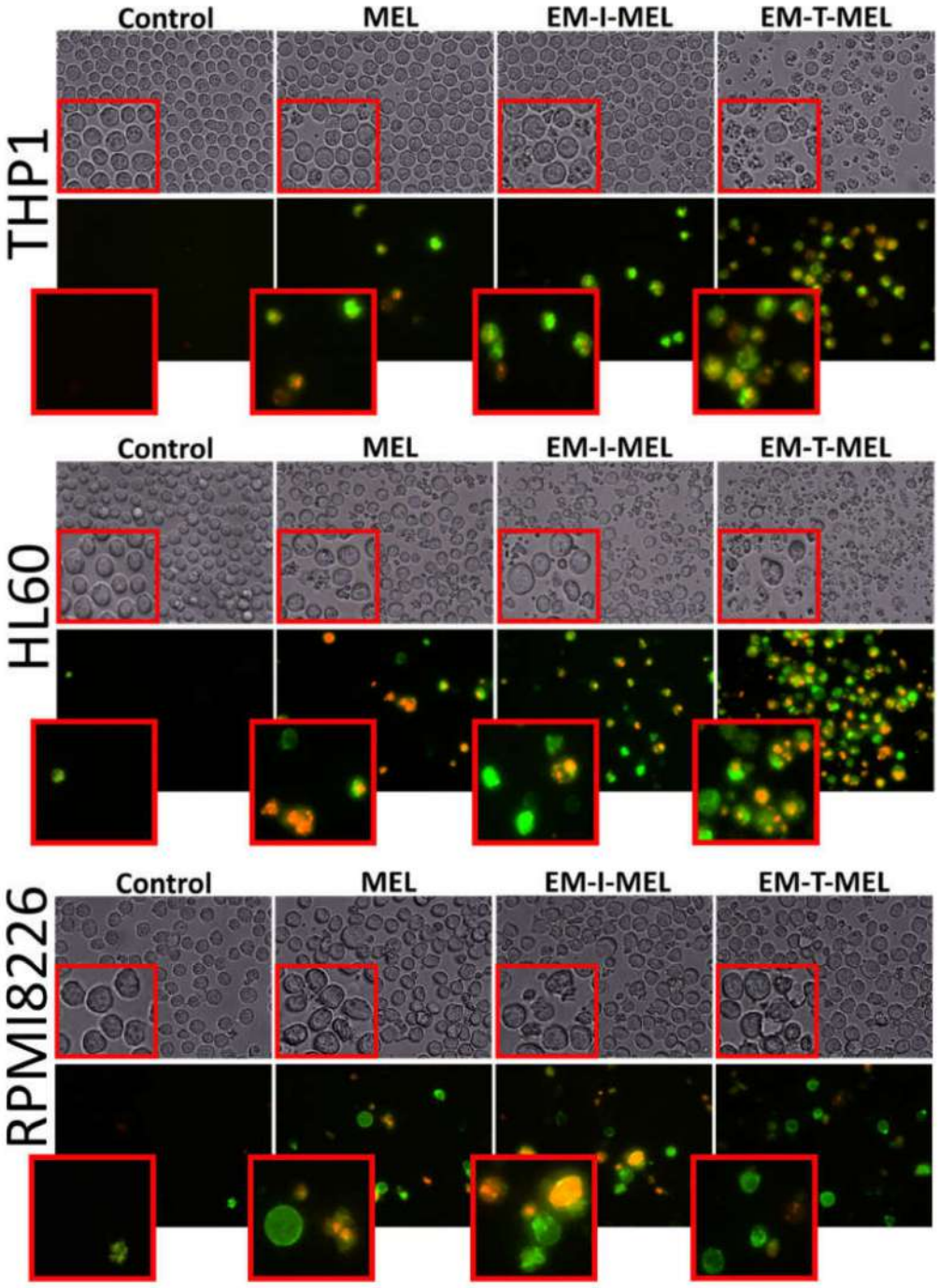

Figure 6. The investigated derivatives induced changes in cell membrane integrity and externalization of phosphatidylserine. We visualized THP1, HL60, and RPMI8226 cells by fluorescence microscopy (Olympus IX70, Japan) after 24 h of incubation with MEL and the test derivatives. The cells were stained with annexin V–fluorescein isothiocyanate (FITC) and PI. After incubation with MEL derivatives, mainly EM–T–MEL cells showed high green (derived from annexin V–FITC) and red fluorescence (derived from PI) indicative of exposed phosphatidylserine (PS) and damage to cell membrane integrity, characteristic features of apoptosis.

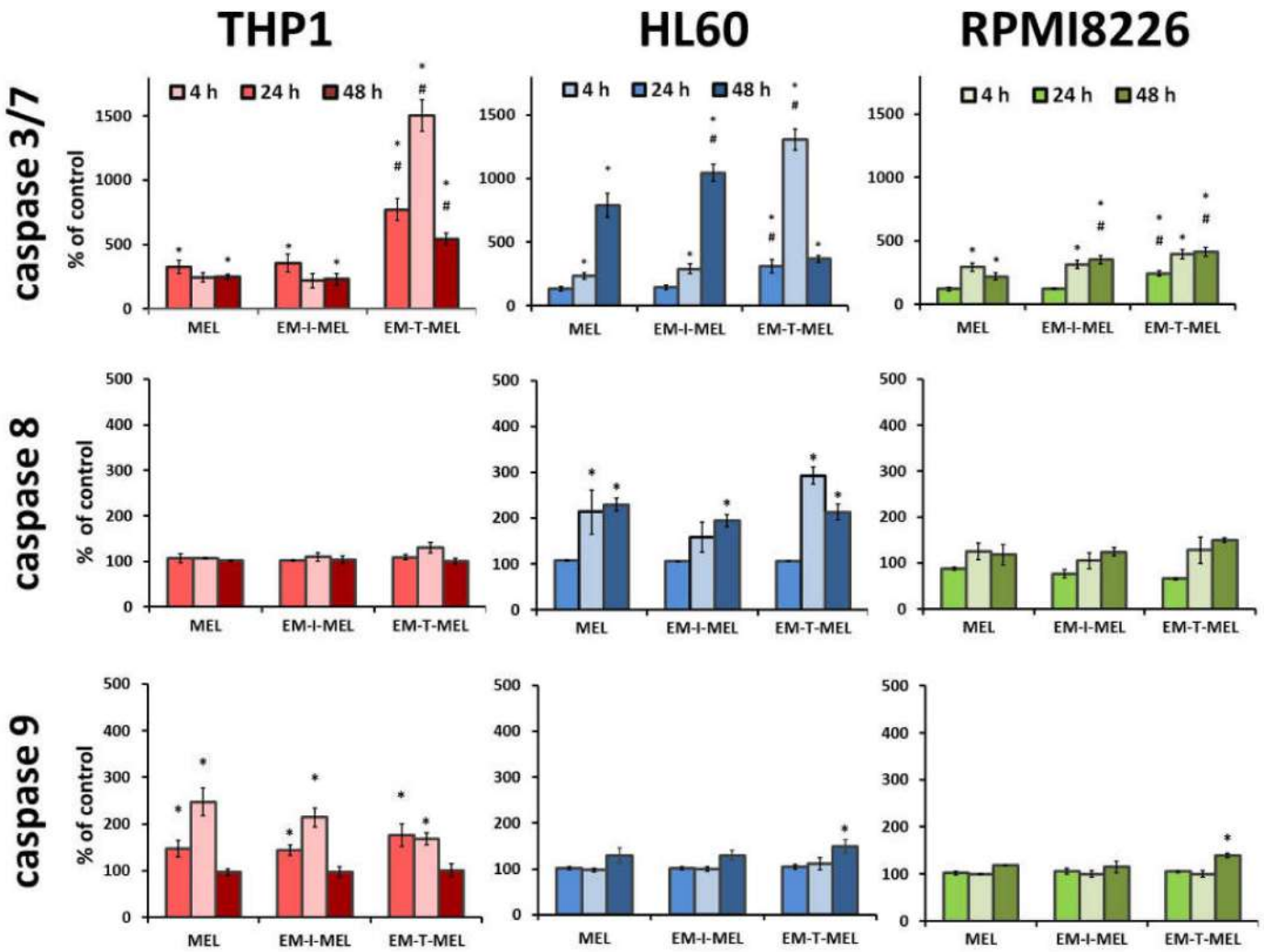

Figure 7. Melphalan derivatives activated executive caspase 3/7 and initiator caspases 8 and 9 in THP1, HL60, and RPMI8226 cells. Cells were incubated for 4, 24, and 48 h with MEL, EM–I–MEL, and EM–T–MEL. The final results are expressed as the percentage of activity of a specific cysteine protease, with the untreated control taken as 100%. All data are from three biological assays and are graphed as the mean ± SD. (*) Statistically significant differences compared to control cells, $p < 0.05$. (#) Statistically significant differences compared to MEL, $p < 0.05$.

The highest green fluorescence intensity was observed in HL60 cells treated with the EM–T–MEL for 24–48 h (ΔΨm dropped to 24.8% vs. control). Already after 18 h of treatment, a statistically significant difference was noticed between the action of the derivative and that of MEL. EM–I–MEL also led to a significant reduction in ΔΨm (to 42%) compared to MEL (to 76%) after 48 h of treatment. In the acute monocytic leukemia cells, strong green fluorescence of JC–1 monomers was observed after treatment with both new melphalan derivatives. Furthermore, in this line, the derivative EM–T–MEL significantly decreased the potential against melphalan. The RPMI8226 line turned out to be the least sensitive to the activity of the test compounds regarding ΔΨm changes. Interestingly, this line was also sensitive to the action of EM–I–MEL and EM–T–MEL, but after a longer incubation time. Chlorophenylhydrazone (CCCP), an uncoupler of oxidative phosphorylation, was used as a positive control for the depolarization of ΔΨm.

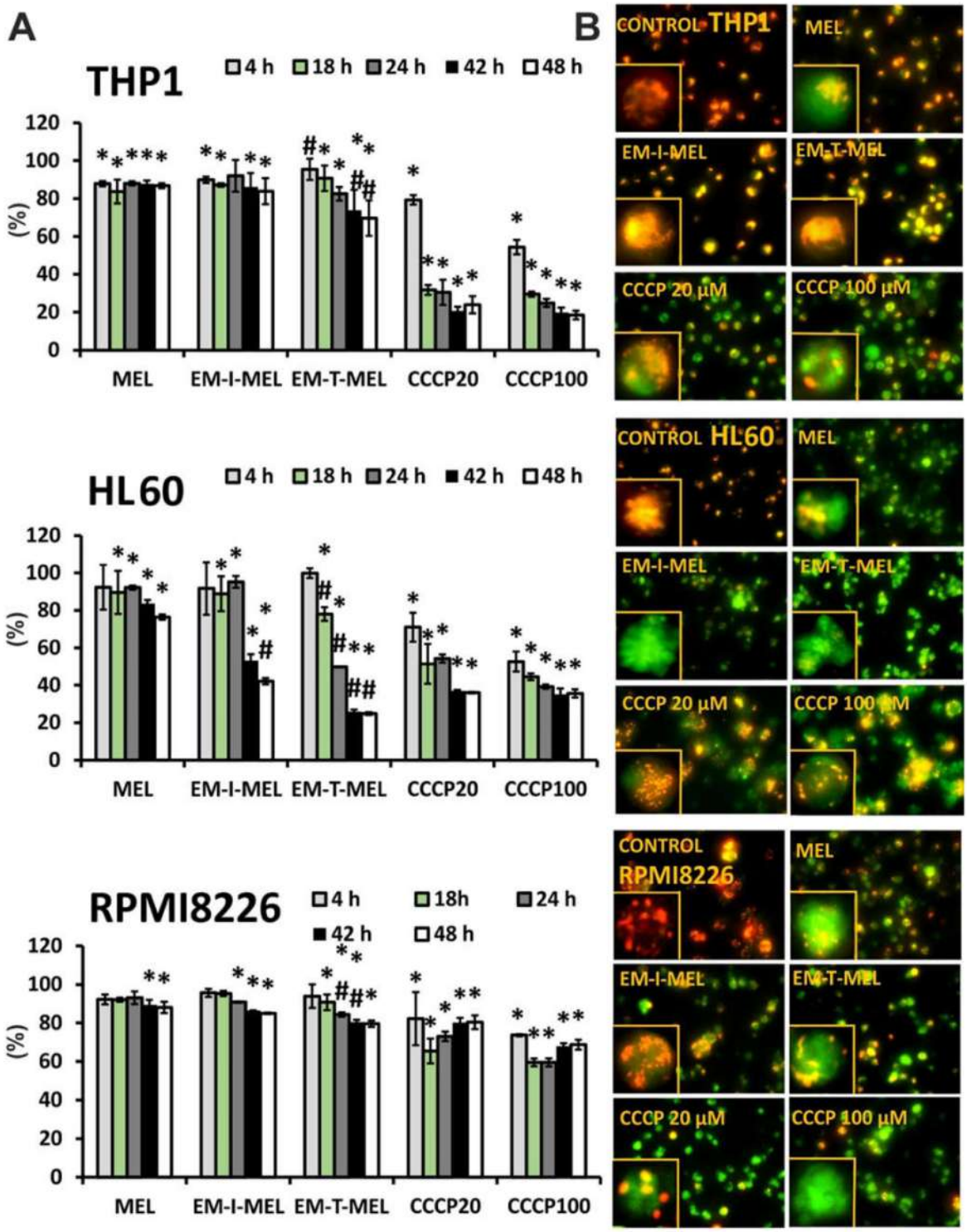

Figure 8. New melphalan derivatives induced a decrease in mitochondrial membrane potential. (**A**) The fluorescence ratio of JC–1 dimers/JC–1 monomers in the control was assumed to be 100%. The cells were stained with the fluorescence probe JC–1 prior to 4–48 h of incubation with MEL, EM–I–MEL, EM–T–MEL, or carbonyl cyanide *m*–chlorophenyl hydrazone (CCCP) (20, 100 µM). All data are from three biological assays and are graphed as the mean ± SD. (*) Statistically significant differences compared to control cells, $p < 0.05$. (#) Statistically significant differences compared to MEL, $p < 0.05$. (**B**) Fluorescent microscopy images of HL60, THP1, and RPMI8226 cells stained with JC–1 probe after 48 h. The cells were viewed under an inverted fluorescence microscope (Olympus IX70, Japan, 400× magnification).

3. Discussion

Blood cancers remain a major health issue despite the high therapeutic efficacy of new treatment options and continuous pharmacological developments. In a previous study [13], we verified and confirmed the hypothesis that chemical modifications to melphalan increased its anticancer properties. We showed that esterification of the carboxyl group was necessary to improve the effectiveness of melphalan. In addition, the additional replacement of the amino group with an amidine group containing two heteroatoms (O and N) in the structure significantly increased the properties of the drug.

The subject of the present research was the analysis of three new melphalan derivatives with increased cytotoxic activity in human neoplastic cells that have not yet been described in the literature. New chemical modifications to old, well-known drugs require a balance between size and lipophilicity to improve cytotoxicity in leukemia therapy. Two of the most effective melphalan modifications were the addition of a morpholine group in our previous work [13] and a thiomorpholine group in the current work. Morpholine and its analogues represent effective heterocycles because of their conformational and physicochemical properties. The oxygen atom in this ring increases binding affinity by participating in donor–acceptor-type interactions with the corresponding receptor. Moreover, the oxygen atom reduces the basicity of the nitrogen atom of the morpholine ring by its electronegative effect [15,16]. Two heteroatoms in the amidine group at the opposite position provide flexible conformation to the ring. Thanks to this construction, this group can participate in lipophilic−hydrophilic interactions. Morpholine modulates properties of the overall structure, as the presence of a weak basic nitrogen at the opposite position of the oxygen atom enhances solubility [17]. Morpholine derivatives can act as antidepressants, analgesics, antitumor agents, antioxidants, antibiotics, or antifungals as well as serving in the treatment of central nervous system disorders [18]. The analog with the rest of the thiomorpholine is part of the previously adopted strategy, because thiomorpholine has two heteroatoms (N and S) in its structure. We attempted to synthesize and research a system that has not been tested so far, i.e., the use of a bicyclic structure consisting of two rings in the amidine group (analog with the rest of the indoline) and the use of a bicyclic structure additionally containing two nitrogen atoms and an oxygen atom. In addition to the described modifications to the amino group, the resulting derivatives were converted to methyl esters according to the established observations that ester analogs are more cytotoxic than the free carboxyl group analogs. We assessed the cytotoxic, genotoxic, and proapoptotic properties against multiple myeloma (RPMI8226) and two types of myeloid leukemia (acute promyelocytic leukemia (HL60) and acute monocytic leukemia (THP1)) to determine the biological activity of the new analogs.

Investigations of the pharmacological properties of new molecular chemical entities (NMEs) or major drug discovery candidates have accelerated in recent years because of the high failure rate of drug candidates in clinical trials. The incorporation of in vitro studies prior to the absorption, distribution, metabolism, elimination, and toxicity (ADMET) study is a promising strategy to improve research on future drug candidates. Drug toxicity is one of the most relevant properties and the most unpredictable characteristic of a drug, as it can be species- and organ-specific. The toxicity of a compound to different cell types can be evaluated using easily available and widely applied in vitro cytotoxicity assays. The advantage of these assays is that they facilitate the process of screening large chemical libraries [19]. Our study used well-known and recommended screening methods to assess the toxicity and intracellular mechanisms associated with the cytotoxic effects of compounds with anticancer potential.

A significant clinical problem in patients with advanced cancer is the high toxicity of chemotherapy. Melphalan is responsible for forming covalent cross-bonds between DNA strands, preventing transcription and replication, leading to cell death. The number of intrastrand cross-links formed is correlated with both the in vitro cytotoxicity of the drug and the patient's response to treatment [20]. We assessed the cytotoxic activity of the test compounds against neoplastic cells and normal PBMCs. The cytotoxic effect of

MEL and its derivatives was dose dependent. The IC_{50} parameter, i.e., the concentration necessary to inhibit the biological process in vitro by 50%, was determined. The EM–T–MEL derivative showed the highest cytotoxicity against neoplastic cells, with the IC_{50} value being about tenfold (THP1), fivefold (HL60), and twofold (RPMI8226) lower than the unmodified compound. Simultaneously, this compound was significantly less (2.5-fold) cytotoxic than melphalan to PBMCs. The EM–I–MEL analog was also more cytotoxic than MEL, exhibiting significantly lower IC_{50} values in the THP1 cancer cell model. Since the cytotoxic activity of the EM–MORPIP–MEL derivative was comparable or less than that of the parent drug, it was eliminated from further analyses. These results confirmed the finding from our previous studies [13] that chemical modifications involving esterification and conversion of an amino group to an amidine group with two heteroatoms exhibit high cytotoxic properties against cancer cells and low cytotoxicity to PBMCs. Esterification and modification of the amino group significantly modify the properties of the compound. Thus, when explaining the different cytotoxic activities of the analyzed compounds, the size, structure, and ring geometry of the attached amine should be taken into account. There have also been reports in the literature that esterification can increase bioavailability and cellular penetration [21–24]. In addition, other in vitro studies have shown that amidine analogs of melphalan reduce the number of estrogen receptor-positive and estrogen receptor-free breast cancer cells [25,26].

Melphalan is mainly transported to the cells via large neutral amino acid transporter 1 (LAT1) [7,27]. It has been shown that the level of LAT1 expression in tumor tissues is significantly higher than in surrounding healthy tissues [28]. Nonsolid tumors exhibit altered LAT1 expression: LAT1 acts as an activating antigen in T cells, and T cell leukemia results in higher levels of LAT1 expression compared to levels in normal activated T cells [27]. We observed higher differences in the sensitivity of normal and leukemic cells in the new derivatives than in melphalan. Leukemic cells require large amounts of nutrients and amino acids for rapid growth and continuous proliferation. The new derivatives, because of the reduced polarity of the molecule in comparison to melphalan, may have wider delivery strategies. EM–T–MEL, EM–I–MEL, or EM–MORPIP–MEL can be transported to cancer cells by other membrane receptors that are overexpressed in leukemia cancer cells: MCT-1, -2, and -4, for lactate transport; OAT-1, for small, hydrophilic organic anion transport; OCTN-1, FLIPT-1, and OCT-6, for organic cation transport; and OATP1B1 and OATP1B3, for large, hydrophobic anion transport [29]. P2X7R, an ATP-gated ion channel, is widespread in cancer cells and overexpressed in AML. Recent studies have indicated that P2X7R-activated macropore opening was shown to enhance the intracellular uptake of drugs including chemotherapeutics such as doxorubicin. P2X7R-activated macropore opening was therefore proposed as tumor cell-specific drug delivery system [30].

Melphalan, as an alkylating drug, is responsible for an increase in the level of the DNA double break marker (γH2AX), induces the phosphorylation of checkpoint kinase 1 (CHK-1) and checkpoint kinase 2 (CHK-2) in MM cells (RPMI8226 and MM1.S) [31], and leads to apoptosis through the formation of intra- and interstitial DNA cross-bonds [32]. Confirming the genotoxic properties of melphalan in selected models of neoplastic cells (THP1, HL60, RPMI8226) and determining whether the new derivatives cause an increase in the level of DNA damage have become further goals of our research. Both the parent drug and the derivatives induced DNA damage in a time-dependent manner. The EM–T–MEL derivative resulted in the highest level of DNA damage in all tested cells, which correlated with the cytotoxicity analysis.

Understanding the mechanism of death of a cancer cell exposed to the test compounds was one of the main research problems of this study. Apoptosis is an important goal of chemotherapy as a process that is strictly regulated and controlled by specific biochemical processes requiring the expression of many different genes. Abnormal apoptosis is a key factor in resistance to chemotherapy. The ability of drugs to induce apoptosis is considered an important criterion in assessing their therapeutic efficacy. Apoptosis is the preferred type of cell death, as it is a noninflammatory physiological process. Unlike necrosis, apoptosis is

characterized by specific morphological and biochemical changes, including cell shrinkage, fragmentation of the cell nucleus, chromatin condensation, disturbance in cell membrane asymmetry, and the formation of small vesicles (ApoBD) [33,34]. One early marker of apoptosis is a change in cell membrane asymmetry and phosphatidylserine translocation. The tested melphalan analogs induced apoptosis in the tumor cells. Based on the results obtained, the test compounds were characterized by different degrees of influence on the leukemic cells and multiple myeloma, manifested by changes in cell morphology. The greatest change was observed after 24 h of incubation with the test compounds, mainly the EM–T–MEL derivative, which correlated with the analysis of the cytotoxicity of the test analogs. Examination of the morphological changes after Hoechst 33342/PI and annexin V–FITC/PI staining suggested that the EM–T–MEL derivative triggered apoptosis-specific markers more clearly than the unmodified MEL in all cell lines tested.

Another aspect of our current study focused on the biochemical changes occurring during apoptosis induced by the melphalan analogs. Melphalan and other DNA cross-linkers increase mitochondrial stress in HeLa and HCT cells and have been shown to be responsible for increasing the cytotoxicity of melphalan [35,36]. Research showed that melphalan induced apoptosis by mediating the mitochondrial permeability transition pore (mPTP) in cervical and colorectal cancer cells [36]. The involvement of mitochondria-dependent mechanisms is critical to the execution of intrinsic apoptotic pathways and is also required for executing the extrinsic apoptotic program. In HL60 cells, $\Delta\Psi m$ collapsed after only 4 h of MEL treatment. Treatment of HL60 cells with a mitochondrial uncoupling agent CCCP (50 µM for 1 h) caused a remarkable drop in $\Delta\Psi m$ [37]. Our data showed that following treatment with melphalan derivatives in cancer cell lines, the mitochondrial membrane potential dropped, especially at longer incubation times of 24–48 h. The changes were larger than those induced by the unmodified parent compound. The new melphalan derivatives, EM–I–MEL and EM–T–MEL, significantly disrupted the potential of the mitochondrial membrane, especially in the promyelocytic cell line. It has been shown that melphalan promotes rapid fragmentation of the mitochondrial network in a time-dependent manner and consequently the early activation of apoptosis.

Comprehension of the mechanisms by which cytotoxic drugs inhibit cancer cell proliferation and induce apoptosis is important for optimizing therapeutic efficacy. Programmed cell death (PCD) is an active, energy-dependent process that requires the activation of many genes and can proceed in various ways involving different cell organelles. Caspases—intracellular enzymes belonging to a large family of serine proteases—are involved in the process of apoptotic cell death. These enzymes are involved both at the initiation stage (initiating caspases include caspases 2, 8, 9, and 10) and at the final stage of apoptosis, the latter of which is referred to as the effector phase (effector caspases include caspases 3, 6, and 7). Caspase 9 is involved mainly in the intrinsic pathway of apoptosis, where mitochondria play a major role in apoptotic signaling and regulation of cell death processes. Caspase 8 is involved mainly in the intrinsic pathway mediated by receptor proteins [34,38]. Incubation with MEL and the test analogs resulted in activation of the effector caspase 3/7. We observed differences in sensitivity of the test analogs toward the tested cancer cells. The most sensitive cell lines were HL60 and THP1, while the least sensitive was the multiple myeloma line. The EM–T–MEL derivative most potently induced caspase 3/7 activation in all cell lines tested. In the case of THP1 and RPMI8226 cells, activation of this cysteine protease occurred after only 4 h of incubation with this analog. Activation of caspase 3/7 was preceded by the initiation of caspase 9 (mainly in THP1 cells) or caspase 8 (mainly in HL60 cells). The intrinsic pathway can be activated in the presence of intracellular signals or in response to the activation of death receptors on the plasma membrane. The intrinsic pathway is triggered by signals such as DNA damage leading to an imbalance between proapoptotic and antiapoptotic proteins in mitochondria and destabilization of mitochondrial membrane potential. In the case of RPMI8226 cells, no increase in the activity of caspase 8 or caspase 9 was observed. The low level of activation of these initiating caspases may suggest activation of a mechanism of cell death other than

apoptosis. Mitotic catastrophe is a pathway of cell death caused mainly by microtubule-stabilizing or -destabilizing factors and DNA damage. It is triggered by mitotic failure due to dysfunctional cell cycle checkpoints and the development of aneuploid cells [39]. Mitotic failure occurs in a p53-independent manner and involves the activation of caspase 2 followed by the release of cytochrome c, activation of caspase 3, chromatin condensation and permeabilization of the mitochondrial membrane, and the subsequent formation [40–42] of mononucleated giant cells (MONGC) or multinucleated giant cells (MNOC) [43]. Mitotic catastrophe activation by melphalan was observed in multiple myeloma cells [44]. This may suggest activation of this death pathway in RPMI8226 cells after incubation with the melphalan analogs analyzed. Understanding the detailed mechanism of multiple myeloma cell death will be the goal of further research on new melphalan analogs.

4. Materials and Methods

4.1. General

Fine chemicals and solvents for synthesizing the analogs were purchased from commercial vendors and used without further purification.

Reactions were monitored by the TLC method. Analyses were performed on aluminum plates precoated with silica gel (Merck 60 F_{254}, 0.25 mm). To develop the chromatogram, the following solvent system was used: methylene chloride/methanol/formic acid/water (82:15:2:1 $v/v/v/v$). Plates were visualized under UV light at 254 and 366 nm.

The chemical purity of MEL, MOR–MEL, and the products obtained in the subsequent stages of synthesis was tested by HPLC. The analyses were performed in a typical Waters system consisting of an autosampler, two pumps, a degasser, and a photodiode detector. The stationary phase was a Chromolith Performance RP18e column at 30 °C, and the mobile phase was a gradient of 0.1% trifluoroacetic acid (TFA) in water and 0.1% TFA in acetonitrile. The flow rate of the mobile phase was 1 ml/min. Relative retention time (RRT) is presented with reference to melphalan (see Figure S1).

Melting point measurements were carried out on an automatic Mettler Toledo MP70 system. For each compound, four capillary measurements were made in parallel, and the results were averaged.

Optical rotation measurements were performed on a Perkin Elmer 341 polarimeter at a wavelength of 589 nm in methanol at 20 °C using a standard 1 ml cuvette.

The IR spectra were recorded on a NICOLET 380 FTIR spectrometer with a high-pressure ATR attachment equipped with a germanium crystal. The characteristic bands were approximately 1690 cm^{-1} (>C=N–amidine) and approximately 1740 cm^{-1} (>C=O) (see Figures S2–S4)

^{1}H NMR, ^{13}C NMR, DEPT, COZY, HMBC, and HSQC spectra were measured using the Bruker AVANCE III HD 500MHz instrument at 500 MHz (^{1}H) and 125 MHz (^{13}C) at 25 °C for solutions in DMSO–d_6 (see Figures S5–S10).

High-resolution mass spectrometry (HRMS) measurements were performed using a Synapt G2–Si mass spectrometer (Waters) equipped with an ESI source and quadrupole-time-of-flight mass analyzer. The mass spectrometer was operated in the positive ion detection mode. The optimized source parameters were: capillary voltage 3.2 kV, cone voltage 30 V, source temperature 110 °C, desolvation gas (nitrogen) flow rate 600 dm^3/h, temperature 350 °C, and nebulizer gas pressure 6.5 bar. To ensure accurate mass measurements, data were collected in the centroid mode. The mass was corrected during acquisition using leucine enkephalin solution as an external reference (Lock-Spray™), which generated a reference ion at m/z 556.2771 Da ($[M+H]^+$) in the positive ESI mode. The results of the measurements were processed using the MassLynx 4.1 software (Waters) incorporated with the instrument (see Figures S11–S16).

4.2. Synthesis

4.2.1. 2-(Morpholinmethylideneamino)-3-[4-[bis(2-chloroethyl) amino] phenyl] Propanoic Acid (MOR–MEL)

Synthetic procedure and analytical data of this compound (under the name 2-(tetrahydro-1,4-oxazynomethylideneamino)-3-[4-[bis(2-chloroethyl) amino] phenyl] propanoic acid) come from: Ireana Oszczapowicz, Małgorzata Łukawska, Joanna Tobiasz, Anna Porębska, Agnieszka Owoc. Nowe pochodne melfalanu, sposób ich wytwarzania, zawierający je środek farmaceutyczny oraz zastosowanie medyczne. PL220880B1, p. 9, example 3. (available in polish language version only).

The reaction was carried out in an argon atmosphere. First, 305 mg (1 mmol) of melphalan was dissolved in 30 mL of methanol. Then, 195 mg (1.2 mmol) of *N*–(dimethoxymethyl) morpholine was added to this solution, and the mixture was stirred until the substrate disappeared (30 min at room temperature, TLC control). Then, the mixture was evaporated to dryness, and 4 ml methanol was added, followed by 35 ml of diethyl ether. The precipitated product was then filtered, washed with diethyl ether, and dried under vacuum. The expected product was obtained after recrystallization from the methanol/diethyl ether mixture and had the following characteristics. Mass: 310 mg (0.77 mmol). Yield: 77%. Off–white crystalline powder. 97.0% (HPLC). RRT (in ref. to MEL): 1.154, 1.201IR (cm^{-1}): 1697 (>C=N–). ^{1}H NMR (300 MHz, DMSO–d_6, δ_{ppm}): 9.30 (s, 1H, COOH), 7.74 (s, 1H, –N=C$\underline{H}$–N–), 7.06 (d, *J* = 8.4 Hz, 2H, $C_{aryl}H_{5/5'}$), 6.71 (d, *J* = 8.4 Hz, 2H, $C_{aryl}H_{6/6'}$), 3.90 (m, 1H, –C_{chiral}H–), 3.77 (m, 2H, –N_{morph}–CH_2–C$\underline{H}_2$–O–), 3.70 (s, 4H, Cl–C$\underline{H}_2$–C$\underline{H}_2$–N), 3.28 (m, 2H, –N_{morph}–C$\underline{H}_2$–CH_2–O–), 3.15 (dd, *J* = 3.9 Hz, *J* = 13.2 Hz, 1H, –$CH_A\underline{H}_B$–CH(N=)–CO_2H), 2.78 (dd, *J* = 10.8 Hz, 1H, –C$\underline{H}_A$$H_B$–$C_{chiral}$H–). Elemental analysis: calc. C—53.85%, H—6.28%, N—10.47%; found: C—53.65%, H—6.16%, N—10.27%.

New Melphalan Derivatives—General Procedure:

First, 1.61 g (4.0 mmol) of MOR–MEL was dissolved in 240 ml of methanol. Then, 8.0 mmol of the appropriate amine was added to this solution, and the mixture was stirred 18–22 h (depending on the amine) at room temperature (TLC control). Next, the mixture was evaporated to dryness, obtaining the crude product as an oil that was then purified by preparative HPLC, leading to the amine derivative of melphalan (oil, purity ca. 90% HPLC).

Then, 1 mmol (418–485 mg) of the melphalan amine derivative, 10 mL DMP, and 1 mL concentrated HCl were stirred for one hour at room temperature. The mixture was evaporated to dryness, and the resulting oil was purified by column chromatography to obtain the appropriate methyl ester with a purity of over 95% (HPLC). The free amine was then dissolved in 5 mL 4 M $HCl_{(g)}$/ethyl acetate to obtain the hydrochloride that precipitated from the solution. The solid was filtered off, washed with cold ethyl acetate, and dried under vacuum at 30 °C to obtain the final product.

The following compounds were synthesized in this manner:

4.2.2. 2-(Indolinmethylideneamino)-3-[4-[bis(2-chloroethyl) amino] phenyl] Propanoic Acid Methyl Ester Hydrochloride (EM–I–MEL):

Off-white crystalline powder. Yield: 25% (not optimized, calculated in relation to MOR–MEL). Purity: 98.80% (HPLC). RRT: 1.690. Mp.: decomposition below the melting point. $[\alpha]_d^{20}$: −37.94° (c = 1, MeOH). IR (cm^{-1}): >C=O (1743), >C=N– (1682). ^{1}H NMR (500 MHz, 25 °C, DMSO–d_6, δ_{ppm}): OCH_3 (3.72, s, 3H), C_{chiral}H (4.65, bs, 1H), C$\underline{H}_A$$H_B$$C_{chiral}$H (3.18, dd, 1H), $CH_A\underline{H}_BC_{chiral}$H (3.02, dd, 1H), $C5_{arom}$H+$C5'_{arom}$H (7.11–7.13, d, 2H,), $C6_{arom}$H+$C6'_{arom}$H (6.65, d, 2H), N–C$\underline{H}_2$–CH_2–Cl (3.62, bs, 4H), N–CH_2–C$\underline{H}_2$–Cl (3.60, s, 4H), –N=CH– (8.81, bs, 1H), $C2_{ind}$H (4.05, bs, 1H), $C3_{ind}$H (3.26, bs, 1H), $C4_{ind}$H+$C6_{ind}$H (7,35, bs, 2H), $C5_{ind}$H (7.26, bs, 1H), $C7_{ind}$H (7.11–7.13, d, 1H,). ^{13}C NMR (125 MHz, 25 °C, DMSO–d_6, δ_{ppm}): OCH_3 (52.51), >C=O (170.4), C3 (36.40), C4 (124.10), C5/C5′ (130.50), C6/C6′ (111.80), C7 (145.15), N–$\underline{C}H_2$–CH_2–Cl (51.96), N–CH_2–$\underline{C}H_2$–Cl (40.96), $C2_{ind}$ (48.07), $C3_{ind}$ (27.24), $C3a_{ind}$ (132.50), $C4_{ind}$ (126.05), $C5_{ind}$ (127.65), $C6_{ind}$ (111.11), $C7a_{ind}$ (149.98). HRMS: calc. for $C_{23}H_{28}N_3O_2Cl_2$: 448.156; found: 448.155.

4.2.3. 2-(Thiomorpholinmethylideneamino)-3-[4-[bis(2-chloroethyl) amino] phenyl] Propanoic Acid Methyl Ester Hydrochloride (EM–T–MEL)

Off–white crystalline powder. Yield: 30% (not optimized, calculated in relation to MOR–MEL). Purity: 96.27% (HPLC). RRT: 1.482. Mp.: decomposition below the melting point. $[\alpha]_d^{20}$: –78.57° (c = 1, MeOH). IR (cm^{-1}): >C=O (1748), >C=N– (1703). ^{1}H NMR (500 MHz, 25 °C, DMSO–d_6, δ_{ppm}): OCH_3 (3.72, s, 3H), $C_{chiral}H$ (4.37, bs, 1H), $C\underline{H}_AH_BC_{chiral}H$ (3.14, dd, 1H), $CH_A\underline{H}_BC_{chiral}H$ (2.90, dd, 1H), $C5_{arom}H$+$C5'_{arom}H$ (7.09, d, 2H), $C6_{arom}H$+$C6'_{arom}H$ (6.71, d, 2H), N–$C\underline{H}_2$–$C\underline{H}_2$–Cl (3.71, s, 4H), –N=CH– (7.83, bs, 1H), $NC\underline{H}_2CH_2S$ (3.61, bs, 4H), $NCH_2C\underline{H}_2S$ (2.62 and 2.35, 2 × bs (3:1), 4H). ^{13}C NMR (125 MHz, 25 °C, DMSO–d_6, δ_{ppm}): OCH_3 (52.49), >C=O (170.40), C2 (61.45), C3 (36.25), C4 (124.10), C5/C5′ (130.64), C6/C6′ (111.80), C7 (145.19), N–$\underline{C}H_2$–CH_2–Cl (52.04), N–CH_2–$\underline{C}H_2$–Cl (41.09), –N=CH– (155.13), $N\underline{C}H_2CH_2S$ (53.90, 47.30), $NCH_2\underline{C}H_2S$ (27.40, 25.80). HRMS: calc. for $C_{19}H_{28}N_3O_2Cl_2$: 432.128; found: 432.127.

4.2.4. 2-[[4-(Piperidin-4-yl)-morpholine] methylideneamino]-3-[4-[bis(2-chloroethyl) amino] phenyl] Propanoic Acid Methyl Ester Hydrochloride (EM–MORPIP–MEL)

Off–white crystalline powder. Yield: 41% (not optimized, calculated in relation to MOR–MEL). Purity: 97.85% (HPLC). RRT: 1.105. Mp.: decomposition below the melting point. $[\alpha]_d^{20}$: –74.39° (c = 1, MeOH). IR (cm^{-1}): >C=O (1744), >C=N– (1696). ^{1}H NMR (500 MHz, 25 °C, DMSO–d_6, δ_{ppm}, conformation changes in both morpholine and piperidine rings caused the multiplication of some signals): OCH_3 (3.71, s, 3H), $C_{chiral}H$ (4.43 and 4.37, bs, 1H), $C\underline{H}_2C_{chiral}H$ (3.07, bs, 2H), $C5_{arom}H$+$C5'_{arom}H$ (7.08, t, 2H), $C6_{arom}H$+$C6'_{arom}H$ (6.82, 6.72, 2d, 2H), N–CH_2–$C\underline{H}_2$–Cl (3.70, bs, 2H), N–$C\underline{H}_2$–CH_2–Cl (3.72, bs, 2H), –N=CH– (8.11, 7.92, 2d, 1H), $N_{pip}CH_A H_B$ (4.53, 3.15, 3.80, 3.35, bs, 4H), $N_{pip}CH_2C\underline{H}_A\underline{H}_B$ (2.37, 2.33, 2.28, 1.84, bs, 4H), $N_{pip}CH_2CH_2C\underline{H}$ (3.45, bs, 1H), $NC\underline{H}_A\underline{H}_BCH_2O$ (3.40, 3.05, 2bs, 4H), $NCH_2C\underline{H}_2O$ (3.86, bs, 4H). ^{13}C NMR (125 MHz, 25 °C, DMSO–d_6, δ_{ppm}): OCH_3 (52.70, 52.64), >C=O (170.29, 170.00), C2 (61.42, 60.68), C3 (35.90, 35.81), C4 (123.91, 123.85), C5/C5′ (130.53, 130.43), C6/C6′ (112.25, 111.97), C7 (145.32, 145.27), N–$\underline{C}H_2$–CH_2–Cl (52.11, 52.05), N–CH_2–$\underline{C}H_2$–Cl (41.31, 41.16), –N=CH– (155.08, 154.64), $N_{pip}CH_2$ (49.80, 49.75, 42.95, 42.83), $N_{pip}CH_2\underline{C}H_2$ (26.05, 25.91, 24.89, 24.57), $N_{pip}CH_2CH_2\underline{C}H$ (60.59, 60.55), $N\underline{C}H_2CH_2O$ (48.42, 48.36, 48 23, 48.06), $NCH_2\underline{C}H_2O$ (63.10). HRMS: calc. for $C_{24}H_{37}N_4O_3Cl_2$: 499.224; found: 499.224.

4.3. In Silico Analysis

A QSAR analysis was performed to see whether the new compounds met the criteria for druglike compounds. To provide a global pharmacokinetics profile of the test molecules, we used the freely accessible SwissADME web tool (http://www.swissadme.ch/, accessed on 5 December 2021) according to rules described in [45].

4.4. Cell Culture

Myeloma cancer cells (RPMI8226 (ATCC® CCL–155™)), promyelocytic leukemia cells (HL60 (ATCC® CCL–240™)), and acute monocytic leukemia cells (THP1 (ATCC® TIB–202™)) were obtained from the American Type Culture Collection (ATCC, Rockville, MD, USA). PBMCs were isolated from buffy coat purchased from the Central Blood Bank (Lodz, Poland). PBMCs were isolated with Histopaque 1077 (Sigma Aldrich, St. Louis, MO, USA) by density gradient centrifugation at 300× *g* for 30 min at 22 °C. The final concentration of lymphocytes was estimated by trypan blue (0.4%, Sigma Aldrich) exclusion assay. All investigated cells were suspended in RPMI 1640 medium supplemented with 1% phytohemaglutinin (only in PBMC growth medium), 10% fetal bovine serum, penicillin (10 U/mL), and streptomycin (50 µg/mL) in standard conditions: 37 °C, 100% humidity, and an atmosphere of 5% CO_2 and 95% air. Cell viability was systematically controlled using trypan blue (0.4%, Sigma). In all experiments, cells in the logarithmic phase of growth were used when their viability was above 95%.

4.5. Cytotoxicity Assay

The cytotoxic properties of melphalan (MEL) and its new derivatives (EM–I–MEL, EM–T–MEL, and EM–MORPIP–MEL) were investigated with the use of resazurin sodium after 48 h of incubation with the test compounds. Living cells were metabolically active and had the ability to reduce resazurin via mitochondrial reductase to a highly fluorescent dye, resorufin. The amount of product formed was directly proportional to the number of viable cells, while the intensity of the color produced was a quantitative measure of cell survival.

Cells were grown in 96-well black plates at 1.5×10^4 cells/well and incubated with various concentrations of test compounds at 37 °C. After 48 h of incubation for each of the wells, resazurin solution (10 μg/mL, final concentration) was added, and the samples were incubated for 90 min. Fluorescence measurement was performed at ~530 nm excitation and ~590 nm emission using a Fluoroskan Ascent FL plate reader (Labsystems, Stockholm, Sweden).

4.6. Determination of Apoptotic and Necrotic Cell Fractions by Double Staining with a Mixture of the Fluorochromes Propidium Iodide and Hoechst 33342

PI is negatively charged and penetrates only cells with damaged cell membranes, which allows the identification of necrotic cells or cells in the late stages of apoptosis. Hoechst 33342, on the other hand, freely penetrates the intact membrane of living and early-apoptotic cells, thus enabling their identification. As a result of the dye penetrating the intact biological membranes, the DNA of the cell nucleus is stained a light blue color. The dye fluorescence intensity is related to the degree of DNA packing, which allows, on the basis of the intensity of fluorescence of the fluorochrome in the cell nucleus, distinguishing strongly fluorescent apoptotic cells containing highly condensed chromatin from weakly fluorescing living cells containing looser chromatin. The simultaneous use of two fluorescent dyes (PI and Hoechst 33342), of which the mechanisms of penetration into the cell and the fluorescence spectra are different, allowed the identification of four types of cells in the sample: live cells (weak, dull light blue fluorescence), early apoptotic cells (bright light blue fluorescence), late apoptotic cells (pink-purple fluorescence), and necrotic cells (intense red fluorescence).

THP1, HL60, and RPMI8226 cells were incubated with the test compounds for 4, 24, and 48 h. After an appropriate incubation time, cells were removed from the culture dishes, centrifuged, and suspended at a final concentration of 1×10^5 cells in 1 mL of PBS. The fluorescent dyes Hoechst 33342 (0.13 mM) and PI (0.23 mM) were added and incubated for 10 min in the dark. The cell suspension was placed on a microscope slide. At least 300 cells per sample were counted in triplicate under an Olympus fluorescence microscope using an NB filter. The percentage of the particular cell types was determined from the total number of cells.

4.7. Visualization of Changes in Cell Membrane Integrity and Externalization of Phosphatidylserine

Visualization of cells stained with annexin V–FITC and PI was applied according to the protocol of the manufacturer, BioVision Incorporated (annexin V–FITC apoptosis kit). This method is a useful tool for distinguishing live cells (not stained with any fluorochrome) from early apoptotic cells (stained with annexin V–FITC only), late apoptotic cells (stained with annexin V–FITC and PI), and necrotic cells (stained with PI only).

Briefly, cells were seeded at a density of 2.5×10^5 cells/well and treated with the test compounds for 24 h. The cells were then washed with PBS and resuspended in 300 μL binding buffer. Then, 3 μL annexin V–FITC and 3 μL PI was added. The mixture was incubated for 10 min on ice. Samples were centrifuged, applied to chamber slides, and then visualized using fluorescence microscopy (Olympus IX70, Tokyo, Japan). Magnification was 200×.

4.8. Activity of Cysteine Proteases (Caspases)

The activation of executive (caspases 3/7) and initiating caspases (involved in the activation of the external (caspase 8) and internal (caspase 9) pathways) is widely known as a reliable indicator of cell apoptosis. DEVD–ProRed™, IETD–R110, and LEHD–AMC were used as fluorogenic markers for the activity of caspases 3/7, 8, and 9, respectively. Following caspase cleavage, the DEVD–ProRed, IETD–R110, and LEHD–AMC caspase substrates generate three different fluorophores, ProRed™ (red fluorescence), R110 (green fluorescence), and AMC (blue fluorescence), which can be easily monitored using flow cytometry.

THP1, HL60, and RPMI8226 cells were seeded in plates (1×10^6), and then the compounds were added at the appropriate concentration. After an appropriate incubation time (4, 24, or 48 h), cells were transferred to cytometric tubes, resuspended in a prepared working solution containing the appropriate substrate (50 µL of substrate into 10 mL assay buffer), and incubated for 30 to 60 min at room temperature, protected from light. Cells were analyzed using a flow cytometer (Becton Dickinson, San Jose, CA, USA) using the following wavelengths: caspase 3/7, ex: 488 nm, em: 620 nm; caspase 8, ex: 490 nm, em: 525 nm; caspase 9, ex: 355 nm, em: 470 nm. The minimum number of events recorded in the sample was 20,000. The results are presented as the median fluorescence in the corresponding channel: PE–Texas Red, FITC, DAPI as % relative to control.

4.9. Mitochondrial Membrane Potential ($\Delta\psi m$)

Cells collected from the culture vessel (15×10^6) were centrifuged (10 min, 1200 rpm), and the culture medium with phenol red was discarded. PBS was added to the pellet, and cells were centrifuged. In the next step, cells were suspended in a working culture medium without phenol red with JC–1 (10 µM) and incubated at 37 °C for 30 min in the dark. The cells were then centrifuged and washed with PBS to remove the dye, which otherwise could have adsorbed on the microplate well plastic and distorted the measurements. Cells prepared in this way were seeded into 96-well microplates at 8×10^4 cells per well. The cells were incubated with the test compounds or CCCP, a mitochondrial uncoupling agent (20 and 100 µM), for 4–24 h. At the end of the treatment, the fluorescence of both JC–1 monomers and dimers was measured on a Fluoroskan Ascent FL microplate reader using filter pairs of 530/590 nm (dimers) and 485/538 nm (monomers). The results shown in the figures are expressed as a ratio of dimer fluorescence to monomer fluorescence in relation to the control fluorescence ratio, taken as 100%. The cells presented in the images were incubated with drugs for 48 h. JC–1 fluorescence was photographed immediately after drug treatment using an inverted Olympus IX70 fluorescence microscope (Olympus, Tokyo, Japan).

4.10. Measurement of DNA Damage (the Alkaline Version of the Comet Assay)

Single-cell agarose gel electrophoresis, commonly referred to as the comet assay, is used to detect alkyl labile sites, as well as single- and double-strand breaks in DNA induced by genotoxic agents. The method involves electrophoretic separation of nuclear DNA so that DNA fragmentation can be observed. The method was performed according to the protocol described in our previous articles [7,13,46].

The cells were plated in 12-well plates (2.5×10^4 cells) and treated with MEL, EM–I–MEL, and EM–T–MEL at the indicated concentrations for 4, 24, and 48 h at 37 °C. The cells were washed with PBS, and the pellet was resuspended in 50 µL of 0.75% low-melting point (LMP) agarose in PBS, pH 7.4. The samples were applied to heated primary slides that had previously been coated with 1% normal-melting point (NMP) agarose. Slides prepared in this manner were then subjected to alkaline lysis (2.5 M NaCl, 100 mM EDTA, 10 mM Tris, 1% Triton X-100, pH 9.0) for a minimum of 1 h at 4 °C. Slides were then placed in developing buffer (300 mM NaOH, 1 mM EDTA) for 20 min and then in electrophoresis buffer (30 mM NaOH, 1 mM EDTA). Electrophoresis was conducted at 29 V and 30 mA for 20 min. Slides were then stained with DAPI (2 µg/mL) in the dark. Fifty randomly selected cells from each slide were analyzed using an Eclipse fluorescence microscope

(Nikon, Japan) attached to a COHU 4910 video camera (Cohu, Inc., San Diego, CA, USA) equipped with a UV–1A filter block and connected to the Lucia-Comet v. 6.0 image analysis system (Laboratory Imaging, Prague, Czech Republic). The percentage of DNA in the comet tail is an indicator of DNA damage.

4.11. Statistical Analysis

Data are presented as the mean ± standard deviation (SD). Analysis of variance (ANOVA) with Tukey's post hoc test was used for multiple comparisons. All statistics were calculated using STATISTICA (StatSoft, Tulsa, OK, USA). A p-value < 0.05 was considered significant. All figures include descriptions of statistically significant changes: * $p < 0.05$ statistically significant difference compared with control cells, # $p < 0.05$ statistically significant difference between samples incubated with melphalan and melphalan derivatives.

5. Conclusions

Research in cancer biology has led to the elucidation of the mechanism of action of anticancer agents. It has also provided a basis for the successful design of new drugs. The development of new analogs of anticancer drugs is a complicated task. Applying chemical principles and analyzing chemical structures together with biological activity enables the synthesis of derivatives with higher biological properties than the parent drug. In vitro studies have confirmed the hypothesis that chemical modification of melphalan leads to significantly higher cytotoxic and genotoxic activities. These modifications include esterifying the carboxyl group and replacing the amino group with amidine containing a thiomorpholine residue with two heteroatoms (N and S) in its structure. The generation of apoptotic bodies and reductions in the mitochondrial membrane potential suggest that these compounds induce apoptosis, the preferred type of cell death.

This studies allowed us to select EM–T–MEL as the most active analog. It also significantly deepened the knowledge on improving the biological activity of the currently used chemotherapeutic agent (Figure 9).

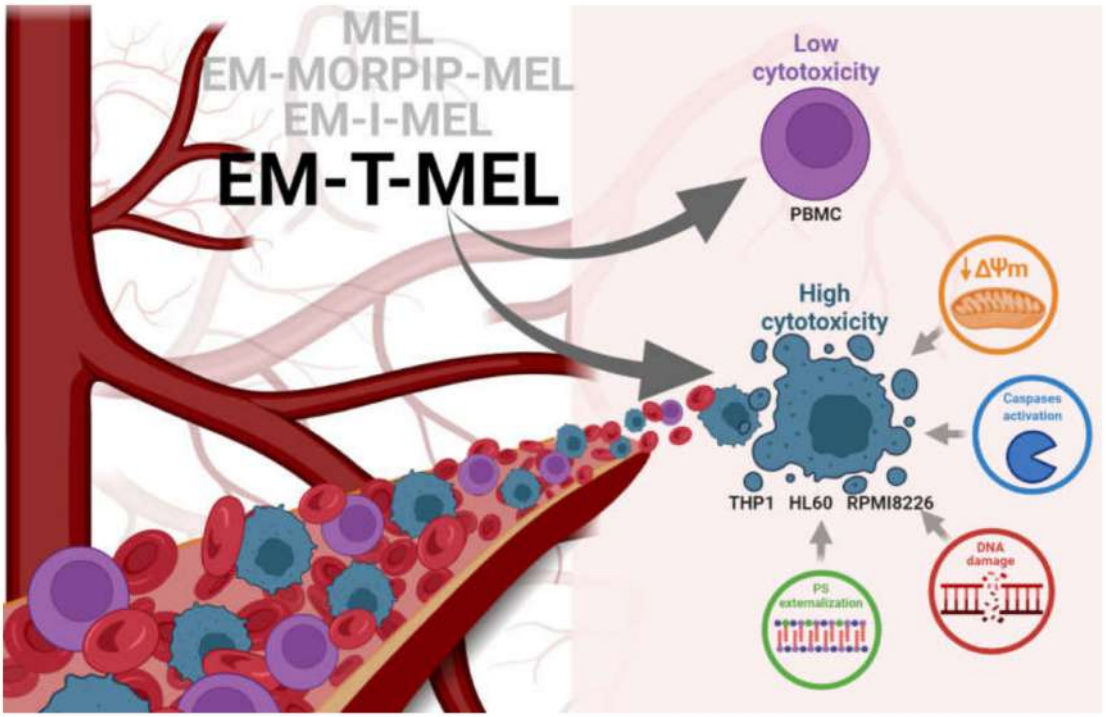

Figure 9. Proposed model of the molecular pathways of the new MEL derivatives with respect to neoplastic cells (THP1, HL60, and RPMI8226) and PBMC.

Supplementary Materials: The following are available online at https://www.mdpi.com/article/10.3390/ijms23031760/s1.

Author Contributions: Conceptualization, A.P., P.K. and A.M.; methodology, A.P., P.K., J.T., A.R., A.G. and A.M.; data curation, A.P. and A.R.; writing—original draft preparation, A.P., P.K., A.R. and A.M.; writing—review and editing, A.P., P.K., A.R., A.G. and A.M. All authors have read and agreed to the published version of the manuscript.

Funding: This work was partially supported under the framework of a statutory project (841333) of the Łukasiewicz Industrial Chemistry Institute funded by the Polish Ministry of Science and Higher Education. Publication's printing cost was co-financed by the European Union from the European Social Fund under the "InterDOC-STARt" project (POWR.03.02.00-00-I033/16-00).

Institutional Review Board Statement: Not applicable.

Informed Consent Statement: Not applicable.

Data Availability Statement: The datasets presented during in the current study are available from the corresponding author on reasonable request.

Acknowledgments: The authors acknowledge Marek Kubiszewski of the Analytical Department, Team of Analytical Research, Łukasiewicz Research Network—Industrial Chemistry Institute for his help in confirming the structures of the compounds obtained by making a detailed analysis of the NMR spectra and identifying individual signals. Figure 9 has been created with BioRender.com.

Conflicts of Interest: The authors declare no conflict of interest.

References

1. Parra, M.; Baptista, M.J.; Genescà, E.; Llinàs-Arias, P.; Esteller, M. Genetics and epigenetics of leukemia and lymphoma: From knowledge to applications, meeting report of the Josep Carreras Leukaemia Research Institute. *Hematol. Oncol.* **2020**, *38*, 432–438. [CrossRef]
2. Oriol, A.; Larocca, A.; Leleu, X.; Hajek, R.; Hassoun, H.; Rodríguez-Otero, P.; Paner, A.; Schjesvold, F.H.; Gullbo, J.; Richardson, P.G. Melflufen for relapsed and refractory multiple myeloma. *Expert Opin. Investig. Drugs* **2020**, *29*, 1069–1078. [CrossRef] [PubMed]
3. Rosiñol, L.; Oriol, A.; Rios, R.; Sureda, A.; Blanchard, M.J.; Hernández, M.T.; Martínez-Martínez, R.; Moraleda, J.M.; Jarque, I.; Bargay, J.; et al. Bortezomib, lenalidomide, and dexamethasone as induction therapy prior to autologous transplant in multiple myeloma. *Blood* **2019**, *134*, 1337–1345. [CrossRef] [PubMed]
4. Pinto, V.; Bergantim, R.; Caires, H.R.; Seca, H.; Guimarães, J.E.; Vasconcelos, M.H. Multiple myeloma: Available therapies and causes of drug resistance. *Cancers* **2020**, *12*, 407. [CrossRef] [PubMed]
5. Singh, R.K.; Kumar, S.; Prasad, D.N.; Bhardwaj, T.R. Therapeutic journery of nitrogen mustard as alkylating anticancer agents: Historic to future perspectives. *Eur. J. Med. Chem.* **2018**, *151*, 401–433. [CrossRef]
6. Yang, J.; Terebelo, H.R.; Zonder, J.A. Secondary Primary Malignancies in Multiple Myeloma: An Old Nemesis Revisited. *Adv. Hematol.* **2012**, *2012*, 801495. [CrossRef]
7. Poczta, A.; Rogalska, A.; Marczak, A. Treatment of Multiple Myeloma and the Role of Melphalan in the Era of Modern Therapies—Current Research and Clinical Approaches. *J. Clin. Med.* **2021**, *10*, 1841. [CrossRef]
8. Bergel, F.; Stock, J.A. Cyto-active Amino-acid and Peptide Derivatives. *J. Chem. Soc.* **1954**, 2409–2417. [CrossRef]
9. Szekerke, B.M.; Wade, R.; Bergel, F. Cyto-active Amino-acids and Peptides. Part XIV. Poly-and Copoly-(amino-acyl) derivatives of melphalan. *J. Chem. Soc. C Organic* **1968**, *14*, 1792–1795. [CrossRef] [PubMed]
10. Everett, J.L.; Baker, M.H.; Bergel, F. Cyto-active Amino-acids and Peptides. Part Xlll Fluorescent Derivatives of Melphalan t and other Amino-acids. *J. Chem. Soc. C Organic* **1968**, 1791–1792. [CrossRef]
11. Gullbo, J.; Tullberg, M.; Våbenø, J.; Ehrsson, H.; Lewensohn, R.; Nygren, P.; Larsson, R.; Luthman, K. Structure-Activity Relationship for Alkylating Dipeptide Nitrogen Mustard Derivatives. *Oncol. Res. Featur. Preclin. Clin. Cancer Ther.* **2003**, *14*, 113–132. [CrossRef] [PubMed]
12. Lu, B.; Huang, D.; Zheng, H.; Huang, Z.; Xu, P.; Xu, H.; Yin, Y.; Liu, X.; Li, D.; Zhang, X. Preparation, characterization, and in vitro efficacy of O-carboxymethyl chitosan conjugate of melphalan. *Carbohydr. Polym.* **2013**, *98*, 36–42. [CrossRef]
13. Gajek, A.; Poczta, A.; Łukawska, M.; Cecuda-Adamczewska, V.; Tobiasz, J.; Marczak, A. Chemical modification of melphalan as a key to improving treatment of haematological malignancies. *Sci. Rep.* **2020**, *10*, 4479. [CrossRef]
14. Małkiewicz, M.A.; Szarmach, A.; Sabisz, A.; Cubała, W.J.; Szurowska, E.; Winklewski, P.J. Blood-brain barrier permeability and physical exercise. *J. Neuroinflammation* **2019**, *16*, 15. [CrossRef]
15. Al-Ghorbani, M.; Bushra, B.A.; Zabiulla, S.V.M.; Mamatha, S.; Khanum, S.A. Piperazine and morpholine: Synthetic preview and pharmaceutical applications. *Res. J. Pharm. Technol.* **2015**, *8*, 611–628. [CrossRef]

16. Al-Ghorbani, M.; Vigneshwaran, V.; Ranganatha, V.L.; Prabhakar, B.T.; Khanum, S.A. Synthesis of oxadiazole-morpholine derivatives and manifestation of the repressed CD31 Microvessel Density (MVD) as tumoral angiogenic parameters in Dalton's Lymphoma. *Bioorganic Chem.* **2015**, *60*, 136–146. [CrossRef] [PubMed]
17. Lenci, E.; Calugi, L.; Trabocchi, A. Occurrence of Morpholine in Central Nervous System Drug Discovery. *ACS Chem. Neurosci.* **2021**, *12*, 378–390. [CrossRef]
18. Arshad, F.; Khan, M.F.; Akhtar, W.; Alam, M.M.; Nainwal, L.M.; Kaushik, S.K.; Akhter, M.; Parvez, S.; Hasan, S.M.; Shaquiquzzaman, M. Revealing quinquennial anticancer journey of morpholine: A SAR based review. *Eur. J. Med. Chem.* **2019**, *167*, 324–356. [CrossRef]
19. Hamid, R.; Rotshteyn, Y.; Rabadi, L.; Parikh, R.; Bullock, P. Comparison of alamar blue and MTT assays for high through-put screening. *Toxicol. Vitr.* **2004**, *18*, 703–710. [CrossRef]
20. Van Kan, M.; Burns, K.E.; Browett, P.; Helsby, N.A. A higher throughput assay for quantification of melphalan-induced DNA damage in peripheral blood mononuclear cells. *Sci. Rep.* **2019**, *9*, 18912. [CrossRef] [PubMed]
21. Bulumulla, C.; Kularatne, R.N.; Catchpole, T.; Takacs, A.; Christie, A.; Gilfoyle, A.; Nguyen, T.D.; Stefan, M.C.; Csaky, K.G. Investigating the effect of esterification on retinal pigment epithelial uptake using rhodamine B derivatives. *Transl. Vis. Sci. Technol.* **2020**, *9*, 18. [CrossRef] [PubMed]
22. Wang, C.-L.; Guo, C.; Zhou, Y.; Wang, R. In vitro and in vivo characterization of opioid activities of C-terminal esterified endomorphin-2 analogs. *Peptides* **2009**, *30*, 1697–1704. [CrossRef] [PubMed]
23. De Oliveira, D.P.; Moreira, T.D.V.; Batista, N.V.; Filho, J.D.D.S.; Amaral, F.A.; Teixeira, M.M.; de Pádua, R.M.; Braga, F.C. Esterification of trans-aconitic acid improves its anti-inflammatory activity in LPS-induced acute arthritis. *Biomed. Pharmacother.* **2018**, *99*, 87–95. [CrossRef]
24. Chvapil, M.; Kielar, F.; Liska, F.; Silhankova, A.; Brendel, K. Synthesis and evaluation of long-acting D-penicillamine derivatives. *Connect. Tissue Res.* **2005**, *46*, 242–250. [CrossRef]
25. Bielawska, A.; Bielawski, K.; Anchim, T. Amidine analogues of melphalan: Synthesis, cytotoxic activity, and DNA binding properties. *Arch. Der Pharm.* **2007**, *340*, 251–257. [CrossRef] [PubMed]
26. Bielawski, K.; Bielawska, A.; Sosnowska, K.; Miltyk, W.; Winnicka, K.; Pałka, J. Novel amidine analogue of melphalan as a specific multifunctional inhibitor of growth and metabolism of human breast cancer cells. *Biochem. Pharmacol.* **2006**, *72*, 320–331. [CrossRef]
27. Zhao, Y.; Wang, L.; Pan, J. The role of L-type amino acid transporter 1 in human tumors. *Intractable Rare Dis. Res.* **2015**, *4*, 165–169. [CrossRef]
28. Hayashi, K.; Jutabha, P.; Endou, H.; Sagara, H.; Anzai, N. LAT1 Is a Critical Transporter of Essential Amino Acids for Immune Reactions in Activated Human T Cells. *J. Immunol.* **2013**, *191*, 4080–4085. [CrossRef]
29. Mynott, R.L.; Wallington-Beddoe, C.T. Drug and Solute Transporters in Mediating Resistance to Novel Therapeutics in Multiple Myeloma. *ACS Pharmacol. Transl. Sci.* **2021**, *4*, 1050–1065. [CrossRef]
30. Pegoraro, A.; Orioli, E.; De Marchi, E.; Salvestrini, V.; Milani, A.; Di Virgilio, F.; Curti, A.; Adinolfi, E. Differential sensitivity of acute myeloid leukemia cells to daunorubicin depends on P2X7A versus P2X7B receptor expression. *Cell Death Dis.* **2020**, *11*, 876. [CrossRef]
31. Lee, C.-K.; Wang, S.; Huang, X.; Ryder, J.; Liu, B. HDAC inhibition synergistically enhances alkylator-induced DNA damage responses and apoptosis in multiple myeloma cells. *Cancer Lett.* **2010**, *296*, 233–240. [CrossRef] [PubMed]
32. Cordelli, E.; Cinelli, S.; Lascialfari, A.; Ranaldi, R.; Pacchierotti, F. Melphalan-induced DNA damage in p53(+/−) and wild type mice analysed by the comet assay. *Mutat. Res.* **2004**, *550*, 133–143. [CrossRef] [PubMed]
33. Xu, H.; He, J.; Zhang, Y.; Fan, L.; Zhao, Y.; Xu, T.; Nie, Z.; Li, X.; Huang, Z.; Lu, B.; et al. Synthesis and in vitro evaluation of a hyaluronic acid-quantum dots-melphalan conjugate. *Carbohydr. Polym.* **2015**, *121*, 132–139. [CrossRef] [PubMed]
34. Keoni, C.L.I.; Brown, T.L. Inhibition of apoptosis and efficacy of pan caspase inhibitor, Q-VD-OPh, in models of human disease. *J. Cell Death* **2015**, *8*, JCD-S23844. [CrossRef] [PubMed]
35. Verrax, J.; Dejeans, N.; Sid, B.; Glorieux, C.; Calderon, P.B. Intracellular ATP levels determine cell death fate of cancer cells exposed to both standard and redox chemotherapeutic agents. *Biochem. Pharmacol.* **2011**, *82*, 1540–1548. [CrossRef] [PubMed]
36. El Dein, O.S.; Gallerne, C.; Brenner, C.; Lemaire, C. Increased expression of VDAC1 sensitizes carcinoma cells to apoptosis induced by DNA cross-linking agents. *Biochem. Pharmacol.* **2012**, *83*, 1172–1182. [CrossRef] [PubMed]
37. Matsura, T.; Kai, M.; Jiang, J.; Babu, H.; Kini, V.; Kusumoto, C.; Yamada, K.; Kagan, V.E. Endogenously Generated Hydrogen Peroxide Is Required for Execution of Melphalan-Induced Apoptosis as Well as Oxidation and Externalization of Phosphatidylserine. *Chem. Res. Toxicol.* **2004**, *17*, 685–696. [CrossRef]
38. Xu, X.; Lai, Y.; Hua, Z.-C. Apoptosis and apoptotic body: Disease message and therapeutic target potentials. *Biosci. Rep.* **2019**, *39*, BSR20180992. [CrossRef]
39. Broker, L.E.; Kruyt, F.A.E.; Giaccone, G. Cell death independent of caspases: A review. *Clin. Cancer Res.* **2005**, *11*, 3155–3162. [CrossRef]
40. Vitale, I.; Manic, G.; Castedo, M.; Kroemer, G. Caspase 2 in mitotic catastrophe: The terminator of aneuploid and tetraploid cells. *Mol. Cell. Oncol.* **2017**, *4*, e1299274. [CrossRef] [PubMed]
41. Čáňová, K.; Rozkydalová, L.; Vokurková, D.; Rudolf, E. Flubendazole induces mitotic catastrophe and apoptosis in melanoma cells. *Toxicol. Vitr.* **2018**, *46*, 313–322. [CrossRef] [PubMed]

42. Mc Gee, M.M. Targeting the Mitotic Catastrophe Signaling Pathway in Cancer. *Mediat. Inflamm.* **2015**, *2015*, 146282. [CrossRef] [PubMed]
43. Erenpreisa, J.; Kalejs, M.; Ianzini, F.; Kosmacek, E.; Mackey, M.; Emzinsh, D.; Cragg, M.; Ivanov, A.; Illidge, T. Segregation of genomes in polyploid tumour cells following mitotic catastrophe. *Cell Biol. Int.* **2005**, *29*, 1005–1011. [CrossRef]
44. Cives, M.; Ciavarella, S.; Rizzo, F.M.; De Matteo, M.; Dammacco, F.; Silvestris, F. Bendamustine overcomes resistance to melphalan in myeloma cell lines by inducing cell death through mitotic catastrophe. *Cell. Signal.* **2013**, *25*, 1108–1117. [CrossRef]
45. Daina, A.; Michielin, O.; Zoete, V. SwissADME: A free web tool to evaluate pharmacokinetics, drug-likeness and medicinal chemistry friendliness of small molecules. *Sci. Rep.* **2017**, *7*, 42717. [CrossRef] [PubMed]
46. Gajek, A.; Rogalska, A.; Koceva-Chyła, A. Aclarubicin in subtoxic doses reduces doxorubicin cytotoxicity in human non-small cell lung adenocarcinoma (A549) and human hepatocellular carcinoma (HepG2) cells by decreasing DNA damage. *Toxicol. Vitr.* **2019**, *55*, 140–150. [CrossRef]

Suplementary materials

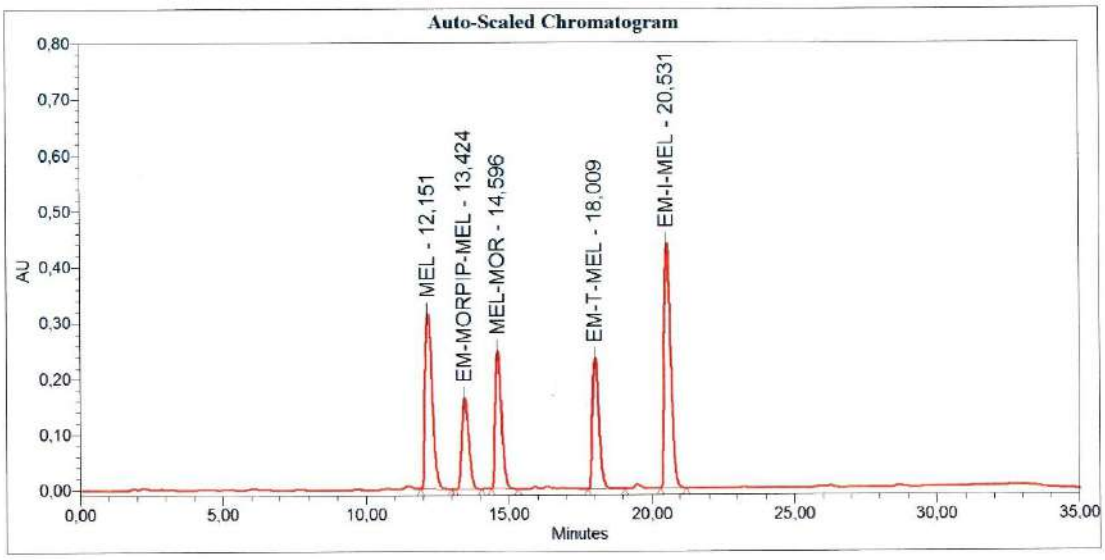

Figure S1. HPLC Chromatogram of MEL, MOR–MEL and new derivatives described in this paper.

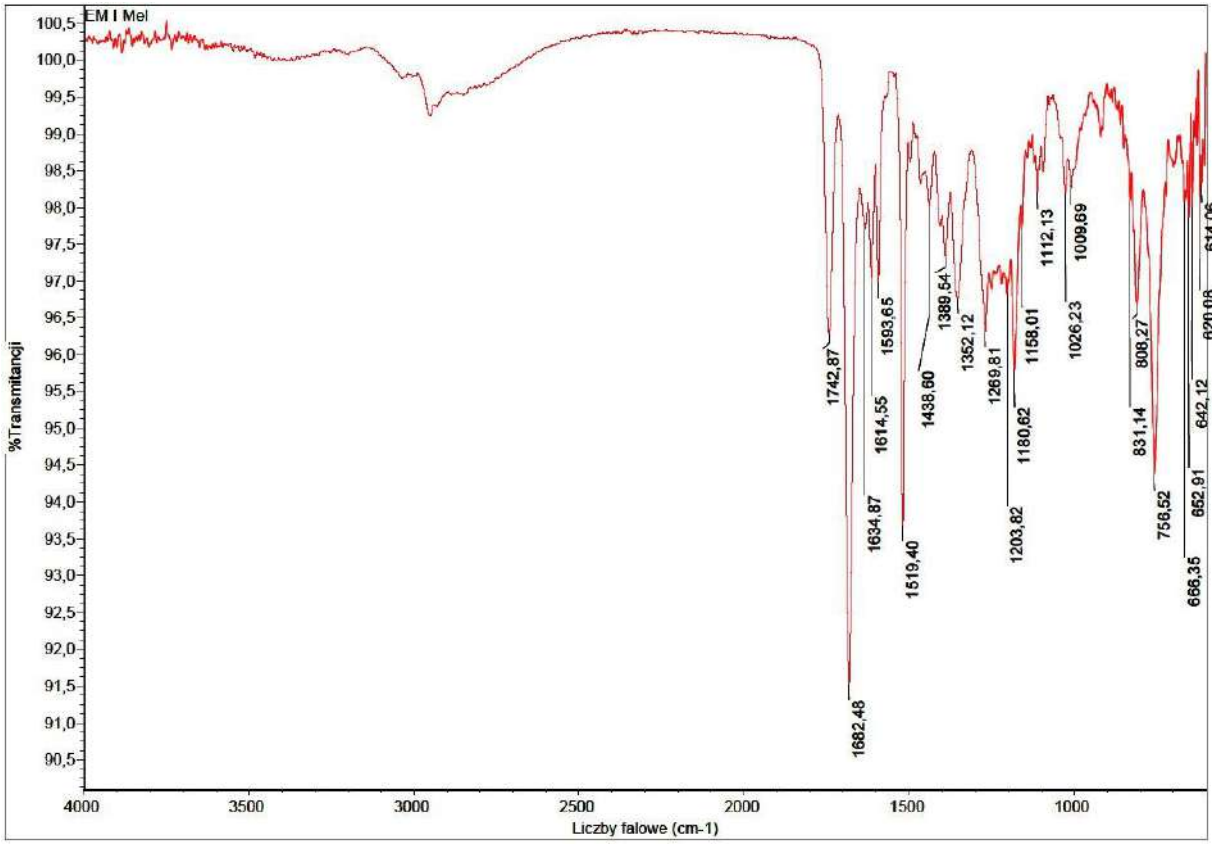

Figure S2. IR spectrum of the EM–I–MEL.

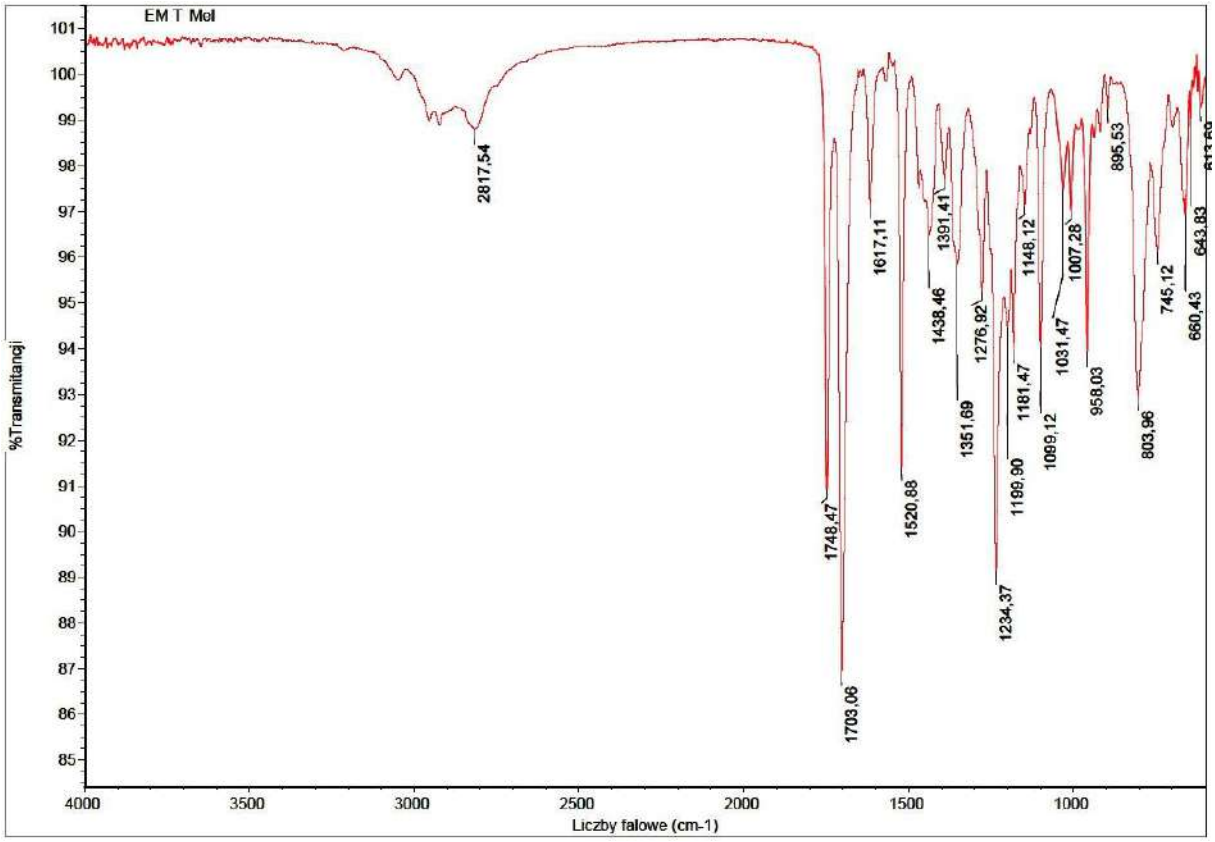

Figure S3. IR spectrum of the EM–T–MEL.

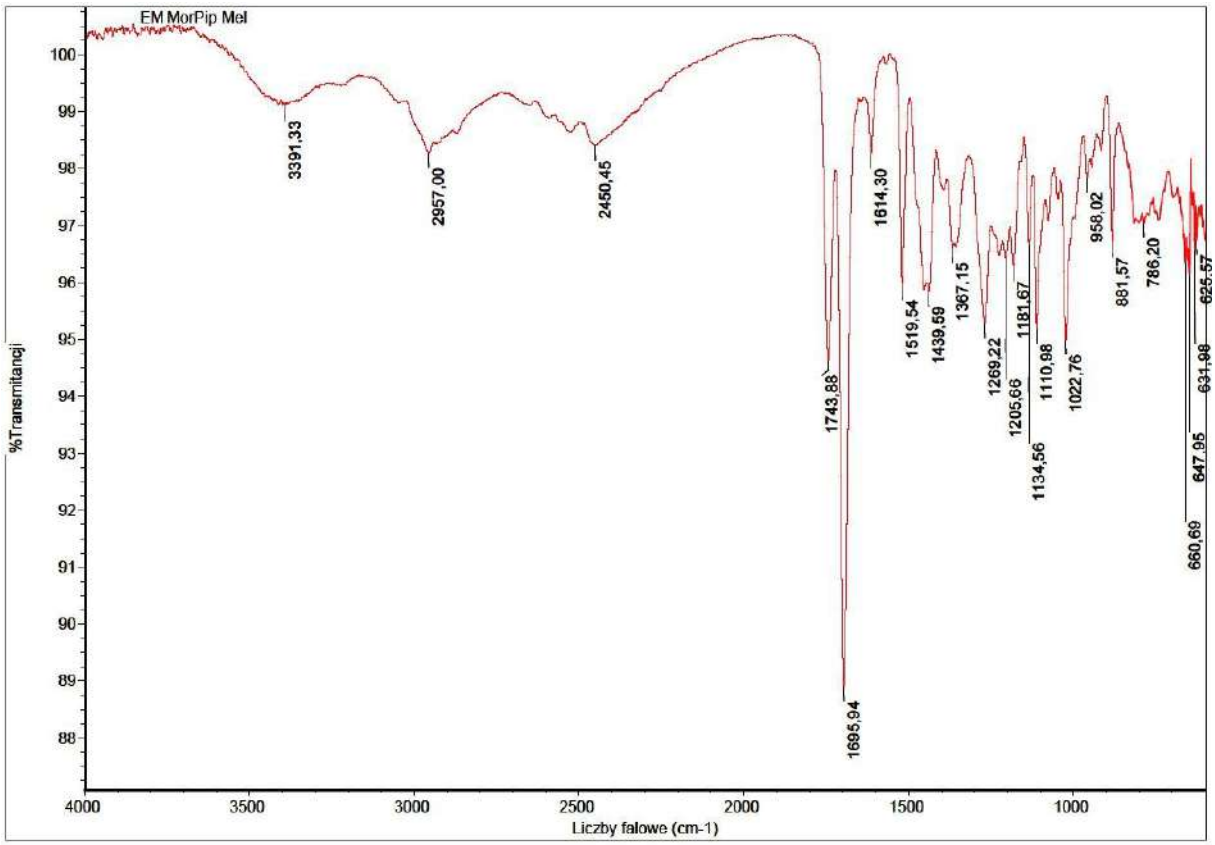

Figure S4. IR spectrum of the EM–MORPIP–MEL.

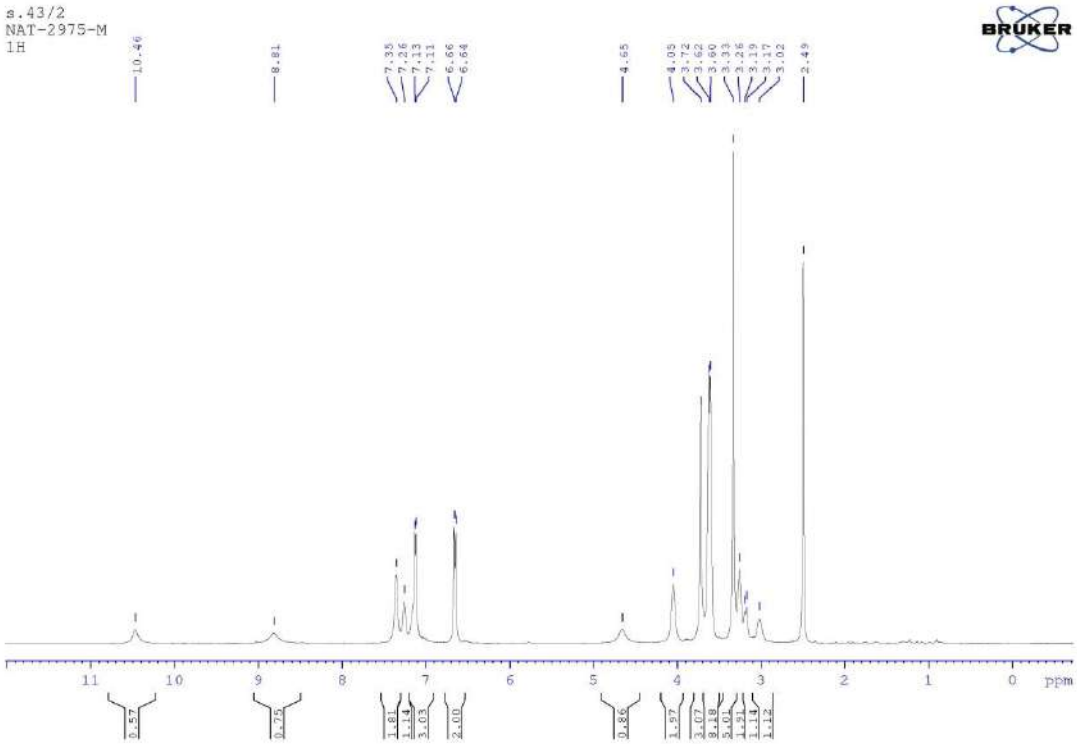

Figure S5. [1]H NMR spectrum of the EM–I–MEL.

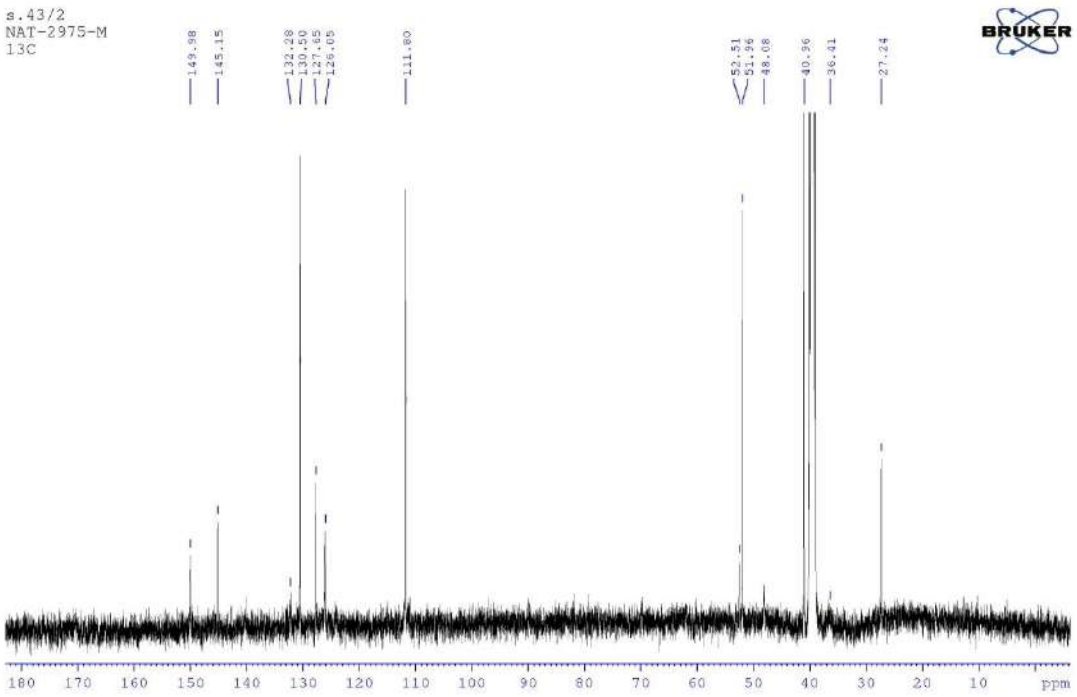

Figure S6. [13]C NMR spectrum of the EM–I–MEL.

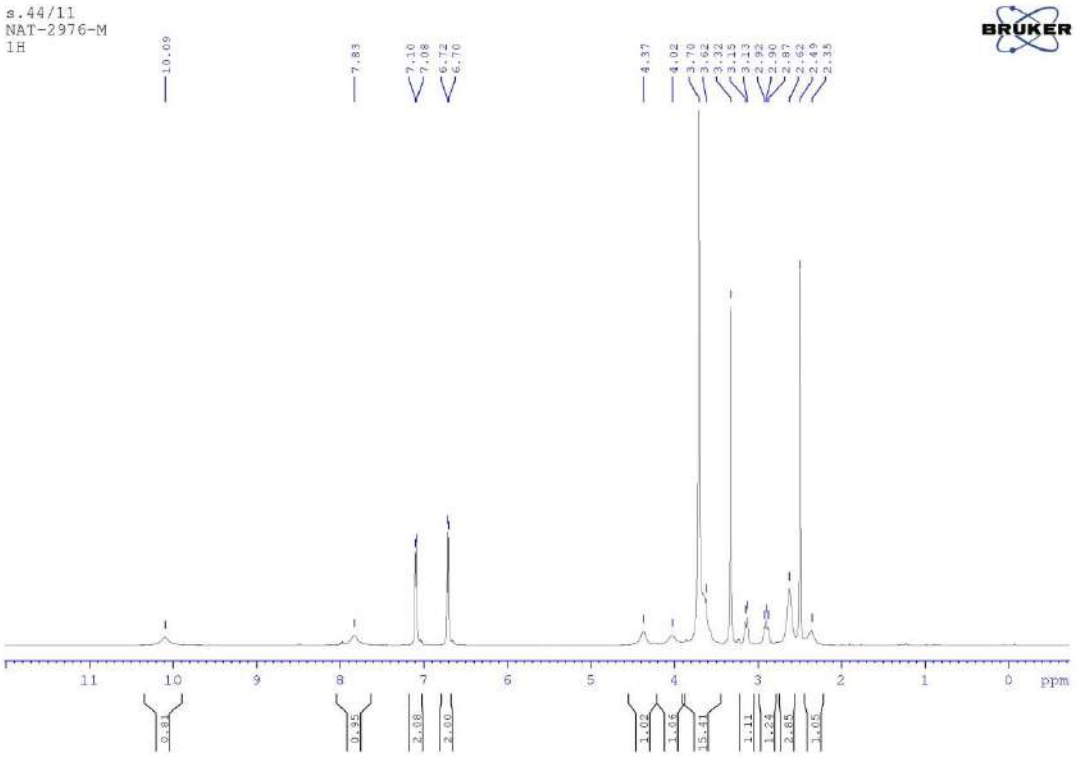

Figure S7. ^{1}H NMR spectrum of the EM–T–MEL.

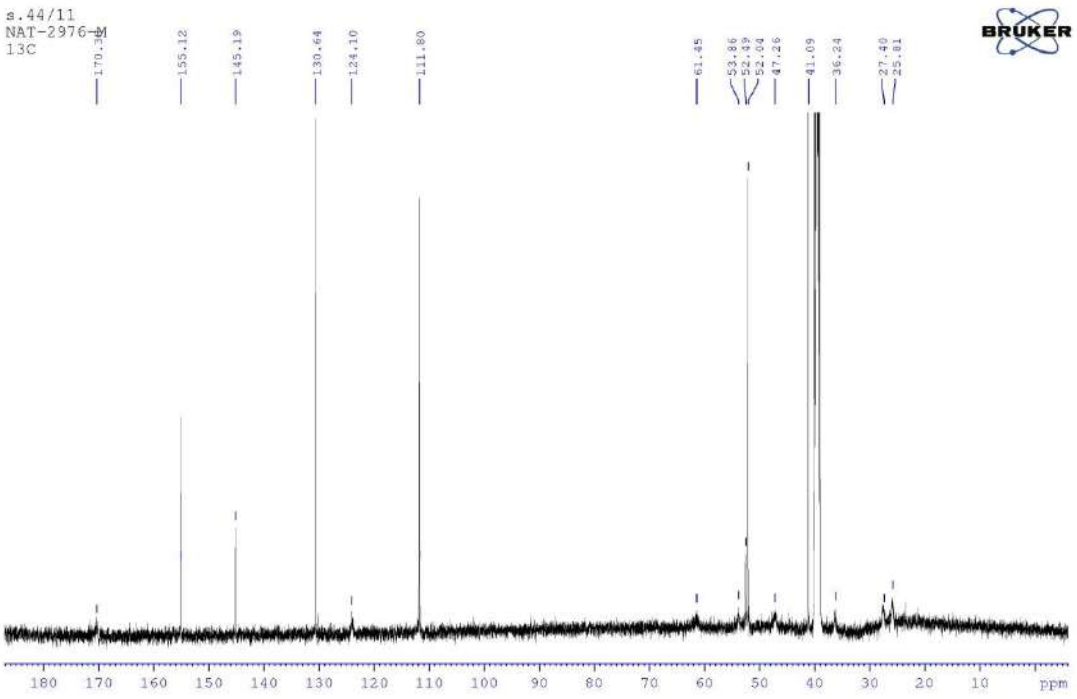

Figure S8. ^{13}C NMR spectrum of the EM–T–MEL.

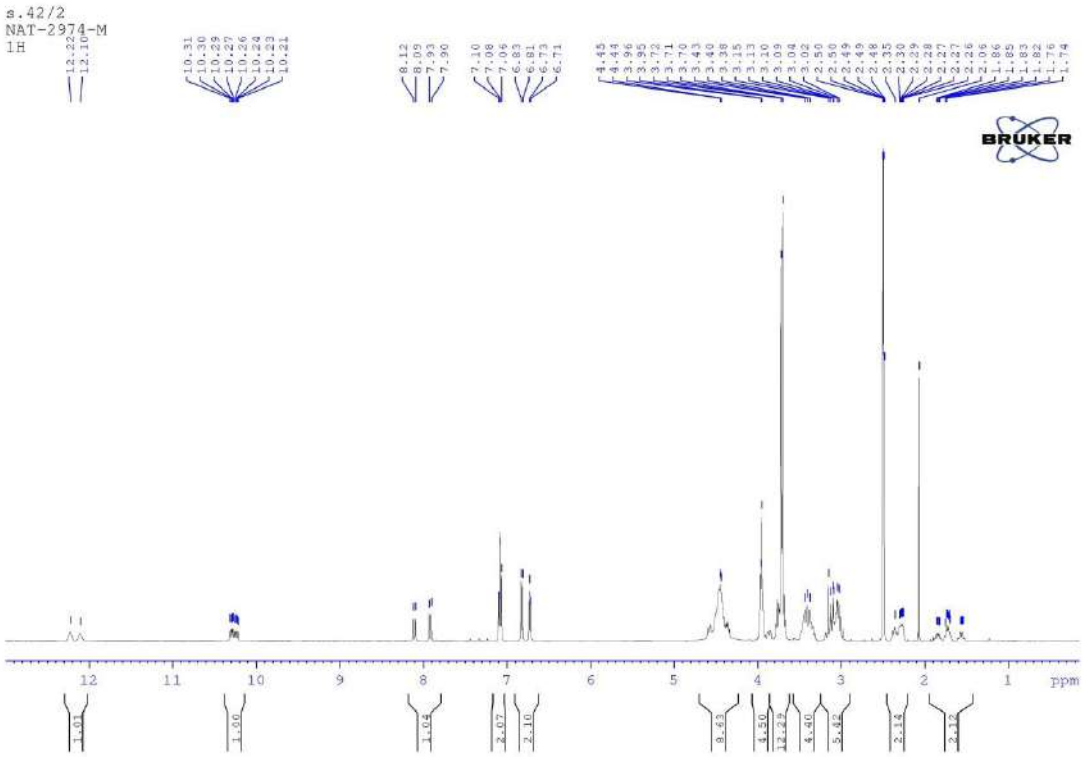

Figure S9. [1]H NMR spectrum of the EM–MORPIP–MEL.

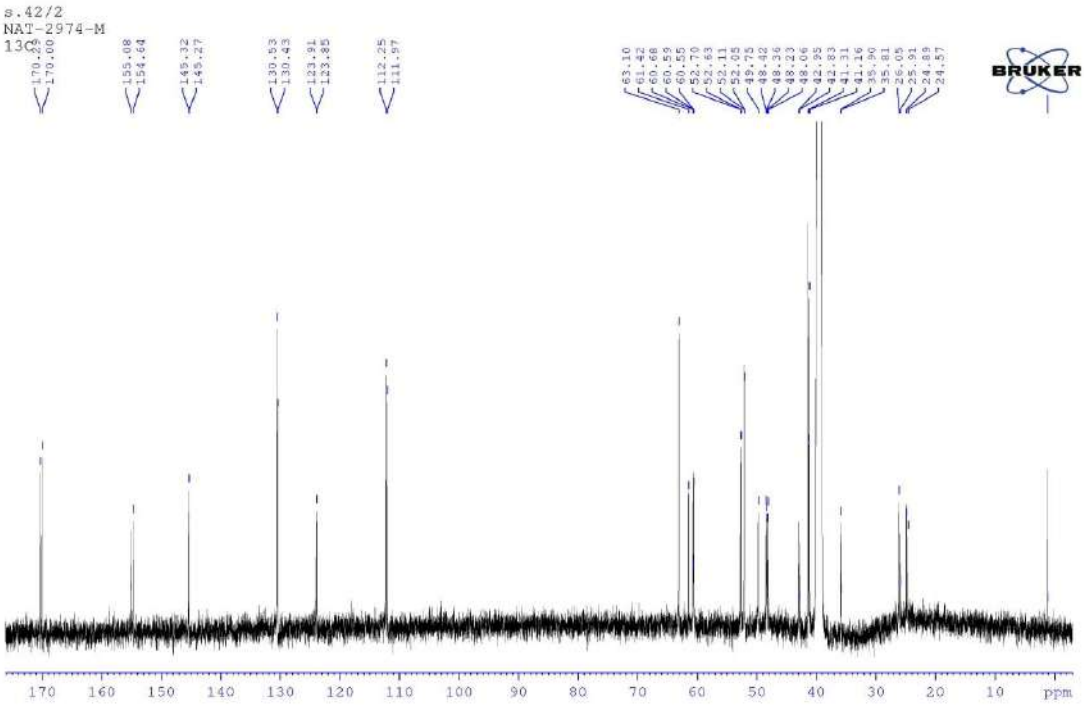

Figure S10. [13]C NMR spectrum of the EM–MORPIP–MEL.

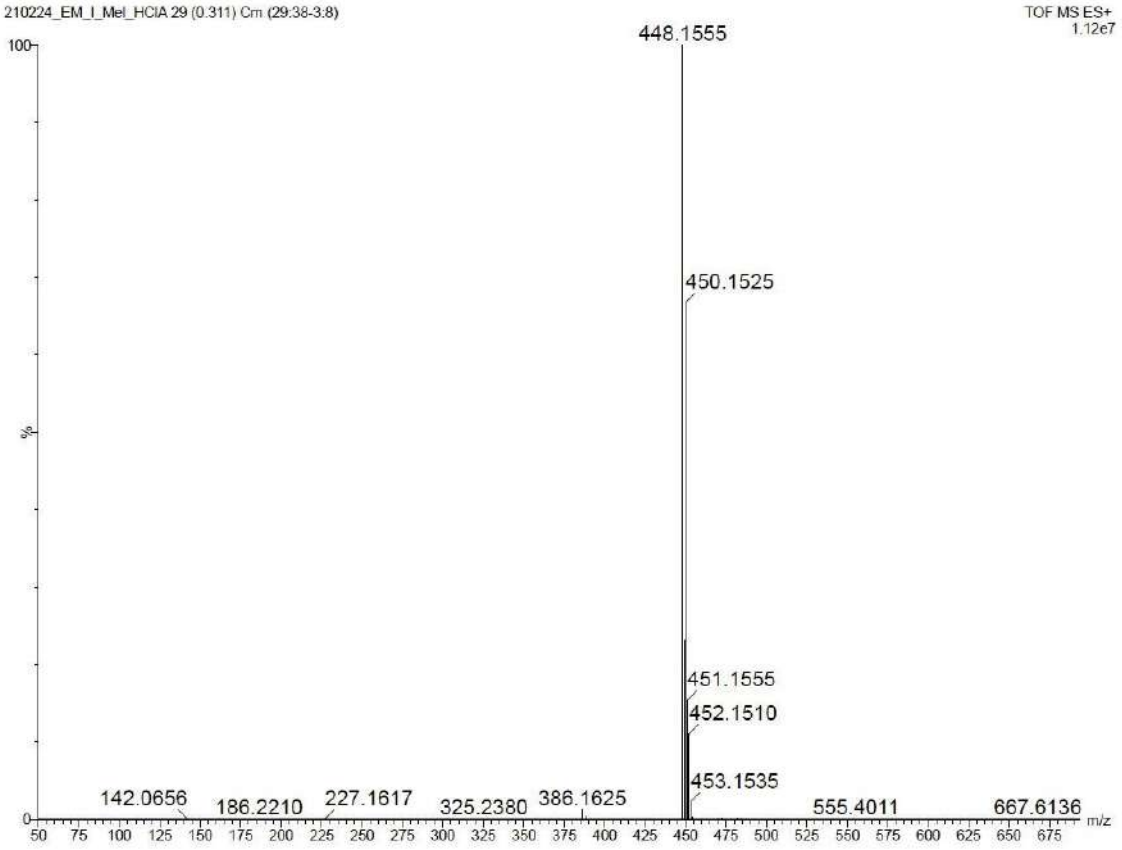

Figure S11. HRMS spectrum of the EM–I–MEL.

Elemental Composition Report **Page 1**

Single Mass Analysis
Tolerance = 5.0 PPM / DBE: min = -1.5, max = 80.0
Element prediction: Off
Number of isotope peaks used for i-FIT = 9

Monoisotopic Mass, Even Electron Ions
404 formula(e) evaluated with 2 results within limits (all results (up to 1000) for each mass)
Elements Used:
C: 0-50 H: 0-80 N: 0-5 O: 0-6 Cl: 1-2

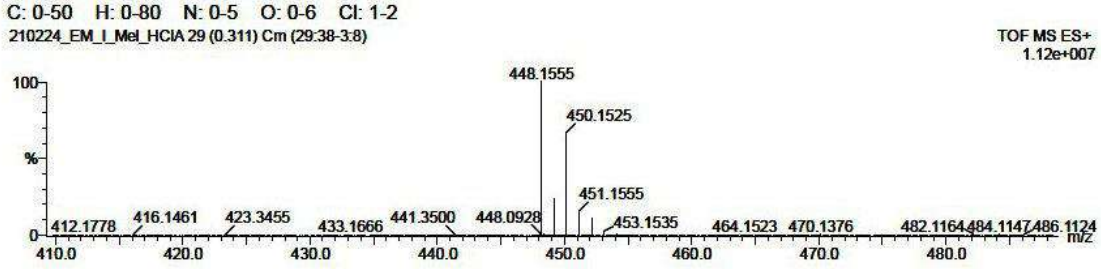

Minimum:				-1.5				
Maximum:		5.0	5.0	80.0				
Mass	Calc. Mass	mDa	PPM	DBE	i-FIT	Norm	Conf(%)	Formula
448.1555	448.1559	-0.4	-0.9	10.5	1625.1	0.000	100.00	C23 H28 N3 O2 Cl2
	448.1540	1.5	3.3	15.5	1646.4	21.272	0.00	C24 H23 N5 O2 Cl

Figure S12. Elemental analysis of the EM–I–MEL.

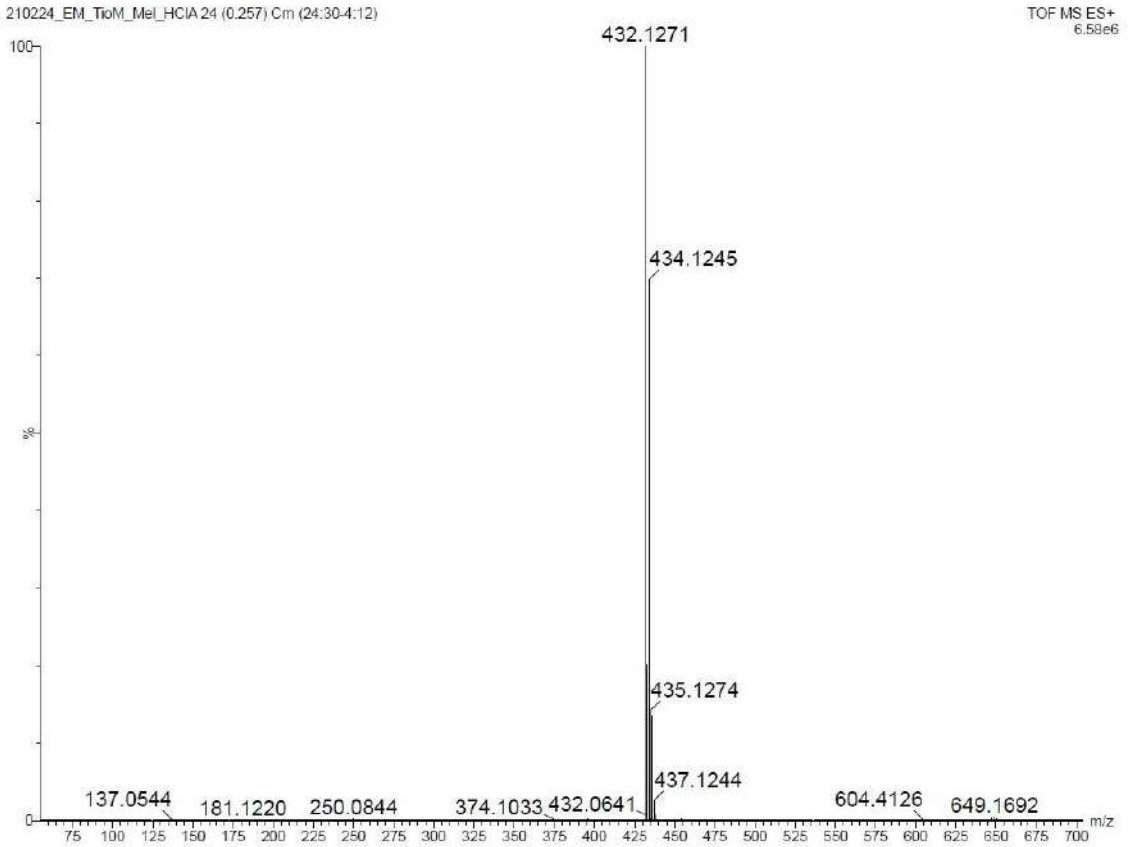

Figure S13. HRMS spectrum of the EM–T–MEL.

Elemental Composition Report **Page 1**

Single Mass Analysis
Tolerance = 5.0 PPM / DBE: min = -1.5, max = 80.0
Element prediction: Off
Number of isotope peaks used for i-FIT = 9

Monoisotopic Mass, Even Electron Ions
356 formula(e) evaluated with 2 results within limits (all results (up to 1000) for each mass)
Elements Used:
C: 0-50 H: 0-80 N: 0-5 O: 0-6 S: 1-1 Cl: 1-2

210224_EM_TioM_Mel_HCIA 24 (0.257) Cm (24:30-4:12)

TOF MS ES+
6.58e+006

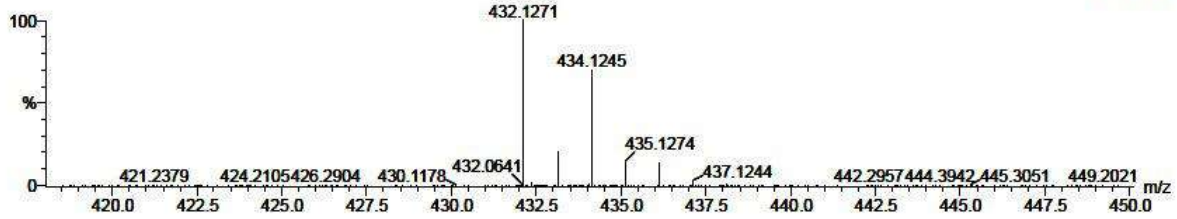

Minimum:				-1.5				
Maximum:		5.0	5.0	80.0				
Mass	Calc. Mass	mDa	PPM	DBE	i-FIT	Norm	Conf(%)	Formula
432.1271	432.1279	-0.8	-1.9	6.5	1080.8	0.000	100.00	C19 H28 N3 O2 S Cl2
	432.1261	1.0	2.3	11.5	1108.6	27.788	0.00	C20 H23 N5 O2 S Cl

Figure S14. Elemental analysis of the EM–T–MEL.

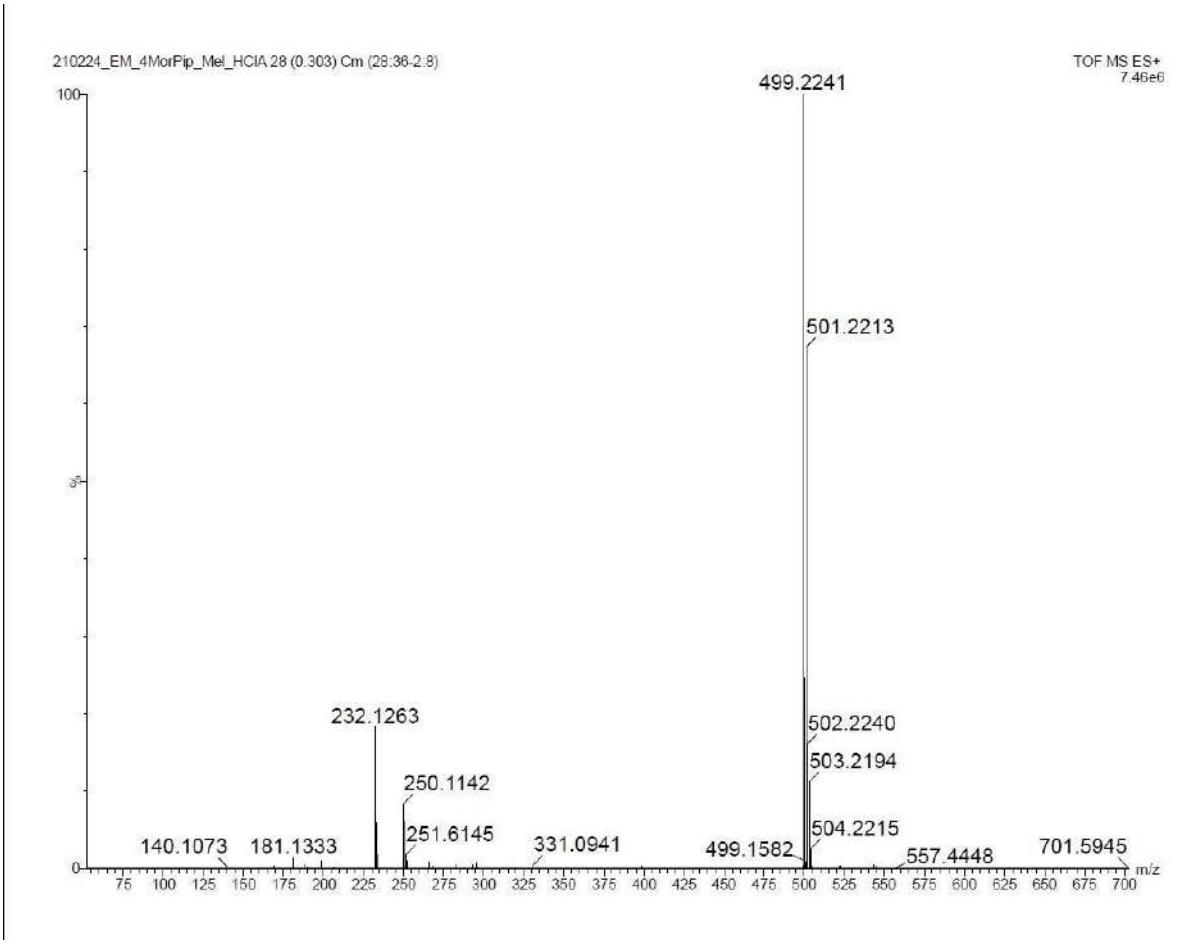

Figure S15. HRMS spectrum of the EM–MORPIP–MEL.

Elemental Composition Report **Page 1**

Single Mass Analysis
Tolerance = 5.0 PPM / DBE: min = -1.5, max = 80.0
Element prediction: Off
Number of isotope peaks used for i-FIT = 9

Monoisotopic Mass, Even Electron Ions
455 formula(e) evaluated with 3 results within limits (all results (up to 1000) for each mass)
Elements Used:
C: 0-50 H: 0-80 N: 0-5 O: 0-6 Cl: 1-2

210224_EM_4MorPip_Mel_HCIA 28 (0.303) Cm (28:36-2:8)

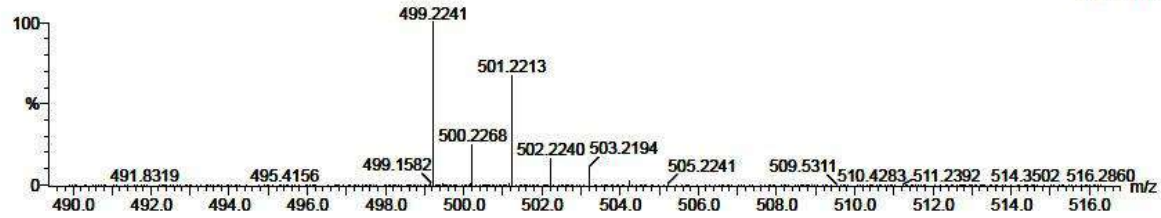

Minimum:				-1.5				
Maximum:		5.0	5.0	80.0				
Mass	Calc. Mass	mDa	PPM	DBE	i-FIT	Norm	Conf(%)	Formula
499.2241	499.2243	-0.2	-0.4	7.5	1271.1	0.000	100.00	C24 H37 N4 O3 Cl2
	499.2251	-1.0	-2.0	11.5	1288.2	17.078	0.00	C29 H36 O5 Cl
	499.2265	-2.4	-4.8	16.5	1288.7	17.583	0.00	C30 H32 N4 O Cl

Figure S16. Elemental analysis of the EM–MORPIP–MEL.

PUBLIKACJA NR IV

Poczta A., Krzeczyński P., Ionov M., Rogalska A., Gaipl U.S., Marczak A. Lubgan D.; *Newly Synthesized Melphalan Analogs Induce DNA Damage and Mitotic Catastrophe in Hematological Malignant Cancer Cells;* Int J Mol Sci. 2022; 23(22): 14258.

- **Praca doświadczalna**
- **IF: 6.208**
- **punkty MEiN: 140 pkt.**

International Journal of
Molecular Sciences

MDPI

Article

Newly Synthesized Melphalan Analogs Induce DNA Damage and Mitotic Catastrophe in Hematological Malignant Cancer Cells

Anastazja Poczta [1,*], Piotr Krzeczyński [2], Maksim Ionov [3], Aneta Rogalska [1], Udo S. Gaipl [4], Agnieszka Marczak [1] and Dorota Lubgan [4]

[1] Department of Medical Biophysics, Faculty of Biology and Environmental Protection, University of Lodz, 141/143 Pomorska St., 90-236 Lodz, Poland
[2] Department of Pharmacy, Cosmetic Chemistry and Biotechnology, Team of Chemistry, Łukasiewicz Research Network—Industrial Chemistry Institute, 8 Rydygiera St., 01-793 Warsaw, Poland
[3] Department of General Biophysics, Faculty of Biology and Environmental Protection, University of Lodz, 141/143 Pomorska St., 90-236 Lodz, Poland
[4] Translational Radiobiology, Department of Radiation Oncology, University Hospital Erlangen Friedrich-Alexander-Universität Erlangen-Nürnberg, Universitätsstr. 27, 91054 Erlangen, Germany
* Correspondence: anastazja.poczta@edu.uni.lodz.pl

Abstract: Myeloablative therapy with highdoses of the cytostatic drug melphalan (MEL) in preparation for hematopoietic cell transplantation is the standard of care for multiple myeloma (MM) patients. Melphalan is a bifunctional alkylating agent that covalently binds to nucleophilic sites in the DNA and effective in the treatment, but unfortunately has limited therapeutic benefit. Therefore, new approaches are urgently needed for patients who are resistant to existing standard treatment with MEL. Regulating the pharmacological activity of drug molecules by modifying their structure is one method for improving their effectiveness. The purpose of this work was to analyze the physicochemical and biological properties of newly synthesized melphalan derivatives (EE-MEL, EM-MEL, EM-MOR-MEL, EM-I-MEL, EM-T-MEL) obtained through the esterification of the carboxyl group and the replacement of the the amino group with an amidine group. Compounds were selected based on our previous studies for their improved anticancer properties in comparison with the original drug. For this, we first evaluated the physicochemical properties using the circular dichroism technique, then analyzed the zeta potential and the hydrodynamic diameters of the particles. Then, the in vitro biological properties of the analogs were tested on multiple myeloma (RPMI8226), acute monocytic leukemia (THP1), and promyelocytic leukemia (HL60) cells as model systems for hematological malignant cells. DNA damage was assessed by immunostaining γH2AX, cell cycle distribution changes by propidium iodide (PI) staining, and cell death by the activation of caspase 2. We proved that the newly synthesized derivatives, in particular EM-MOR-MEL and EM-T-MEL, affected the B-DNA conformation, thus increasing the DNA damage. As a result of the DNA changes, the cell cycle was arrested in the S and G2/M phases. The cell death occurred by activating a mitotic catastrophe. Our investigations suggest that the analogs EM-MOR-MEL and EM-T-MEL have better anti-cancer activity in multiple myeloma cells than the currently used melphalan.

Keywords: blood cancer; DNA damage γH2AX; drug structure modification; melphalan; mitotic catastrophe

Citation: Poczta, A.; Krzeczyński, P.; Ionov, M.; Rogalska, A.; Gaipl, U.S.; Marczak, A.; Lubgan, D. Newly Synthesized Melphalan Analogs Induce DNA Damage and Mitotic Catastrophe in Hematological Malignant Cancer Cells. *Int. J. Mol. Sci.* **2022**, *23*, 14258. https://doi.org/10.3390/ijms232214258

Academic Editor: Lina Sabatino

Received: 31 October 2022
Accepted: 15 November 2022
Published: 17 November 2022

1. Introduction

Hematopoietic malignancies are a heterogeneous group of cancers that affect the bone marrow, blood, and lymph nodes. They account for 10% of all annual cancer deaths worldwide. The second most common hematologic malignancy, after non-Hodgkin's lymphoma, is multiple myeloma (MM). The disease is most often manifested by hypercalcemia, renal failure, anemia, and bone changes [1–3].

The therapeutic arsenal for MM patients includes drugs with various mechanisms of action, such as alkylating agents (melphalan, bendamustine), immunomodulatory drugs (thalidomide, lenalidomide, pomalidomide), histone deacetylase inhibitors (vorinostat, panobinostat), proteasome inhibitors (bortezomib, carfilzomib, ixazomib), and monoclonal antibodies (daratumumab, isatuximab) [4]. Treatment strategies vary depending on the patient's age, comorbidities, disease stage, cytogenetic parameters, and other factors. For the treatment of primary patients under the age of 70 years without serious comorbidities, the treatment program includes high-dose melphalan (MEL), followed by autologous stem cell transplantation [5,6].

The cytotoxic properties of melphalan are due to its alkylating properties [7]. The alkylation of DNA takes place in two steps, involving the first and then the second chloroethyl group in the melphalan molecule, which create a highly reactive aziridinium intermediate cation [4,8]. Then, the resulting reactive intermediates rapidly alkylate guanine or adenine sites of the DNA to form the primary monoadduct. After the formation of the primary DNA monoadduct, the second chloroethyl group acts in this same manner. However, the secondary cyclization reaction is much slower than the first. The 2′-hydroxyethyl derivatives are the predominant DNA changes resulting from melphalan treatment, because DNA–DNA cross-links play a key role in the biological activity of melphalan. As a result of alkylation, many different DNA adducts can be formed: monoadduct (if the reactive intermediate interacts with the H_2O molecule, the adduct remains a DNA monoadduct), DNA–protein cross-linking (if it reacts with an adjacent protein), intra-strand cross-linking (if the reaction takes place with guanine or adenine of the same DNA strand as the initial monoadduct), and inter-strand cross-linking (if the interaction is with the opposite strand of DNA) [9–11]. DNA–DNA cross-linking is usually associated with cell death or loss of a chromosome. The intra- or inter-strand lesions may be promutagenic or fatal [10].

Although using a high concentration of MEL in myeloablative therapy in preparation for hematopoietic cell transplantation remains the standard of care for MM patients [4], relapses are still common, with periods of remission becoming shorter and shorter. Therefore, new approaches are urgently needed for patients who are resistant to existing therapies [12].

Regulating the pharmacological activity of drug molecules by modifying their structure is one method of improving their effectiveness. The chemical structure of a drug determines its physicochemical properties, absorption, distribution, metabolism, excretion, and toxicity, which ultimately affects its pharmacological activity [13]. In our previous studies [14,15], we have shown that esterification of the carboxyl group is necessary to improve the effectiveness of MEL. In addition, replacing the amino group with an amidine group containing a thiomorpholine, indoline, or morpholine residue in the structure increases the properties of the drug. The new analogs synthesized by us have been designed to have good drug-like properties, which was confirmed by in silico studies [15]. In vitro studies of the biological properties, including the cytotoxic, pro-apoptotic, and genotoxic properties, showed the new derivatives to have improved properties. Simultaneously, a decreased cytotoxic effect in the tested derivatives was observed against peripheral blood mononuclear cells (PBMC) [14,15]. Such derivatives could potentially be of therapeutic importance. However, they require additional tests, including elucidating the mechanism of action that leads to their cytotoxic and genotoxic effects. The purpose of this work was to analyze the physicochemical and biological properties within our scientific framework of five synthesized derivatives (EE-MEL, EM-MEL, EM-MOR-MEL, EM-I-MEL, EM-T-MEL) in comparison with the original drug, melphalan. In particular, we focused on analyzing their effects on DNA and on understanding the cell death pathway in three cancer cell lines: multiple myeloma (RPMI8226), acute monocytic leukemia (THP1), and acute promyelocytic leukemia (HL60).

2. Results

2.1. Chemical Modifications of the Melphalan Molecule Alter the Conformation of B-DNA

To analyze the ability of melphalan and the investigated melphalan derivatives (EE-MEL, EM-MEL, EM-MOR-MEL, EM-I-MEL, EM-T-MEL) to affect DNA secondary

structures, the circular dichroism (CD) technique was applied. This method is widely used to study the conformation of biomolecules, and is based on the difference in absorption of left and right circularly polarized light. The obtained spectrum was typical for the B-formation of DNA (as described in [16,17]) with characteristic peaks: positive around λ = 280 nm and negative around λ = 245 nm. The positive band appears as a result of a stacking interaction between the DNA nitrogen bases, while the negative band indicates the right-handedness of the B-DNA double helix [18]. CD spectra were recorded in the λ = 230–320 nm range. The CD results are presented as molar ellipticity (θ) in deg × cm^2 × $dmol^{-1}$ (Figure 1A). All the drugs had an impact on the DNA. The greatest changes in ellipticity were observed for EM-T-MEL and EM-MOR-MEL.

The conformational transition of DNA can be traced by changes in the positions and intensities of the CD spectral peaks (Figure 1A,B) [19]. The shift in the peak from 280 nm to higher wavelengths (EM-T-MEL: 287 nm; EM-MOR-MEL: 288 nm), followed by a decrease in intensity, indicated that the DNA form changed from form A to form B [20]. The ellipticity of the DNA changed with increasing derivative concentration (5–300 μM). At the highest concentration of EM-T-MEL, the CD peak intensity at λ = 280 nm decreased and reached a minimum at λ = 268 nm. An increase in intensity was determined at λ = 245 nm, reaching a maximum at λ = 238. The EM-MOR-MEL derivative caused relevant changes in ellipticity as well. This compound caused a decrease in the intensity of the CD peaks and two negative CD peaks (for the highest concentration: λ = 271 nm and λ = 248 nm). The ability of MEL and its derivative EM-T-MEL to form complexes with DNA was confirmed and also studied by computer modeling (Figure 1C).

2.2. Melphalan and Its Derivatives Exhibit a Negative Zeta Potential

Zeta potential measurements provide information about the surface charge of tested compounds and their complexes with DNA (Figure 2A). The zeta potential of naked DNA was negative (approximately −23 mV). MEL and all tested analogs were negatively charged as well. The zeta potential of the original MEL molecule ranged from −27 mV (2.5 μM) to −58 mV (10–100 μM). The addition of negatively charged DNA increased the zeta potential to values ranging from −8 mV (2.5 μM) to −44 mV (10 μM). The EM-T-MEL derivative at a concentration of 25 μM had the lowest zeta potential (approximately −70 mV). The addition of DNA resulted in a significant increase in the zeta potential, by up to −53 mV. For the other compounds, we also observed low zeta potential values for the samples with and without DNA. Adding increasing concentrations of the compounds to the DNA caused a gradual but significant decrease in the zeta potential. EM-MEL and EM-MOR-MEL in the already lowest concentration of 5 μM, MEL at 10 μM, and the remaining derivative at 25 μM induced increased (due to higher concentrations) modifications in the zeta potential.

The hydrodynamic diameters of the tested compounds and their complexes with DNA were measured by the dynamic light scattering (DLS) technique (Figure 2B). We did not observe an increase in the average size of the complex when the tested compounds were added to DNA compared to the sample containing DNA only. The DLS results showed that melphalan and its tested analogs did not cause an increase in the DNA hydrodynamic diameter.

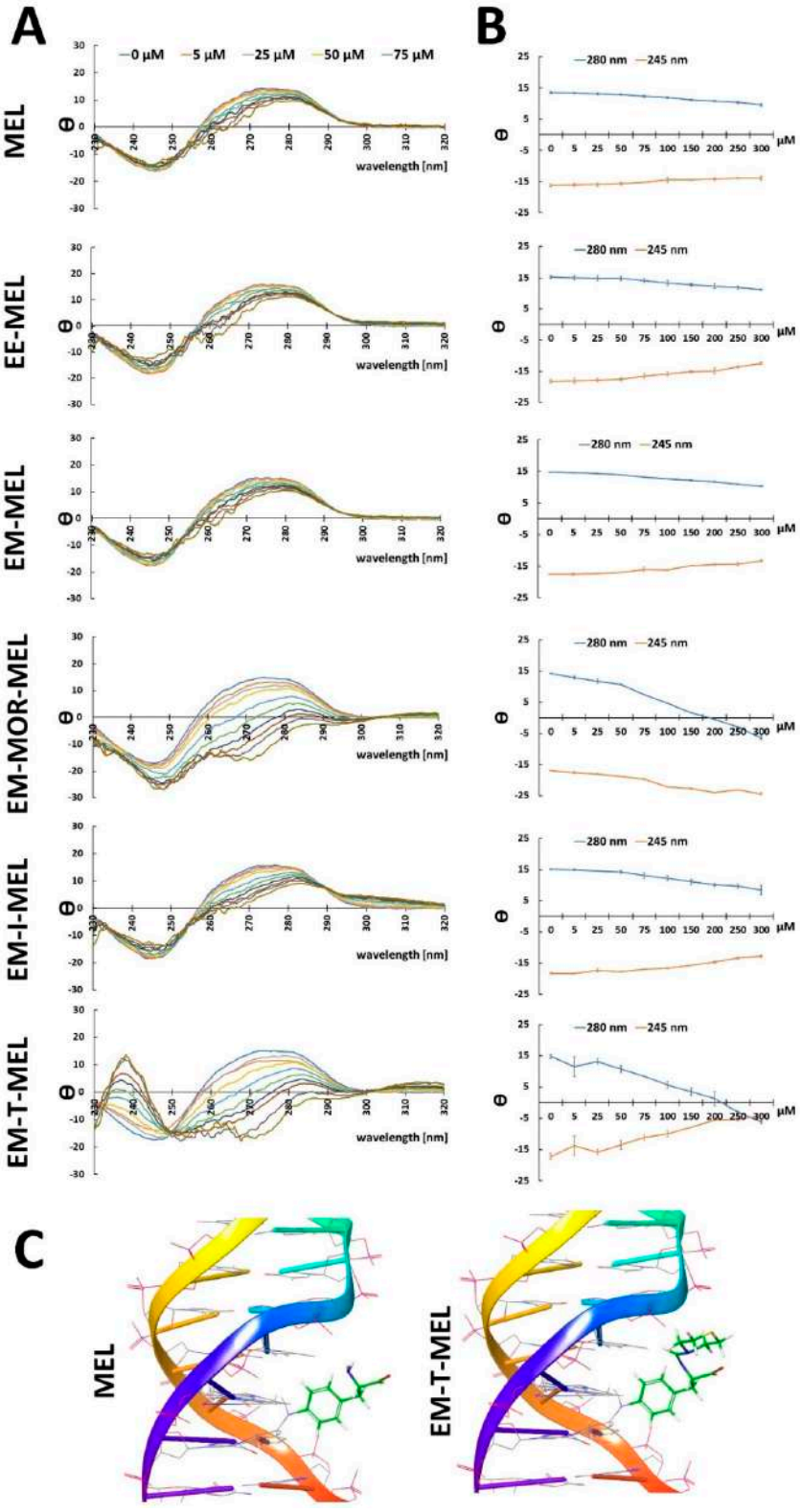

Figure 1. Chemical modifications of the melphalan molecule affect the B-DNA structure. (**A**) The CD spectra of DNA in the presence of MEL, EE-MEL, EM-MEL, EM-MOR-MEL, EM-I-MEL, and EM-T-MEL. (**B**) Changes in θ/θ0 parameter at λ = 245 nm and λ = 280 nm in the presence of MEL, EE-MEL, EM-MEL, EM-MOR-MEL, EM-I-MEL, and EM-T-MEL. Results are the mean ± standard deviation (SD), *n* = 3. (**C**) Visualizations showing the binding site to DNA of the original drug MEL and the most potent derivative EM-T-MEL. The visualizations were created in PyMOL (Schrödinger, Inc.). Computer simulation was performed for one DNA molecule and one ligand molecule.

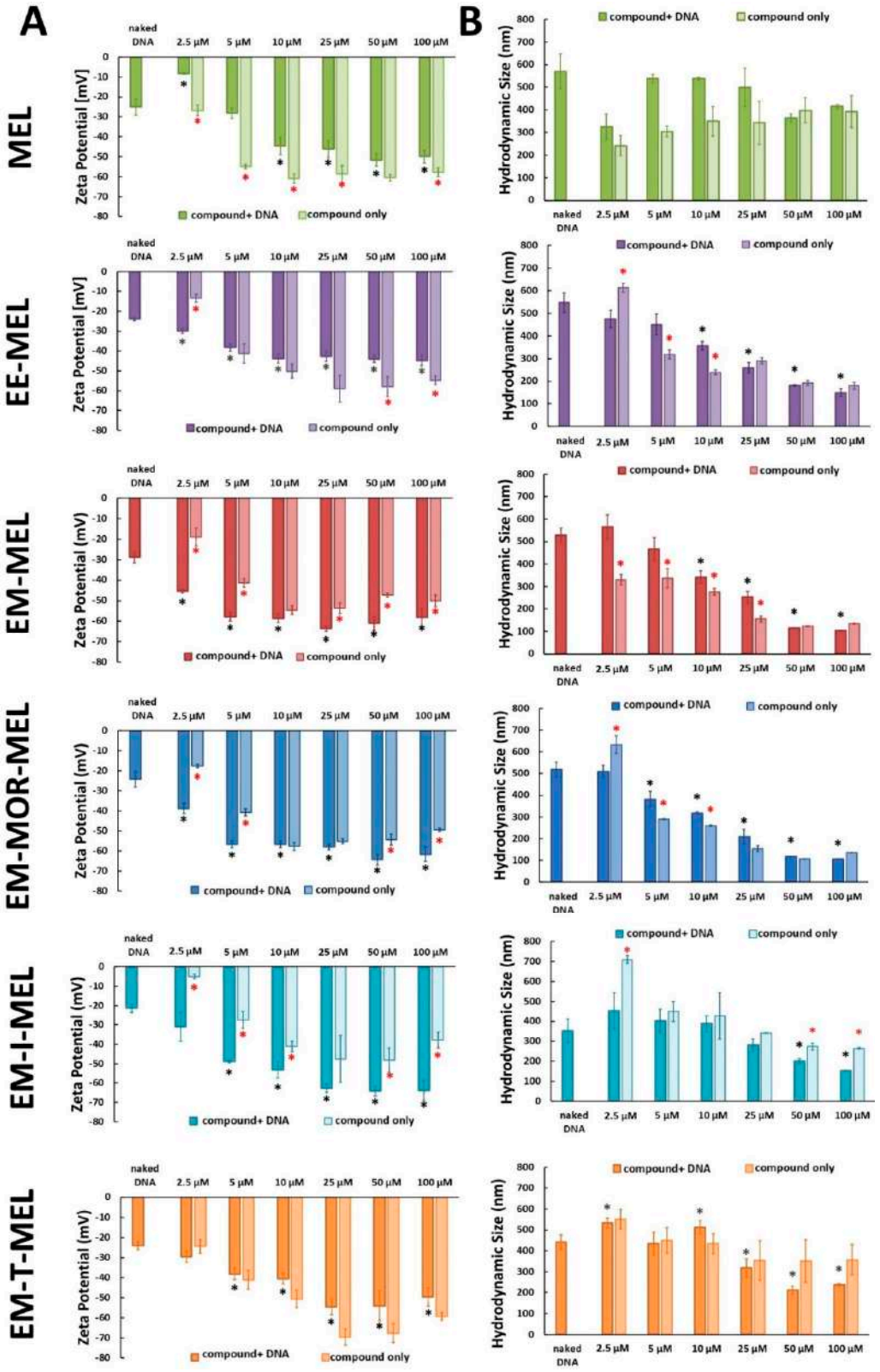

Figure 2. (**A**) Zeta potential of the original drug and all tested analogs with and without DNA. (**B**) The hydrodynamic size of MEL, EE-MEL, EM-MEL, EM-MOR-MEL, EM-I-MEL, and EM-T-MEL with and without DNA. Results are the mean ± SD. (black asterisks *) Statistically significant differences between a sample containing only DNA vs. a sample containing DNA and the tested compound, $p < 0.05$; (red asterisks *) statistically significant differences between a sample containing DNA and the tested compound vs. a sample containing only tested compound, $p < 0.05$, n = 3.

2.3. Tested Derivatives Induce DNA Damage Detected by γH2AX Analysis

The ability of MEL and its derivatives to induce DNA double-strand breaks (DSBs) was tested by an immunostaining assay (Figure 3). Cells irradiated with 1 Gy were used as a positive control in the staining process. All tested cell lines were sensitive to 1 Gy irradiation. All compounds, including the original drug MEL, led to a significant increase in γH2AX foci (cut off: 5 foci per cell, $p < 0.001$) in all three cell lines (THP1, HL60, RPMI8226) in relation to each untreated control (Table 1). In the case of THP1, the greatest changes were noticed after 24 h incubation with EM-T-MEL and 48 h incubation with EE-MEL, EM-MEL, EM-I-MEL, and EM-T-MEL. When compared to the original drug MEL, the greatest changes were noticed after 24 h incubation with EM-T-MEL. The 48 h incubation with all compounds led to a statistically significant ($p < 0.001$) increase in γH2AX foci compared to the control. This effect was strongly visible for EE-MEL, EM-MEL, EM-I-MEL, and EM-T-MEL (all drugs except EM-MOR-MEL). The HL60 cells were overall more sensitive than the THP1 cells. The damage was already apparent after 4 h for all drugs in relation to the untreated cells. HL60 showed a higher sensitivity to the modified drugs than the original MEL compound. Significant changes were observed after 4 h treatment with EM-T-MEL, 24 h treatment with all analogs, and 48 h treatment with all tested analogs except EM-I-MEL. RPMI8226 cells responded similarly to THP1 when compared to the untreated controls. When compared to the original MEL, the increase in the number of foci reached a maximum after 4 h and 24 h with EE-MEL, and 24 h with EM-T-MEL. The most explicit effect of an approximately 5.5-fold increase in the abundance of foci was observed after 24 h incubation with EM-T-MEL.

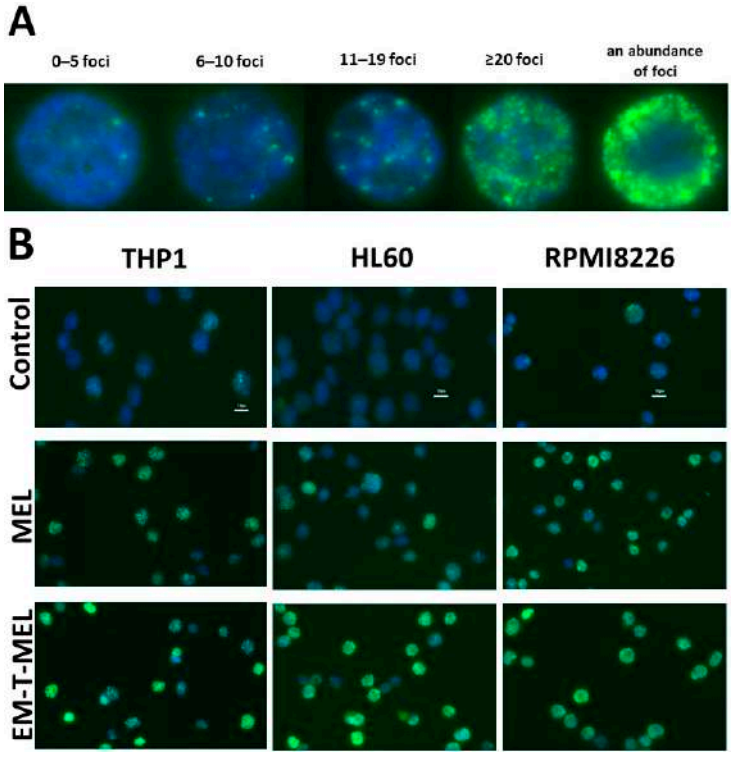

Figure 3. (**A**) Representative photos showing RPMI8226 cells with a number of foci (0–5; 6–10; 11–19; ≥20; an abundance of foci) per cell. (**B**) Detection and localization of γH2AX histone foci in THP1, HL60, and RPMI8226 cells based on the highly specific antigen–antibody binding reaction. Sample images after 24 h of incubation. Cells were incubated with a phospho-(Ser139) mouse monoclonal IgG specific anti-H2AX antibody, and next with Alexa Fluor TM 488 goat anti-mouse IgG secondary antibody as described in the Materials and Methods section. The cell nuclei were stained with 4′,6-diamidino-2-phenylindole (DAPI) solution. The cells were visualized under a fluorescence microscope. Magnification: 400x, scale bar: 10 μm.

Table 1. γH2AX foci per cell after treatment with melphalan and its derivatives. Data are the number of foci per cell (%). All data are from two biological assays (n = 200; 100 cells counted in each case). Statistically significant *p* values (ANOVA with Tukey's *post hoc*) for cells > 5 foci/cell compared to the control or original MEL drug are shown.

THP1 (n = 200)								
				4 h				
foci/cell	Control	1 Gy	MEL	EE_MEL	EM-MEL	EM_MOR_MEL	EM_I_MEL	EM_T_MEL
0–5	155 (77.5%)	30 (15%)	73 (36.5%)	63 (31.5%)	70 (35%)	109 (54.5%)	87 (43.5%)	59 (29.6)
6–10	22 (11%)	50 (25%)	69 (34.5%)	40 (20%)	43 (21.5%)	29 (14.5%)	43 (21.5%)	47 (23.6%)
11–19	5 (2.5%)	42 (21%)	12 (6%)	43 (21.5%)	25 (12.5%)	28 (14%)	23 (11.5%)	32 (16.1%)
≥20	11 (5.5%)	45 (22.5%)	31 (15.5%)	31 (15.5%)	45 (22.5%)	27 (13.5%)	36 (18%)	36 (18.1%)
an abundance of foci	7 (3.5%)	33 (16.5%)	15 (7.5%)	23 (11.5%)	17 (8.5%)	7 (3.5%)	11 (5.5%)	25 (12.6%)
compared to control		$p = 0.000177$	$p = 0.000177$	$p = 0.000177$	$p = 0.000177$	$p = 0.000177$	$p = 0.000177$	$p = 0.000177$
compared to MEL		$p = 0.000177$						
				24 h				
0–5	152 (76%)		43 (21.5%)	34 (17.1%)	30 (15%)	28 (14%)	64 (32%)	16 (8%)
6–10	45 (22.5%)		56 (28%)	48 (24.1%)	34 (17%)	33 (16.5%)	47 (23.5%)	25 (12.5%)
11–19	3 (1.5%)		40 (20%)	43 (21.6%)	39 (19.5%)	36 (18%)	36 (18%)	29 (14.5%)
≥20	0 (0%)		49 (24.5%)	44 (22.1%)	59 (29.5%)	57 (28.5%)	49 (24.5%)	66 (33%)
an abundance of foci	0 (0%)		12 (6%)	30 (15.1%)	38 (19%)	46 (23%)	4 (2%)	64 (32%)
compared to control			$p = 0.000177$	$p = 0.000177$	$p = 0.000177$	$p = 0.000177$	$p = 0.000177$	$p = 0.000177$
compared to MEL								$p = 0.000374$
				48 h				
0–5	118 (59%)		43 (21.5%)	11 (5.5%)	24 (12%)	30 (15%)	15 (7.5%)	9 (4.5%)
6–10	50 (25%)		50 (25%)	16 (8%)	39 (19.5%)	22 (11%)	39 (19.5%)	23 (11.5%)
11–19	19 (9.5%)		40 (20%)	17 (8.5%)	60 (30%)	35 (17.5%)	40 (20%)	31 (15.5%)
≥ 20	8 (4%)		42 (21%)	67 (33.5%)	54 (27%)	64 (32%)	57 (28.5%)	59 (29.5%)
an abundance of foci	5 (2.5%)		25 (12.5%)	89 (44.5%)	23 (11.5%)	49 (24.5%)	49 (24.5%)	78 (39%)
compared to control			$p = 0.000177$	$p = 0.000177$	$p = 0.000177$	$p = 0.000177$	$p = 0.000177$	$p = 0.000177$
compared to MEL				$p = 0.000180$	$p = 0.034157$		$p = 0.000271$	$p = 0.000177$
HL60 (n = 200)								
				4 h				
foci/cell	Control	1 Gy	MEL	EE_MEL	EM-MEL	EM_MOR_MEL	EM_I_MEL	EM_T_MEL
0–5	180 (90.5%)	19 (9.5%)	130 (65%)	140 (70%)	126 (63%)	117 (58.5%)	127 (63.5%)	90 (45%)
6–10	14 (7%)	62 (31%)	45 (22.5%)	39 (19.5%)	42 (21%)	50 (25%)	29 (14.5%)	37 (18.5%)
11–19	2 (1%)	84 (42%)	11 (5.5%)	10 (5%)	16 (8%)	15 (7.5%)	28 (14%)	24 (12%)
≥ 20	3 (1.5%)	18 (9%)	13 (6.5%)	11 (5.5%)	8 (4%)	17 (8.5%)	15 (7.5%)	37 (18.5%)

Table 1. *Cont.*

THP1 (n = 200)								
an abundance of foci	0 (0%)	17 (8.5%)	1 (0.5%)	0 (0%)	8 (4%)	1 (0.5%)	1 (0.5%)	12 (6%)
compared to control		$p = 0.000177$	$p = 0.000177$	$p = 0.000177$	$p = 0.000177$	$p = 0.000177$	$p = 0.000177$	$p = 0.000177$
compared to MEL		$p = 0.000177$						$p = 0.000177$
				24 h				
0–5	150 (75%)		104 (52.5%)	23 (11.6%)	37 (18.7%)	60 (30%)	71 (35.5%)	37 (18.8%)
6–10	39 (19.5%)		41 (20.7%)	32 (16.2%)	32 (16.2%)	39 (19.5%)	44 (22%)	33 (16.8%)
11–19	9 (4.5%)		23 (11.6%)	20 (10.1%)	24 (12.1%)	31 (15.5%)	21 (10.5%)	29 (14.7%)
≥ 20	2 (1%)		21 (10.6%)	88 (44.4%)	68 (34.3%)	50 (25%)	53 (26.5%)	58 (29.4%)
an abundance of foci	0 (0%)		9 (4.5%)	35 (17.7%)	37 (18.7%)	20 (10%)	11 (5.5%)	40 (20.3%)
compared to control			$p = 0.000177$	$p = 0.000177$	$p = 0.000177$	$p = 0.000177$	$p = 0.000177$	$p = 0.000177$
compared to MEL				$p = 0.000177$	$p = 0.000177$	$p = 0.000177$	$p = 0.000177$	$p = 0.000177$
				48 h				
0–5	182 (91%)		53 (26.5%)	11 (5.6%)	18 (9%)	8 (4%)	57 (28.5%)	37 (18.5%)
6–10	18 (9%)		22 (11%)	17 (8.6%)	26 (13%)	19 (9.5%)	18 (9%)	27 (13.5%)
11–19	0 (0%)		13 (6.5%)	23 (11.7%)	27 (13.5%)	33 (16.5%)	16 (8%)	19 (9.5%)
≥ 20	0 (0%)		54 (27%)	61 (31%)	61 (30.5%)	58 (29%)	61 (30.5%)	52 (26%)
an abundance of foci	0 (0%)		58 (29%)	85 (43.1%)	68 (34%)	82 (41%)	48 (24%)	65 (32%)
compared to control			$p = 0.000177$	$p = 0.000177$	$p = 0.000177$	$p = 0.000177$	$p = 0.000177$	$p = 0.000177$
compared to MEL				$p = 0.000177$	$p = 0.000177$	$p = 0.000177$		$p = 0.005658$
RMPI8226 (n = 200)								
				4 h				
foci/cell	Control	1 Gy	MEL	EE_MEL	EM-MEL	EM_MOR_MEL	EM_I_MEL	EM_T_MEL
0–5	155 (77.5%)	30 (15%)	73 (36.5%)	63 (31.5%)	70 (35%)	109 (54.5%)	87 (43.5%)	59 (29.6%)
6–10	22 (11.0%)	50 (25%)	69 (34.5%)	40 (20%)	43 (21.5%)	29 (14.5%)	43 (21.5%)	47 (23.6%)
11–19	5 (2.5%)	42 (21%)	12 (6%)	43 (21.5%)	25 (12.5%)	28 (14%)	23 (11.5%)	32 (16.1%)
≥ 20	11 (5.5%)	45 (22.5%)	31 (15.5%)	31 (15.5%)	45 (22.5%)	27 (13.5%)	36 (18%)	36 (18.1%)
an abundance of foci	7 (3.5%)	33 (16.5%)	15 (7.5%)	23 (11.5%)	17 (8.5%)	7 (3.5%)	11 (5.5%)	25 (12.6%)
compared to control		$p = 0.000177$	$p = 0.000177$	$p = 0.000177$	$p = 0.000177$	$p = 0.000177$	$p = 0.000177$	$p = 0.000177$
compared to MEL				$p = 0.011650$				
				24 h				
0–5	152 (76%)		43 (21.5%)	34 (17.1%)	30 (15%)	28 (14%)	64 (32%)	16 (8%)
6–10	45 (22.5%)		56 (28%)	48 (24.1%)	34 (17%)	33 (16.5%)	47 (23.5%)	25 (12.5%)
11–19	3 (1.5%)		40 (20%)	43 (21.6%)	39 (19.5%)	36 (18%)	36 (18%)	29 (14.5%)
≥ 20	0 (0%)		49 (24.5%)	44 (22.1%)	59 (29.5%)	57 (28.5%)	49 (24.5%)	66 (33%)
an abundance of foci	0 (0%)		12 (6%)	30 (15.1%)	38 (19%)	46 (23%)	4 (2%)	64 (32%)

Table 1. *Cont.*

THP1 (n = 200)							
compared to control		$p = 0.000177$	$p = 0.000177$	$p = 0.000177$	$p = 0.000177$	$p = 0.000177$	$p = 0.000177$
compared to MEL			$p = 0.000347$				$p = 0.002221$
			48 h				
0–5	118 (59%)	43 (21.5%)	11 (5.5%)	24 (12%)	30 (15%)	15 (7.5%)	9 (4.5%)
6–10	50 (25%)	50 (25%)	16 (8%)	39 (19.5%)	22 (11%)	39 (19.5%)	23 (11.5%)
11–19	19 (9.5%)	40 (20%)	17 (8.5%)	60 (30%)	35 (17.5%)	40 (20%)	31 (15.5%)
≥ 20	8 (4%)	42 (21%)	67 (33.5%)	54 (27%)	64 (32%)	57 (28.5%)	59 (29.5%)
an abundance of foci	5 (2.5%)	25 (12.5%)	89 (44.5%)	23 (11.5%)	49 (24.5%)	49 (24.5%)	78 (39%)
compared to control		$p = 0.000177$	$p = 0.000177$	$p = 0.000177$	$p = 0.000177$	$p = 0.000177$	$p = 0.000177$
compared to MEL							

2.4. Melphalan and Its Derivatives Induce G2/M Arrest

The cell cycle was measured by propidium iodide DNA staining using a flow cytometric technique. The results are shown in Figure 4. Changes in the distribution for each stage were time and compound dependent. We revealed that the greatest effect was induced by EM-T-MEL.

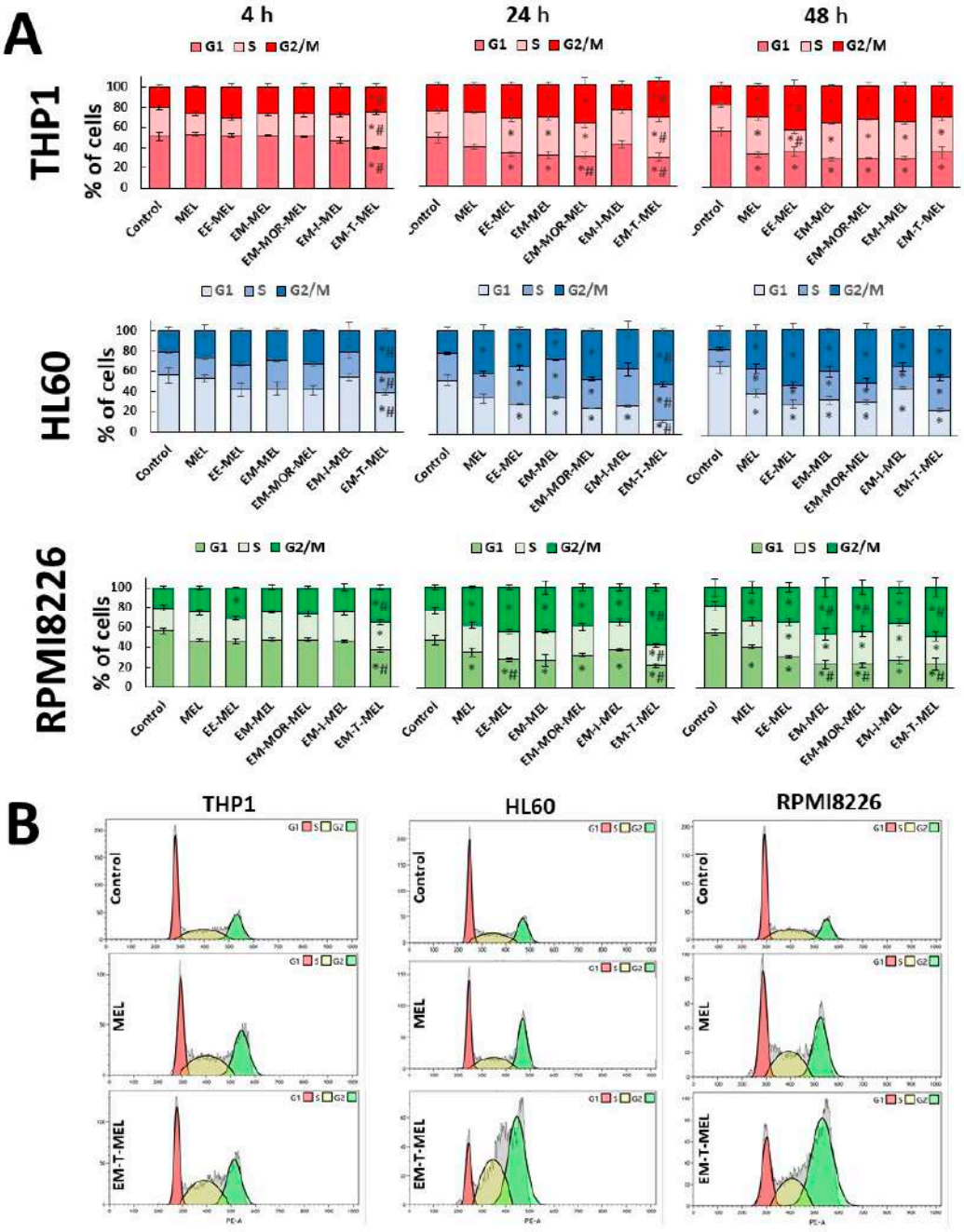

Figure 4. Melphalan and its derivatives induced cell cycle arrest. HL60, THP1, and RPMI8226 cells were incubated for 4, 24, and 48 h with MEL, EE-MEL, EM-MEL, EM-MOR-MEL, EM-I-MEL, and EM-T-MEL. (**A**) Distribution of the cell cycle phases. All data are from three biological assays and are graphed as the mean ± SD. (*) Statistically significant differences compared to the control cells, $p < 0.05$. (#) Statistically significant differences compared to unmodified MEL, $p < 0.05$. (**B**) Representative histograms of cell cycle analysis.

Treatment with EM-T-MEL significantly ($p < 0.05$) changed the distribution of the cell cycle compared to the untreated cells. Compared with the unmodified drug, the time-

dependent incubation of cells with EM-T-MEL had the greatest effect on the RPMI8226 cell line, followed by the THP1 and HL60 cells. There was an accumulation of cells in the G2/M phase. In the THP1 cells, there was also an accumulation of cells in the S phase. It is worth noting that changes for this derivative were observed after 4 h of incubation. The level of cells arrested in G2/M after 24 h and 48 h increased by about 2-fold compared to the controls. HL-60 cells in this phase constituted 52% of the cell population at 24 h and 45% at 48 h. This was similar to RPMI8226 cells, in which 58% of the cell population at 24 h and 49% at 48 h, were in the G2/M phase. Simultaneously, the G1 cell population decreased, thereby causing a reversal of the cell cycle profile. In the case of THP1, there was a significant ($p < 0.05$) increase in the G2/M fraction (24 h: 35% of cells; 48 h: 31% of cells) as well as the S fraction (24 h: 40% of cells, 48 h: 35% of cells) at the expense of the G1 phase. Minor but significant ($p < 0.05$) changes in the distribution of the cell cycle were also observed after treating the cells with EE-MEL, EM-MEL, MOR-MEL (24 h, 48 h), and EM-I-MEL (after 48 h). Melphalan, compared to EM-T-MEL, caused less enrichment of cells in the G2/M phase (<30% in HL60 and THP; about 36% in RPMI8226).

2.5. Tested Compounds Activate Caspase 2 in a Multiple Myeloma Cell Line

Caspase 2 plays an important role in initiating the mitotic catastrophe process. The final results are expressed as a percentage of their activity, with the fluorescence value of the untreated control as 100% (Figure 5).

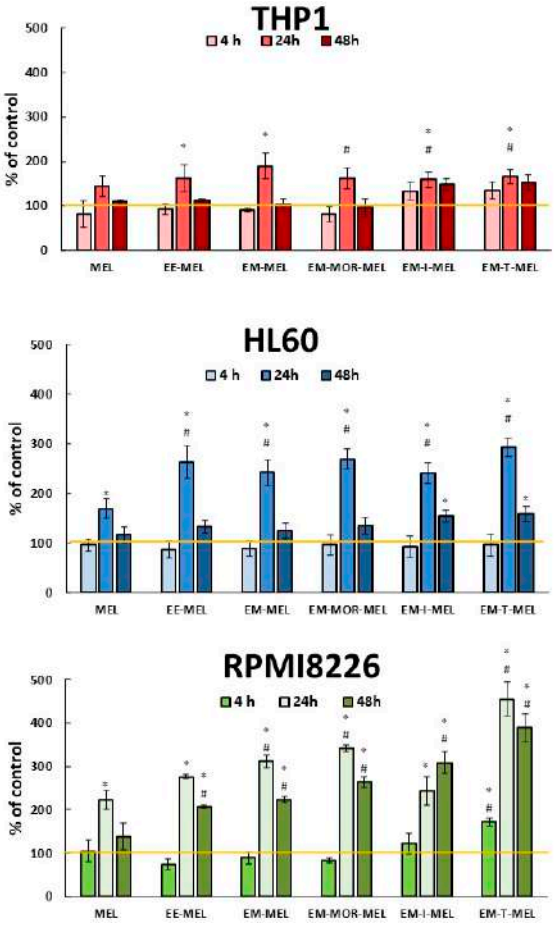

Figure 5. Melphalan derivatives-induced caspase 2 activation. HL60, THP1, RPMI8226 cells were incubated for 4, 24, and 48 h with MEL, EE-MEL, EM-MEL, EM-MOR-MEL, EM-I-MEL, and EM-T-MEL. The final results are expressed as the percentage of activity of a specific cysteine protease, with the untreated control taken as 100%. All data are from three biological assays, and are graphed as the mean ± SD. (*) Statistically significant differences compared to the control cells, $p < 0.05$. (#) Statistically significant differences compared to MEL at the same time point, $p < 0.05$.

RPMI8226 cells were the most sensitive to increased caspase 2 activity after longer incubation with all tested derivatives when compared to both leukemia cell lines. Only EM-T-MEL caused changes after 4 h. The greatest activation of caspase 2 occurred after 24 h treatment and for all tested drugs. After this time, statistically significant ($p < 0.005$) changes compared to unmodified MEL (222% ± 21) were observed for EM-MEL (311% ± 15), EM-MOR-MEL (342% ± 8), and EM-T-MEL (455% ± 37). Increasing the incubation time with all tested derivatives up to 48 h was not associated with significantly higher caspase 2 activity. Leukemia cells showed less (HL60) or no increased activity (THP) of caspase 2 compared to RPMI8226 cells. In the case of HL60, most changes were observed after 24 h of incubation with all tested drugs. All modified drugs had more effects than the original drug MEL on caspase 2.

3. Discussion

The discovery of new drugs and their pharmacological evaluation is a constant research task of modern science and technology. Understanding the mechanisms of drug actions and their clinical implications is gaining increasing attention in the field of potent drug discovery. Elucidating the mechanisms by which cytotoxic drugs inhibit cancer cell proliferation and induce cell death is essential for optimizing therapeutic efficacy. It is also the basis for the design of new drugs.

In our previous research [14,15], we focused on the synthesis and preliminary biological analysis of new melphalan derivatives with enhanced anti-cancer properties. These studies allowed us to select the five most promising derivatives: melphalan ethyl ester (EE-MEL), melphalan methyl ester (EM-MEL), and melphalan methyl esters with an additional modification in the amine group, which was replaced with an amidine group containing a ring of morpholine (EM-MOR-MEL), indoline (EM-I-MEL), or thiomorpholine (EM-T-MEL). All these derivatives showed higher cytotoxic, genotoxic, and pro-apoptotic properties against multiple myeloma cells (RPMI8226) and leukemic cells (THP1, HL60) than melphalan. In this study, we elucidated the modes of action of selected analogs on tumor cell DNA compared to the original drug melphalan.

Physicochemical methods are key approaches to understanding drug—macromolecule interactions. DNA and proteins are important biomolecules responsible for all necessary cellular metabolism in the biological system. Importantly, interaction studies provide insight into the structure activity relationship of a drug, which is important in designing more effective drugs [21]. CD spectral changes for DNA in the presence of increasing amounts of MEL and its analogs were recorded to gain detailed insight into the mechanism of interaction with DNA. The helix with the right-handed β-C/N-glycosidic bonds and asymmetric DNA pattern in the B form gave a characteristic CD spectrum with a positive band at 280 nm (attributable to the base alignment) and a negative band at 245 nm (due to the right-handed DNA helix) [22,23]. Variations in typical band positions and ellipticities are indicative of suitable conformational transitions in the DNA double helix, due to its interaction with the drug [18]. DNA has three different binding sites: groove binding, binding to a phosphate group, and intercalation [22]. A classical intercalator aligns axially between the DNA base pairs, which in turn leads to an increase in the length of the DNA strand and, thus, to a change in the spiral. This increases the intensity of the positive and negative DNA bands with a shift to higher wavelengths [22–24]. On the other hand, the groove binders do not show any shifts or changes in the intensity of the positive and negative bands [25].

In the presence of all tested compounds, a decrease in the intensity of the positive peak with a simultaneous shift to higher waves and an increase in the intensity of the negative peak were observed. The largest changes were observed for EM-T-MEL. The significant reduction in ellipticity in the negative band (245 nm) may have been associated with the destabilization and unwinding of the spiral [26]. For EM-MOR-MEL, a decrease in the intensity of the positive and negative peaks was observed. The shift to higher wavelengths is attributed to conformational transitions from the B to A form, and is additionally

associated with decreased ellipticity. This indicates that the complexes modify the base alignment of DNA without inducing significant changes in supramolecular helicity [25]. Due to large changes in ellipticity for EM-MOR-MEL and EM-T-MEL, we can assume that there was partial intercalation [23,27]. Our research showed that unmodified MEL interacted with DNA in a non-intercalation binding mode. It is known that the major site of the alkylation of melphalan is guanine N7 in the major groove [28]. Studies by Bielawska et al. have shown that amidine analogs of melphalan bound to AT-rich sequences in the minor grooves [29].

The results of the circular dichroism analyses were confirmed using other biophysical methods, such as zeta potential measurements and the dynamic light scattering technique. It was shown that melphalan and the tested analogs did not cause the formation of conjugates with DNA because both MEL and all tested analogs were negatively charged.

The cellular response to DNA damage involves a complex network of signaling pathways that lead to cell cycle arrest or cell death [30]. One of these events is the phosphorylation of the histone H2AX to form γH2AX [31]. In eukaryotes, DNA is packed into nucleosomes whose core is an octameric particle consisting of two histones of the classes H2A, H2B, H3, and H4. H2AX is a secondary component of the histone H2A. H2AX phosphorylation is a marker of a DNA double-strand break. Within minutes of DSB formation, several thousand H2AX near the DSB site are phosphorylated at serine 139 to form foci in the nucleus that are microscopically visible by immunofluorescence staining [32]. The results of other researchers have shown that γH2AX foci formation can be used as a pharmacodynamic marker of DNA inter-strand cross-link formation for both nitrogen mustard and platinum-based drugs [33,34]. Our in vitro studies showed that the response to DNA damage in the form of γH2AX foci formation after treatment with the tested compounds was time-dependent for all three cell lines (RPMI8226, H60, and THP1) investigated.

The statistically significant highest ability to phosphorylate histone H2AX was demonstrated by EM-T-MEL, which showed considerably better effects than the original MEL after 24 h and 48 h for THP1; after 4 h, 24 h, and 48 h for HL60; and after 24 h for RPMI8226 cells. These results were consistent with our previous assessment of the levels of DNA damage from these derivatives in the comet test [14,15]. Studies by other groups [35] have confirmed that melphalan is responsible for an increase in γH2AX levels and the induction of phosphorylation of checkpoint kinase 1 (CHK-1) and checkpoint kinase 2 (CHK-2) in MM cells (RPMI8226 and MM1.S).

The antiproliferative properties of antitumor compounds result from their ability to inhibit the division cycle of neoplastic cells. As a result of the genotoxic effects of MEL and the new analogs, the DNA damage response pathway was activated. There was an accumulation of cells in the S- and G2/M phases at the expense of the G1 phase. Studies by other scientists [35,36] have indicated that after treatment with alkylating drugs, including MEL, the most affected phase in terms of cell progression (cytostatic effect) was G2/M [36,37]. Changes in the cell cycle distribution for the tested cell lines depended on the time and sensitivity to the test compound. Treatment with EM-T-MEL significantly affected the distribution of the cell cycle, leading to an accumulation of RPMI8226 and HL60 in the G2/M phase and THP1 additionally in the S-phase at four hours after treatment. Dysfunction of the S-phase checkpoint is one of the main causes of mitotic catastrophe [38]. For the other analogs, the shifted distribution of the cell cycle occurred later: between 24–48 h for EE-MEL, EM-MEL, and MOR-MEL, and after 48 h for EM-I-MEL. Overall, compared to EM-T-MEL, the original drug caused much less enrichment of cells in the G2/M phase.

Our previous studies [14,15] have shown that MEL derivatives exhibited strong pro-apoptotic properties, mainly in leukemic cells (THP-1 and HL-60). The assessment was based on numerous analyses of cell morphological and biochemical changes. THP1 and HL60 cells were particularly sensitive to caspase 3 activation via the mitochondrial apoptosis activation pathway, as opposed to multiple myeloma cells (RPMI8226). It was also shown previously that cells of the RPMI8226 line showed the characteristics of late stages

of apoptosis. However, they were least sensitive to caspase 3 activation. No increases in the activation levels of caspase 8 or 9 were observed. This may have indicated the initiation of other molecular mechanisms leading to cell death. All of the tested derivatives induced an accumulation of RPMI8226 cells in the G2/M phase. Cell cycle arrest in this phase is related to the mitotic catastrophe process [38,39] due to defects in the mitotic apparatus, DNA damage, and mitotic checkpoint errors that make complete mitosis impossible. This process is not a typical form of programmed cell death. Other scientists have contributed to the development of mitotic catastrophe by looking at various types of cell death (apoptosis, autophagy, and necrosis), as well as the effect of therapeutic agents acting directly on the DNA [38,40]. The initiation of mitotic catastrophe leads to morphological and biochemical changes in the cells [41]. Cells unable to complete mitosis are characterized by an abnormal increase in cyclin B1 levels [42,43], and are delayed in the G2/M transition, leading to nuclear changes. Multiple nuclei, macronuclei, and micronuclei are formed as a result of chromosome scattering, chromosome breaks, and the disruption of karyokinesis in the metaphase. Reconfiguration of the mitochondrial network can also be considered a morphological feature of mitotic catastrophe [38]. In addition to morphological changes in cell nuclei and mitochondria, the state of mitotic catastrophe is also characterized by an accumulation of H2AX, a biochemical marker of DNA damage [38,44]. Cells undergoing mitotic catastrophe do not show DNA fragmentation that is typical of apoptosis or DNA breaks detected by terminal deoxynucleotidyl transferase biotin-dUTP nick end labeling (TUNEL). Our previous studies [14] for DNA damage analysis (using the TUNEL method) showed a poor response after incubation with all tested compounds, as well as a lack of DNA fragmentation into segments equal to multiples of nucleosome length [42] typical for "classic" apoptosis [45]. This encouraged us to continue the investigations on the mitotic catastrophe process.

One of the most important regulators of mitotic catastrophe is caspase 2 [38,46,47]. The outcome/ending of mitotic catastrophe may be related to the molecular profile of the cell [48]. Thus, to activate this caspase, PIDDosome is formed, which consists of three proteins: the p53-induced death domain protein (PIDD), the RIP-associated Ich-1/Ced-3 homologous protein with a death domain (RAIDD), and caspase 2 [49]. On the other hand, caspase 2 participates in cell cycle regulation by stabilizing p53 and cleaving its inhibitor Mdm2, which are essential for the cellular response during abnormal chromosome segregation and the development of mitotic catastrophe [38]. Melphalan has been shown to activate mitotic catastrophe in RPMI8226 cells [37]. Our study on caspase 2 activation in multiple myeloma cells and leukemic cells showed a significant increase in caspase activity, mainly after 24 h incubation. The RPMI8226 cell line turned out to be the most sensitive. The greatest changes were observed after incubation with EM-T-MEL.

Mitotic catastrophe is characterized by nuclear changes that lead to multinucleation and/or micronucleation [38,42]. Under conditions of mitotic catastrophe, changes occur in the cell nucleus, in which the mitochondria are also involved. Changes in the mitochondrial network have been shown to accelerate the development of mitotic catastrophe [38,41,48]. The induction of mitotic catastrophe by doxorubicin leads to the remodeling of mitochondrial structure and the fragmentation of mitochondria in colon cancer cells. Moreover, in breast cancer cells, mitochondrial fission promotes radiation-induced mitotic catastrophe and increases Ca^{2+} levels in the cytosol [38].

In the present study, we focused on another important regulator of mitotic catastrophe, caspase 2, which is involved in maintaining genome stability. Polyploid and aneuploid cells are prone to mitotic catastrophe. As part of the PIDDosome complex, caspase 2 participates in the elimination of extra centrosomes and regulates ploidy and cell proliferation. In addition, caspase 2 activates the PCD process in cells with abnormal numbers of chromosomes and centrosomes, which also prevents the development of mitotic catastrophe [38]. Caspase 2 deficiency results in the predisposition of cancer cells to aneuploidy, due to B-cell CLL/lymphoma 9-like (BCL9L) protein dysfunction [38,50]. Our results showed high caspase 2 activity after treatment with new highly genotoxic analogs, mainly in multiple

myeloma cells, which indicated high genomic instability. Based on the data, we concluded that high caspase 2 activity may be associated with the removal of cells with mitotic aberrations to reduce aneuploidy, so we did not expect a large number of cells with a mitotic catastrophe phenotype. The reconfiguration of the mitochondrial network can also be considered a morphological feature of mitotic catastrophe [38]. Our previous data [14,15] showed that mitochondrial membrane potential decreased after treatment with melphalan analogs in cancer cell lines. We also observed subtle increases in the activation of the exocrine caspase 3. Based on the current and previous studies, we can suspect that one of the pathways of multiple myeloma cell death may be mitotic catastrophe [41,42,48].

4. Materials and Methods

4.1. Materials

4.1.1. Melphalan Derivatives

This study used MEL (2S)-2-amino-3-[4-[bis(2-chloroethyl)amino]phenyl]propanoic acid and its five analogs: EE-MEL (2S)-2-amino-3-[-4-[bis(2-chloroethyl)amino]phenyl] propanoic acid ethyl ester; EM-MEL (2S)-2-amino-3-[-4-[bis (2-chloroethyl)amino]phenyl] propanoic acid ethyl ester; EM-MOR-MEL (2S)-2-(morpholinmethylideneamino)-3-[4-[bis(2-chloroethyl)amino]phenyl] propanoic acid methyl ester; EM-I-MEL (2S)-2-(indoli nmethylideneamino)-3-[4-[bis(2-chloroethyl)amino]phenyl]propanoic acid methyl ester; and EM-T-MEL (2S)-2-(thiomorpholinmethylideneamino)-3-[4-[bis(2-chloroethyl)amino] phenyl] propanoic acid methyl ester (Figure 6). Their synthesis has been reviewed in our previous publications [14,15].

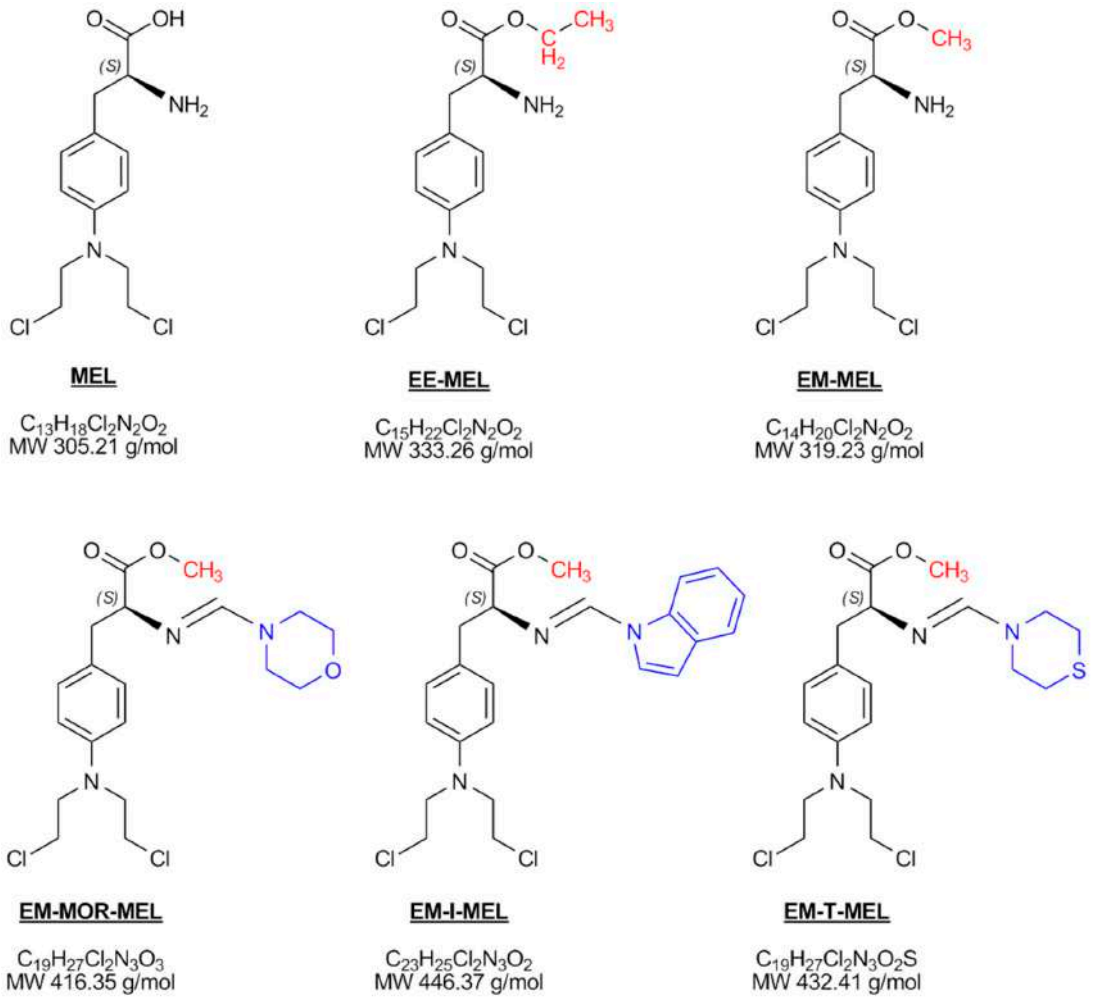

Figure 6. Chemical structure of melphalan (MEL) and its tested derivatives.

4.1.2. Cell Culture, Drug Concentration, and Treatment Time

The acute monocytic leukemia cell line THP1 (ATCC® TIB–202™), promyelocytic leukemia cell line HL60 (ATCC® CCL–240™), and the multiple myeloma cell line RPMI8226 (ATCC® CCL–155™) were obtained from the American Type Culture Collection (ATCC, Rockville, MD, USA). All the investigated cells were cultured in RPMI 1640 medium supplemented with 10% fetal bovine serum, penicillin (10 U/mL), and streptomycin (50 µg/mL) in standard conditions: 37 °C, 100% humidity, and an atmosphere of 5% CO_2 and 95% air. Cell viability was systematically controlled using 0.4% trypan blue. In all experiments, cells in a logarithmic growth phase were used when their viability was above 95%.

One concentration of the drugs for each cell line was chosen for the study: THP1: 0.3 µM; HL60: 0.7 µM; RPMI8226: 3 µM. These were the same as in previous studies evaluating the biological properties of melphalan analogs [14,15]. In all experiments, cells were treated for 4 h, 24 h, and 48 h. Simultaneously, control cultures were incubated similarly without further treatment. For the immunostaining assay, a positive control from irradiated cells was prepared. The cells were irradiated with 1 Gy of ionizing radiation by an ISOVOLT Titan X-ray generator (GE, Ahrensburg, Germany) [51,52].

4.2. Methods

4.2.1. Circular Dichroism as a Technique for the Analysis of the Alteration of DNA Conformation

The circular dichroism spectra of deoxyribonucleic acid from the calf thymus were measured using a J-815CD spectrometer (Jasco, Japan). Complexes of DNA/MEL or MEL derivatives were prepared in a 10 mM Na-phosphate buffer, with a pH of 7.4. The concentration of DNA in the samples was 250 µg/mL. However, the concentrations of compounds in the samples were 5 µM, 25 µM, 50 µM, 75 µM, 100 µM, 150 µM, 200 µM, 250 µM, and 300 µM. The measurements were made in a Helma quartz cell with a thickness of 0.5 cm. The scan parameters were as follows: wavelengths of 230–320 nm; scan speed of 100 nm/min, and bandwidth of 1.0 nm. The slit was set on the auto mode, and n = 3. The mean ellipticity was calculated using software provided by Jasco.

4.2.2. Zeta Potential Measurement and DLS for Measuring the Hydrodynamic Diameters of the Particles

Zeta potential was measured using laser Doppler velocimetry by Zetasizer Nano ZS-90 (Malvern Instruments, United Kingdom) and calculated using the Smoluchowski equation. Complexes of DNA/MEL or MEL derivatives were prepared in a 10 mM Na-phosphate buffer, with a pH of 7.4. The concentration of DNA in the samples was 30 µg/mL. The concentrations of compounds in the samples were 2.5 µM, 5 µM, 10 µM, 25 µM, 50 µM, and 100 µM. Measurements were made with or without DNA. Data analysis was performed using Malvern software and given as the mean ± standard deviation (SD) obtained from five measurements in seven cycles at room temperature (RT) for each sample.

Hydrodynamic diameters of the complexes were measured by the DLS method in a photon correlation spectrometer (Zetasizer Nano ZS-90, Malvern Instruments, Malvern, UK). The wavelength was set at 633 nm, the refraction factor was 1.33, and the detection angle was 900. Complexes of DNA/MEL or MEL derivatives were prepared in a 10 mM Na-phosphate buffer, with a pH of 7.4. Measurements were made with or without DNA. The data analysis was performed using Malvern software and is given as the mean ± SD obtained from five measurements in five cycles at RT for each sample.

4.2.3. Immunofluorescence Staining of γH2AX for DNA Damage Detection

The essence of the test was the detection and localization of γH2AX histone foci, based on the highly specific antigen–antibody binding reaction. Based on previous publications, a protocol for fixing [53,54] and staining [55,56] non-adherent cells was prepared.

Cells were treated in Petri dishes with all tested compounds, as described above. Additionally, a positive control was prepared in which the cells irradiated with 1 Gy.

Cells were washed with PBS (300 rpm, 5 min, RT), spotted on the surface of defatted glass slides, and incubated for 10 min to adhere cells to the coverslips. Adherent cells were fixed in 4% formaldehyde solution with 0.1% Triton X-100. Permeabilized cells were washed with Tris-buffered saline (TBS) and blocked with 1% BSA in PBS overnight. After incubation and washing with TBS, staining was performed. Cells were incubated with a phosphorylated (Ser139) mouse monoclonal IgG-specific anti-H2AX antibody at a dilution of 1:2500 (BioLegend, San Diego, United States) suspended in TBS buffer supplemented with 1% BSA. Incubation was for 1 h in the dark in a humid chamber at 24 °C. Then, a washing step with TBS was performed. The cells were then incubated with Alexa Fluor TM 488 goat anti-mouse IgG secondary antibody at a dilution of 1:400 (Thermo Fisher Scientific, Waltham, MA, USA) suspended in TBS buffer supplemented with 1% BSA. Incubation was for 3 h in the dark in a humid chamber at 24 °C. The cell nuclei were then stained with 4′,6-diamidino-2-phenylindole (DAPI) solution (0.1 ng/mL). Microscopic analysis (Zeiss Axio Plan 2, Göttingen, Germany) was started, and digital recordings were taken using the MetaSystem software (Altlussheim, Germany). The photos were analyzed with ImageJ (LOCI, University of Wisconsin). The number of foci in each cell was counted; 100 cells were counted from each image.

4.2.4. Flow Cytometry for Cell Cycle Analysis

Flow cytometry was used to quantify the cellular DNA content. Cells were treated as described above. After incubation, cells were harvested, washed with PBS, and fixed in 70% ethanol (minimum 24 h; 4 °C). Following ethanol fixation, the cells were washed in PBS and centrifuged at 7000× *g* for 10 min at 4 °C. Harvested cells were stained by adding 300 µL of PBS containing PI and RNase at final concentrations of 75 µM and 20 µg/mL, respectively. The samples were incubated for 1 h in complete darkness at 37 °C. The stained cells were analyzed using flow cytometry (Becton Dickinson, San Jose, CA, USA), and the percentage of cells in each cell phase was calculated [57].

4.2.5. Activity of Caspase 2

The test was based on detecting the cleavage of substrate VDVAD (Val-Asp-Val-Ala-Asp)-AFC (7-amino-4-trifluoromethycoumarin). VDVAD-AFC emits blue light (λ = 400 nm). However, after substrate cleavage by caspase 2, free AFC emits yellow-green fluorescence (λ = 505 nm), which can be quantified with a fluorometer plate reader. The activities of caspase 2 were estimated with a caspase 2 assay kit (Fluorometric) according to the manufacturer's protocols (Abcam, Cambridge, UK).

Cells were treated on Petri dishes with tested compounds as described above. Next, cells were counted and placed in 96-well black fluorometric plates (1×10^6/well). Cells were resuspended in 50 µL of chilled cell lysis buffer and incubated on ice for 10 min. Reaction buffer (50 µL) containing 10 mmol of DTT and 5 µL of the 1 mM VDVAD-AFC substrate was added to each well and incubated for 2 h at 37 °C. The measurement was done on a Fluoroscan Ascent FL plate reader (Labsystem, Stockholm, Sweden) using a 400 nm excitation filter and a 505 nm emission filter. Caspase 2 activity was expressed as a ratio of fluorescence of the treated sample relative to the corresponding untreated control, which was taken as 100%.

4.2.6. Statistical Analysis

Data are presented as the mean ± standard deviation (SD) unless indicated otherwise.

For analyzing changes from the baseline (control cell culture without treatment or the original drug MEL), the analysis of variance (ANOVA) with Tukey's post hoc test was used. The data from two independent biological assays (100 cells counted in each case, n = 200) were merged for the immunostaining analysis. Foci-positive cells were labeled as cells with more than five foci according to or based on a previous study [32]. The statistical analyses were performed using STATISTICA (StatSoft, Tulsa, OK, USA). The level of significance for all analyses was set at $\alpha = 0.05$ (two-tailed). All figures include descriptions of statistically

significant changes: * $p < 0.05$ signifies a statistically significant difference compared to control cells, and # $p < 0.05$ signifies a statistically significant difference compared to MEL.

5. Conclusions

In this study, we proved that tumor cell DNA is the main molecular target for the chemically modified analogs of the widely used anti-cancer drug melphalan.

The newly synthesized derivatives, in particular EM-MOR-MEL and EM-T-MEL, affected the B-DNA conformation, which increased the DNA damage detected by γH2AX analysis. As a result of the DNA changes, the cell cycle was arrested in the S and G2/M phases. The cell death occurred by activating a mitotic catastrophe as a special example of apoptosis. Our investigations suggest that the analogs EM-MOR-MEL and EM-T-MEL have better anti-cancer activity in multiple myeloma cells than the currently used melphalan, at least in the in vitro models applied.

Author Contributions: Conceptualization, A.P., A.M. and D.L.; methodology, A.P., M.I., U.S.G., A.M. and D.L.; investigation, A.P.; data curation, A.P. and D.L.; writing—original draft preparation, A.P. and D.L.; writing—review and editing, A.P., P.K., M.I., A.R., U.S.G., A.M. and D.L.; visualization, A.P. and P.K.; supervision, A.M. and D.L. All authors have read and agreed to the published version of the manuscript.

Funding: A research internship enabling scientific cooperation between the University of Lodz and University Hospital Erlangen, Friedrich-Alexander-Universität Erlangen-Nürnberg, was co-financed by the European Union from the European Social Fund under the "InterDOC-STARt" project (POWR.03.02.00-00-I033/16-00).

Institutional Review Board Statement: Not applicable.

Informed Consent Statement: Not applicable.

Data Availability Statement: The datasets presented during in the current study are available from the corresponding author upon reasonable request.

Acknowledgments: The authors acknowledge: Benjamin Frey and Tina Jost of Translational Radiobiology, Department of Radiation Oncology, University Hospital Erlangen Friedrich-Alexander-Universität Erlangen-Nürnberg for valuable laboratory support and Luis E. Muñoz of the Department of Internal Medicine 3-Rheumatology and Immunology, University Hospital Erlangen Friedrich-Alexander-Universität Erlangen-Nürnberg for giving THP1 cells. We thank Bartosz Trzaskowski PhD, D.Sc. of Centre of New Technologies (CeNT), University of Warsaw for preparing the DNA—drug visualizations.

Conflicts of Interest: The authors declare no conflict of interest.

References

1. Joshua, D.E.; Bryant, C.; Dix, C.; Gibson, J.; Ho, J. Biology and therapy of multiple myeloma. *Med. J. Aust.* **2019**, *210*, 375–380. [CrossRef] [PubMed]
2. Castaneda, O.; Baz, R. Multiple Myeloma Genomics—A Concise Review. *Acta Med. Acad.* **2019**, *48*, 57–67. [CrossRef] [PubMed]
3. Rajkumar, S.V. Multiple myeloma: Every year a new standard? *Hematol. Oncol.* **2019**, *37*, 62–65. [CrossRef] [PubMed]
4. Poczta, A.; Rogalska, A.; Marczak, A. Treatment of Multiple Myeloma and the Role of Melphalan in the Era of Modern Therapies—Current Research and Clinical Approaches. *J. Clin. Med.* **2021**, *10*, 1841. [CrossRef]
5. Aksenova, A.Y.; Zhuk, A.S.; Lada, A.G.; Zotova, I.V.; Stepchenkova, E.I.; Kostroma, I.I.; Gritsaev, S.V.; Pavlov, Y.I. Genome Instability in Multiple Myeloma: Facts and Factors. *Cancers* **2021**, *13*, 5949. [CrossRef]
6. Sureda, A.; Bader, P.; Cesaro, S.; Dreger, P.; Duarte, R.F.; Dufour, C.; Falkenburg, J.H.F.; Farge-Bancel, D.; Gennery, A.; Kröger, N.; et al. Indications for allo- and auto-SCT for haematological diseases, solid tumours and immune disorders: Current practice in Europe, 2015. *Bone Marrow Transplant.* **2015**, *50*, 1037–1056. [CrossRef]
7. Dima, D.; Jiang, D.; Singh, D.J.; Hasipek, M.; Shah, H.S.; Ullah, F.; Khouri, J.; Maciejewski, J.P.; Jha, B.K. Multiple Myeloma Therapy: Emerging Trends and Challenges. *Cancers* **2022**, *14*, 4082. [CrossRef]
8. Singh, R.K.; Kumar, S.; Prasad, D.N.; Bhardwaj, T.R. Therapeutic journery of nitrogen mustard as alkylating anticancer agents: Historic to future perspectives. *Eur. J. Med. Chem.* **2018**, *151*, 401–433. [CrossRef]
9. van Kan, M.; Burns, K.E.; Helsby, N.A. A systematic review of inter-individual differences in the DNA repair processes involved in melphalan monoadduct repair in relation to treatment outcomes. *Cancer Chemother. Pharmacol.* **2021**, *88*, 755–769. [CrossRef]

10. Mohamed, D.; Linscheid, M. Separation and identification of trinucleotide–melphalan adducts from enzymatically digested DNA using HPLC–ESI–MS. *Anal. Bioanal. Chem.* **2008**, *392*, 805–817. [CrossRef]
11. Loeber, R.L.; Michaelson-Richie, E.D.; Codreanu, S.G.; Liebler, D.C.; Campbell, C.R.; Tretyakova, N.Y. Proteomic Analysis of DNA−Protein Cross-Linking by Antitumor Nitrogen Mustards. *Chem. Res. Toxicol.* **2009**, *22*, 1151–1162. [CrossRef] [PubMed]
12. Qu, B.; Xu, Y.; Lu, Y.; Zhuang, W.; Jin, X.; Shi, Q.; Yan, S.; Guo, Y.; Shen, Z.; Che, J.; et al. Design, synthesis and biological evaluation of sulfonamides inhibitors of XPO1 displaying activity against multiple myeloma cells. *Eur. J. Med. Chem.* **2022**, *235*, 114257. [CrossRef] [PubMed]
13. Mao, F.; Ni, W.; Xu, X.; Wang, H.; Wang, J.; Ji, M.; Li, J. Chemical Structure-Related Drug-Like Criteria of Global Approved Drugs. *Molecules* **2016**, *21*, 75. [CrossRef] [PubMed]
14. Gajek, A.; Poczta, A.; Łukawska, M.; Cecuda-Adamczewska, V.; Tobiasz, J.; Marczak, A. Chemical modification of melphalan as a key to improving treatment of haematological malignancies. *Sci. Rep.* **2020**, *10*, 4479. [CrossRef] [PubMed]
15. Poczta, A.; Krzeczyński, P.; Tobiasz, J.; Rogalska, A.; Gajek, A.; Marczak, A. Synthesis and In Vitro Activity of Novel Melphalan Analogs in Hematological Malignancy Cells. *Int. J. Mol. Sci.* **2022**, *23*, 1760. [CrossRef]
16. Vorlíčková, M.; Kejnovská, I.; Bednářová, K.; Renčiuk, D.; Kypr, J. Circular Dichroism Spectroscopy of DNA: From Duplexes to Quadruplexes. *Chirality* **2012**, *24*, 691–698. [CrossRef]
17. Vanloon, J.; Harroun, T.; Yan, H. Circular dichroism spectroscopy of DNA duplexes at near-biological concentrations. *Bioorg. Med. Chem. Lett.* **2021**, *43*, 128053. [CrossRef]
18. Agarwal, S.; Chadha, D.; Mehrotra, R. Molecular modeling and spectroscopic studies of semustine binding with DNA and its comparison with lomustine–DNA adduct formation. *J. Biomol. Struct. Dyn.* **2015**, *33*, 1653–1668. [CrossRef]
19. Agarwal, S.; Jangir, D.K.; Mehrotra, R. Spectroscopic studies of the effects of anticancer drug mitoxantrone interaction with calf-thymus DNA. *J. Photochem. Photobiol. B* **2013**, *120*, 177–182. [CrossRef]
20. Efthimiadou, E.K.; Sanakis, Y.; Katsarou, M.; Raptopoulou, C.P.; Karaliota, A.; Katsaros, N.; Psomas, G. Neutral and cationic mononuclear copper(II) complexes with enrofloxacin: Structure and biological activity. *J. Inorg. Biochem.* **2006**, *100*, 1378–1388. [CrossRef]
21. Subastri, A.; Durga, A.; Harikrishna, K.; Sureshkumar, M.; Jeevaratnam, K.; Girish, K.; Thirunavukkarasu, C. Exploration of disulfiram dealings with calf thymus DNA using spectroscopic, electrochemical and molecular docking techniques. *J. Lumin* **2016**, *170*, 255–261. [CrossRef]
22. Kellett, A.; Molphy, Z.; Slator, C.; McKee, V.; Farrell, N.P. Molecular methods for assessment of non-covalent metallodrug–DNA interactions. *Chem. Soc. Rev.* **2019**, *48*, 971–988. [CrossRef] [PubMed]
23. Molphy, Z.; Montagner, D.; Bhat, S.S.; Slator, C.; Long, C.; Erxleben, A.; Kellett, A. A phosphate-targeted dinuclear Cu(II) complex combining major groove binding and oxidative DNA cleavage. *Nucleic Acids Res.* **2018**, *46*, 9918–9931. [CrossRef] [PubMed]
24. Pawar, S.K.; Jaldappagari, S. Intercalation of a flavonoid, silibinin into DNA base pairs: Experimental and theoretical approach. *J. Mol. Recognit.* **2019**, *33*, e2812. [CrossRef]
25. Meenongwa, A.; Brissos, R.F.; Soikum, C.; Chaveerach, P.; Gamez, P.; Trongpanich, Y.; Chaveerach, U. DNA-interacting and biological properties of copper(ii) complexes from amidino-O-methylurea. *New J. Chem.* **2014**, *39*, 664–675. [CrossRef]
26. Shahabadi, N.; Moghadam, N.H. Determining the mode of interaction of calf thymus DNA with the drug sumatriptan using voltammetric and spectroscopic techniques. *Spectrochim. Acta A Mol. Biomol. Spectrosc.* **2012**, *99*, 18–22. [CrossRef]
27. Inamdar, P.R.; Sheela, A. Spectroscopic investigations on partial intercalative binding behaviour of terpyridine based copper(II) complexes with DNA. *J. Photochem. Photobiol. B* **2016**, *159*, 133–141. [CrossRef]
28. Reddy, B.; Sondhi, S.; Lown, J. Synthetic DNA minor groove-binding drugs. *Pharmacol. Ther.* **1999**, *84*, 1–111. [CrossRef]
29. Bielawska, A.; Bielawski, K.; Anchim, T. Amidine Analogues of Melphalan: Synthesis, Cytotoxic Activity, and DNA Binding Properties. *Arch. Pharm.* **2007**, *340*, 251–257. [CrossRef]
30. Petsalaki, E.; Zachos, G. DNA damage response proteins regulating mitotic cell division: Double agents preserving genome stability. *FEBS J.* **2020**, *287*, 1700–1721. [CrossRef]
31. Fragkos, M.; Jurvansuu, J.; Beard, P. H2AX Is Required for Cell Cycle Arrest via the p53/p21 Pathway. *Mol. Cell. Biol.* **2009**, *29*, 2828–2840. [CrossRef]
32. Ishihama, M.; Toyooka, T.; Ibuki, Y. Generation of phosphorylated histone H2AX by benzene metabolites. *Toxicol. Vitr.* **2008**, *22*, 1861–1868. [CrossRef]
33. Clingen, P.; Wu, J.-H.; Miller, J.; Mistry, N.; Chin, F.; Wynne, P.; Prise, K.; Hartley, J. Histone H2AX phosphorylation as a molecular pharmacological marker for DNA interstrand crosslink cancer chemotherapy. *Biochem. Pharmacol.* **2008**, *76*, 19–27. [CrossRef] [PubMed]
34. Spanswick, V.J.; Lowe, H.L.; Newton, C.; Bingham, J.P.; Bagnobianchi, A.; Kiakos, K.; Craddock, C.; Ledermann, A.J.; Hochhauser, D.; Hartley, A.J. Evidence for different mechanisms of 'unhooking' for melphalan and cisplatin-induced DNA interstrand cross-links in vitroand in clinical acquired resistant tumour samples. *BMC Cancer* **2012**, *12*, 436. [CrossRef] [PubMed]
35. Lee, C.-K.; Wang, S.; Huang, X.; Ryder, J.; Liu, B. HDAC inhibition synergistically enhances alkylator-induced DNA damage responses and apoptosis in multiple myeloma cells. *Cancer Lett.* **2010**, *296*, 233–240. [CrossRef]
36. Lupi, M.; Cappella, P.; Matera, G.; Natoli, C.; Ubezio, P. Interpreting cell cycle effects of drugs: The case of melphalan. *Cancer Chemother. Pharmacol.* **2006**, *57*, 443–457. [CrossRef] [PubMed]

37. Cives, M.; Ciavarella, S.; Rizzo, F.M.; De Matteo, M.; Dammacco, F.; Silvestris, F. Bendamustine overcomes resistance to melphalan in myeloma cell lines by inducing cell death through mitotic catastrophe. *Cell Signal.* **2013**, *25*, 1108–1117. [CrossRef]
38. Sazonova, E.V.; Petrichuk, S.V.; Kopeina, G.S.; Zhivotovsky, B. A link between mitotic defects and mitotic catastrophe: Detection and cell fate. *Biol. Direct* **2021**, *16*, 25. [CrossRef]
39. Čáňová, K.; Rozkydalová, L.; Vokurková, D.; Rudolf, E. Flubendazole induces mitotic catastrophe and apoptosis in melanoma cells. *Toxicol. Vitr.* **2018**, *46*, 313–322. [CrossRef]
40. Denisenko, T.V.; Sorokina, I.V.; Gogvadze, V.; Zhivotovsky, B. Mitotic catastrophe and cancer drug resistance: A link that must to be broken. *Drug Resist. Update* **2015**, *24*, 1–12. [CrossRef]
41. Castedo, M.; Perfettini, J.-L.; Roumier, T.; Andreau, K.; Medema, R.; Kroemer, G. Cell death by mitotic catastrophe: A molecular definition. *Oncogene* **2004**, *23*, 2825–2837. [CrossRef] [PubMed]
42. Mc Gee, M.M. Targeting the Mitotic Catastrophe Signaling Pathway in Cancer. *Mediat. Inflamm.* **2015**, *2015*, 146282. [CrossRef] [PubMed]
43. Verhees, F.; Legemaate, D.; Demers, I.; Jacobs, R.; Haakma, W.E.; Rousch, M.; Kremer, B.; Speel, E.J. The Antiviral Agent Cidofovir Induces DNA Damage and Mitotic Catastrophe in HPV-Positive and -Negative Head and Neck Squamous Cell Carcinomas In Vitro. *Cancers* **2019**, *11*, 919. [CrossRef]
44. Imreh, G.; Norberg, H.V.; Imreh, S.; Zhivotovsky, B. Chromosomal breaks during mitotic catastrophe trigger γH2AX–ATM–p53-mediated apoptosis. *J. Cell Sci.* **2016**, *129*, 1950. [CrossRef]
45. Roninson, I.B.; Broude, E.V.; Chang, B.-D. If not apoptosis, then what? Treatment-induced senescence and mitotic catastrophe in tumor cells. *Drug Resist. Update* **2001**, *4*, 303–313. [CrossRef] [PubMed]
46. Vitale, I.; Manic, G.; Castedo, M.; Kroemer, G. Caspase 2 in mitotic catastrophe: The terminator of aneuploid and tetraploid cells. *Mol. Cell. Oncol.* **2017**, *4*, e1299274. [CrossRef]
47. Haschka, M.; Karbon, G.; Fava, L.; Villunger, A. Perturbing mitosis for anti-cancer therapy: Is cell death the only answer? *EMBO Rep.* **2018**, *19*, e45440. [CrossRef]
48. Vakifahmetoglu, H.; Olsson, M.; Zhivotovsky, B. Death through a tragedy: Mitotic catastrophe. *Cell Death Differ.* **2008**, *15*, 1153–1162. [CrossRef]
49. Jang, T.-H.; Park, H.H. PIDD mediates and stabilizes the interaction between RAIDD and Caspase-2 for the PIDDosome assembly. *BMB Rep.* **2013**, *46*, 471–476. [CrossRef]
50. Dawar, S.; Lim, Y.; Puccini, J.; White, M.; Thomas, P.; Bouchier-Hayes, L.; Green, D.R.; Dorstyn, L.; Kumar, S. Caspase-2-mediated cell death is required for deleting aneuploid cells. *Oncogene* **2016**, *36*, 2704–2714. [CrossRef]
51. Scheper, J.; Hildebrand, L.S.; Faulhaber, E.-M.; Deloch, L.; Gaipl, U.S.; Symank, J.; Fietkau, R.; Distel, L.V.; Hecht, M.; Jost, T. Tumor-specific radiosensitizing effect of the ATM inhibitor AZD0156 in melanoma cells with low toxicity to healthy fibroblasts. *Strahlenther. Onkol.* **2022**, *in press*. [CrossRef] [PubMed]
52. Zhang, X.; Bobeica, M.; Unger, M.; Bednarz, A.; Gerold, B.; Patties, I.; Melzer, A.; Landgraf, L. Focused ultrasound radiosensitizes human cancer cells by enhancement of DNA damage. *Strahlenther. Onkol.* **2021**, *197*, 730–743. [CrossRef]
53. Tsang, M.; Gantchev, J.; Ghazawi, F.M.; Litvinov, I.V. Protocol for adhesion and immunostaining of lymphocytes and other non-adherent cells in culture. *BioTechniques* **2017**, *63*, 230–233. [CrossRef] [PubMed]
54. Nakayama, T.; Mihara, K.; Kawata, J.; Kimura, H.; Saitoh, H. Adhesion of suspension cells on a coverslip in serum-free conditions. *Anal. Biochem.* **2014**, *466*, 1–3. [CrossRef] [PubMed]
55. Bürkel, F.; Jost, T.; Hecht, M.; Heinzerling, L.; Fietkau, R.; Distel, L. Dual mTOR/DNA-PK Inhibitor CC-115 Induces Cell Death in Melanoma Cells and Has Radiosensitizing Potential. *Int. J. Mol. Sci.* **2020**, *21*, 9321. [CrossRef]
56. Dobler, C.; Jost, T.; Hecht, M.; Fietkau, R.; Distel, L. Senescence Induction by Combined Ionizing Radiation and DNA Damage Response Inhibitors in Head and Neck Squamous Cell Carcinoma Cells. *Cells* **2020**, *9*, 2012. [CrossRef]
57. Poczta, A.; Rogalska, A.; Łukawska, M.; Marczak, A. Antileukemic activity of novel adenosine derivatives. *Sci. Rep.* **2019**, *9*, 14135. [CrossRef]

Oświadczenia współautorów publikacji

WYDZIAŁ BIOLOGII
i OCHRONY ŚRODOWISKA
Uniwersytet Łódzki

Łódź, 15.12.2022

mgr Anastazja Poczta
Katedra Biofizyki Medycznej
Wydział Biologii i Ochrony Środowiska
Uniwersytet Łódzki
ul. Pomorska141/143
90-236 Łódź

OŚWIADCZENIE

Oświadczam, że jestem współautorem artykułu przeglądowego opublikowanego w czasopiśmie *Journal of Clinical Medicine* pt. *Treatment of Multiple Myeloma and the Role of Melphalan in the Era of Modern Therapies-Current Research and Clinical Approaches* (IF: 4.964; punkty MEiN: 140 pkt.), autorstwa Anastazji Poczta, Anety Rogalskiej oraz Agnieszki Marczak.

Mój wkład w powstanie niniejszego artykułu polegał na współudziale w tworzeniu koncepcji pracy, zebraniu literatury na dany temat badawczy, napisaniu poszczególnych rozdziałów artykułu, wykonaniu ilustracji, przygotowaniu wstępnego kształtu manuskryptu, jego edycji oraz przygotowywaniu odpowiedzi na recenzje. Pełniłam również funkcję autora korespondencyjnego.

Mój wkład w powstanie tej pracy oceniam na 80%.

Anastazja Poczta
mgr Anastazja Poczta

WYDZIAŁ BIOLOGII
i OCHRONY ŚRODOWISKA
Uniwersytet Łódzki

Łódź, 15.12.2022

dr hab. Aneta Rogalska, prof. UŁ
Katedra Biofizyki Medycznej
Wydział Biologii i Ochrony Środowiska
Uniwersytet Łódzki
ul. Pomorska141/143
90-236 Łódź

OŚWIADCZENIE

Oświadczam, że jestem współautorem artykułu przeglądowego opublikowanego w czasopiśmie *Journal of Clinical Medicine* pt. *Treatment of Multiple Myeloma and the Role of Melphalan in the Era of Modern Therapies-Current Research and Clinical Approaches* (IF: 4.964; punkty MEiN: 140 pkt.), autorstwa Anastazji Poczta, Anety Rogalskiej oraz Agnieszki Marczak.

Mój wkład w powstanie niniejszego artykułu polegał na współudziale w tworzeniu koncepcji pracy, w szczególności rozdziału dotyczącego komórek macierzystych i badań klinicznych oraz na udziale w przygotowywaniu odpowiedzi na recenzje.

Mój wkład w powstanie tej pracy oceniam na 10%.

Aneta Rogalska
.....
dr hab. Aneta Rogalska, prof. UŁ

WYDZIAŁ BIOLOGII
i OCHRONY ŚRODOWISKA
Uniwersytet Łódzki

Łódź, 15.12.2022

prof. dr hab. Agnieszka Marczak
Katedra Biofizyki Medycznej
Wydział Biologii i Ochrony Środowiska
Uniwersytet Łódzki
ul. Pomorska141/143
90-236 Łódź

OŚWIADCZENIE

Oświadczam, że jestem współautorem artykułu przeglądowego opublikowanego w czasopiśmie *Journal of Clinical Medicine* pt. *Treatment of Multiple Myeloma and the Role of Melphalan in the Era of Modern Therapies-Current Research and Clinical Approaches* (IF: 4.964; punkty MEiN: 140 pkt.), autorstwa Anastazji Poczta, Anety Rogalskiej oraz Agnieszki Marczak.

Mój wkład w powstanie niniejszego artykułu obejmował opiekę merytoryczną, współudział w tworzeniu koncepcji pracy oraz udział w przygotowywaniu odpowiedzi na recenzje.

Mój wkład w powstanie tej pracy oceniam na 10%.

A. Marczak

.....

prof. dr hab. Agnieszka Marczak

WYDZIAŁ BIOLOGII
i OCHRONY ŚRODOWISKA
Uniwersytet Łódzki

Łódź, 15.12.2022

dr Arkadiusz Gajek
Katedra Biofizyki Medycznej
Wydział Biologii i Ochrony Środowiska
Uniwersytet Łódzki
ul. Pomorska141/143
90-236 Łódź

OŚWIADCZENIE

Oświadczam, że jestem współautorem artykułu naukowego opublikowanego w czasopiśmie *Scientific Reports* pt. *Chemical modification of melphalan as a key to improving treatment of haematological malignancies* (IF: 4.964; punkty MEiN: 140 pkt.), autorstwa Arkadiusza Gajka, Anastazji Poczta, Małgorzaty Łukawskiej, Violetty Cecudy- Adamczewskiej, Joanny Tobiasz, Agnieszki Marczak.

Mój wkład w powstanie niniejszego artykułu polegał na współudziale w tworzeniu koncepcji pracy, współudziale w przeprowadzaniu eksperymentów takich jak: pomiary właściwości cytotoksycznych testem redukcji resazuryny, analiza fragmentacji DNA przy pomocy alkalicznej wersji testu kometowego oraz testu TUNEL (ang. TdT-mediated dUTP Nick-End Labeling assay), analiza zaburzeń strukturalnych błony komórkowej metodą podwójnego barwienia z wykorzystaniem mieszaniny fluorochromów: jodek propidyny i aneksyna V-FITC, analiza kondensacji chromatyny z wykorzystaniem mieszaniny fluorochromów: Vybrant® DyeCycle™ Violet oraz SYTOX® AADvanced™ oraz współudział w przygotowaniu manuskryptu i odpowiedzi na uwagi recenzentów.
Pełniłem również funkcję autora korespondencyjnego.

Mój wkład w powstanie tej pracy oceniam na 40% (Współautorstwo równocenne z Panią mgr Anastazją Pocztą – co zaznaczono na etapie publikacji artykułu).

Arkadiusz Gajek
.....
dr Arkadiusz Gajek

WYDZIAŁ BIOLOGII
i OCHRONY ŚRODOWISKA
Uniwersytet Łódzki

Łódź, 15.12.2022

mgr Anastazja Poczta
Katedra Biofizyki Medycznej
Wydział Biologii i Ochrony Środowiska
Uniwersytet Łódzki
ul. Pomorska141/143
90-236 Łódź

OŚWIADCZENIE

Oświadczam, że jestem współautorem artykułu naukowego opublikowanego w czasopiśmie *Scientific Reports* pt. *Chemical modification of melphalan as a key to improving treatment of haematological malignancies* (IF: 4.964; punkty MEiN: 140 pkt.), autorstwa Arkadiusza Gajka, Anastazji Poczta, Małgorzaty Łukawskiej, Violetty Cecudy- Adamczewskiej, Joanny Tobiasz, Agnieszki Marczak.

Mój wkład w powstanie niniejszego artykułu polegał na współudziale w przeprowadzaniu eksperymentów:

- ocena właściwości cytotoksycznych testem redukcji resazuryny,
- pomiary fragmentacji DNA przy pomocy alkalicznej wersji testu kometowego oraz testu TUNEL (ang. TdT-mediated dUTP Nick-End Labeling assay),
- analiza zaburzeń strukturalnych błony komórkowej metodą podwójnego barwienia z wykorzystaniem mieszaniny fluorochromów: jodek propidyny i aneksyna V-FITC,
- pomiary i analiza kondensacji chromatyny z wykorzystaniem mieszaniny fluorochromów: Vybrant® DyeCycle™ Violet oraz SYTOX® AADvanced™,
- pomiary i analiza aktywności kaspaz 3/7, 8,9 z zastosowaniem sond fluorescencyjnych,
- badanie wewnątrzkomórkowego poziomu jonów wapnia za pomocą sondy fluorescencyjnej Fluo-4NW
- oznaczenia związane z limfocytami.

Ponadto do moich obowiązków, podczas realizacji tej pracy należało:

- współudział w tworzeniu koncepcji pracy,
- zebranie odpowiedniej literatury,
- analiza statystyczna, opracowanie, opis wyników i dyskusja w oparciu o istniejące doniesienia literaturowe,
- przygotowanie wstępnego kształtu manuskryptu,
- przygotowywanie odpowiedzi na recenzje.

Mój wkład w powstanie pracy jest równocenny z wkładem Pana dr. Arkadiusza Gajka, co zaznaczono na etapie druku publikacji i wynosi 40%.

Anastazja Poczta
mgr Anastazja Poczta

dr inż. Małgorzata Łukawska

OŚWIADCZENIE

Oświadczam, że jestem współautorem artykułu naukowego opublikowanego w czasopiśmie *Scientific Reports* pt. *Chemical modification of melphalan as a key to improving treatment of haematological malignancies* (IF: 4.964; punkty MEiN: 140 pkt.), autorstwa Arkadiusza Gajka, Anastazji Poczta, Małgorzaty Łukawskiej, Violetty Cecudy- Adamczewskiej, Joanny Tobiasz, Agnieszki Marczak.

Mój wkład w powstanie niniejszego artykułu obejmował koncepcję struktury chemicznej analogów melfalanu, syntezę tychże analogów oraz opisanie aspektów chemicznych ich otrzymywania wraz z analizą ich struktury, współpracę przy nadaniu pracy ostatecznego kształtu publikacji oraz udział w odpowiedziach na uwagi recenzentów.

Mój wkład w powstanie tej pracy oceniam na 5%.

.....

dr inż. Małgorzata Łukawska

Łódź, 15.12.2022

dr Violetta Cecuda- Adamczewska
Instytut Biotechnologii i Antybiotyków
Sieć Badawcza ŁUKASIEWICZ
ul. Starościńska 5
02-516 Warszawa

OŚWIADCZENIE

Oświadczam, że jestem współautorem artykułu naukowego opublikowanego w czasopiśmie *Scientific Reports* pt. *Chemical modification of melphalan as a key to improving treatment of haematological malignancies* (IF: 4.964; punkty MEiN: 140 pkt.), autorstwa Arkadiusza Gajka, Anastazji Poczta, Małgorzaty Łukawskiej, Violetty Cecudy- Adamczewskiej, Joanny Tobiasz, Agnieszki Marczak.

Mój wkład w powstanie niniejszego artykułu polegał na syntezie badanych związków.

Mój wkład w powstanie tej pracy oceniam na 5%.

Adamczewska

.....

dr Violetta Cecuda- Adamczewska

Warszawa, 15.12.2022

Joanna Tobiasz
Instytut Biotechnologii i Antybiotyków
Sieć Badawcza ŁUKASIEWICZ
ul. Starościńska 5
02-516 Warszawa

OŚWIADCZENIE

Oświadczam, że jestem współautorem artykułu naukowego opublikowanego w czasopiśmie *Scientific Reports* pt. *Chemical modification of melphalan as a key to improving treatment of haematological malignancies* (IF: 4.964; punkty MEiN: 140 pkt.), autorstwa Arkadiusza Gajka, Anastazji Poczta, Małgorzaty Łukawskiej, Violetty Cecudy- Adamczewskiej, Joanny Tobiasz, Agnieszki Marczak.

Mój wkład w powstanie niniejszego artykułu polegał na syntezie badanych związków.

Mój wkład w powstanie tej pracy oceniam na 5%.

.....

Joanna Tobiasz

WYDZIAŁ BIOLOGII
i OCHRONY ŚRODOWISKA
Uniwersytet Łódzki

Łódź, 15.12.2022

prof. dr hab. Agnieszka Marczak
Katedra Biofizyki Medycznej
Wydział Biologii i Ochrony Środowiska
Uniwersytet Łódzki
ul. Pomorska141/143
90-236 Łódź

OŚWIADCZENIE

Oświadczam, że jestem współautorem artykułu naukowego opublikowanego w czasopiśmie *Scientific Reports* pt. *Chemical modification of melphalan as a key to improving treatment of haematological malignancies* (IF: 4.964; punkty MEiN: 140 pkt.), autorstwa Arkadiusza Gajka, Anastazji Poczta, Małgorzaty Łukawskiej, Violetty Cecudy- Adamczewskiej, Joanny Tobiasz, Agnieszki Marczak.

Mój wkład w powstanie niniejszego artykułu obejmował współudział w przygotowaniu koncepcji i planu wykonywanych badań, opiekę merytoryczną, udział w analizie i dyskusji uzyskanych wyników oraz odpowiedziach na recenzje.

Mój wkład w powstanie tej pracy oceniam na 5%.

A. Marczak

.....

prof. dr hab. Agnieszka Marczak

WYDZIAŁ BIOLOGII
i OCHRONY ŚRODOWISKA
Uniwersytet Łódzki

Łódź, 15.12.2022

mgr Anastazja Poczta
Katedra Biofizyki Medycznej
Wydział Biologii i Ochrony Środowiska
Uniwersytet Łódzki
ul. Pomorska141/143
90-236 Łódź

OŚWIADCZENIE

Oświadczam, że jestem współautorem artykułu naukowego opublikowanego w czasopiśmie *International Journal of Molecular Sciences* pt. *Synthesis and In Vitro Activity of Novel Melphalan Analogs in Hematological Malignancy Cells* (IF: 6.208; punkty MEiN: 140 pkt.), autorstwa Anastazji Poczta, Piotra Krzeczyńskiego, Joanny Tobiasz, Anety Rogalskiej, Arkadiusza Gajka oraz Agnieszki Marczak.

Mój wkład w powstanie niniejszego artykułu polegał przeprowadzaniu następujących oznaczeń:

- oceny właściwości cytotoksycznych nowych analogów melfalanu testem redukcji resazuryny,
- oceny właściwości genotoksycznych nowych analogów melfalanu przy użyciu alkalicznej wersji testu kometowego,
- oznaczanie frakcji komórek apoptotycznych i nekrotycznych metodą podwójnego barwienia z wykorzystaniem mieszaniny fluorochromów: jodek propidyny i Hoechst 33342
- analiza zaburzeń strukturalnych błony komórkowej metodą podwójnego barwienia z wykorzystaniem mieszaniny fluorochromów: jodek propidyny i aneksyna V,
- analiza aktywności kaspaz 3/7, 8,9 z zastosowaniem sond fluorescencyjnych,
- badanie zmian potencjału błony mitochondrialnej za pomocą sondy fluorescencyjnej JC–1 (5,5',6,6'-tetrachloro-1,1',3,3'–tetraetylobenzimidazolokarboksyjanina)
- współudział w analizach *in silico*.

Ponadto do moich obowiązków, podczas realizacji tej pracy należało:

- współudział w tworzeniu koncepcji pracy,
- zebranie odpowiedniej literatury na dany temat badawczy,
- analiza statystyczna, opracowanie i opis wyników bazując na istniejących doniesieniach literaturowych,
- przygotowanie wstępnego kształtu manuskryptu, edycja oraz przygotowywanie odpowiedzi na recenzje.

Pełniłam również funkcję autora korespondencyjnego.

Mój wkład w powstanie tej pracy oceniam na 55 %.

Anastazja Poczta

mgr Anastazja Poczta

Łukasiewicz
ICHP

Łódź, 15.12.2022

dr inż. Piotr Krzeczyński
Zakład Farmacji, Chemii Kosmetycznej i Biotechnologii
Sieć Badawcza–ŁUKASIEWICZ
Instytut Chemii Przemysłowej
imienia Profesora Ignacego Mościckiego
ul. Rydygiera 8
01–793 Warszawa

OŚWIADCZENIE

Oświadczam, że jestem współautorem artykułu naukowego opublikowanego w czasopiśmie *International Journal of Molecular Sciences* pt. *Synthesis and In Vitro Activity of Novel Melphalan Analogs in Hematological Malignancy Cells* (IF: 6.208; punkty MEiN: 140 pkt.), autorstwa Anastazji Poczta, Piotra Krzeczyńskiego, Joanny Tobiasz, Anety Rogalskiej, Arkadiusza Gajka oraz Agnieszki Marczak.

Mój wkład w powstanie niniejszego artykułu obejmował:

- zaplanowanie i współwykonanie syntez związków opisanych w pracy
- wykonanie badań fizykochemicznych związków opisanych w pracy oraz opracowanie wyników
- współudział w napisaniu manuskryptu publikacji
- współudział w odpowiedziach recenzentom.

Mój wkład w powstanie tej pracy oceniam na 15%.

P. Krzeczyński

.....

dr inż. Piotr Krzeczyński

Łukasiewicz
ICHP

Warszawa, 15.12.2022

Joanna Tobiasz
Zakład Farmacji, Chemii Kosmetycznej i Biotechnologii
Instytut Chemii Przemysłowej
Sieć Badawcza ŁUKASIEWICZ
Ul. Rydygiera 8
01-793 Warszawa

OŚWIADCZENIE

Oświadczam, że jestem współautorem artykułu naukowego opublikowanego w czasopiśmie *International Journal of Molecular Sciences* pt. *Synthesis and In Vitro Activity of Novel Melphalan Analogs in Hematological Malignancy Cells* (IF: 6.208; punkty MEiN: 140 pkt.), autorstwa Anastazji Poczta, Piotra Krzeczyńskiego, Joanny Tobiasz, Anety Rogalskiej, Arkadiusza Gajka oraz Agnieszki Marczak.

Mój wkład w powstanie niniejszego artykułu polegał na:

- zaplanowaniu i wykonaniu syntez związków opisanych w pracy,
- ustaleniu warunków metody analizy HPLC, wykonaniu analiz czystości chemicznej związków opisanych w pracy oraz opracowaniu wyników.

Mój wkład w powstanie tej pracy oceniam na 15%.

Joanna Tobiasz

WYDZIAŁ BIOLOGII
i OCHRONY ŚRODOWISKA
Uniwersytet Łódzki

Łódź, 15.12.2022

dr hab. Aneta Rogalska, prof. UŁ
Katedra Biofizyki Medycznej
Wydział Biologii i Ochrony Środowiska
Uniwersytet Łódzki
ul. Pomorska141/143
90-236 Łódź

OŚWIADCZENIE

Oświadczam, że jestem współautorem artykułu naukowego opublikowanego w czasopiśmie *International Journal of Molecular Sciences* pt. *Synthesis and In Vitro Activity of Novel Melphalan Analogs in Hematological Malignancy Cells* (IF: 6.208; punkty MEiN: 140 pkt.), autorstwa Anastazji Poczta, Piotra Krzeczyńskiego, Joanny Tobiasz, Anety Rogalskiej, Arkadiusza Gajka oraz Agnieszki Marczak.

Mój wkład w powstanie niniejszego artykułu obejmował współudział w analizie zmian potencjału błony mitochondrialnej za pomocą sondy fluorescencyjnej JC–1 (5,5',6,6'-tetrachloro-1,1',3,3'–tetraetylobenzimidazolokarboksyjanina), udział w analizie i dyskusji uzyskanych wyników oraz odpowiedziach na recenzje.

Mój wkład w powstanie tej pracy oceniam na 5 %.

Aneta Rogalska
.....
dr hab. Aneta Rogalska

WYDZIAŁ BIOLOGII
i OCHRONY ŚRODOWISKA
Uniwersytet Łódzki

Łódź, 15.12.2022

dr Arkadiusz Gajek
Katedra Biofizyki Medycznej
Wydział Biologii i Ochrony Środowiska
Uniwersytet Łódzki
ul. Pomorska141/143
90-236 Łódź

OŚWIADCZENIE

Oświadczam, że jestem współautorem artykułu naukowego opublikowanego w czasopiśmie *International Journal of Molecular Sciences* pt. *Synthesis and In Vitro Activity of Novel Melphalan Analogs in Hematological Malignancy Cells* (IF: 6.208; punkty MEiN: 140 pkt.), autorstwa Anastazji Poczta, Piotra Krzeczyńskiego, Joanny Tobiasz, Anety Rogalskiej, Arkadiusza Gajka oraz Agnieszki Marczak.

Mój wkład w powstanie niniejszego artykułu obejmował współudział w analizie zaburzeń strukturalnych błony komórkowej metodą podwójnego barwienia z wykorzystaniem mieszaniny fluorochromów: jodek propidyny i aneksyna V-FITC, oraz edycję pierwotnej wersji manuskryptu.

Mój wkład w powstanie tej pracy oceniam na 5 %.

Arkadiusz Gajek
.....
dr Arkadiusz Gajek

WYDZIAŁ BIOLOGII
i OCHRONY ŚRODOWISKA
Uniwersytet Łódzki

Łódź, 15.12.2022

prof. dr hab. Agnieszka Marczak
Katedra Biofizyki Medycznej
Wydział Biologii i Ochrony Środowiska
Uniwersytet Łódzki
ul. Pomorska141/143
90-236 Łódź

OŚWIADCZENIE

Oświadczam, że jestem współautorem artykułu naukowego opublikowanego w czasopiśmie *International Journal of Molecular Sciences* pt. *Synthesis and In Vitro Activity of Novel Melphalan Analogs in Hematological Malignancy Cells* (IF: 6.208; punkty MEiN: 140 pkt.), autorstwa Anastazji Poczta, Piotra Krzeczyńskiego, Joanny Tobiasz, Anety Rogalskiej, Arkadiusza Gajka oraz Agnieszki Marczak.

Mój wkład w powstanie niniejszego artykułu obejmował współudział w przeprowadzeniu analizy *in silico* badanych związków, współudział w przygotowaniu koncepcji i planu wykonywanych badań, opiekę merytoryczną, udział w analizie i dyskusji uzyskanych wyników oraz odpowiedziach na recenzje.

Mój wkład w powstanie tej pracy oceniam na 5 %.

A. Marczak

.....

prof. dr hab. Agnieszka Marczak

WYDZIAŁ BIOLOGII
i OCHRONY ŚRODOWISKA
Uniwersytet Łódzki

Łódź, 15.12.2022

mgr Anastazja Poczta
Katedra Biofizyki Medycznej
Wydział Biologii i Ochrony Środowiska
Uniwersytet Łódzki
ul. Pomorska141/143
90-236 Łódź

OŚWIADCZENIE

Oświadczam, że jestem współautorem artykułu naukowego opublikowanego w czasopiśmie *International Journal of Molecular Sciences* pt. *Newly Synthesized Melphalan Analogs Induce DNA Damage and Mitotic Catastrophe in Hematological Malignant Cancer Cells* (IF: 6.208; punkty MEiN: 140 pkt.), autorstwa Anastazji Poczta, Piotra Krzeczyńskiego, Maksima Ionova, Anety Rogalskiej, Udo S. Gaipl, Agnieszki Marczak oraz Doroty Lubgan.

Mój wkład w powstanie niniejszego artykułu polegał na przeprowadzaniu następujących oznaczeń:

- analiza widm dichroizmu kołowego,
- pomiar potencjału zeta oraz wielkości średnicy hydrodynamicznej
- badanie fosforylacji histonu H2AX poprzez barwienie immunofluorescencyjne,
- analiza aktywności kaspazy 2,
- analiza zmian rozkładu cyklu komórkowego metodą cytometrii przepływowej.

Ponadto do moich obowiązków, podczas realizacji tej pracy należało:

- współudział w tworzeniu koncepcji pracy,
- zebranie odpowiedniej literatury na dany temat badawczy,
- analiza statystyczna, opracowanie i opis wyników bazując na istniejących doniesieniach literaturowych,
- przygotowanie wstępnego kształtu manuskryptu, edycja oraz przygotowywanie odpowiedzi na recenzje.

Pełniłam również funkcję autora korespondencyjnego.

Mój wkład w powstanie tej pracy oceniam na 60%.

Anastazja Poczta

mgr Anastazja Poczta

Łukasiewicz
ICHP

Łódź, 15.12.2022

dr inż. Piotr Krzeczyński
Zakład Farmacji, Chemii Kosmetycznej i Biotechnologii
Sieć Badawcza–ŁUKASIEWICZ
Instytut Chemii Przemysłowej
imienia Profesora Ignacego Mościckiego
ul. Rydygiera 8
01–793 Warszawa

OŚWIADCZENIE

Oświadczam, że jestem współautorem artykułu naukowego opublikowanego w czasopiśmie *International Journal of Molecular Sciences* pt. *Newly Synthesized Melphalan Analogs Induce DNA Damage and Mitotic Catastrophe in Hematological Malignant Cancer Cells* (IF: 6.208; punkty MEiN: 140 pkt.), autorstwa Anastazji Poczta, Piotra Krzeczyńskiego, Maksima Ionova, Anety Rogalskiej, Udo S. Gaipl, Agnieszki Marczak oraz Doroty Lubgan.

Mój wkład w powstanie niniejszego artykułu polegał na współudziale w napisaniu manuskryptu publikacji oraz współudziale w odpowiedziach recenzentom.

Mój wkład w powstanie tej pracy oceniam na 10%.

P. Krzeczyński

.....

dr inż. Piotr Krzeczyński

WYDZIAŁ BIOLOGII
i OCHRONY ŚRODOWISKA
Uniwersytet Łódzki

Łódź, 15.12.2022

dr hab. Maksim Ionov, prof. UŁ
Katedra Biofizyki Ogólnej
Wydział Biologii i Ochrony Środowiska
Uniwersytet Łódzki
ul. Pomorska141/143
90-236 Łódź

OŚWIADCZENIE

Oświadczam, że jestem współautorem artykułu naukowego opublikowanego w czasopiśmie *International Journal of Molecular Sciences* pt. *Newly Synthesized Melphalan Analogs Induce DNA Damage and Mitotic Catastrophe in Hematological Malignant Cancer Cells* (IF: 6.208; punkty MEiN: 140 pkt.), autorstwa Anastazji Poczta, Piotra Krzeczyńskiego, Maksima Ionova, Anety Rogalskiej, Udo S. Gaipl, Agnieszki Marczak oraz Doroty Lubgan.

Mój wkład w powstanie niniejszego artykułu obejmował opiekę merytoryczną i współudział w analizie i opisaniu uzyskanych wyników podczas wykonywania następujących eksperymentów: analiza zmian dichroizmu kołowego, pomiar potencjału zeta, wielkości średnicy hydrodynamicznej.

Mój wkład w powstanie tej pracy oceniam na 5%.

.....
dr hab. Maksim Ionov, prof. UŁ

WYDZIAŁ BIOLOGII
i OCHRONY ŚRODOWISKA
Uniwersytet Łódzki

Łódź, 15.12.2022

dr hab. Aneta Rogalska, prof. UŁ
Katedra Biofizyki Medycznej
Wydział Biologii i Ochrony Środowiska
Uniwersytet Łódzki
ul. Pomorska141/143
90-236 Łódź

OŚWIADCZENIE

Oświadczam, że jestem współautorem artykułu naukowego opublikowanego w czasopiśmie *International Journal of Molecular Sciences* pt. *Newly Synthesized Melphalan Analogs Induce DNA Damage and Mitotic Catastrophe in Hematological Malignant Cancer Cells* (IF: 6.208; punkty MEiN: 140 pkt.), autorstwa Anastazji Poczta, Piotra Krzeczyńskiego, Maksima Ionova, Anety Rogalskiej, Udo S. Gaipl, Agnieszki Marczak oraz Doroty Lubgan.

Mój wkład w powstanie niniejszego artykułu obejmował współudział w opracowaniu wyników dotyczących analizy rozkładu faz cyklu komórkowego oraz udział w dyskusji i w przygotowaniu odpowiedzi na recenzje.

Mój wkład w powstanie tej pracy oceniam na 5%.

Aneta Rogalska
dr hab. Aneta Rogalska, prof. UŁ

Universitätsklinikum Erlangen

Strahlenklinik 91012 Erlangen

To
whom it may concern

Strahlenklinik
Direktor: Prof. Dr. med. Rainer Fietkau
Leitung Translationale Strahlenbiologie - Fokus Strahlenimmunbiologie
Prof. Dr. rer. nat. habil. Udo S. Gaipl
Telefon: 09131 85-44258
Fax: 09131 85-35796
E-Mail: udo.gaipl@uk-erlangen.de
Universitätsstraße 27, 91054 Erlangen
https://www.strahlenklinik.uk-erlangen.de/forschung/translationale-strahlenbiologie/
Öffentliche Verkehrsmittel:
Buslinie 293, Haltestelle Lorlebergplatz
Ihr Zeichen, Ihre Nachricht vom:

Unser Zeichen:
(bitte bei Antwort immer angeben)
UG / Decl_AP_12_2022
16.12.2022

Declaration of co-authorship

Dear Sirs,

I hereby declare that I am a co-author of the article "*Newly Synthesized Melphalan Analogs Induce DNA Damage and Mitotic Catastrophe in Hematological Malignant Cancer Cells*" published in the *International Journal of Molecular Sciences* (IF: 6,208), by Anastazja Poczta, Piotr Krzeczyński, Maksim Ionov, Aneta Rogalska, Udo S. Gaipl, Agnieszka Marczak and Dorota Lubgan.

My contribution to this article included participation in the development of the methodology, writing, review and editing of the work. I estimate my contribution to this paper at 5%.

Sincerely,

Prof. Dr. Udo Gaipl
Head of Translational Radiobiology

WYDZIAŁ BIOLOGII
i OCHRONY ŚRODOWISKA
Uniwersytet Łódzki

Łódź, 15.12.2022

prof. dr hab. Agnieszka Marczak
Katedra Biofizyki Medycznej
Wydział Biologii i Ochrony Środowiska
Uniwersytet Łódzki
ul. Pomorska141/143
90-236 Łódź

OŚWIADCZENIE

Oświadczam, że jestem współautorem artykułu naukowego opublikowanego w czasopiśmie *International Journal of Molecular Sciences* pt. *Newly Synthesized Melphalan Analogs Induce DNA Damage and Mitotic Catastrophe in Hematological Malignant Cancer Cells* (IF: 6.208; punkty MEiN: 140 pkt.), autorstwa Anastazji Poczta, Piotra Krzeczyńskiego, Maksima Ionova, Anety Rogalskiej, Udo S. Gaipl, Agnieszki Marczak oraz Doroty Lubgan.

Mój wkład w powstanie niniejszego artykułu obejmował współudział w przygotowaniu koncepcji i planu wykonywanych badań, opiekę merytoryczną, udział w analizie i dyskusji uzyskanych wyników oraz odpowiedziach na recenzje.

Mój wkład w powstanie tej pracy oceniam na 5%.

A. Marczak

.....

prof. dr hab. Agnieszka Marczak

Erlangen, 15.12.2022

PD Dr. Dr. habil. med. Dorota Lubgan
Translational Radiobiology,
Department of Radiation Oncology,
University Hospital Erlangen
Friedrich-Alexander-Universität Erlangen-Nürnberg,
Universitätsstr. 27, 91054 Erlangen, Germany

OŚWIADCZENIE

Oświadczam, że jestem współautorem artykułu naukowego opublikowanego w czasopiśmie *International Journal of Molecular Sciences* pt. *Newly Synthesized Melphalan Analogs Induce DNA Damage and Mitotic Catastrophe in Hematological Malignant Cancer Cells* (IF: 6.208; punkty MNiSW: 140 pkt.), autorstwa Anastazji Poczta, Piotra Krzeczyńskiego, Maksima Ionova, Anety Rogalskiej, Udo S. Gaipl, Agnieszki Marczak oraz Doroty Lubgan.

Mój wkład w powstanie niniejszego artykułu obejmował współudział w tworzeniu koncepcji pracy, opiekę merytoryczną nad eksperymentem dotyczącym badania fosforylacji histonu H2AX, a także udział w analizie i dyskusji uzyskanych wyników oraz odpowiedziach na recenzje.

Mój wkład w powstanie tej pracy oceniam na 10%.

.....

PD Dr. Dr. habil. med. Dorota Lubgan